Université Libre de Bruxelles
Faculté des Sciences
Service de Chimie-Physique

Generalized Markov Coarse Graining and the Observables of Chaos

Dónal Nicholas MacKernan

Dissertation presented in fulfillment
of the conditions for earning the
Scientific Degree of

Doctor in the Physical Sciences

Brussels, June, 1997

Acknowledgments

A long time ago I telephoned Professor Grégoire Nicolis from the United States and said that I would be in Berlin for a while, and could easily pass through Brussels to discuss the possibility of doing a doctoral thesis with him if he so desired. I came, and did discuss, or rather chatted with him for an hour or so in the company of Catherine Nicolis, after which he suggested that I visit all the sub-groups of the department to devise a thesis topic. He added at the end that he also had some ideas, but did not want possibly to bias my choice. I have continually experienced this welcome, support and freedom of choice from him and the entire department ever since. I am very grateful to him for enabling this visit to turn into thesis and to Catherine Nicolis. Ioannis Antoniou also helped me at this beginning, scientifically, and otherwise. The group of Jean-Pierre Boon, and in particular Alain Noullez taught me programming in C, and was always very hospitable. Alain left for Nice, and then Jörg Weimar arrived who was always happy to help me in any computer problem: C, Unix or even Latex. On this silicon note, I should also express my gratitude to Yves Steyt who selflessly spent days and days fixing up my Linux system. Discussions with Pierre Gaspard were always insightful, and often humorous in a quiet way. I fought, played and learned a lot with and from Daniel Alonso. John William Turner always had a good reference to a well posed problem. I had many a stimulating discussion with David Daems, Francisco Bosco, Jérome Losson, Giorgio Sonnino, Sudhir Jain and in particular Zdzislaw Suchanecki.

But life in the department has not only been scientific: Pierre Charles Romond, Jacques Lauzeral, Gianluca Guidi, Volker Cahlenbuhr, Astero Provata, Alberto Suarez, Charilaos Kougias, Carlo Pierleoni and Sona Prakash made it much more. So did Mustapha Tlidi, Ioannis Kourakis and Andre Wilch. I have spent many years sharing an office with M'Fedall Hillali, and discussing all manners of things, invariably over a cup of coffee.

José Halloy, Anne de Wit, Alain Destexhe and Geneviève Dupont have provided good company since I first arrived. Later I have had the pleasure of knowing Daniele Carati, Stéphane Metens, Olivier Lejeune, Isabella Susa, Christo Christov, José Verdasca, José Pontes, Nadia Hassani, Alain Goriely, Ira Tereshenkova, Carlos Lorenzo, Rolando Guzzi, Marc Op De Beek, Kostas Karamanos, Katja Rateitschak, Irene Burghardt, Marc Houggardi, Hans Schepers, El Korchi Drisse, Felipe Barra and Michaêl Theunissen.

I would also like to thank many others of the department: Florence Baras, Malek Mansour for his indefatigable wit, Serge Pahaut, Philippe Peeters, Guy Dewel, Pierre Borckmans, Michele Sanglier, Jean Louis Deneubourg and all his group, in particular Simon Goss, Arnauld Leoni, Philippe Rasse, Thierry Van Damme and the late Rafael Venroy. I am grateful to Pierre Kinet, Irène Saverino and Sonia Wellens for all the help they have provided.

I have had good relations with many of those associated with the International Solvay institutes of physics and chemistry: among them Professor Ilya Prigogine, Jacob Levitan, Dean Driebe and especially Anusha Latifi. I also benefited often from the kindness of Nadine Galand and Mireille Kies-Vercruysse.

I cannot forget the wonderful crazy Danish connection, Ole Lund, Ole Jensen, Ole Viggo and Robin Engelhardt, or further north to Finland, Minna Makiranta and Petteri Kettunen or to Siberia, and Alexander Baranovski.

During my visits to the Humboldt university, Berlin, I have also enjoyed many illuminating discussions with Werner Ebeling, Jan Freund and Lutz Schimansky Geier. Still in Berlin, I have discussed various mathematical problems late into several nights with Jörg Schmeling and Dirk Henning of the Free university. I also thank the Aue family for the hospitality they always showed to me. In a more Bavarian (or Cambridge) direction, more late nights, enjoyable and often mathematical discussions have been my lot with Oscar Bandtlow. The same can be said for the Amsterdam direction with Réne Kuiving; and a toward Milan/Como with Giorgio Mantica.

I am very grateful to Michel Mareschal for sharing his insight about molecular dynamics, and to Jean-Paul Ryckaert for his insight into polymer physics.

And to the whole thesis jury: Radu Balescu, Predrag Cvitanovic', Pierre Gaspard, Michel Mareshal, Grégoire Nicolis and John William Turner, I offer my thanks for their time and criticism.

To all these people, and my other friends in Brussels, Thankyou.

I also wish to thank two old dear friends with whom this chaotic journey commenced, Vasilis Basios and Dimitrius Vasiliadis. Long may it continue.

I have been fortunate to receive financial support from the European Commision under the Science programme, and from the Belgian federal office for Scientific, Technical and Cultural Affairs through the Pôles d'attraction Interuniversitaires programme. To each of these instututions I express my gratitude.

Finally, I wish to thank Colm, Caitriona, Paddy, Dara, my late grand parents, the rest of my family and Oscar and Oisin for being there always.

Dónal MacKernan, Brussels June 1997

Address

Université Libre de Bruxelles
Centre for nonlinear phenomena and complex systems,
C.P. 231, Campus Plaine, B-1050 Brussels.

Electronic Address

dmack@ulb.ac.be
http://homepages.ulb.ac.be/~dmack/

Contents

Chapter 1

Chaos and the Observer: Reducing the Infinite to the Finite

1.1 Introduction

The Collins Thesaurus [47] lists as synonyms of chaotic *anarchic, confused, deranged, disordered, lawless, purposeless, rampageous, riotous, topsy-turvy, tumultuous, uncontrolled.* On the presumption that these are unattractive attributes chaotic dynamical systems were largely avoided or ignored until the nineteen seventies by the scientific community. But, we now know that chaotic systems can be highly ordered in their long time behaviour. Moreover, if one applies tiny perturbations, their chaotic nature often allows them to be controlled with a degree of flexibility far beyond that of regular systems. The main thesis on which the present dissertation is based is that a large class of deterministic chaotic systems can be described statistically as an essentially finite dimensional process, even though a priori, such a description should be infinite dimensional [1]. Thus, while from a trajectory based perspective our ability to predict the future of such systems is severely limited, from a probabilistic point of view, their behaviour can be completely characterised for all time. We will describe local statistical behaviour which enables one to describe the evolution of point-like initial conditions, and global behaviour, which primarily is concerned with the properties of time-correlations of observables (such as position) which are continuous over the system's entire phase space, of Lyapunov exponents and of topological entropy.

While chaos theory has only recently attracted wide-spread interest, examples of systems now termed chaotic have been studied at least since the time of Gauss. Never the less for a long time almost all work in dynamics was analytical and was restricted to linear systems or weakly non-linear models that could be solved perturbatively given nearby linear solutions. Poincaré showed, in the late nineteenth century, that perturbative techniques could sometimes fail, after which research in dynamical systems became largely dormant, with some notable exceptions such as the work of Birkhoff, Lyapunov and the Andronov school. An awakening occurred with the work of Kolmogorov and later Arnold and

[1] while the systems we consider are low dimensional, the function space of probability densities, which are typically L^1 functions, is infinite dimensional

Moser who were able to regularise perturbation techniques in certain cases. Around this time, there was also a growth in interest in ergodic theory, with which we may associate mathematicians such as Anosov, Sinai and Smale (who took a geometrical approach) to mention but a few. The ergodic hypothesis, wherein the long-time average behaviour of a system has a sufficient degree of regularity that it can be described through a distribution function, is a widely assumed truth, particularly for high dimensional systems. It enables us to state that certain averages, and correlations are intrinsic properties of the system and not dependent on its initial preparation. Experimentally and numerically, many large systems seem to satisfy the hypothesis, but this is notoriously difficult to prove.

Despite the great success of this period, dynamical systems theory remained essentially the preserve of mathematicians. In the seventies, the meteorologist Lorenz, perhaps as an echo of the previous decade, coined the popular phrase "the butterfly effect" [61], to describe the sensitivity of his three dimensional deterministic model to small changes in initial conditions. The Nature review article by May[69], indicated that chaos, and non-linear systems in general could have some relevance in biological modeling, while the publications of Feigenbaum on the period-doubling cascade highlighted the fact that simple one-dimensional maps, applied recursively, could share many of the characteristics of high dimensional systems, qualitatively and quantitatively. Since then, chaotic-like behaviour has been observed in such diverse fields as fluid dynamics, optics, chemistry, and biology[42]. Indeed, in certain medical areas, tools of dynamical systems theory have been adapted and used as diagnostic aids - where the presence of chaos is an indicator of health and normalcy. More generally, chaos is one facet of the order and complexity manifested by low and high dimensional nonlinear systems typical of nature[82, 77].

1.2 Dynamical Systems and Chaos

To describe the properties of an evolving natural system, one must first identify quantities which can be measured. We expect the values of the measurements to change over time, as a result of underlying dynamics. Let us call the set of all conceivable values that the measurements may give, the phase space Ω of the system, and each set of values that the system may have at a given time t, its state at time t, $\vec{x}_t$. If we are fortunate, we may find a simple rule, which uniquely determines the future state, given that we know its present state. We will call this deterministic rule, together with Ω, a dynamical system,

$$\vec{x}_t = \vec{f}_t(x_0). \tag{1.1}$$

If time t is continuous, the dynamical system is often called a flow, and if it is discrete, it is referred to as a map. For many systems, the dynamical equations are invertible, so that given the present state of the system, one can in theory determine its past. If the dynamical equations are invertible, and phase space volume is conserved [2] then the system is said to be reversible. For conservative systems satisfying Hamiltons equations, such as an isolated classical system, consisting of a finite number of particles. the term

[2] Consider any region of phase space, and imagine a swarm of points that fill the region completely. Roughly speaking, if the volume of phase space occupied by the swarm as the systems evolves does not change as the swarm moves about phase space, then the system is said to be conservative.

microscopic reversibility is used. A simple example of a system that can be modeled as a low dimensional Hamiltonian system is an ideal child's swing, where there is no friction at the support of the swing or with the air, leading to energy dissipation to the exterior. As our phase space, we could choose the angle from the vertical of the swing and the rate of change of the angle with time. Of course, a more realistic model will take friction into account, and will not be reversible, as the final stationary state will be independent of its history.

Suppose, at time 0, the state of the system $\vec{x}_0$ is not known precisely, but rather there is some tiny uncertainty of magnitude ϵ. We may then depict the initial state, as a small ball of diameter ϵ in phase space, with center $\vec{x}_0$. If the uncertainty in our knowledge of the future state of the system grows exponentially with time, then the system is said to be chaotic. This is not the case in the two examples of the swing, although it is possible for certain Hamiltonian systems. On the other hand, if for some reason we kick the swing periodically, then its motion may become chaotic, depending on the frequency, and magnitude of the kicks. Actually the dynamics of the kicked swing [89] can be surprisingly complicated [3], and is of more physical significance that one might credit [17, 91]. It is also similar to a ball bouncing on a massive oscillating table[44]. Suppose that we decided to measure the rate of change of the angle, every time it was vertical. In the first case, we would obtain only two values, which depend solely on the initial state. In the second, the swing would eventually stop. In the third, if the motion is still periodic, we would obtain a finite number of values, but if it becomes chaotic we would measure an infinity of values. [4] This type of measurement, where one measures one quantity (or quantities) , every time another quantity reaches a specified value is called a Poincaré section. and produces a set of points on a hypersurface of Ω, which in the case of the swing is one dimensional. The way in which each pair of consecutive points is visited on the hypersurface is called a first return map (although it may not be a true map at all, e.g. in some regions, it may be an n to m transformation (with $n > m$), and therefore not deterministic). The function which gives the time between each visit to a point on the hypersurface, is called the return time function. When the first return map is a true map, then it and the hypersurface upon which it acts is also a dynamical system. This is the most common way that chaotic maps are obtained experimentally, or numerically. They are typically easier to investigate than a flow, which is why they are widely used. In this thesis we shall only be concerned with maps, which themselves can give rise to quite intricate dynamics.

1.3 Statistical Description

As pointed out in the preceeding section, initial conditions are never known precisely for real systems, so we may always associate an uncertainty (of magnitude ϵ) with the initial state. If the system is chaotic, then the uncertainty will grow too large in a relatively short time, for us to specify even approximately its current state. While in theory the

[3]It is also related to the kicked rotator, which has been used as a tractable model, for example, to investigate the properties of quantum systems whose classical analogous can behave chaotically.

[4]We should remark, that one could obtain an infinity of points, and the system need not be chaotic, for example, the motion can be quasiperiodic.

system is deterministic, in practice a description at the level of point trajectories is not realistic. We could, however, depict the initial condition as a swarm of points contained in a ball (of radius equal ϵ) in Ω, and describe the evolution of the swarm. It is surprising that the collective dynamics of the swarm can often be easier to characterise than that of the motion of an individual point[52, 107, 84, 86, 85]. In particular, the swarm may exhibit patterns, while the motion of a single point may appear totally erratic. If one can systematically account for these patterns, one may be able to describe quantitatively its general properties. This is the spirit of the techniques that we have used in this thesis, namely to find these patterns by examining carefully the properties of the map, and then to classify dynamical systems, according to the complexity of the patterns that each class may exhibit. But to have any hope that these patterns may be reasonably regular we need to consider the limit of an infinite number of points, where the swarm might be expected to lose its discrete appearance, and become itself an integrable function. If we take this limit, and renormalize the swarm to obtain probability densities, we can speak of the probability of the system being in a given region of Ω, and calculate average quantities, such as the average position of the "swarm" and so on. In fact, probability densities have their evolution governed by a well known linear operator, the Frobenius-Perron operator $\mathcal{U}$ [56], which can be derived from the iterative map (see eq.(1.1)). Specifically, if $\rho_t(\vec{x})$ is a probability density at time t (now assumed to be discrete), its state a time $t+1$ is given by the relation

$$\rho_{t+1}(\vec{x}) = \mathcal{U}\rho_t(\vec{x}) = \int_\Omega \delta(\vec{f}(\vec{y}) - \vec{x})\rho_t(\vec{y})d\vec{y}. \tag{1.2}$$

Probability densities are a priori, at least, integrable functions, and this space (L^1 or L^2) is infinite dimensional. For chaotic systems, the spectrum of $\mathcal{U}$ acting on this space becomes continuous[5], for reversible systems it fills the unit circle (see chapter 5). However, the qualitative observation that swarms can exhibit simple patterns suggests that we do not need to consider the evolution of arbitrary probability densities, but, rather, only those which are either related to the patterns, or correspond to some natural preparations, or measurements of the system. One part of the task ahead is to identify these function spaces. We will see that for large classes of chaotic systems, the infinite dimensional problem of characterising $\mathcal{U}$ reduces to an essentially finite dimensional problem, through appropriate choices of function spaces/observables tailored to each particular system. In this context, one should note that when one makes a statistical prediction, one states the probability of an "event" occuring, or the mean value of an observable at a given instant, and that reduces to the evaluation of integrals of the type

$$\int_\Omega A(\vec{x})\rho_t(\vec{x})d\vec{x} = < A >_{\rho_t}, \tag{1.3}$$

where $A(\vec{x})$ is an integrable function which may represent a characteristic function equal to one in the region of interest, and zero outside, or is some observable such as position. Therefore it is the value of the integral which is of primary physical significance, not the integrand. This distinction is not so important in our analysis for one dimensional chaotic systems, but is vital for higher dimensional reversible systems, where we manipulate the

[5]For one-dimensional maps the spectrum fills the unit disc in the complex plane (see 2)

integrand without changing the value of the integral. Our techniques will allow us to evaluate eq.(1.3) through essentially finite matrix operations so that

$$< A >_{\rho_t} = \sum_{j=0} \sum_{i=0} b_j W^t_{ji} a_i. \tag{1.4}$$

The eigenvalues of W generally[6] define characteristic times of the system, in particular decay rates. The representation where W is diagonal, or in its Jordan form, constitutes for our purposes a spectral decomposition.

Another method to characterise chaotic systems is through their long time average properties. While at first glance, this method seems quite different from that just outlined but is just a sub-case. As mentioned earlier, typically chaotic systems satisfy the ergodic hypothesis. Thus, given an observable $A(\vec{x})$, the average

$$\lim_{T\to\infty} \frac{\sum_{t=0}^{T-1} A(\vec{f}^t(\vec{x}_0))}{T} = \int_\Omega A(\vec{x})\rho_{eq}(\vec{x})d\vec{x} = < A >_{eq}, \tag{1.5}$$

is essentially independent of the initial state $\vec{x_0}$, and is alternatively given as a mean with respect to the invariant density $\rho_{eq}(\vec{x})$. Time correlation functions can also be expressed through $\rho_{eq}(\vec{x})$, so that, given two observables $A(\vec{x}), B(\vec{x})$,

$$\begin{aligned} C_{AB}(\tau) &= \lim_{T\to\infty} \frac{\sum_{t=0}^{T-1}(A(\vec{f}^{t+\tau}(\vec{x}_0)) - < A >_{eq})(B(\vec{f}^t(\vec{x}_0)) - < B >_{eq})}{T} \\ &= \int_\Omega (A(\vec{f}^\tau(\vec{x})) - < A >_{eq})(B(\vec{x}) - < B >_{eq})\rho_{eq}(\vec{x})d\vec{x}. \end{aligned} \tag{1.6}$$

Now, the iterative map also defines a linear operator known as the Koopman operator,

$$KA(\vec{x}) = A(\vec{f}(\vec{x})), \tag{1.7}$$

which is the adjoint of $\mathcal{U}$ in the sense that

$$\int_\Omega K[A(\vec{x})]B(\vec{x})d\vec{x} = \int_\Omega A(\vec{x})\mathcal{U}B(\vec{x})d\vec{x}. \tag{1.8}$$

Thus, we may express $C_{AB}(\tau)$ as

$$C_{AB}(\tau) = \int_\Omega (A(\vec{x}) - < A >_{eq})\mathcal{U}^\tau[(B(\vec{x}) - < B >_{eq})\rho_{eq}(\vec{x})]d\vec{x}, \tag{1.9}$$

so we can evaluate $C_{AB}(\tau)$ if we can determine ρ_{eq}, and the properties of integrals like $< A >_{\rho_t}$. In this context, let us mention that $\rho_{eq}(x)$ is invariant under $\mathcal{U}$, i.e, $\mathcal{U}\rho_{eq}(\vec{x}) = \rho_{eq}(\vec{x})$.

[6]The exception is if the system is intermittent, where we may still in some cases use a matrix represntation up to a good approximation, but valid only for finite times. However, nothing conclusive can be said of the spectra, although they are believed to be non-discrete.

1.4 Obtaining an Essentially Finite Representation

We stated earlier that the spirit of the techniques developed in this thesis rests on the observation that for many chaotic systems, evolving probability densities exhibit patterns, and that through a quantitative description of such patterns, one can reduce an a priori infinite dimensional problem to an essentially finite one. But why do such patterns emerge? The answer to this question is the mathematical foundation of our work, which we shall now sketch using four representative examples: the Bernouli shift, the tent map, the logistic map, and the baker map.

As a preliminary, let us first show the form of the Frobenius-Perron operator for one dimensional chaotic maps. One can readily derive it from eq.(1.2), using the properties of Dirac-delta distributions,

$$\rho_{t+1}(x) = \mathcal{U}\rho_t(x) = \sum_\alpha \rho_t(f_\alpha^{-1}(x))|\frac{d}{dx}f_\alpha^{-1}(x)|\chi_{I_\alpha}(x), \tag{1.10}$$

where $f_\alpha(x)$ are the monotonic branches of the map, and $\chi_{I_\alpha}(x)$ equals one in the range of the α'th monotonic branch, and is zero otherwise. Clearly the local inverses of the map play a vital role in $\mathcal{U}$.

The Bernouli shift map is defined as,

$$b(x) = \begin{cases} b_L(x) = 2x & \text{if } x < \frac{1}{2} \\ b_R(x) = 2x - 1 & \text{otherwise} \end{cases} . \tag{1.11}$$

Each inverse branch maps the unit interval into itself : $b_L^{-1}([0,1]) = [0,\frac{1}{2}]$, $b_R^{-1}([0,1]) = [\frac{1}{2},1]$, and can obviously be extended into the complex plane. This is useful because it allows us to relate their complex geometrical properties to the convergence rates of matrix representations of $\mathcal{U}$ with respect to appropriate basis functions. In the case of the Bernoulli shift, the inverse images of any disc in the complex plane of radius $r > 1$, centre at $\frac{1}{2}$ are also contained within the same disc. Discs are intimately related to Taylor expansions of analytic functions, and matrix representations of $\mathcal{U}$ with respect to monomials[7]. Given an initial density $\rho_0(x)$, analytic in such a disc, $\mathcal{U}\rho_0(x)$ one can readily show that the evolving probability density can always be written as

$$\rho_t(x) = \hat{\rho}_t(x)\chi_{[0,1]}(x), \tag{1.12}$$

where $\hat{\rho}_t(x)$ is analytic in at least the disc of radius r'. In the present case $r' < r$. It is this factorization which allows us to avail of complex analysis. Similar statements may be made with respect to a Chebyshev basis, where a family of confocal ellipsi play the same role as circles here.

Let us now turn to the tent map,

$$T_\mu(x) = \begin{cases} T_L(x) = \mu x & \text{if } x < \frac{1}{2} \\ T_R(x) = \mu(1-x) & \text{otherwise} \end{cases} . \tag{1.13}$$

[7] As is well known if a functions $\psi(z)$ is analytic in a disc of radius $r > 1$, then it can be expanded so that $\forall |z| < r$, $\psi(z) = \sum_{k=0}^{\infty} c_k z^k$, where $|c_k| < \frac{M_r}{r^k}$, and M_r is the maximum value of $|\psi(z)|$ on the circle of radius r.

If $\mu = 2$, the system is very similar to the Bernouli shift. Let us instead consider a value of μ, where the iterates of the critical point $\frac{1}{2}$ fall in a finite time onto a periodic orbit, and define our phase space to be the interval $[0, T(\frac{1}{2})]$. The iterates of the critical point may be used to partition Ω, which is so special that it has the name, the minimal Markov partition. Any Markov partition (in one dimension) has the property that the inverse image of any cell is always contained within a cell. Now given an initial analytic density on Ω, with each consecutive application of $\mathcal{U}^t$, new discontinuities will appear at each successive iterate of the critical point. The inverse branches can be analytically continued, as we did for the Bernoulli shift to show that any density which is piecewise analytic over the partition, will remain remain so, as it evolves. This is why the minimal Markov partition is so special. It "nails down", as it were, the non-analytic points that can be produced by $\mathcal{U}$, given an initialy analytic density. With this knowledge, we may construct an appropriate piecewise polynomial basis, to obtain a matrix representation of $\mathcal{U}$ acting on, for example, the space of functions piecewise analytic over the latter partition. Even if the iterates of the critical point are countably infinite, we can use a finite number of them to construct a quasi-minimal Markov because in practice, for an evolving density (if it is initialy smooth), the relative magnitude of discontinuities at later iterates of the critical point decreases so rapidly that we need only take into account a finite number of them.

Let us now inspect the logistic map,

$$L_r(x) = rx(1-x). \tag{1.14}$$

One major difference between it and the tent and Bernoulli maps is the extremum. This means that the derivatives of the local inverses will have a singularity at $L_r(\frac{1}{2})$, and as $L_r(x)$ is a second order polynomial, this singularity is of square root type, while the local inverses have a square root dependence at this point. One may choose the value of r so that the iterates of the critical point form a finite set, and so that only square-root singularities occur at these points in an evolving probability density, given that it was initialy analytic. With this knowledge, one may identify a invariant function space, and construct an appropriate orthogonal basis. At this point, we should point out that constructing an appropriate basis is not always a trivial task, as will become clear later.

These one-dimensional examples illustrate the three key features responsible for the emergence of patterns in evolving densities:

1. The existence and nature of the minimal Markov partition
2. The nature of non-analyticities present in the local inverses
3. the essentially contractive nature of the local inverses [8]

With this information, one may then identify an invariant function space(s) and construct a basis, tailored to each system.

We may now proceed to our two-dimensional example. The baker map is a 2-d conservative map acting on the unit rectangle. It is constructed from the Bernoulli shift,

$$\vec{B}(x,y) = \begin{cases} (b_L(x), b_L^{-1}(y)) & \text{if } x < \frac{1}{2} \\ (b_R(x), b_R^{-1}(y) & \text{otherwise} \end{cases}. \tag{1.15}$$

[8] Although the logistic is evidently not everywhere hyperbolic, in a certain sense, it is equivalent to an expanding map

Three key features of this map need to be pointed out. First, there is clearly a global coupling between the x and y co-ordinates, but locally, these directions are independent. Second, a one-dimensional expanding map, the Bernouli shift, is the Poincaré section of the baker for constant y. Third, is the obvious fact that the inverse of $b_L^{-1}(y)$ and $b_R^{-1}(y)$ are expanding analytic maps. While these remarks are quite trivial for the baker, it turns out that this structure, albeit in a more complicated setting, is present for a large variety of two-dimensional, reversible chaotic maps. We shall show that these properties enable us to utilise the techniques valid for one dimensional chaotic maps, and in particular, to calculate expressions such as eq.(1.4).

Finally, let us mention that the techniques developed in this thesis originated from a Markov coarse grained approach to chaotic systems[79, 21, 78, 81, 54, 77]. In this approach one first partitions the phase space into cells, and then portrays each point trajectory as a sequence of cell to cell transitions. This portrayal is referred to as symbolic dynamics, and is a powerful method for classifying trajectories of various types and for unraveling aspects of the systems' complexity[26, 19] that would remain blurred in a traditional description limited to trajectories. An additional interest in symbolic dynamics is that strings of symbols play a fundamental role in many natural phenomena. For example DNA and RNA molecules are in part, characterised through sequences of the four symbols A, C, G and T (or U), according to whether the nucleic acid subunit (nucleotide) contains the base adenine, cytosine, guanine and thymine (or uracil). Indeed, most messages conveying information such as books, music, computer programs or electrical activity of the brain can be viewed through symbolic strings[29, 30, 28, 90].

A statistical description can be naturally associated with the symbols, where instead of speaking of the value of a probability density at a given point, one merely states the probability to be in one or a set of cells. One can then speak of the probability of a series of cell to cell transitions. If an appropriate partition is choosen, one sometimes obtains a closed and finite set of equations governing all coarse grained probabilistic predictions, and this is usually generated through a finite stochastic matrix. In that case one can say that the system is a Markov process, satisfying a master equation similar to a stochastic Markov process. This thesis can be viewed as a generalization of a Markov coarse grained approach, to a function analytic setting. The generalization enables one to solve large classes of problems which cannot be resolved from a purely Markov coarse grained perspective. More importantly, it identifies the key dynamical features allowing such a description to be executed, and the crucial role of the choice of observable/ measurable function.

1.5 Outline of Results

This thesis is organized as follows

- In chapter 2 the principal results in the current literature on one-dimensional maps are given, and Markov coarse graining is generalized for piecewise linear Markov maps, and equivalent repellers. The connection between our representations and the zeta- function formalism is established. In so doing, we point out that for piecewise linear Markov maps, where the minimal Markov partition consists of more than one cell, the dynamical zeta functions cannot be expected to give all the decay rates of time correlation functions of analytical observables. This is due to a subtle counting error, which fortunately can be easily corrected. We then show that local statistical properties can be described through an appropriate basis related to the systems periodic orbits, and derive a formula for the corresponding spectra. Finally, we show how spaces of functions including singular, but integrable functions can be constructed so that there exist eigenvalues of $\mathcal{U}$ arbitrarily close to one in magnitude in the unit disc. Thus, we can define highly localized states that decay arbitrarily slowly.

- All the previous results, with the exception of the latter are generalized to any Markov analytic map (and equivalent repellers) in chapter 3. We show rigorously, and constructively, how spectral decompositions of $\mathcal{U}$ can be obtained. The formula for spectra related to local statistical properties is demonstrated to be valid not just for Markov analytic maps, but for a much larger class of dynamical systems. This chapter is the analytical foundation of the later chapters.

- The case of non-hyperbolic, but chaotic maps (of the S-unimodal type) is treated in chapter 4. This includes in particular, the logistic map. Singular, but integrable probability densities are generic to these systems, necessitating the construction of special orthogonal basis. We establish that these systems are statistically isomorphic to Markov analytic maps. This means that all the results of the previous chapter are applicable here too. We argue heuristicaly that these techniques can also be applied to non-Markov maps, and provide numerical results remarkably consistent with this claim. Finally, a formula for the dependence of the spectral gap, as a function of the control parameter is obtained.

- In chapter 5 classes of two-dimensional chaotic systems both dissipative and conservative are considered. All the results of chapter 3 are generalized. In particular, we show that the results of any statistical measurement (involving piecewise analytic observables) can be calculated through an essentially finite dimensional matrix. Thus an effective spectral decomposition can be obtained, where the eigenvalues lie within the unit disc (with the exception of eigenvalues corresponding to invariant states). We close the chapter by commenting on the origins of macroscopic irreversability.

- In the final chapter we discuss applications, and partial results on: intermittentcy, non-Markov maps, stochastic resonance-like phenomena and sensitive dependence of chaotic systems to time dependent perturbations. We conclude the thesis by outlining what we believe to be the merits and limitations of the techniques developed in this work.

Chapter 2

Generalized Markov Coarse Graining and Spectral Decompositions of piecewise linear Maps

2.1 Introduction

Low-dimensional chaotic maps have a deceptively simple appearance, yet their dynamical behaviour can be extraordinarily intricate, and difficult to characterise. A system's phase space may have regions of chaotic and stable motion (quasi-periodic and periodic) intermingled. Even one-dimensional chaotic maps such as the logistic can be difficult to characterise. Thus, as a first step towards an analysis of these complex systems, we shall discuss the properties of piecewise linear maps. We will see in later chapters that almost all of the results obtained here can be generalized to one-dimensional non-linear chaotic maps, and classes of two-dimensional maps.

In chapter 1 it was explained that long-time average properties of ergodic chaotic systems can, in principle, be determined through a knowledge of the properties of $\mathcal{U}$ acting on probability densities. Thus, whatever one's statistical perspective, it seems reasonable to focus attention on $\mathcal{U}$. As $\mathcal{U}$ is a linear operator[56, 67] a natural way to characterize it is by its eigenvalues (as these usually define characteristic times of the system) and associated eigenstates. Now, given any probability density $\rho(x)$, which must be, by definition, an integrable function, $\mathcal{U}\rho(x)$ will also be a probability density. Thus, the space of integrable functions (L^1) is invariant under $\mathcal{U}$, and so it would seem natural to seek a representation of $\mathcal{U}$ acting on L^1 through an appropriate basis. Unfortunately, the spectra of $\mathcal{U}$ acting on L^1 fill up the unit disc in the complex plane [31, 94], and are of little obvious value in characterising the system. Moreover, $\mathcal{U}$ has the properties that its spectra depend on the space of functions upon which it acts. This is often considered to be a liability, as it follows that there is no unique set of characteristic times. But, it is in fact an advantage, as one can, in many cases, identify specific functions spaces and observables, with a given set of spectra. For example, each Markov analytic map has the property that the space of functions piecewise analytic over the minimal Markov partition is invariant under $\mathcal{U}$. Mayer[70] has shown that the spectra of $\mathcal{U}$ acting on this function space is discrete. There are many other possible choices of invariant function space, for these systems. We will introduce one related to the system's periodic orbits that is suitable for describing local statistical properties. Thus, the choice of function space $\mathcal{F}$ can be related to the scales of the phenomena that can be probed in phase space through the probabilistic description.

Before identifying various invariant function spaces, let us first outline the Markov coarse grained approach to the description of the statistical properties of chaotic systems. One starts by partitioning the phase space into cells which define local regions. For an M cell partition $\mathcal{P}$, a linear operator E performing the coarse graining can be defined,

$$E\rho(x) = \sum_{i=1}^{M} \left(\frac{1}{\Delta_i} \int_{C_i} \rho(y) dy \right) \chi_{c_i}(x), \tag{2.1}$$

where $\chi_{c_i}(x)$ equals one if x belongs to the i^{th} cell C_i and is zero otherwise, and Δ_i is the size of C_i. When the relation

$$(E\mathcal{U}E)^n = E\mathcal{U}^n E \tag{2.2}$$

is valid, the coarse grained description of the evolution is generated by a time independent finite dimensional matrix,

$$\mathcal{W} = E\mathcal{U}E, \tag{2.3}$$

and a Markov coarse graining (MCG) is said to be possible. Of course the definition of $\mathcal{W}$ in itself does not imply the validity of eq.(2.2). A sufficient (but not necessary) condition for this is that the coarse graining and evolution operators commute when acting on coarse grained functions[1]

$$[E,\mathcal{U}]E = (E\mathcal{U} - \mathcal{U}E)E = E\mathcal{U}E - \mathcal{U}E = 0. \tag{2.4}$$

Concrete examples of MCG's have been constructed both for conservative and dissipative dynamical systems. One class of such examples, which is the chief concern of this chapter are piecewise linear maps on the unit interval[79, 21, 78, 81, 63, 73] whose non-differentiable points fall in a finite number of iterations onto a periodic orbit(s). Such maps are called piecewise linear Markov maps. The set of iterates of the non-differentiable points form a minimal Markov[70] partition and with respect to this partition, a MCG exists. Indeed, in this case, $E\mathcal{U}E - \mathcal{U}E = 0$, so that the space $\mathcal{F}$ of functions piecewise constant over the cells of the partition, is invariant under $\mathcal{U}$. Hence, the eigenvalues and right eigenvectors of $\mathcal{W}$, define eigenvalues and eigenfunctions of $\mathcal{U}$ restricted to $\mathcal{F}$ and invariant densities are easily calculated [43]. The logarithms of the absolute values of the spectra equal the decay rates observed in time correlation functions of observables lying in $\mathcal{F}$. Finer scale descriptions can be easily made by adding to the points defining the minimal Markov partition either a finite number of successive inverse images of one or more of these points; or by adding all the points of a finite number of periodic orbits of the iterative law $f(x)$. Both methods of partition refinement can be done simultaneously, and with respect to the new partition, a MCG also exists.

[1] One may show for any Markov map that there exists an MCG where E is defined with respect to an invariant measure μ absolutely continuous with respect to Lebesgue (rather than the uniform measure as above), and where $\mathcal{U}$ is replaced by a transfer operator which is the adjoint (with respect to the measure) of the Koopman operator defined as $Kg(x) = g(S(x))$. In general this transfer operator will not be the same $\mathcal{U}$

A simple generalization of spaces of piecewise constant functions are spaces of piecewise polynomials. That is, spaces of functions that are polynomial within each cell of $\mathcal{P}$ but are permitted to have discontinuities at each cell boundary. As it turns out, piecewise polynomial spaces of any order are also invariant under U. Hence, a matrix representation $\mathcal{W}$ of $\mathcal{U}$ acting on these spaces can be calculated with respect to a piecewise polynomial basis, such as monomials (where expansion coefficients correspond to those of a Taylor series), or any set of orthogonal polynomials (e.g. Chebyshev polynomials, Legendre polynomials), where each basis function has support over a given cell. This choice of basis determines a larger class of initial densities/observables whose statistical properties can be determined through the corresponding $\mathcal{W}$. The class consists at least of all functions which can expanded through the basis as a uniformly convergent series. In the case of a monomial expansions, this space $\mathcal{F}$ includes functions, which over each cell, have complex extensions into discs of radius related to the width of the cell. For piecewise Chebyshev functions, the space includes all functions which within each cell are continuous, and whose derivatives are functions of bounded variation (in this chapter we shall only use a piecewise monomial basis). Again, eigenfunctions and eigenvalues of $\mathcal{U}$ are defined through the eigenvalues and eigenvectors of $\mathcal{W}$, and are easily calculated. The left and right normalized eigenvectors of $\mathcal{W}$ form a bi-orthonormal set. Suppose now that $\vec{g}$ denotes the expansion coefficients of a function $g(x) \in \mathcal{F}$, truncated at a suitable order, with a truncation error ϵ. Using the bi-orthonormal basis defined by the eigenvectors, we may expand $g(x)$ in terms of the right eigenfunctions of $\mathcal{U}$, the error in the expansion being no larger than ϵ. Thus, spectral decompositions of $\mathcal{U}$ can be obtained. The extension of classical coarse graining to this more general and representative function space is the principal goal of the present chapter.

The term Frobenius-Perron transform for $\mathcal{U}$ appears to have been first coined by Ulam [105], in work which lead to a well-known conjecture bearing his name. He considered a simple class of piecewise linear maps, and noticed that for the tent map (slope 2), that an MCG was possible for a partition of cells of equal size. He used the phrase Frobenius-Perron in allusion to the Frobenius-Perron theorem, which states that for a finite dimensional matrix, where all matrix elements are positive and non-zero[2], there exists an eigenvector $\vec{v}$ and corresponding maximum eigenvalue r such that for any vector $\vec{q}$,

$$\lim_{n->\infty} \frac{W^n \vec{q}}{||W^n \vec{q}||} \to \vec{v}. \tag{2.5}$$

In the case of the tent map, the invariant vector of $\mathcal{W}$ (which is an irreducible stochastic matrix) tends to the invariant density of $\mathcal{U}$. Ulam's conjecture is that the invariant eigenvector of W in the limit of an infinitely fine partition of uniform cell size, will coincide with the invariant density of $\mathcal{U}$ for any chaotic map, including the logistic map at parameter 4. The conjecture is not correct for the logistic map, as the invariant density is singular, but is valid for piecewise C_2 maps with minimum expansion rate equal[60] to two. However, a partition having all cells of equal size is generally not optimal, in that for piecewise linear Markov maps, a finite MCG is possible. Moreover, the Ulam conjecture does not address the properties of less dominant eigenfunctions and corresponding eigenvalues, which

[2]One may also consider the case of finite an irreducible stochastic matrix, where the maximum eigenvalue equals one

determine, for example, the system's decay rates.

The motivation for obtaining invariant densities by these, and the several other authors lies in establishing the ergodic properties of these systems. In this regard, we should define a number of terms commonly used in ergodic theory. Let $(\Omega, \mathcal{A}, \mu)$ be a measure space [56, 67], where Ω is the phase space, $\mathcal{A}$ is the σ algebra[3] of measurable sets, and μ is a probability measure [4]. Let $S : \Omega \to \Omega$ be a measurable map. A measure is called invariant if

$$\mu(S^{-1}(\Delta)) = \mu(\Delta), \tag{2.6}$$

where Δ is any set such that $\Delta \in \mathcal{A}$. A system is ergodic if every invariant set A is such that $\mu(A) = 0$ or $\mu(\Omega \backslash A) = 0$. A system is mixing if

$$\forall A, B \in \sigma, \lim_{n\to\infty} \mu(A \bigcap S^{-n}(B)) = \mu(A)\mu(B). \tag{2.7}$$

A third property, of great importance for dissipative systems is exactness. A system is exact if

$$\lim_{n\to\infty} \mu(S^n(A)) = 1, \tag{2.8}$$

for each A such that $\mu(A) > 0$ and $S^n(A) \in \mathcal{A}$. Exactness implies mixing, and in turn ergodicity. Exact maps may be related to a class of chaotic reversible higher dimensional maps called K automorphisms, which will be analysed in chapter 5. However, the relation between mixing and the spectral properties of $\mathcal{U}$ acting on given function spaces is not clear in general. Fortunately, the work of Lasota and Yorke on the existence of invariant measures on C_2 piecewise expanding maps [57] established that the space of functions of bounded variation is invariant under $\mathcal{U}$. This led to a series of theorems, which include the following interesting results. Let $\rho(x)$ be any function in L^1. The Frobenius-Perron operator [5] may be decomposed as

$$\mathcal{U}\rho(x) = \sum_{i=1}^{r} \Lambda^{\dagger}{}_i(\rho) g_i(x) + Q\rho(x), \tag{2.9}$$

where r is an integer, the $\Lambda^{\dagger}{}_i$'s are bounded linear functionals, the $g_i(x)$'s are non-negative probability densities, and $Q : L^1 \to L^1$ is a bounded linear operator. The densities g_i and Q have the following properties:

1. The g_i's have mutually disjoint support, so that $g_i(x)g_j(x) = 0$, if $i \neq j$.
2. $\mathcal{U}g_i(x) = g_{\beta(i)}(x)$
3. $||\mathcal{U}^n Q\rho(x)|| \to 0$, as $n \to \infty$.

[3] A collection $\mathcal{A}$ of subsets of a set X is a σ algebra if:(a) When $A \in \mathcal{A}$ then $X \backslash A \in \mathcal{A}$; (b) Given a finite or infinite sequence $\{A_k\}$ of disjoint subsets of X,$\bigcup_k A_k \in \mathcal{A}$; and (c) $X \in \mathcal{A}$.

[4] A real-valued function μ defined on a σ-algebra $\mathcal{A}$ is a measure if: (a) $\mu(\emptyset) = 0$; and (b) $\mu(A) \geq 0$ for all $A \in \mathcal{A}$; (c) $\mu\left(\bigcup_k A_k\right) = \sum_k \mu(A_k)$ if $\{A_k\}$ is a finite or infinite sequence of pairwise disjoint subsets of $\mathcal{A}$

[5] This is in fact valid for any smoothing Markov operator

A system is ergodic if $\beta(i)$ is a cyclic permutation, and is exact if $r = 1$. Indeed, if a system is mixing, then $r = 1$, so that for systems satisfying the criteria of the theorem, mixing also implies exactness. Obviously, in the case of a cyclic permutation of period p, there will be p distinct eigenvalues of $\mathcal{U}$ equal to the p^{th} roots of unity. Similar results have been obtained by Hoffbauer and Keller[50] and others, where one considers the properties of $\mathcal{U}$ acting on the space of functions of bounded variation. In this case, $||\mathcal{U}^n Q\rho(x)||$ decays exponentially.

Let us now outline the main results in the literature for one dimensional piecewise linear maps. The main subjects of concern have been the behaviour of time correlation functions, and the calculation of invariant measures rather than a full analysis of the Frobenius-Perron operator. In the context of the present chapter, the work of Mori *et al*[73], and Györgi *et al* [45] are particularly relevant. They investigated the properties of time correlation functions of polynomial observables, by considering the corresponding eigenvalue problem of $\mathcal{U}$. In a related work[102, 106] evidence was provided that certain piecewise linear maps that do not possess finite minimal Markov partitions can be well approximated as Markov maps, which is important because the Markov property is rarely satisfied exactly. However, this problem has not yet been resolved conclusively[27, 64]. Roeperstorff [93] and later others[48, 38, 4] obtained a spectral decomposition of U for r-adic maps (e.g. Bernouili shift map). We should mention that given a piecewise linear chaotic map, one may also construct a statistically equivalent non-linear one through smooth conjugate transformations, and in some cases, the converse is also possible. Two examples are the logistic map at parameter 4, where the conjugate transformation was found by Ulam, and the Chebyshev maps, where the conjugate transformation was obtained by Adler and Rivlin[2]. For the latter, Roepersdorff also obtained a spectral decomposition of the corresponding $\mathcal{U}$.

The present chapter extends this earlier work to all piecewise linear Markov maps and repellers and to a wider class of function spaces such as spaces of piecewise analytic functions. Further it reveals the existence of a wider class of eigenvalues related to the unstable periodic orbits. Finally, it provides a systematic algorithm for constructing the transition matrix governing the evolution of probability vectors which are the representation of the densities in each function space.

An outline of the rest of the chapter and principal results is as follows.

- In section 2.2 we define piecewise linear Markov maps and repellers and generalize the notion of Markov coarse graining to obtain a spectral decomposition of $\mathcal{U}$. In this case, $\mathcal{U}$ is restricted to the space of functions that can be expressed, exactly or up to a good approximation, over each cell of $\mathcal{P}$ as a finite Taylor expansion. The spectra are arranged in groups corresponding to the order of the piecewise monomial space.

- In section 2.3 we consider the case where $\mathcal{P}$ is the minimal Markov partition. This partition defines the space of piecewise analytic functions having the least number of discontinuities) which is invariant under $\mathcal{U}$. The spectra of $\mathcal{U}$ restricted to this space also give the possible decay rates of time correlation functions of any analytic observable. We relate the spectra to the zeros of the corresponding zeta functions [23, 7]. In so doing, we show for general Markov maps, where the Markov partition consists of more than one cell, that the dynamical zeta functions typically does not contain all the expected decay rates that correlation functions of analytic observables may exhibit. This point has been overlooked by several authors[70, 66], and may be related to Manning multiples [68]. We close the section by deriving a simple general formula for the appropriate correction factors.

- In section 2.4 we consider the case of refined partitions suitable for local statistical descriptions. In particular, we derive a simple formula for their spectra. Each eigenvalue corresponds to a given periodic orbit, and the associated time correlation functions exhibit a periodic decay. The spectra given by this formula for periodic orbits that are elements of the minimal Markov partition are directly related to fore-mentioned correction factors.

- The results of sections 2.3 and 2.4 are illustrated in 2.5 with simple examples of maps from the tent family.

- In section 2.6 the eigenvalues associated with measurable functions that are generalized piecewise polynomials (powers of x raised to a fractional or to a complex exponent) are considered. It turns out that exponents can be chosen so that the corresponding spectra lie anywhere in the unit circle. Arbitrarily slowly decaying eigenstates can thus be constructed which are highly localized about the periodic orbits.

2.2 Generalized Markov coarse graining in a piecewise monomial basis

A piecewise linear or analytic map $f : \mathbf{I} \to \mathbf{I}$, where $\mathbf{I} = [0, 1]$, is Markov if it has the following properties [70]:

(i) The number of non-differentiable points $d_1, d_2, .., d_N$ is finite.

(ii) Their iterates form a finite set of points $\mathcal{P}_{\mathcal{M}}$ $\{a_0, a_1, .., a_{N'}\}$, where $a_k < a_{k+1}, a_0 = 0$ and $a_{N'} = 1$.

(iii) There exists an integer k such that $|\frac{d}{dx} f^k(x)| > 1$ for some $k \geq 1$ and $\forall x \in \mathbf{I}$.

The set of points $\mathcal{P}_{\mathcal{M}}$ can be used to partition the unit interval into cells $C_i = [a_{i-1}, a_i]$. The resulting partition is referred to as the minimal Markov partition[6]. We remark that in some cases the minimal Markov partition may consist of only one cell, the unit interval itself.

The probability density $\rho_n(x)$ at time n, descriptive of the statistical state of the system, assumed to be an L^1 function, evolves according to the Frobenius-Perron operator (cf

[6]Note certain authors include the critical points (i) as well as the points (ii) in the definition of the minimal Markov partition.

eq.(1.10))

$$\begin{aligned}\rho_{n+1}(x) = \mathcal{U}\rho_n(x) &= \int_0^1 \delta(x - f(y))\rho_n(y)dy \\ &= \sum_\alpha \rho_n(f_\alpha^{-1}(x))|\frac{d}{dx}f_\alpha^{-1}(x)| \end{aligned} \qquad (2.10)$$

where $f_\alpha^{-1}(x)$ denote the inverse branches of $f(x)$. It is understood from hereon that if an inverse branch $f_\alpha^{-1}(x)$ is not defined for a point x, then the corresponding term in the sum eq.(2.10) is set equal to zero at this point. Throughout the rest of this chapter derivatives will often be indicated by the following suffices: $\frac{d}{dx}f(x) = f'(x)$ and $\frac{d^n}{dx^n}f(x) = f^{(n)}(x)$.

We shall also be interested in the properties of a class of piecewise linear repellers. Let $f(x)$ denote the map of any system belonging to this class. $f(x)$ has the properties:

(i) The unit interval $\mathbf{I}$ is mapped onto a union of itself and another set of points D, where $\mathbf{I}$ and D are mutually disjoint.

$$f(\mathbf{I}) = \mathbf{I}\bigcup D. \qquad (2.11)$$

(ii) Points that leave $\mathbf{I}$ never return

$$\forall n,\ f^n(D)\bigcap \mathbf{I} = \emptyset. \qquad (2.12)$$

(iii) The iterates of non-differentiable points of $f(x)$ that are in $\mathbf{I}$ are finite in number and define $\mathcal{P}_\mathcal{M}$. This implies that the iterates of non-differentiable points that remain in $\mathbf{I}$ are mapped onto one or more periodic orbits.

(iv) There exists a k such that$|\frac{d}{dx}f^k(x)| > 1$ for some $k \geq 1$ and $\forall x \in \mathbf{I}$.

We shall restrict the Frobenius-Perron operator $\mathcal{U}$ so that it acts only on functions whose support is not outside the unit interval, thus ignoring what happens to densities after they have left $\mathbf{I}$. The set of points $\mathcal{P}_\mathcal{M}$ for repellers will effectively form, for our purposes, a minimal Markov partition of $\mathbf{I}$. From here on, $f(x)$ denotes a map belonging to either of the above classes.

We now need to define the type of function basis and its dual which will be used in the representations of $\mathcal{U}$. As will be clear shortly, each possible basis is associated with any M-cell Markov partition $\mathcal{P}$ of the following class: the minimal Markov partition and refinements formed by adding to the points defining $\mathcal{P}_\mathcal{M}$ either: (a) a finite number of successive inverse images of one or more of these points; or (b) all the points of a finite number of periodic orbits of $f(x)$. Both methods of partition refinement can be performed simultaneously.

We define the monomial family whose support is the cell $C_i = (a_{i-1}, a_i)$ as

$$\phi_i(n,x) = \begin{cases} (x - a_{i-1})^n, & \text{if } x \in C_i; \\ 0, & \text{otherwise,} \end{cases} \qquad (2.13)$$

where $n = 0, 1, 2, \ldots$. The open intervals used to define the cells is chosen to avoid possible ambiguities. Let Φ_N be the function space spanned by the set of monomial families of order N associated with the partition $\mathcal{P}$, $\{\phi_i(n,x) : i = 1, 2, \ldots, M, \ \ and \ \ n = 0, 1, \ldots N\}$. The dual functional to a monomial of order n, having support in the cell $C_i = [a_{i-1}, a_i]$ is

$$\phi_i^\dagger(n,x) \ = \ \lim_{\epsilon \to 0^+} \frac{(-1)^n}{n!} \frac{d^n}{dx^n} \delta(x - \epsilon - a_{i-1}). \tag{2.14}$$

The above functionals define the functional space $\Phi_N^\dagger$ which is the dual space to Φ_N. We note that the set of $\phi_i^\dagger$'s simply gives the expansion coefficients of the Taylor series of a function $g(x)$ evaluated at the left boundary a_{i-1} of the cell C_i

$$\int_0^1 \phi_i^\dagger(n,x) g(x) dx = \lim_{\epsilon \to 0^+} \frac{1}{n!} \, g^{(n)}(a_{i-1} + \epsilon). \tag{2.15}$$

Note that to avoid ambiguities at the cell boundaries only right derivatives are considered, and Dirac-delta distributions are defined as

$$\int g(x) \delta(x - a) = \lim_{\epsilon \to 0^+} g(a + \epsilon). \tag{2.16}$$

It is straight forward to show that $\phi_i(n,x)$ and the corresponding dual form a bi-orthonormal set

$$\int_0^1 \phi_i^\dagger(n,x) \phi_j(m,x) dx = \delta(i,j) \delta(n,m). \tag{2.17}$$

We next need to identify the sort of function $g(x)$ that can be represented, finitely with respect to our basis, either exactly or up to a good approximation[7] This will certainly be the case if the expansion of $g(x)$ in each cell C_i is uniformly convergent. A sufficient condition for this is obtained by simply using Taylor's mean value theorem with Lagrange's form of remainder, and demanding that the remainder be very small. If the n^{th} derivative of $g(x)$ exists for all $x \in C_i$, then

$$g(a_{i-1} + x) = S_n(x) + R_n(x), \tag{2.18}$$

where

$$\begin{aligned} S_n(x) \ &= \ \sum_{r=0}^{n-1} \frac{x^r}{r!} \, g^{(r)}(a_{i-1}), \\ R_n(x) \ &= \ \frac{x^n}{n!} g^{(n)}(a_{i-1} + \theta x), \end{aligned} \tag{2.19}$$

and $0 \leq \theta \leq 1$. Obviously, we will obtain uniform convergence if over each cell of the partition derivatives of $g(x)$ arbitrary order are bounded. Alternatively, we can simply demand over each cell C_i, that $g(x)$ can be analytically into a complex disc centre a_{i-1}, with radius greater than the width of the cell. Let us denote either of these function spaces by Ξ.

We shall now compile a number of identities needed for the following sections which are valid for all piecewise linear Markov maps and repellers, and the fore-mentioned partitions:

[7] Note that simply demanding continuity of $g(x)$, or even analyticity is not sufficient. For example, if $g(x)$ has a pole in the complex plane close to C_i, then such an expansion is likely to diverge for some points in C_i.

1. Any inverse branch $f_\alpha^{-1}(x)$ of a map $f(x)$ has the properties:

$$\forall C_i,\, C_j : f_\alpha^{-1}(C_i) \bigcap C_j \neq \emptyset \Rightarrow f_\alpha^{-1}(C_i) \subset C_j. \tag{2.20}$$

   A corollary of the first identity is that for each cell C_i, $f(C_i)$ is a union of cells.

2. The derivatives of the inverse branches are piecewise constant over each cell,

$$\forall x \in C_i,\, \frac{d^2}{dx^2} f_\alpha^{-1}(x) = 0. \tag{2.21}$$

3. Consider a monomial of order n whose support is over the union of k adjacent cells of a partition,

$$\psi(x) = \begin{cases} (x - a_{i-1})^n, & \text{if } x \in C_i \bigcup C_{i+1} .. \bigcup C_{i+k-1} \\ 0\ , & \text{otherwise.} \end{cases} \tag{2.22}$$

   One can easily show that

$$\psi(x) = \sum_{j=i}^{i+k-1} \phi_j(n,x) + \sum_{j=i}^{i+k-1} \sum_{l=0}^{n-1} a_{jl} \phi_j(l,x), \tag{2.23}$$

   except perhaps at the points $a_i, a_{i+1}, ..a_{k-2}$, where a_{jl} are expansion coefficients. As these points are finite in number, their exclusion has no measurable effect after integration. Note that the coefficients of $\phi_j(n,x)$ in eq.(2.23) equal one.

4. Using identities (2.20) to (2.23) one can easily show that the function space Φ_n is invariant under U. That is

$$[E_n, \mathcal{U}]E_n = E_n \mathcal{U} E_n - \mathcal{U} E_n = 0, \tag{2.24}$$

   where the projector E_n acting on a function $g(x)$,

$$E_n g(x) = \sum_{l=0}^{n} \sum_{j=1}^{M} \left(\int_0^1 \phi_j^\dagger(l,y) g(y) dy \right) \phi_j(l,x) \tag{2.25}$$

   can be viewed as a generalized coarse graining operator.

Therefore, $\mathcal{U}\phi_i(l,x)$ is a linear combination of the basis elements, which implies that $\mathcal{U}$ can be represented as a time-independent transition matrix when acting on these states. More specifically,

$$\begin{aligned} \mathcal{U}\phi_i(n,x) &= \sum_\alpha \phi_i(n, f_\alpha^{-1}(x)) |f_\alpha^{-1\prime}(x)| \\ &= \sum_{l=0}^{n} \sum_{j=1}^{M} W_{lj\,ni} \phi_j(l,x). \end{aligned} \tag{2.26}$$

For expository convenience we have written the expansion coefficients $W_{lj\,ni}$ as a fourth order tensor, although they really form a matrix. A crucial property of this basis is that monomial families of order N can undergo transitions to linear combinations of monomial families of order no higher than N. As a result, if the basis elements are ordered according to

$$\begin{aligned}
&\phi_1(0,x),\phi_2(0,x),\cdots,\phi_M(0,x),\\
&\phi_1(1,x),\phi_2(1,x),\cdots,\phi_M(1,x),\\
&\phi_1(n,x),\phi_2(n,x),\cdots,\phi_M(n,x),
\end{aligned} \tag{2.27}$$

the matrix $\mathcal{W}$ has the block form

$$W = \begin{pmatrix} w(0) & . & . & . & . \\ 0 & w(1) & . & . & . \\ 0 & 0 & w(2) & . & . \\ 0 & 0 & 0 & . & . \\ 0 & 0 & 0 & 0 & . \end{pmatrix}, \tag{2.28}$$

where the $w(i)$ and the dots denote M by M matrices, and M is the number of cells in the relevant partition. We can immediately use standard results of linear algebra to explore the properties of $\mathcal{U}$ through its matrix representation W when acting on the above states. In particular, the fact that the basis functions and their corresponding dual distributions form a bi-orthonormal set (eq. (2.17)) leads to the following results.

1. The right(left) basis elements for which W is in its Jordan form give the expansion coefficients for the basis of functions (distributions) for which U restricted to $\Phi_n^\dagger \otimes \Phi_n$ is in its Jordan form.

2. This canonical basis of functions $\{v_i(x)\}$ and its dual $\{v_i^\dagger(x)\}$ form a bi-orthonormal set, that is
$$\int v^\dagger{}_i(x)v_i(x)dx \;=\; \delta_{ij}, \tag{2.29}$$

3. Any function in Ξ can be expanded first in terms of the piecewise monomial basis, and truncated at an order where the truncation error is less than any specified value. We can then safely expand the truncated function using eq.(2.29) in terms of the canonical basis, with no further error. Thus a spectral decomposition is readily obtained through a finite number of algebraic manipulations.

2.3 Eigenvalue problem of the transition matrix $\mathcal{W}$ and connection with the zeta function formalism

In section 2.2 a simple method for obtaining spectral decompositions for piecewise analytic spaces was presented. Initial densities residing in this space evolve with a time-independent matrix and the invariant density or measure (when unique) can be straight-forwardly obtained. Thus, all the statistical moments associated with long time averages for observables (for example, position x) in this function space can be easily calculated, including time correlation functions and their corresponding decay properties. It is, therefore, natural to inquire about the connection between this method and one of the most elegant methods yet developed for investigating the statistical properties of a hyperbolic dynamical systems, namely the zeta function formalism developed by Ruelle and others[95, 96, 10, 15, 9]. From a physical perspective, the formalism has been successfully applied by several authors including [38, 39, 40, 23, 7] but despite this success, the range of systems for which it is valid has not yet been fully established.

One of the purposes of this formalism is to relate the decay rates of time correlation functions of appropriate observables to the zeros of the function,

$$Z_s(z) = \det(1 - z\mathcal{U}), \tag{2.30}$$

through the zeros of the function

$$\tilde{Z}_s(z) = \prod_{k=1}^{\infty} \frac{1}{\zeta_k(z)}, \tag{2.31}$$

where

$$\zeta_k(z) = \prod_p \left(1 - \frac{z^{n_p}}{|\wedge_p|\wedge_p^{k-1}}\right)^{-1}, \tag{2.32}$$

$\prod_p, n_p$ and $\wedge_p$ denote the product over all periodic orbits, the period of the p^{th} periodic orbit and its relative stability or instability factor $f'(x_1)f'(x_2)...f'(x_p)$ respectively. $\zeta_k(z)$ is an example of a dynamical zeta function. The zeros of $Z_s(z)$ equal the reciprocals of the eigenvalues of $\mathcal{U}$ if $\mathcal{U}$ is a nuclear operator[70] of order less than or equal to $\frac{2}{3}$[8]. In the zeta function formalism one seeks to relate the zeros of $Z_s(z)$ to the zeros of $\tilde{Z}_s(z)$. For all Markov analytic maps it was believed that

$$Z_s(z) = \tilde{Z}_s(z). \tag{2.33}$$

We will show that equality above generally holds[9] only if the space of analytic functions is invariant under $\mathcal{U}$, and will derive a simple correction factor equal to

$$\frac{Z_s(z)}{\tilde{Z}_s(z)}$$

which is valid for all piecewise linear Markov maps. The generalization to all Markov analytic maps (i.e also with curvature) will be given in the next chapter.

We will see that the functions Z_s and $\tilde{Z}_s$ are indeed equal to each other for Markov analytic maps whose corresponding $\mathcal{U}$ leave the space of analytic functions invariant, which is the case when the minimal Markov partition consists of only one cell, i.e the unit interval. However, Z_s and $\tilde{Z}_s$ are generally not equal for maps possessing a multi-cell minimal

[8]We do not know if $Z_s(z)$ equals $\tilde{Z}_s(z)$ under weaker conditions. Note also that the form of $\tilde{Z}_s(z)$ is slightly different in higher dimensions.

[9]That $Z_s(z)$ does not always equal $\tilde{Z}_s(z)$ was noticed by Manning, but as far as we understand, for a different class of maps where the difference between the two functions arises from periodic boundary conditions. In that case the space of analytic functions can be invariant under $\mathcal{U}$. A simple example is the r-addic map on the circle rather than the interval, another is the Arnold cat map. Moreover, no explicit general formula for that correction factor, known as a Manning multiple, was apparently obtained.

Markov partition, where fixed points or periodic orbits form the interface between cells. In this case, a piecewise analytic function space rather than an analytic one is invariant under $\mathcal{U}$. This leads to a subtle difference in the relation of the trace of $\mathcal{U}$ to the periodic orbits of the map simply because of the difference in function space, and as a result the identification of the trace to certain partition functions[10]. In the following we will use the

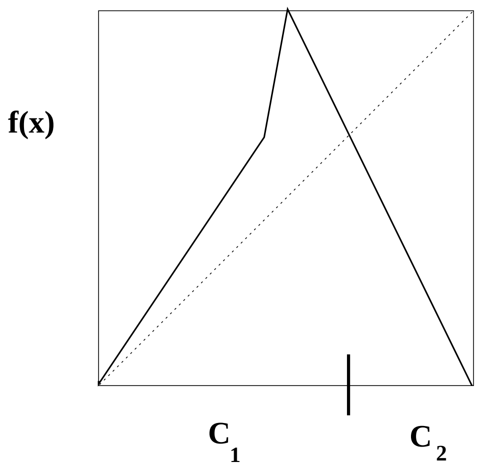

Figure 2.1: A piecewise linear Markov map, where a fixed point forms the interface between the two cells of the minimal Markov partition. Clearly the cell C_2 cannot undergo a transition to itself in one iteration via the right branch of the map.

trace formula

$$\begin{aligned} \det(1 - zT) &= \exp\left(\mathrm{Tr}\,(\ln(1 - zT)\right) \\ &= \exp(-\sum_{n=1}^{\infty} \frac{z^n}{n} \mathrm{Tr}\,(T^n)) \end{aligned} \tag{2.34}$$

valid for nuclear operators T of order zero and nonsingular matrices[70] to relate the eigenvalues of W to an expression involving $Z_s(s)$. The secular equation of W, for a piecewise monomial space of order N, reduces to

$$\det(I - z\mathcal{W}) = \prod_{k=0}^{N} \det(1 - zw(k)), \tag{2.35}$$

because of $\mathcal{W}$'s block form, as was pointed out at the end of the previous section. Let us now apply formula (2.34) to $\det(1 - zw(k)$:

$$\begin{aligned} \det(1 - zw(k)) &= \exp[\mathrm{Tr}\,(\ln(1 - zw(k))] \\ &= \exp\left(-\sum_{n=1}^{\infty} \frac{z^n}{n} \mathrm{Tr}\,(w(k)^n)\right). \end{aligned} \tag{2.36}$$

[10]Consider, the analysis by Mayer[70], page 198, with the example illustrated in fig.2.1. For simplicity, take the case $m = n = 1$. One can easily show that eq.(70) has a contribution from each of the fixed points of the map, whereas eq.(71) only has a contribution form the fixed point at the origin. Thus, eqs. (70) and (71) do not coincide. Eq. (70) is a partition function, and eq. (71) which is correctly evaluated is essentially a trace.

In calculating the trace of $w(k), \sum_i w_{ii}(k)$, where $w_{ii}(k)$ is the coefficient of transition of $\phi_i(k,x)$ to itself, we notice that the relevant terms in eq.(2.26) satisfy

$$f_\alpha^{-1}(C_i) \subset C_i. \tag{2.37}$$

It follows that

$$w_{ii}(k) = \sum_{f_\alpha^{-1}(C_i)\subset C_i} \int \phi_i^\dagger(k,x)\phi_i(k, f_\alpha^{-1}(x))|f_\alpha^{-1\prime}(x)|dx. \tag{2.38}$$

We now observe that eq.(2.37) implies that there is a fixed point x^* of $f_\alpha^{-1}(x)$ either contained in the interior of C_i, or if $f_\alpha^{-1}(x)$ is monotonic increasing and x^* coincides with one of the cell boundaries. Using Eqs. (2.20) and (2.21) we obtain a simple expression for the inverse branch,

$$\forall x \in C_i,\ f_\alpha^{-1}(x) = \frac{x}{f'(x_*)} + c, \tag{2.39}$$

where c is a constant. Therefore,

$$\phi_i(k, f_\alpha^{-1}(x))|f_\alpha^{-1\prime}(x)| = \frac{(\frac{x}{f'(x_*)} + c)^k}{|f'(x_*)|}. \tag{2.40}$$

Thus,

$$w_{ii}(k) = \sum_{x_*\in Int(C_i)} \frac{1}{f'^k(x_*)|f'(x_*)|} + \sum_{x_*\in B(C_i)} \frac{1}{f'^k(x_*)|f'(x_*)|} \tag{2.41}$$

where the first sum is over fixed points lying in the interior of the cell $(Int(C_i))$ and the second sum is over fixed points lying on the boundary of the cell $(B(C_i) = \{a_{i-1}, a_i\}$ associated with monotonic increasing branches. We may rearrange the right hand side of eq.(2.41),

$$\mathrm{Tr}\,(w(k)) = \left(\sum_{x_*} \frac{1}{f'^k(x_*)|f'(x_*)|} + \sum_{y_{*1}} \frac{1}{f'^{k+1}(y_{*1})} - \sum_{y_{*2}} \frac{1}{f'^k(y_{*2})|f'(y_{*2})|}\right), \tag{2.42}$$

where the consecutive summations are over all fixed points, and fixed points having the following properties:

1. The inverse branch having y_{*1} as a fixed point is defined on either side of y_{*1}.
2. The inverse branch having y_{*2} as a fixed point is monotonic decreasing, but is defined only to one side of y_{*2}.

One may verify eq.(2.42) through the following observations. First, the fixed points $\{y_{*2}\}$ do not contribute to the trace. Second, consider two cells

$$C_i = [a_{i-1}, y_{*1}],\ C_{i+1} = [y_{*1}, a_i],$$

where y_{*1} forms the interface. If y_{*1} is a fixed point of a monotonic increasing branch, then

$$f_\alpha^{-1}(C_i) \subset C_i \text{ and } f_\alpha^{-1}(C_{i+1}) \subset C_{i+1}.$$

Thus the fixed point will give the same contribution twice. On the other hand, if $f_\alpha^{-1}(x)$ is monotonic decreasing, then the latter transitions do not occur, and the fixed point should not contribute to the trace. One can show in a similar fashion that

$$\mathrm{Tr}\,(w(k)^n) = \left(\sum_{x_*} \frac{1}{f^{n\prime k}(x_*)|f^{n\prime}(x_*)|} + \sum_{y_{*1}} \frac{1}{f^{n\prime k+1}(y_{*1})} - \sum_{y_{*2}} \frac{1}{f^{n\prime k}(y_{*2})|f^{n\prime}(y_{*2})|}\right). \quad (2.43)$$

where the sums are now over the fixed points of $f^n(x)$. In the sequel, any type of periodic orbit will be denoted by p. In addition, class 1 periodic orbits will also be denoted by p_1, and class 2 periodic orbits will be denoted by p_2.

Let us now come back to eq.(2.36). Any periodic orbit p of period N_p will contributing to eq.(2.43) only if N_p is a divisor of n. We shall denote the set of all periodic orbits whose period N_p is a divisor of n by N_p/n. We shall adopt the argument and notation of Artuso et al[23, 7]. In general, the n^{th} order trace picks up contributions from N_p/n. Therefore

$$\mathrm{Tr}\,w(k)^n = \sum_{N_p/n} N_p t_p^{\frac{n}{N_p}} + \sum_{N_{p_1}/n} N_{p_1} \hat{t}_{p_1}^{\frac{n}{N_{p1}}} - \sum_{N_{p_2}/n} N_{p_2} t_{p_2}^{\frac{n}{N_{p2}}} \quad (2.44)$$

where

$$t_p = \frac{1}{f^{N_p\prime}(x_*)^k|f^{N_p\prime}(x_*)|}, \text{ and } \hat{t}_{\hat{p}} = \frac{1}{f^{N_{\hat{p}}\prime}(x_*)^{k+1}} \quad (2.45)$$

and x_* is a fixed point of $f^{N_p}(x_*)$. Let $r = \frac{n}{N_p}$. We can express eq.(2.36) as

$$\begin{aligned}
\det(1 - zw(k)) &= exp\left(-\sum_p\sum_{r=1}^{\infty}\frac{(z^{N_p}t_p)^r}{r} - \sum_{p_1}\sum_{r=1}^{\infty}\frac{(z^{N_{p1}}\hat{t}_{p_1})^r}{r} + \sum_{p_2}\sum_{r=1}^{\infty}\frac{(z^{N_{p2}}t_{p_2})^r}{r}\right) \\
&= exp\left(\sum_p ln(1 - z^{N_p}t_p) + \sum_{p_1} ln(1 - z^{N_{p1}}\hat{t}_{p_1}) - \sum_{p_2} ln(1 - z^{N_{p2}}t_{p_2})\right) \\
&= \prod_p (1 - z^{N_p}t_p)\prod_{p_1}(1 - z^{N_{p1}}\hat{t}_{p_1})\frac{1}{\prod_{p_2}(1 - z^{N_{p2}}t_{p_2})} \\
&= \frac{\eta_k(z)\xi_k(z)}{\zeta_k(z)},
\end{aligned} \quad (2.46)$$

where

$$\eta_k(z) = \prod_{\hat{p}}(1 - z^{N_{\hat{p}}}\hat{t}_{\hat{p}}), \quad (2.47)$$

$$\xi_k(z) = \frac{1}{\prod_{p_2}(1 - z^{N_{p2}}t_{p_2})}. \quad (2.48)$$

Thus,

$$\det(1 - z\mathcal{U}) = \prod_{k=1}^{\infty}\frac{\eta_k(z)\xi_k(z)}{\zeta_k(z)} = \tilde{Z}_s(z)\prod_{k=1}^{\infty}\eta_k(z)\xi_k(z), \quad (2.49)$$

and

$$\frac{Z_s(z)}{\tilde{Z}_s(z)} = \prod_{k=1}^{\infty}\eta_k(z)\xi_k(z). \quad (2.50)$$

Let us now make the observations: (i) the number of periodic orbits producing in $\eta_k(z)$ $\xi(z)$ are finite; and (ii) the zeros of $\eta_k(z)$ describe a decaying oscillation with period $\hat{p}$ if $\hat{t}_{\hat{p}}$ is positive, and period $2\hat{p}$ is $\hat{t}_{\hat{p}}$ is negative. If the elements of more than one periodic orbit form the interfaces between cells (which can be the case if there is more than one critical point) then the above oscillations will occur for all such periodic orbits. Again, we stress that the functions $\eta_k(z)$ and $\xi_k(z)$ do not occur in eq.(2.49) if the space of analytic functions is invariant under $\mathcal{U}$. Finally let us remark that one may identify which

$$\frac{\eta_k(z)\xi_k(z)}{\zeta_k(z)}$$

are relevant for a given set of observables. That is, if a set of observables can be expressed (exactly or up to a good approximation) as linear combinations of piecewise monomials (associated with $\mathcal{P}_{\mathcal{M}}$) of order no higher than N, only the $\frac{\eta_k(z)\xi_k(z)}{\zeta_k(z)}$ for $k \leq N$ are relevant for the corresponding time correlation functions. Thus, the nature of the link between our method and the zeta function formalism is clearly established.

2.4 Effect of refinement of the minimal Markov partition with periodic orbits

Point-like initial conditions where the associated initial uncertainty is very small, can be modeled as a highly peaked probability distributions, having support over a small local region. How do such distributions evolve? One may also be interested in the frequency that a local region is visited, or how long a highly localised distribution takes to decay, and the nature of any oscillations. Such questions cannot be easily answered in terms of a global statistical description. Indeed, in some cases the spectra associated with such local properties can be more dominant (the eigenvalues can have greater magnitude) than decay rates associated with global statistical properties. We also note that the investigation of the properties of statistical systems at different length scales has attracted much interest recently. In this section, we will try to address these questions, and in particular, investigate the spectral properties of $\mathcal{U}$ in this local context.

The studying of local statistical behavior involves the calculation of statistical moments associated with observables having support over local regions. This is not possible with analytic observables whose support is over the entire interval, because the calculation of their statistical moments entails an integration over all of phase space. Consequently, they can only describe essentially global aspects of the system. Such "global“ aspects were the subject of the last section, where we characterized the spectra of spectral decompositions associated with $\mathcal{P}_{\mathcal{M}}$. To describe local statistical behavior, we shall now use the results of section 2.2 to characterize the eigenvalues of spectral decompositions associated with refined partitions. The partitions are formed by adding to the points defining $\mathcal{P}_{\mathcal{M}}$ all the points of a finite number of periodic orbits. The periodic orbits are chosen so that the points defining the new partition $\mathcal{P}$ lie on or close to the boundaries of the local regions of interest. We shall establish the following properties:

1. There exists a countable infinity of eigenvalues of $\mathcal{U}$ associated with each periodic orbit $\{x_1, x_2, \ldots, x_p\}$.

2. Corresponding to each eigenvalue there is a unique eigenfunction which is contained in the space of monomial families associated with the partition $\mathcal{P}$.

3. The eigenvalues are

$$\begin{aligned}\{\lambda\} &= \frac{1}{\sqrt[p]{(f^{p\prime}(x_l))^{k+1}}}, \\ &= \left|\frac{1}{\sqrt[p]{(f^{p\prime}(x_l))^{k+1}}}\right| \exp(i\gamma\pi j/p),\end{aligned} \tag{2.51}$$

where

$$\gamma = \begin{cases} 1, & \text{if } (f^{p\prime}(x_l))^{k+1} < 0; \\ 2, & \text{otherwise,} \end{cases} , \tag{2.52}$$
$$k = 0, 1, 2, 3..., \; and \; j = 1, 2, 3, ...p$$

and x_l belongs to a periodic orbit of period p.

They describe a decaying oscillatory mode with period p if the argument of the p^{th} root is positive, and $2p$ if it is negative. They play no role for time correlation functions of observables that are piecewise analytic with respect to $\mathcal{P}_{\mathcal{M}}$. However, they are relevant for the statistical moments of measurable functions, where each function has the following properties. 1. It can be well approximated over each cell of $\mathcal{P}$ as a finite Taylor series. 2. It has at least one discontinuity (or discontinuity in a derivative of lower order than the order of truncation in the Taylor expansion) at or close to an element of one of the periodic orbits used to refine $\mathcal{P}_{\mathcal{M}}$.

We now proceed to the proof of the above statements.
Let $\Phi_n = \{\phi_i(n, x)\}$ denote the function space spanned by the basis of monomial families of order N associated with a $\mathcal{P}_{\mathcal{M}}$ having M cells. For each point of the periodic orbit x_i define the set of monomials having support $[x_i, a_{i*}]$ as

$$\psi_i(k, x) = \begin{cases} (x - x_i)^k, & \text{if } x \in [x_i, a_{i*}]; \\ 0, & \text{otherwise;} \end{cases} \tag{2.53}$$

where C_{i_*} denotes a cell of $\mathcal{P}_{\mathcal{M}}$ such that $x_i \in C_{i*} = [a_{i*-1}, a_{i*}]$ and $k = 0, 1, 2, .., N$. We extend the space Φ_n to a space $\tilde{\Phi}_n$ by adding the monomials (eq.(2.53)) as new basis functions to the set spanning Φ_n. The new additional dual basis distributions are

$$\begin{aligned}&\psi_i^{\dagger}(n, x) \\ &= \frac{(-1)^n}{n!}\frac{d^n}{dx^n}(\delta(x - x_i) - \delta(x - a_{i*-1})).\end{aligned} \tag{2.54}$$

One can readily verify that the extended basis and its dual form a bi-orthonormal set. By eqs.(2.20) to (2.23) $\tilde{\Phi}_n$ is an invariant function space of $\mathcal{U}$. Therefore, denoting for convenience the new basis by $\{\tilde{\phi}_i(n, x)\}$ we have, in analogy to eq.(2.26),

$$\mathcal{U}\tilde{\phi}_i(n, x)$$

$$
\begin{aligned}
&= \sum_{\alpha} \tilde{\phi}_i \left(n, f_\alpha^{-1}(x)\right) |{f^{-1}}'_\alpha(x)| \\
&= \sum_{l=0}^{n} \sum_{j=1}^{M+1} \breve{W}_{lj\,ni} \tilde{\phi}_j(l,x),
\end{aligned}
\tag{2.55}
$$

where $\breve{W}_{lj\,ni}$ is the matrix representation of $\mathcal{U}$ in this basis. A monomial $\psi_i(n,x)$ of order n having a discontinuity at x_i, will have a discontinuity at x_{i+1} after one iteration, but not at any other points of the periodic orbit. Furthermore, $\mathcal{U}\psi_i(n,x)$ is a linear combination of monomials, including $\psi_{i+1}(k,x)$, where $k = 0,1,2\ldots,n$. Discontinuities at x_{i+1} in the sum eq. (2.55) only occur for the term whose corresponding inverse branch $f_\alpha^{-1}(x)$, maps x_{i+1} to x_i. Using this fact together with eqs. (2.20) to (2.23) one can easily show that

$$
\begin{aligned}
&\psi_i(n, {f^{-1}}_\alpha(x))|{f^{-1}}'_\alpha(x)| \\
&= \frac{\psi_{i+1}(n,x)}{f'(x_i)^{n+1}} + \Upsilon,
\end{aligned}
\tag{2.56}
$$

where Υ consists of terms which do not contribute to the transition to $\psi_{i+1}(n,x)$. It follows that,

$$
\begin{aligned}
&\int \psi_j^\dagger(n,x)\mathcal{U}\psi_i(n,x)dx \\
&= \int \psi_j^\dagger(n,x)\psi_i(n, f_\alpha^{-1}(x))|f_\alpha^{-1}(x)|dx \\
&= \int \psi_j^\dagger(n,x)\frac{\psi_{i+1}(n,x)}{f'(x_i)^{n+1}}dx \\
&= \frac{\delta(j,i+1)}{f'(x_i)^{n+1}}.
\end{aligned}
\tag{2.57}
$$

Consider the following arrangement of the basis functions for $k = 0,1,2,\ldots,n$:

$$
\begin{aligned}
&\phi_1(k,x), \phi_2(k,x), \ldots, \phi_m(k,x), \\
&\psi_1(k,x), \psi_2(k,x), \ldots, \psi_p(k,x),
\end{aligned}
\tag{2.58}
$$

where, for each value of k, the basis functions associated $\mathcal{P}_\mathcal{M}$ occur first, followed by the basis functions associated with the periodic orbit. Then the n^{th} order block of the matrix representation $\breve{W}$ of $\mathcal{U}$ for this basis has the schematic form

$$
\breve{\mathcal{W}} = \begin{pmatrix} A(n) & B(n) \\ 0 & C(n) \end{pmatrix}.
\tag{2.59}
$$

$A(n)$ is a M by M matrix giving the transition coefficients of elements of $\{\phi_i(k,x)\}$ going to elements of $\{\phi_j(k,x)\}$. $B(n)$ is a p by M matrix giving the transition of elements of $\{\psi_i(k,x)\}$ going to elements of $\{\phi_j(k,x)\}$. $C(n)$ is a p by p matrix giving the transition coefficients of elements of $\{\psi_i(k,x)\}$ going to elements of $\{\psi_j(k,x)\}$. If the periodic orbit is a fixed point x_* (i.e. $p=1$), then $C(n)$ is a 1 by 1 matrix, so that $C(n) = f'^{-(n+1)}(x_*)$.

For any orbit of higher period, $C(n)$ has the form

$$C(n) = \begin{pmatrix} 0 & 0 & 0 & 0 & \kappa(x_p) \\ \kappa(x_1) & 0 & 0 & 0 & 0 \\ 0 & \kappa(x_2) & 0 & 0 & 0 \\ \vdots & \vdots & 0 & 0 & 0 \\ 0 & 0 & 0 & \kappa(x_{p-1}) & 0 \end{pmatrix}, \tag{2.60}$$

where $\kappa(x) = f'^{-(n+1)}(x)$, and, as before, monomial families of order n cannot undergo transitions to higher orders. Therefore, the secular equation reduces to

$$\begin{aligned} |\breve{\mathcal{W}} - \lambda I| &= \prod_{k=0}^{k=N} |w(k) - \lambda I| \\ &= \prod_{k=0}^{k=N} |A(k) - \lambda I| \, |C(k) - \lambda I|, \end{aligned} \tag{2.61}$$

so the eigenvalues arising from the refinements are the eigenvalues of $C(k)$. These are, precisely, the ones listed in eq. (2.51). In fact, there are strong analytical reasons to believe that the results of this section can be generalized to everywhere expanding piecewise analytic maps which do not have to possess a minimal Markov partition[64].

2.5 Examples

We shall now illustrate the results of the preceding sections on simple chaotic maps. Let us first consider the tent map

$$f(x) = \begin{cases} mx, & \text{if } 0 \le x \le 0.5; \\ m(1-x), & \text{otherwise} \end{cases}, \tag{2.62}$$

for $m \ge 2$. If $m > 2$ then the map is a repeller, so that the support of the invariant measure is a cantor set [34]. However, the only effect in the evolution of initialy smooth densities [104] is that at each iteration their norm can decrease if part of the density leaves the interval $\mathbf{I} = [0, 1]$. That is, within the interval the evolving density never has a fractal support. The Frobenius-Perron operator takes the form

$$\rho_{n+1}(x) = \frac{1}{m}\left(\rho_n(\frac{x}{m}) + \rho_n(1 - \frac{x}{m})\right). \tag{2.63}$$

We are only concerned with the evolution of densities (or portions thereof) while they remain in the interval $[0, 1]$. The effective minimal Markov partition coincides with the unit interval itself. Following section 2.2 a bi-orthonormal set is provided by the monomials with support the unit interval, i.e,

$$1,\ x,\ x^2,\ x^3, \ldots x^n, \ldots, \tag{2.64}$$

and their corresponding duals

$$
\begin{aligned}
&\delta(x),\ -\frac{d}{dx}\delta(x),\ \frac{(-1)^2}{2!}\frac{d^2}{dx^2}\delta(x),\\
&\frac{(-1)^3}{3!}\frac{d^3}{dx^3}\delta(x),\ldots,\frac{(-1)^n}{n!}\frac{d^n}{dx^n}\delta(x),\ldots
\end{aligned}
\tag{2.65}
$$

For this basis it is easy to see that the transition matrix is upper triangular, with diagonal elements

$$
\frac{2}{m},\ 0,\ \frac{2}{m^3},\ 0,\ \frac{2}{m^5},\ldots \tag{2.66}
$$

The diagonal terms are just the eigenvalues, and their reciprocals equal the poles of the zeta function $Z(z)$ defined in section 2.3. When $m > 2$, the eigenvalue $\frac{2}{m}$ gives the escape rate out of the unit interval for an initialy uniform distribution. The zero eigenvalues show that monomials of odd order cannot undergo transitions to themselves in one iteration, which is due to the symmetry of the map about $\frac{1}{2}$. Due to a certain similarity between these repellers, and the r-addic map[93, 48, 38, 4], one can easily show that the eigenfunctions of $\mathcal{U}$ restricted to the space of analytic functions are the Bernoulli polynomials

$$
B_n(x),\ n = 0, 1, 2, \cdots. \tag{2.67}
$$

As a result their corresponding eigendistributions/duals are just

$$
\begin{aligned}
D_0(x) &= \theta(x)\theta(1-x)\\
D_n(x) &= \frac{(-1)^{n-1}}{n!}\left(\delta^{(n-1)}(x-1) - \delta^{(n-1)}(x)\right),
\end{aligned}
\tag{2.68}
$$

where $\theta(x)$ is the Heavy-side step function. It will be more convenient to not use the Bernoulli polynomials in the following extension of the function space.

Let us now refine the minimal partition with the addition of the fixed point $x_* = \frac{m}{1+m}$, and extend the basis with monomials having as support $[x_*, 1]$, i.e.

$$
\begin{aligned}
&\chi_{[x_*,1]}(x),\ (x-x_*)\chi_{[x_*,1]}(x),\ldots\\
&\ldots,(x-x_*)^n\chi_{[x_*,1]}(x)\ldots,
\end{aligned}
\tag{2.69}
$$

the new dual basis elements being

$$
\tilde{\delta}(x),\ -\frac{d}{dx}\tilde{\delta}(x),\ldots,(-1)^n\frac{d^n}{dx^n}\tilde{\delta}(x),\ldots, \tag{2.70}
$$

where

$$
\tilde{\delta}(x) = \delta(x-x_*) - \delta(x). \tag{2.71}
$$

One can readily show that the extended basis and its dual form a bi-orthonormal set. Applying Eq.(2.51) one finds

$$
\begin{aligned}
\{\lambda\} &= \frac{1}{\sqrt[p]{(f^{p\prime}(x_*))^{k+1}}},\\
&= \frac{1}{m}\exp(i\pi\gamma j/p),
\end{aligned}
\tag{2.72}
$$

where $k = 0, 1, 2, 3, \ldots, j = 1, 2, 3, \ldots, p$ and

$$\gamma = \begin{cases} 1, & \text{if } (f^{p\prime}(x_*))^{k+1} < 0; \\ 2, & \text{otherwise.} \end{cases} \tag{2.73}$$

The first few eigenvalues generated by the above refinement are then $\frac{-1}{m}, \frac{1}{m^2}, \frac{-1}{m^3}, \ldots$ and the overall transition matrix has the form of eq. (2.28),

$$W_{ki} = \begin{pmatrix} 2m^{-1} & m^{-1} & m^{-1} & m^{-1} & m^{-1} & m^{-1} & \cdots \\ 0 & -m^{-1} & 0 & -m^{-1} & 0 & -m^{-1} & \cdots \\ 0 & 0 & 0 & -m^{-2} & -2m^{-2} & -2m^{-2} & \cdots \\ 0 & 0 & 0 & m^{-2} & 0 & 2m^{-2} & \cdots \\ 0 & 0 & 0 & 0 & 2m^{-3} & m^{-3} & \cdots \\ 0 & 0 & 0 & 0 & 0 & m^{-3} & \cdots \\ \vdots & \vdots & \vdots & \vdots & \vdots & 0 & \cdots \end{pmatrix}, \tag{2.74}$$

while each successive 2 by 2 block along the diagonal has the form of eq.(2.59). Actually for this map W is diagonalizable so that the right(left) eigenvectors of W define eigenfunctions (dual eigendistributions) of the Frobenius-Perron operator $\mathcal{U}$, which can be normalized to form a bi-orthonormal set. More generally W with respect to its canonical basis reduces to its Jordan form. The eigenfunctions corresponding to the first four eigenvalues $(\frac{2}{m}, \frac{-1}{m}, 0, \frac{1}{m^2})$ are:

$$\begin{aligned} v_1(x) = {} & \chi_{[0,1]}(x); \\ v_2(x) = {} & \frac{-\chi_{[0,1]}(x)}{3} + \chi_{[x_*,1]}(x); \\ v_3(x) = {} & \chi_{[0,1]}(x) - 2x\chi_{[0,1]}(x); \\ v_4(x) = {} & \frac{m^2\chi_{0,1]}(x)}{(2m-1)(1+m)} - \frac{m\chi_{[x_*,1]}}{1+m} \\ & -x\chi_[0,1](x) + (x - x_*)\chi_{[x_*,1]}(x). \end{aligned} \tag{2.75}$$

The dual eigen-distributions can be expanded in terms of the dual basis. For the eigendistributions corresponding to the eigenfunctions above, the first four terms in the expansion are:

$$\begin{aligned} v_1^\dagger(x) = {} & \delta(x) + \frac{1}{3}\tilde{\delta}(x) - \frac{1}{2}\frac{d}{dx}\delta(x) \\ & -\frac{2(3-m)}{3(2m-1)}\frac{d}{dx}\tilde{\delta}(x) + \ldots; \\ v_2^\dagger(x) = {} & \tilde{\delta}(x) + \frac{m}{m+1}\frac{d}{dx}\tilde{\delta}(x) + \ldots; \\ v_3^\dagger(x) = {} & \frac{1}{2}\left(\frac{d}{dx}\delta(x) + \frac{d}{dx}\tilde{\delta}(x)\right) + \ldots; \\ v_4^\dagger(x) = {} & -\frac{d}{dx}\tilde{\delta}(x) + \ldots\,, \end{aligned} \tag{2.76}$$

where $\tilde{\delta}(x)$ is the same as before. Let $g(x)$ be any function which can be well approximated with the first two terms of a Taylor series (see eq. (2.18)) over each cell of the partition. $g(x)$ can be expanded in terms of the eigenfunctions of eq. 2.75,

$$g(x) \cong \sum_{i=0}^{4} \left(\int_0^1 v_i^{\dagger}(y) g(y) dy \right) v_i(x). \tag{2.77}$$

It is simple to extend this treatment to higher orders and to other periodic orbits.

For values of m less than two the tent map no longer sends the unit interval onto itself. However for $m > \sqrt{2}$ the interval $[f(f(\frac{1}{2})), f(\frac{1}{2})] = [a, b]$ is mapped onto itself, so that our results will be directly applicable if the critical point is mapped onto a periodic orbit or fixed point. A slope value for which the analysis is particularly simple is $m = \frac{1+\sqrt{5}}{2}$. The minimal Markov partition is $\{a, \frac{1}{2}, b\}$. Again we can refine the partition with the fixed point x_*, and in addition consider the dynamics in the interval $[0, a]$, so that the new Markov partition is $\{0, a, \frac{1}{2}, x_*, b, \}$. The analysis proceeds as in the last example. The eigenvalues associated with the decay out of the region $[0, a]$ are simply

$$\{m^{-1}, m^{-2}, m^{-3}, ...\}. \tag{2.78}$$

The eigenvalues associated with the fixed point are

$$\frac{-1}{m}, \frac{1}{m^2}, \frac{-1}{m^3}, ... \tag{2.79}$$

The eigenvalues corresponding to the minimal Markov partition are

$$1, \frac{-1}{m^3}, \frac{-1}{m^3} e^{1.0944 i\pi}, \frac{-1}{m^3} e^{-1.0944 i\pi}, ... \tag{2.80}$$

2.6 Extensions to non-analytic basis functions

So far we have described the properties of $\mathcal{U}$ acting on spaces of piecewise analytic functions associated with the minimal Markov partitions and its refinements. We have seen explicitly that the choice of partition and corresponding function space determines the possible spectra, and thus characteristic times that can be observed in time correlation functions. Since there is no reason that the initial density or observable should always be analytic, it is natural to inquire about the spectral properties of U when acting on non-piecewise analytic functions.

Consider first a simple generalization of a monomial, x raised to a non-integer power α, $\psi(x) = x^{\alpha}$, and the tent map with $m \geq 2$. We have then

$$\mathcal{U}\psi(x) = \frac{(\frac{x}{m})^{\alpha}}{m} + \frac{(1 - \frac{x}{m})^{\alpha}}{m}. \tag{2.81}$$

The first term is proportional to $\psi(x)$, while the second is expandable as an infinite power series. No exact representation of $\mathcal{U}$ in terms of a finite matrix can now be expected. However, since $m > 1$ and $x \in [0, 1]$, we can still apply the method of section 2.2 since the expansion converges sufficiently, and calculate the new eigenfunction to any desired accuracy. The new eigenvalue is clearly $m^{\alpha+1}$, which has the same form as the eigenvalues associated with monomials having the unit interval as support. For $-1 < \alpha < 0$, $\psi(x)$ is divergent at zero but nevertheless integrable. We can choose α so that the corresponding eigenvalue lies anywhere between zero and one. Indeed, if α is complex with its real part greater than -1 $\psi(x)$ remains integrable (with integrable singularities at zero if $\mathrm{Re}(\alpha) < 0$) and eigenvalues can be obtained anywhere in the unit circle, implying that the corresponding characteristic times can be arbitrarily long. We can extend the basis to include the function $(1-x)^\alpha$, finding that its corresponding eigenvalue is zero.

Let us now consider the problem of general piecewise linear Markov maps. We need to define functions that are a generalization of non-integer powers of x, and then show how a finite invariant functions space containing them can be constructed. Therefore, let

$$\tilde{\psi}_i(\alpha,\eta,c,x) = \begin{cases} (x-a_{i-1}+c)^\alpha, & \text{if } \eta = \mathrm{L} \text{ and } x \in C_i; \\ (a_i - x + c)^\alpha, & \text{if } \eta = R \text{ and } x \in C_i; \\ 0, & \text{otherwise,} \end{cases} , \tag{2.82}$$

where $c \geq 0$, and the index η, has two possible values L and R, to denote each of the non-zero functions of eq.(2.82). In the sequel we shall refer to these functions as generalized piecewise monomials ($G.P.M.$) if $c = 0$, and generalized piecewise polynomials ($G.P.P.$) if $c \neq 0$. We shall show that no matter how many times $\mathcal{U}$ is applied to a $G.P.M.$ with exponent α, the resulting density can be expanded in terms of a finite number of $G.P.M.$'s, $G.P.P.$'s and piecewise monomials. The key element of the proof is that if $\mathcal{U}$ is applied to a $G.P.P.$, the result is a linear combination of $G.P.P.$'s having the same exponent α, but a larger c. Let $m_{\beta,j}$ denote the value of $|f'(f_\beta^{-1}(x))|$, $x \in C_j$. If the functions in eq. (2.51) are evolved one time step one finds

$$\tilde{\psi}_j(\alpha,\eta,c,f_\beta^{-1}(x))|f_\beta^{-1\prime}(x)| = \frac{\tilde{\psi}_k(\alpha,\eta',\hat{c},x,)}{m_{\beta,k}^{\alpha+1}}, \tag{2.83}$$

for

$$x \in C_k \textit{ and } f_\beta^{-1}(C_k) \bigcap C_j \neq \emptyset,$$

where

$$\begin{aligned} \hat{c} &\geq c\, m_{\beta,k} \begin{cases} \text{if} & a_{j-1} \in f_\beta^{-1}(C_k) \\ \text{or} & a_j \in f_\beta^{-1}(C_k) \end{cases} , \\ \hat{c} &> c\, m_{\beta,k} \ \textit{otherwise}, \end{aligned} \tag{2.84}$$

as easily proved using relations (2.20) and (2.21). If $\hat{c} > a_k - a_{k-1}$, $\tilde{\psi}_j(\alpha,\hat{c},x)$ can be expressed as a uniformly convergent power series in x, for all $x \in C_j$. Moreover, if $c \neq 0$, $\mathcal{U}^n\tilde{\psi}_j(\alpha,c,x)$ can be expanded in a similar fashion after a finite number of iterations since $\hat{c}$ is growing exponentially quickly. In fact, after a maximum of N_{max} iterations $\hat{c}$ is either zero or greater than the width of the largest cell. N_{max} is the smallest integer greater than

$$\frac{\log(\frac{\Delta_1 m_1}{\Delta_2})}{\log(m_2)}, \tag{2.85}$$

where Δ_1, Δ_2, m_1, m_2 denote the width of the largest and smallest cells, the maximum slope, and the minimum slope respectively. This expression is obtained by noting in eq.(2.82) that either $c = 0$, or $c > \frac{\Delta_2}{m_2}$, and then exploiting eq.(2.84). Therefore if an initial density is a given $G.P.M.$, in the subsequent evolution it can be expressed as a linear combination of piecewise monomials, a finite number $G.P.M.$'s and $G.P.P.$'s (where the number of different values of c is finite). Thus, an invariant function space can be constructed having the above functions as a basis. Only certain transitions between the basis functions are possible, as indicated in the following table:

	$G.P.M.$	$G.P.P.$	$P.M.$
$G.P.M.$	yes (a)	no	no
$G.P.P.$	yes (b)	yes (d)	no
$P.M.$	yes (c)	yes (e)	yes (f)

, (2.86)

where $P.M.$ denotes piecewise monomials. Thus, the matrix W generating the evolution of the states has the schematic form,

$$\mathcal{W} = \begin{pmatrix} A & 0 & 0 \\ B & D & 0 \\ C & E & F \end{pmatrix}, \tag{2.87}$$

where the matrix blocks A, B, C, D, E, F correspond to transitions (a), to (f) listed in table (2.86), and the eigenvalues of W are the eigenvalues of A, D and F respectively. The eigenvalues of F are just the eigenvalues of U acting on the space of piecewise monomial functions. All the eigenvalues of D are zero, because a $G.P.P.$ as it evolves can never undergo a transition to itself (see eq.(2.84)). The eigenvalues of A when $\mathcal{P}$ is the minimal Markov partition are difficult to characterize for general piecewise linear Markov maps. However, if $\mathcal{P}$ is a refined partition of the type considered in section 2.4, the eigenvalues associated with periodic orbits can be easily calculated. The derivation is very similar to that of section 2.4, except that for every exponent α there are two $G.P.M.$'s,

$$(x_l - x)^\alpha \chi_{[a_{i*-1}, x_l]}(x)$$

and

$$(x - x_l)^\alpha \chi_{[x_l, a_{i*}]}(x),$$

corresponding to each point of the periodic orbit, whereas in section 2.4 there is only one piecewise monomial for every integer exponent k [11]. One can readily show that the corresponding eigenvalues are solution of the secular equations

$$\begin{aligned} \lambda^p - \frac{1}{|f^{p\prime}(x_l)|^{(\alpha+1)}} &= 0, \; \textit{if } f^{p\prime}(x_l) > 0, \\ \lambda^{2p} - \frac{1}{|f^{p\prime}(x_l)|^{2(\alpha+1)}} &= 0, \; \textit{if } f^{p\prime}(x_l) < 0, \end{aligned} \tag{2.88}$$

where x_l is any element of the periodic orbit. Therefore the eigenvalues are

$$\frac{1}{|f^{p\prime}(x_l)|^{\frac{\alpha+1}{p}}} \exp\left(\frac{2\pi j}{p}\right), \tag{2.89}$$

[11] The definition of a_{i*} was given directly after eq.(2.53)

if $f^{p\prime}(x_l) > 0$ where $j = 0, 1, 2, \cdots, p-1$, and

$$\frac{1}{|f^{p\prime}(x_l)|^{\frac{\alpha+1}{2p}}} \exp\left(\frac{\pi j}{p}\right), \tag{2.90}$$

if $f^{p\prime}(x_l) < 0$ where $j = 0, 1, 2, \ldots, p-1, p, p+1, \ldots 2p-1$. The eigenmodes describe a periodic oscillatory decay if the imaginary part of α is given by

$$\alpha_I = \frac{g\ 2\pi}{\log(|f^{p\prime}(x_l)|)}, \tag{2.91}$$

where g is any fraction, and an aperiodic oscillatory decay otherwise. Again, if the real part of α, α_R is close to -1, then the eigenvalues decay arbitrarily slowly. Of course, as observables are normally real valued, when α is complex the basis eq. (2.82) ($c = 0$) needs to be extended for its complex conjugate α^*. In this case the observables or initial densities of interest are typically of the form

$$\begin{aligned} &\tilde{\psi}_i(\alpha, L, 0, x) + \tilde{\psi}_i(\alpha*, L, 0, x) \\ &= 2(x - a_{i-1})^{\alpha_R} \cos(\alpha_I \log(x - a_{i-1}))\chi_i(x). \end{aligned} \tag{2.92}$$

A striking property of this type of function is that it oscillates infinitely quickly as x approaches a_{i-1} if α_I is non-zero.

Let us illustrate the latter results with the tent map, choosing the partition $\{0, x_*, 1\}$, so

$$a_0 = 0,\ a_1 = x_* = \frac{m}{m+1},\ a_2 = 1 \tag{2.93}$$

and

$$\begin{aligned} \psi_1(\alpha, L, 0, x) &= x^\alpha \chi_{[0,x_*]}(x), \\ \psi_1(\alpha, R, 0, x) &= (x_* - x)^\alpha \chi_{[0,x_*]}(x), \\ \psi_2(\alpha, L, 0, x) &= (x - x_*)^\alpha \chi_{[x_*,1]}(x), \\ \psi_2(\alpha, R, 0, x) &= (1 - x)^\alpha \chi_{[x_*,1]}(x). \end{aligned} \tag{2.94}$$

Evolving each of these functions once we obtain

$$\begin{aligned} &\mathcal{U}\psi_1(\alpha, L, 0, x) = \frac{(\frac{x}{m})^\alpha}{m} + \frac{(1 - \frac{x}{m})^\alpha}{m}, \\ &\mathcal{U}\psi_1(\alpha, R, 0, x) \\ &= \frac{(x_* - \frac{x}{m})^\alpha}{m} + \frac{(\frac{x - x_*}{m})^\alpha}{m}\chi_{[x_*,1]}(x), \\ &\mathcal{U}\psi_2(\alpha, L, 0, x) = \frac{(\frac{x_* - x}{m})^\alpha}{m}\chi_{[0,x_*]}(x), \\ &\mathcal{U}\psi_2(\alpha, R, 0, x) = \frac{(\frac{x}{m})^\alpha}{m}\chi_{[0,x_*]}(x). \end{aligned} \tag{2.95}$$

The right hand side of each of the last four equations can be written as linear combinations of the functions eq. (2.94) and the monomials

$$x^k \chi_{[0,x_*]}(x),\ (x - x_*)^k \chi_{[x_*,1]}(x), \tag{2.96}$$

where $k = 0, 1, 2, \ldots$ Again we can find a value of k such that the monomial expansions have converged sufficiently so that truncation produces a negligible error. Thus, we can find a finite dimensional function space including the generalized piecewise monomials (eqn. (2.94)) that up to an arbitrary approximation is invariant under $\mathcal{U}$. The new eigenvalues corresponding to the fixed point are

$$\lambda_{\pm} = \pm \frac{1}{|f'(x_*)|^{\alpha+1}}. \tag{2.97}$$

2.7 Conclusion

Spectral decompositions of the Frobenius-Perron operator have been obtained for all piecewise-linear Markov maps and associated repeller-like maps. This was achieved by restricting the operator to an invariant space spanned by a piecewise monomial basis associated with any Markov partition $\mathcal{P}$ of the following class: the minimal Markov partition, its self refinements, and refinements made with the addition of the elements of a finite number of periodic orbits. This representation is relevant for all initial densities or measurable functions that , over each cell of a $\mathcal{P}$, can be expressed (or suitably approximated) as a finite Taylor series. The main results are:

1. The spectra and right eigenfunctions for the zeroth order monomial projection correspond to those obtained in earlier work using a Markov coarse graining projection [79, 21, 78, 81, 63], [80].

2. The eigenvalues can be grouped into sets (eq.(2.46), each corresponding to a piecewise monomial space of a given order.

3. Right and left eigenfunctions or eigen-distributions associated with periodic orbits have been constructed, and a simple general formula for their spectra (eq.(2.51)) has been given. This construction enables local behavior to be predicted, in particular the characteristic times of time correlation functions, which generally exhibit a periodic oscillatory decay.

4. The decay rates associated with observables that are generalized piecewise polynomials (powers of x raised to a fractional or to a complex exponent) have been considered (eq.(2.82)). Eigenvalues (eq.(2.89) and eq.(2.90)) and methods for obtaining eigenfunctions have been given. Exponents can be chosen so that the corresponding spectra lie anywhere in the unit circle, thus arbitrarily slowly decaying eigenstates can be constructed that are highly localized about the periodic orbits.

Our results confirm further the conclusion of recent work [31, 4] that the spectra of the Frobenius-Perron operator, and thus the possible measurable characteristic times for chaotic maps, depend critically on the function space under consideration. More importantly they show how invariant function spaces can be constructed in a systematic and efficient manner according to the set of observables that are of immediate interest. In the next chapter, we will show how these results can be generalized to all Markov analytic maps and equivalent repellers. This will require us to use Chebyshev polynomials, which are far more powerful than monomials, both analytically and numerically.

Chapter 3

Markov Analytic Maps

3.1 Introduction

The chaotic behaviour of Markov analytic maps can be surprisingly intricate. This class of one dimensional dynamical systems includes at one extreme monotone Bernoulli and tent maps, and at another almost intermittent maps, where periods of slow evolution are followed by explosive bursts of activity. Their common features are that they are eventually everywhere expanding, and there exist piecewise analytic functions spaces $\mathcal{F}$ invariant under the corresponding Frobenius-Perron operator $\mathcal{U}$. As a consequence, spectra of $\mathcal{U}$ restricted to $\mathcal{F}$ is discrete. As we shall see later, aspects of their statistical behaviour, and techniques and proofs developed here to obtain matrix representations of $\mathcal{U}$, can be generalized to the physically important class of unimodal maps, as well as to two-dimensional conservative maps such as Anosov automorphisms, and hyperbolic non-Markov maps. These techniques can also be used to study local statistical behaviour, including the evolution of probability densities describing almost point-like initial conditions.

Hitherto, methods of performing the latter calculations have only been developed case by case, by explicitly or implicitly choosing a basis which is both complete in $\mathcal{F}$ and with respect to which the matrix representation W_{ji} of $\mathcal{U}$ is highly convergent[98, 70, 95, 96]. With the exception of the techniques to be developed in the present chapter, no general constructive method exists which is applicable to all Markov analytic maps. Thus, **here maps can have curvature** unlike the previous chapter, and so piecewise polynomial function spaces will not generally be invariant under $\mathcal{U}$. Indeed, the inverse branches of maps can even have singularities close to the real axis, which obviously complicates the choice of basis for representations of $\mathcal{U}$. Moreover, from a practical point of view, representations should be readily obtained numerically, and errors induced by truncation of the representation should be well controlled. This will allow one, for example, to explore the statistical properties of a variety of one parameter families of maps as the corresponding control parameter is varied. With these motivations, let us now outline the chapter.

- In section 3.2 we consider systems whose Frobenius-Perron operator leaves the space of analytic functions invariant. We show explicitly that the choice of polynomial basis can have a dramatic effect on the the convergence of the matrix representation. In particular, for certain systems a monomial basis leads to a divergent, and therefore meaningless representation.

- In section 3.3 the issue of basis dependent convergence for the latter maps is considered from the perspective of Chebyshev polynomials[18]. We relate this to the geometrical properties in the complex plane[92, 25] of such maps and the basis. In particular, we prove that the corresponding matrix representations converge exponentially quickly. This is of great importance as Chebyshev polynomials are ideal for rapid numerical computations[88] because they satisfy a discrete orthogonality relation as well as an integral one, and a finite Chebyshev approximation (e.g order N) of any continuous function on a bounded interval is closely related to the corresponding minimax polynomial (the best polynomial approximation of order N to that function).

- In section 3.4 the previous result is generalized by showing how basis sets of orthogonal polynomials tailored to any Markov map can be constructed through a simple algorithm. This will also allow us to consider local statistical properties and the evolution of highly localized initial densities.

- In section 3.5 we show how the eigenfunctions and spectra of $\mathcal{U}$ acting on invariant piecewise analytic function spaces can be calculated through appropriate matrix representations. If piecewise polynomial spaces are invariant under $\mathcal{U}$, then the corresponding eigenfunctions and their spectra can be exactly determined by solving for the eigenvectors and eigenvalues of a finite dimensional matrix. More generally the representation must be truncated, producing approximate eigenfunctions and eigenvalues. However the error in the dominant eigenfunctions and eigenvalues decreases at least exponentially with the order of truncation. The neglected eigenvalues are in magnitude of the order of the error. Thus, we may obtain a spectral decomposition of $\mathcal{U}$ with arbitrary accuracy.

- In section 3.6 we show that when a finite representation is used for the evolution of probability densities, or the calculation of time correlation functions, the truncation error as a function of time can be well controlled.

- In section 3.7 we relate the spectra of $\mathcal{U}$ acting on the space of functions piecewise analytic over the minimal Markov partition to the dynamical zeta functions. In particular, we find that if for a system, the space of analytic functions is not invariant under $\mathcal{U}$ then the zeros of the dynamical zeta functions cannot be expected to give all the decay rates of time correlation functions of analytical observables. This is due to a subtle counting problem overlooked by several authors (including ourselves !). Fortunately, for one dimensional Markov analytic maps, the correction to the dynamical zeta function is straight forward, and is of the form of an extra factor, generally a rational function.

- In section 3.8 we develop the description of local statistical properties through the use of finite numbers of periodic orbits. In particular we show that the formula for the spectra associated with local behaviour derived in chapter 2 for piecewise linear maps is also valid for all Markov analytic maps. The spectra given by this formula for periodic orbits that are elements of the minimal Markov partition are directly related to correction factor of the dynamical zeta function. The section is completed with examples where we demonstrate role of these spectra in the time correlation functions of observables having local support.

3.2 Basis-dependent convergence of matrix representations

3.2.1 Preliminaries

Consider a one-dimensional map on the interval $\mathcal{I} = [-1, 1]$,

$$x_{n+1} = f(x_n), \tag{3.1}$$

with the properties that the domain of each inverse branch ${f_\alpha}^{-1}(x)$ is $\mathcal{I}$, and has an extension $g_\alpha(z)$ into a complex domain $D \supset \mathcal{I}$ where

$$\forall z \in D,\ g_\alpha(z) \text{ is analytic;} \tag{3.2}$$

and

$$\forall z \in D,\ |\frac{d}{dz} g_\alpha(z)| \leq \Lambda. \tag{3.3}$$

We are interested in systems which are hyperbolic ($\Lambda < 1$) or eventually hyperbolic. If the map is only eventually hyperbolic then $\Lambda > 1$, but there exists a τ such that

$$\forall t \geq \tau,\ |\frac{d}{dx} f^t(x)| > 1, \tag{3.4}$$

so that

$$\forall t \geq \tau,\ \forall z \in \mathcal{D},\ |\frac{d}{dz} {g^t}_\alpha(z)| \leq \Lambda_t < 1, \tag{3.5}$$

where ${g^t}_\alpha(z)$ is the complex extension of the inverse branch of the t^{th} iterate of the map.

As we have seen in the preceeding chapters, any probability density $\rho_n(x)$ at time n, evolves according to the the Frobenius-Perron operator $\mathcal{U}$,

$$\begin{aligned} \rho_{n+1}(x) = \mathcal{U}\rho_n(x) &= \int_0^1 \delta(x - f(y))\rho_n(y)dy \\ &= \sum_\alpha \rho_n(f_\alpha^{-1}(x))|\frac{d}{dx} f_\alpha^{-1}(x)| \qquad (3.6) \\ &= \sum_\alpha \mathcal{U}_\alpha \rho_n(x) \qquad (3.7) \end{aligned}$$

In the present case, the inverse branches are defined for all $x \in \mathcal{I}$. As any analytic function can be locally expanded as a uniformly convergent Taylor series, let's see under what conditions a monomial basis can be used to obtain a matrix representation of $\mathcal{U}$, that is, when is the expansion

$$\begin{aligned} \mathcal{U}x^n &= \sum_\alpha \mathcal{U}_\alpha x^n && (3.8)\\ &= \sum_\alpha \sum_{m=0}^{\infty} W_{\alpha m n} x^m \\ &= \sum_{m=0}^{\infty} W_{mn} x^m && (3.9) \end{aligned}$$

well defined, and how quickly does the sum converge. Let us focus on a typical term in eq.(3.8),

$$(f_\alpha^{-1}(x))^n \Big|\frac{d}{dx} f_\alpha^{-1}(x)\Big|,$$

and examine the properties of its complex extension into $\mathcal{D}$,

$$(g_\alpha(z))^n \frac{d}{dz} g_\alpha(z)\sigma_\alpha,$$

where σ_α equals 1 if $f_\alpha^{-1}(x)$ is monotonic increasing, and -1 otherwise. This term can be expanded as a uniformly convergent Taylor series[55] provided $g_\alpha(z)$ has no singularities in a circle of radius $1+\epsilon$ with centre at the origin of the complex plane. *Furthermore, if each inverse branch sends the set of points in a disc of radius* $r > 1$ *into a disc of radius* $\hat{r}$, then for any real phase θ,

$$max(|g_\alpha(r\exp(i\theta))|) \leq \hat{r}, \tag{3.10}$$

and

$$(g_\alpha(z))^n \frac{d}{dz} g_\alpha(z)\sigma_\alpha = \sum_{m=0}^{\infty} W_{\alpha m n} z^m, \tag{3.11}$$

where

$$|W_{\alpha m n}| \leq \Lambda \frac{\hat{r}^n}{r^m}. \tag{3.12}$$

Thus, there exist discs of radius $r > 1$ such that

$$|W_{mn}| \leq c \frac{\hat{r}^n}{r^m}, \tag{3.13}$$

where c is a constant. Moreover, if the inverse branch has a complex extension in a large enough disc C_r about the origin, then

$$|W_{\alpha m n}| \leq \Lambda \frac{(\Lambda r)^n}{r^m}. \tag{3.14}$$

To see this, first note that every $g_\alpha(z)$ has a fixed point $x^* \in \mathcal{I}$; and let $z = r\exp^{i\theta}$. Then, using the mean value theorem,

$$\begin{aligned} |g_\alpha(r\exp^{i\theta}) - 0| &\leq |g_\alpha(r\exp^{i\theta}) - x^*| + |x^*| \\ &\leq \Lambda(r+1) + 1. && (3.15) \end{aligned}$$

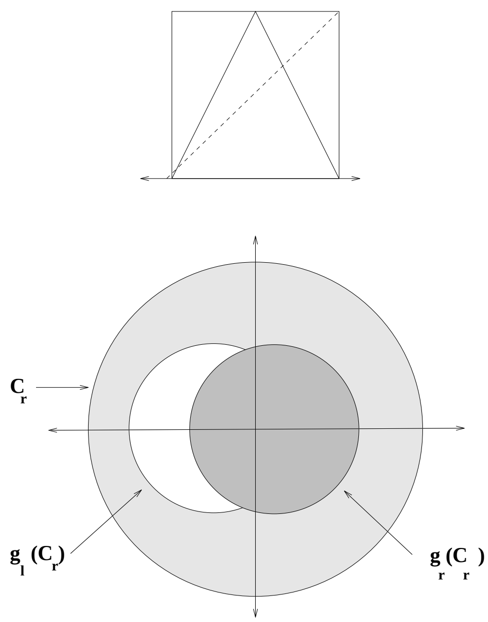

Figure 3.1: The tent map, and the images of a disc C_r via the complex extensions of its left and right inverse branches ($g_l(z) = \frac{z}{2}$ and $g_r(z) = 1 - \frac{z}{2}$ respectively).

Simple examples are the Bernouli and tent maps with slope 2 so that $\Lambda = \frac{1}{2}$, as exhibited in fig.3.1. This figure provides a geometrical illustration of the requirements of convergent matrix representations of $\mathcal{U}$ with respect to a monomial basis. The monomials have a special relationship to the discs, as the image of any disc C_r via a monomial z^n is the disc C_{r^n}. If the image of C_r via each $g_\alpha(z)$ lies within the disc C_r, then exponential convergence of the matrix representation is guaranteed. For Chebyshev polynomials, the role played here by circles (the boundary of the discs) is played by a family of confocal ellipsi[92].

Suppose $\hat{r} < r$, then for any $\epsilon > 0$, there exists an N_α such that

$$\left|(f_\alpha^{-1}(x))^n\right|\frac{d}{dx}f_\alpha^{-1}(x)| - \sum_{m=0}^{N_\alpha} W_{\alpha nm}x^m| < \epsilon, \tag{3.16}$$

independently of the value of n. Let N_{max} denote the supremum of the N_α's over all the inverse branches. Then

$$\left|\mathcal{U}x^n - \sum_{n=0}^{N_{max}}\sum_{m=0}^{N_{max}}(W)_{nm}x^n\right| < \epsilon. \tag{3.17}$$

Now ϵ grows exponentially smaller as we increase the basis size given that eq.(3.10) is satisfied. Therefore, analytic densities expandable as a uniformly convergent Taylor series can be evolved with arbitrary accuracy for any finite time with a finite matrix.

The simplest class of systems having this property are piecewise linear maps like the Bernouli and tent maps (slope 2), where each inverse branch has a complex extension which is entire, everywhere contractive and conformal, and

$$|W_{nm}| \le C\Lambda^{-m}, \tag{3.18}$$

where C is a constant. Moreover, for piecewise linear maps, as r in eq.(3.12) can be arbitrarily large, we find $W_{nm} = 0$ if $n > m$.

Less trivial examples are provided by two one parameter family of maps, defined through their local left and right inverses,

$$\begin{aligned} L_a(x) &= a(x+1) + \frac{1}{2}(\frac{1}{2} - a)(x^2 + 2x + 1) - 1 \\ R_a(x) &= -L_a(-x), \end{aligned} \tag{3.19}$$

and

$$\begin{aligned} \hat{L}_a(x) &= a(x+1) + \frac{1}{2}(\frac{1}{2} - a)(x^2 + 2x + 1) - 1 \\ \hat{R}_a(x) &= -\hat{L}_a(x). \end{aligned} \tag{3.20}$$

At $a = 0.5$, the inverse maps of eq.(3.19) correspond to those of the Bernoulli shift, whereas the inverse maps of eq.(3.20) correspond to those of the tent map (slope 2). The following plots establish that if the stability factor of the fixed point(s) of the original map is greater than one (which corresponds to $0 < a < 1$, then there exists an $r > 1$ such that

$$\forall \theta \in \Re, \left| \hat{f}_\alpha^{-1}(r \exp(i\theta)) \right| = r' < r \tag{3.21}$$

The upper surface in figure 3.2 corresponds to $|r \exp^{i\theta}|^2$ and is displayed for reference.

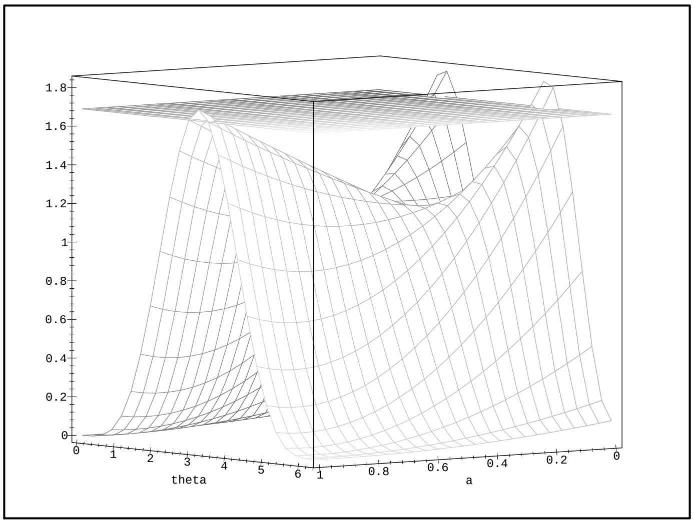

Figure 3.2: 3-d plot of the magnitude squared of the left inverse for a fixed radius $r = 1.3$ as a function of control parameter a, and phase theta

We notice for $\delta \leq a < 1$ that the contour displayed lies below the surface $|r|^2 = 1.69$, where $0 < \delta \ll 1$. . The contour pierces the surface for $a = 1$ and $a = 0$, suggesting that eq.(3.21) may not be satisfied at these values of a. Indeed, one can easily show analytically for $a = 1$ and $\forall \epsilon > 0$

$$\lim_{t \to \infty} L^t(-1-\epsilon) \to -\infty.$$

In this case the systems described by eqs.(3.19,3.20) exhibit intermittent-like behaviour, and the spectra of each associated $\mathcal{U}$ is believed not to be discrete. Fortunately, for all other values of a, we obtain convergent matrix representation of $\mathcal{U}$ with respect to a monomial basis, and the spectra are easily determined. In subsection 3.3.3 we will investigate the spectral properties of the one parameter family of maps given by eq.(3.20).

3.2.2 Monomial representations and eventually hyperbolic maps

Clearly, discs C_r, $r > 1$ being mapped into smaller discs about the origin by all the inverse branches of a system leads to exponentially convergent representations. This is typically the case if the inverse branches are analytic and contractive in large complex domains about the origin (see eq.(3.15)). But these conditions may be violated. The system may, for example only be eventually hyperbolic, or the curvature of the inverse branches may be too high, and yet a convergent monomial repesentation of $\mathcal{U}$ for appropriate classes of initial probability densities $\{\rho(x)\}$ may still be possible, as we shall now see. We suppose that $\{\rho(x)\}$ have complex extensions in a disc of sufficiently large radius $r_0 > 1$ centred at the origin such that

$$\forall z \in C_{r_0},\ \rho(z) \text{ is analytic.} \tag{3.22}$$

The latter equation implies that the initial density can be represented by a vector $\vec{\rho_0}$ defined by the Taylor expansion coefficients;

$$\rho(z) = \sum_{n=0}^{\infty} \rho_n z^n, \tag{3.23}$$

where

$$|\rho_n| \leq \frac{M}{{r_0}^n}, \tag{3.24}$$

and M is the maximum value of $\rho(z)$ on the circle of radius r_0. By a convergent representation $\mathcal{W}$ of $\mathcal{U}$ for a this class of initial densities we mean that

$$\forall t,\ \mathcal{U}^t\rho(x) = \sum_{m=0}^{\infty}\sum_{n=0}^{\infty} \mathcal{W}^t_{mn}\rho_n x^m, \tag{3.25}$$

in the sense of uniform convergence. As each monomial is bounded above by one, this amounts to demanding that

$$\forall t,\ \mathcal{W}^t\vec{\rho} \tag{3.26}$$

converges absolutely, if r_0 is large enough.

We will now prove eq.(3.25) is valid for any map $f(x)$ which is eventually hyperbolic, provided:

I $\forall t$, $\forall \alpha$, $g^t_\alpha(z)$ is analytic in a disc C_r, $r > 1$;

II There exists a disc C_q of radius $q > 1$, whose image via any $g^t_\alpha(z)$ lies within the disc C_r;

III the initial density is analytic in a disc of sufficiently large radius r_0 (see eqs.(3.22)-(3.24))

A simple example of a uniformly hyperbolic system satisfying these conditions is illustrated in fig.(3.1). In contrast, the fig. 3.3 demonstrates that the conditions above only require eventual hyperbolicity.

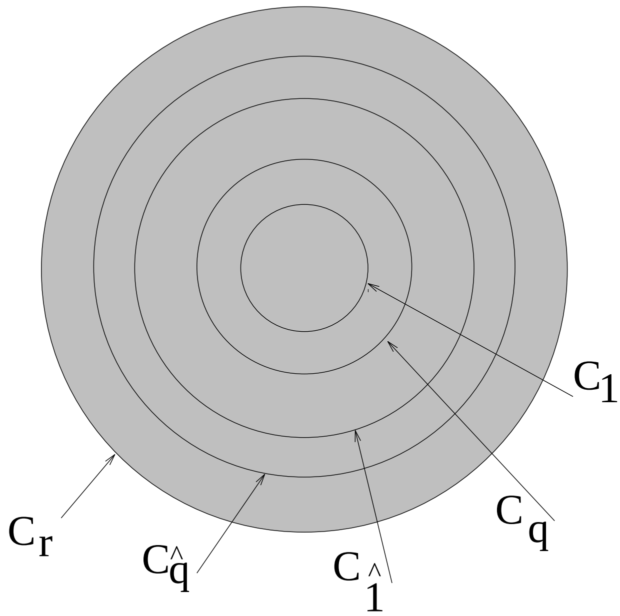

Figure 3.3: Illustration of condition **I** and **II** for any $g^t_\alpha(z)$. The concentric discs, from the inner to the outer represent: the unit disc C_1, a disc C_q of radius q, the smallest disc $C_{\hat{1}}$ containing the image of the unit disc, the smallest disc $C_{\hat{q}}$ containing the image of the disc C_q, and the largest disc C_r wherein $g^t_\alpha(z)$ is analytic. The initial density must be analytic in a disc of radius greater that $\hat{q}$ (condition **III**).

Proof:

Consider separately the contributions to $\mathcal{W}\vec{\rho}$ from each inverse branch,

$$\begin{aligned} |\sum_{m_1=0}^{\infty}\sum_{m_0=0}^{\infty} W_{m_1 m_0}\rho_{m_0}| &\le \sum_\alpha \sum_{m_1=0}^{\infty}\sum_{m_0=0}^{\infty} |W_{\alpha m_1 m_0}\rho_{m_0}| \\ &\le \sum_\alpha \sum_{m_1=0}^{\infty}\sum_{m_0=0}^{\infty} \Lambda_\alpha \frac{1}{r_1^{m_1}} (\frac{\hat{r_1}}{r_0})^{m_0} , \end{aligned} \tag{3.27}$$

where we've used eq.(3.12). Thus sufficient conditions for the convergence of $\mathcal{W}\vec{\rho}$ are that for each inverse branch $g_\alpha(z)$, there exists a disc C_{r_1}, $r_1 > 1$ such that $\forall z \in C_{r_1}$, $g_\alpha(z)$ is analytic and $|g_\alpha(z)| \le \hat{r_1} < r_0$. Let us denote the radius of the largest disc where each

$g_\alpha(z)$ is analytic by r. Our conditions are then

$$1 < r_1 < r \text{ and } \frac{\hat{r_1}}{r_0} < 1, \tag{3.28}$$

which may obviously impose a constraint on the required domain of analyticity of $\rho(z)$.

Next, we consider separately the contributions from each sequence of inverse branches $(g_{\alpha_1} \circ g_{\alpha_2}(z))$, to $\mathcal{W}^2\vec{\rho}$ using eq.(3.9)

$$\begin{aligned} |\mathcal{W}^2\vec{\rho}| &= \sum_{\alpha_2}\sum_{\alpha_1} |\sum_{m_2=0}^{\infty}\sum_{m_1=0}^{\infty}\sum_{m_1=0}^{\infty}\sum_{m_0=0}^{\infty} W_{\alpha_2 m_2 m_1} W_{\alpha_1 m_1 m_0}\rho_{m_0}| \\ &\leq M\Lambda_{\alpha_2}\Lambda_{\alpha_1}\sum_{\alpha_2}\sum_{\alpha_1}\sum_{m_2=0}^{\infty}\sum_{m_1=0}^{\infty}\sum_{m_1=0}^{\infty}\sum_{m_0=0}^{\infty}\frac{1}{r_2^{m_2}}\left(\frac{\hat{r_2}}{r_1}\right)^{m_1}\left(\frac{\hat{r_1}}{r_0}\right)^{m_0}. \end{aligned} \tag{3.29}$$

Sufficient conditions for convergence are that there exists a disc C_{r_1}, with and a disc C_{r_2} with $1 < r_2 < r_1 < r$ such that

$$g_{\alpha_2}(C_{r_2}) \hat{\subset} C_{\hat{r}_2} \hat{\subset} C_{r_1} \text{ and } g_{\alpha_1}(C_{r_1}) \hat{\subset} C_{\hat{r}_1} \hat{\subset} C_{r_0}, \tag{3.30}$$

where $A \hat{\subset} B$ if $A \subset B$ and $A \neq B$. In other words,

$$\frac{\hat{r_2}}{r_1} < 1 \text{ and } \frac{\hat{r_1}}{r_0} < 1. \tag{3.31}$$

That such discs exist follows from conditions **I, II, III**, and the maximum modulus theorem[55] for analytic functions[1].

Let us now use the monomial basis to obtain a representation of $\mathcal{U}^t$,

$$\begin{aligned} \mathcal{U}^t x^n &= \sum_{m=0}^{\infty} Q_{tmn} x^m \\ &= \sum_{\beta}\sum_{m=0}^{\infty} Q_{t\beta mn} x^m \end{aligned} \tag{3.32}$$

where $Q_{t\beta mn}$ is defined through the relation

$$\sigma_\beta({g^t}_\beta(z))^n \frac{d}{dz}{g^t}_\beta(z) = \sum_{m=0}^{\infty} Q_{t\beta mn} z^m, \tag{3.33}$$

and

$${g^t}_\beta(z) = g_{\alpha_1} \circ g_{\alpha_2} \circ \cdots \circ g_{\alpha_{t-1}} \circ g_{\alpha_t}(z). \tag{3.34}$$

It is easy to show by induction that $\mathcal{W}^t\vec{\rho}$ converges absolutely if

$$\forall s,\ 2 \leq s \leq t,\ \mathcal{W}Q_{s-1}\vec{\rho} \tag{3.35}$$

[1] Let D be a bounded region and suppose that $g^t_\alpha(z)$ is analytic and non-constant in D and on the boundary of D. Then $|g^t_\alpha(z)|$ cannot have a maximum at an interior point of D. Consequently, the maximum of $|g^t_\alpha(z)|$ is taken on the boundary of D.

converges absolutely. Therefore, our problem reduces to establishing the conditions for convergence of eq.(3.35). For $t = 2$, the conditions are given by eq.(3.31), so let us now consider $t > 2$. As before, we can focus on the contributions to these matrices from each sequence of inverse branches separately (see eq.(3.33)). From condition **I** there exists a disc C_{q_t}, $1 < q_t < r$ such that the image of the disc via each inverse branch $g^t_\beta(z)$ is contained in a disc disc $C_{\hat{q}_t}$ of radius $\hat{q}_t$. Thus, eq.(3.13) implies

$$|Q_{t\beta mn}| \leq C\frac{\hat{q_t}^n}{q_t^m}, \tag{3.36}$$

where C is a constant. Sufficient conditions the convergence of $Q_{t\beta}\vec{\rho}$ are that $\hat{q}_t < r_0$ which are fulfilled for all inverse branches provided r_0 is sufficiently large. Now as eq.(3.31) is satisfied,

$$Q_{2m_2m_0} = \sum_{m_1=0}^{\infty} \mathcal{W}_{m_2m_1}\mathcal{W}_{m_1m_0}. \tag{3.37}$$

Let us check the conditions of convergence for $\mathcal{W}Q_2\vec{\rho}$,

$$|\sum_{m_2=0}^{\infty}\sum_{m_0=0}^{\infty}\mathcal{W}_{m_3m_2}Q_{2m_2m_0}\rho_{m_0}| \leq \frac{1}{r_3^{m_3}}C'\sum_{m_2=0}^{\infty}\sum_{m_0=0}^{\infty}(\frac{\hat{r}_3}{q_2})^{m_2}(\frac{\hat{q}_2}{r_0})^{m_0}, \tag{3.38}$$

where C' is a constant. Sufficient conditions for convergence of eq.(3.38) are

$$\frac{\hat{r}_3}{q_2} < 1 \text{ and } \frac{\hat{q}_2}{r_0} < 1, \tag{3.39}$$

which are satisfied by conditions **I, II, III** again provided r_0 is large enough. More generally sufficient conditions for the convergence of eq.(3.35) reduce to

$$\frac{\hat{r}_s}{q_{s-1}} < 1, \text{ and } \frac{\hat{q}_{s-1}}{r_0} < 1, \tag{3.40}$$

where $2 \leq s \leq t$. As the system is by assumption eventually hyperbolic (eq.(3.4), the image of C_{q_t} via any any inverse branch $g^t_\beta(z)$ for large t must tend to its fixed point $x^* \leq 1$, so that

$$\lim_{t\to\infty}\hat{q}_t \leq 1. \tag{3.41}$$

Thus, we need only check that (3.40) is satisfied for a finite number of values of s. Now, let us denote the supremum of $\{\hat{q}_s\}$ by $\hat{q}_{sup}$, then eq.(3.40) will obviously be satisfied if

$$r_0 > \hat{q}_{sup}. \tag{3.42}$$

Therefore, the statistical properties of functions/initial densities which are analytic in a disc of radius greater than $\hat{q}_{sup}$ can certainly be calculated through our representation for all time.

□

In contrast, suppose a given system is never even eventually hyperbolic, but conditions **I,II** are satisfied for a finite time T. Then if r_0 is large enough (i.e. condition **III** is satisfied) we may still use our representation for a time T. This observation is important for type 3 intermittentcy where there exist marginally stable fixed points. It implies that for finite times our representation converges can can be truncated, so that probability densities can be evolved, and time correlation functions can be evaluated reliably, provided r_0 is sufficiently large. However, as $\hat{q}_{sup}$ will keep increasing with time, one is forced to increase the truncation order with time. For intermittent maps, numerical computations indicate that the basis size necessary for a good approximation grows linearly with T.

3.2.3 Singularities close to the real axis

One can construct examples of Markov analytic maps where the space of analytic functions with support on $\mathcal{I}$ is invariant under $\mathcal{U}$, and yet where a monomial expansion does not converge at all. Consider for instance the map whose left inverse is defined as

$$L(x) = -0.5575 + 0.5x + 0.01x^2 + \frac{0.095}{x^2 + 0.9} \tag{3.43}$$

which has a pole on the imaginary axis close to the origin in the complex plane. We can choose the right branch to be $R(x) = -L(-1)$ for instance, although this detail is not important here. The following figures of the left inverse branch and its first derivative demonstrate that eq.(3.3) is indeed satisfied (i.e the left inverse is contractive). This

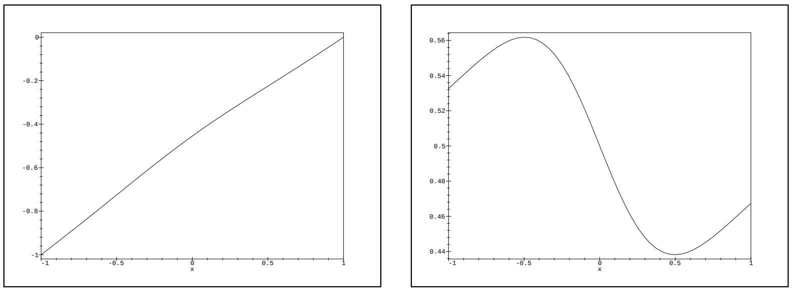

Figure 3.4: Left: Left inverse branch. Right: derivative of the left inverse branch.

example illustrates the need to find basis sets where convergent matrix representations exist. Clearly a monomial basis is not always adequate.

3.3 Convergent Chebyshev representations

It is well known that any function which is continuous, and whose first derivative is bounded, can be expanded in terms of a uniformly convergent Chebyshev series, and if the function is analytic about the interval $\mathcal{I}$, then the expansion coefficients decrease exponentially quickly [18, 92]. One may ask if the Frobenius-Perron operator of any hyperbolic or eventually hyperbolic map leaves the space of analytic functions invariant, can an exponentially convergent matrix representation like eq.(3.12) always be obtained with respect to a Chebyshev function basis ? This is the case, and is particularly significant because Chebyshev polynomials satisfy a discrete orthogonality relation as well as a continuous one, and so are ideal for rapid numerical computations [88]. The proof will be developed from a geometrical and analytical perspective. We will see that a one parameter family of confocal ellipsi in the complex plane play a role for Chebyshev polynomials completely analogous to that of circles for monomials in Taylor expansions. This will be reflected in almost identical proofs of their convergence properties. Fig.(3.5) is a a geometrical

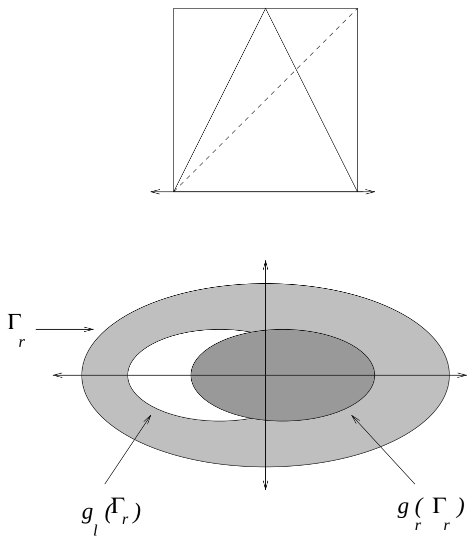

Figure 3.5: The tent map, and the images of the interior of an ellipse Γ_r via the complex extensions of its left and right inverse branches ($g_l(z) = \frac{z}{2}$ and $g_r(z) = 1 - \frac{z}{2}$ respectively).

illustration of a map whose local inverses (the complex extensions thereof) satisfy the requirements of convergent matrix representations with respect to Chebyshev polynomials. The Chebyshev polynomials have a special relationship with a family of confocal ellipsi ($\{\Gamma_r\}$, $r > 1$), the image of any such ellipse Γ_r via $T_n(z)$ is another member $\Gamma_{r'}$ of the family. We shall see that if the image of Γ_r via each $g_\alpha(z)$ lies within the disc Γ_r, then exponential convergence of the matrix representation is guaranteed.

3.3.1 General formulation

The Chebyshev polynomials

$$T_n(x) = cos(ncos^{-1}(x)),\ n = 0, 1, 2... \tag{3.44}$$

obey the orthogonality relation

$$\int_{-1}^{1} \frac{T_n(x)T_m(x)}{\sqrt{1-x^2}}dx = \begin{cases} \pi\delta_{n,m} & \text{if } n \neq 0 \\ \frac{\pi\delta_{n,m}}{2} & \text{if } n = 0 \end{cases} \tag{3.45}$$

We want to determine the rate of convergence of a matrix representation of $\mathcal{U}$ with respect to a Chebyshev basis,

$$\mathcal{U}T_n(x) = \sum_0^\infty W_{mn}T_m(x), \tag{3.46}$$

where

$$W_{mn} = \left\{ \begin{array}{ll} \frac{2}{\pi}\int_{-1}^{1} T_m(x)\mathcal{U}T_n(x)dx & \text{if } m = 0 \\ \\ \frac{1}{\pi}\int_{-1}^{1} T_m(x)\mathcal{U}T_n(x)dx & \text{otherwise} \end{array} \right\}. \tag{3.47}$$

Now, any function $\psi(x)$ which is continuous, and of bounded variation can be expanded in terms of a uniformly convergent Chebyshev series[18],

$$\psi(x) = \sum_0^\infty A_n T_n(x), \tag{3.48}$$

where for $n \neq 0$

$$A_n = \frac{1}{\pi}\int_{-1}^{1} \frac{T_n(x)\psi(x)}{\sqrt{1-x^2}}dx. \tag{3.49}$$

The integral eq.(3.48) on making a change of variable $x \to \theta = \arccos(x)$ becomes

$$A_n = \frac{1}{\pi}\int_{-\pi}^{\pi} \psi(\cos(\theta))cos(n\theta)d\theta, \tag{3.50}$$

and on making another change of variable,

$$\theta \to z = re^{i\theta},\ r = 1,$$

we obtain

$$\begin{aligned} |A_n| &= \left| \frac{1}{2\pi}\int_{C_r} \psi(\frac{z+z^{-1}}{2})\frac{z^n+z^{-n}}{2}\frac{dz}{z} \right| \\ &\leq \left| \frac{1}{4\pi}\int_{C_r} \psi(\frac{z+z^{-1}}{2})z^{n-1}dz \right| + \left| \frac{1}{4\pi}\int_{C_r} \psi(\frac{z+z^{-1}}{2})z^{-n-1}dz \right|, \end{aligned} \tag{3.51}$$

where C_r denotes the circle of radius one. The only singularities in $z + z^{-1}$ occur at the origin and at infinity, so by Cauchy's theorem we may change the contours to $C_{\frac{1}{r}}$ and C_r with $r > 1$ in the last two terms respectively, without changing the value of the integrals provided that $\psi(\frac{z+z^{-1}}{2})$ has no additional singularities in the new domains. Denoting the maximum value of $|\psi(\frac{z+z^{-1}}{2})|$ on C_r by M_r, we find

$$|A_n| \leq \frac{M_r}{r^n}. \tag{3.52}$$

Now as z draws out a circle of radius r or r^{-1}, $\frac{z+z^{-1}}{2}$ draws out an ellipse in the complex plane with foci $-1, 1$, semi-axis major

$$\varpi_r = \frac{1}{2}(r + r^{-1}), \tag{3.53}$$

and semi-axis minor

$$\varsigma_r = \frac{1}{2}(r - r^{-1}). \tag{3.54}$$

Thus, M_r is the maximum value of $|\psi(z)|$ on the ellipse Γ_r. The ellipsi form a confocal family parameterised by r. When r is large then

$$\varpi_r \approx \varsigma_r \approx \frac{r}{2}, \tag{3.55}$$

and the ellipse is almost a circle of radius $\frac{r}{2}$. At the other extreme, if $r = 1 + \delta$, and $\delta \ll 1$, then

$$\varpi_r = 1 + \frac{\delta^2}{2},\ \varsigma_r = \delta, \tag{3.56}$$

up to second order in δ, so the ellipse barely lies out of $\mathcal{I}$.

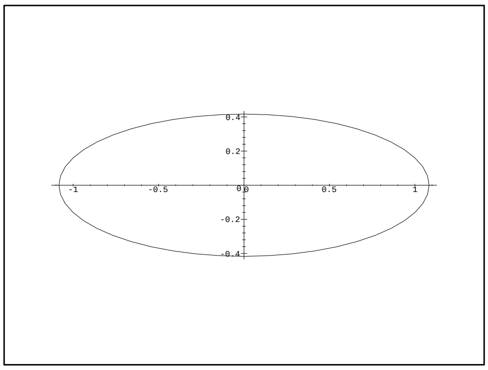

Figure 3.6: ellipse $\Gamma_{r=1.5}$, and foci $-1, 1$.

Let us denote the set of points enclosed by Γ_r as Ξ_r. Inspired by the results of section 3.2, we will show that if each inverse branch $g_\alpha(z)$ sends the points of Ξ_r, $r > 1$ into $\Xi_{\hat{r}}$ then the matrix coefficients will decay at least as quickly as

$$W_{mn} \leq \Lambda \frac{\varpi_{\hat{r}^n}}{r^m} = \Lambda \frac{\hat{r}^n + \hat{r}^{-n}}{2r^m} \tag{3.57}$$

Proof:

We first note that one can easily obtain the identity,

$$T_n(\frac{z + z^{-1}}{2}) = \frac{z^n + z^{-n}}{2}, \tag{3.58}$$

provided $0 < |z| < \infty$. Thus, a Chebyshev polynomial T_w having as its domain points w on the ellipse Γ_r will have as its range the points $w' \in \Gamma_{r^n}$ in particular the maximum magnitude equals the value of the semi-axis major.

$$max(T_n(w)) = \varpi_{r^n}. \tag{3.59}$$

The analogy with circles in the complex plane and monomials is clear. As in the previous section, we can determine the properties of $\mathcal{U}$, by examining the effect of each contributing inverse branch $g_\alpha(z)$ on the Chebyshev polynomials,

$$T_n(g_\alpha(z))\frac{d}{dz}g_\alpha(z)\sigma_\alpha = \sum_0^\infty W_{\alpha mn}T_m(z) \tag{3.60}$$

The truth of statement 3.57 is easily established using eqs. (3.3), (3.59) and (3.52), and then summing up the contributions of each branch,

$$W_{mn} = \sum_\alpha W_{\alpha mn}. \tag{3.61}$$

$\square$

3.3.2 Convergence of W

We see that if $\hat{r} < r$ in eq.(3.57), then W_{mn} decays exponentially quickly in n and m. All the observations made in sub-section 3.2.1 regarding the convergence of $\mathcal{W}$ for piecewise linear maps are also valid here. This should not be a surprise, as we have already noted that large ellipsi resemble circles. Indeed, the analogies go further, the results of subsection 3.2.2 can be translated into similar results for Chebyshev polynomials, the only difference being that they are valid for any eventually hyperbolic map whose $\mathcal{U}$ leaves invariant the space of functions analytic in an arbitrarily small domain about the interval $\mathcal{I}$. A representation $\mathcal{W}$ of $\mathcal{U}$ with respect to Chebyshev polynomials exists if the initial densities $(\{\rho(x)\}$ are analytic functions,

$$\forall t,\ \mathcal{U}^t\rho(x) = \sum_{m=0}^\infty\sum_{n=0}^\infty \mathcal{W}^t_{mn}\rho_n T_m(x), \tag{3.62}$$

in the sense of uniform convergence. As each Chebyshev polynomial with domain $\mathcal{I}$ is bounded above by one, this reduces to demanding that

$$\forall t,\ \mathcal{W}^t\vec{\rho} \tag{3.63}$$

converges absolutely. We will now prove eq.(3.25) is valid for any map $f(x)$ which is eventually hyperbolic, provided $\forall t$, $\forall\alpha$:

I $\forall t$, $\forall\alpha$, $g^t_\alpha(z)$ is analytic in an elliptic interior Ξ_r, $r > 1$;

II There exists an elliptic interior Ξ_q, $q > 1$ whose image via any $g^t_\alpha(z)$ lies completely within Ξ_r;

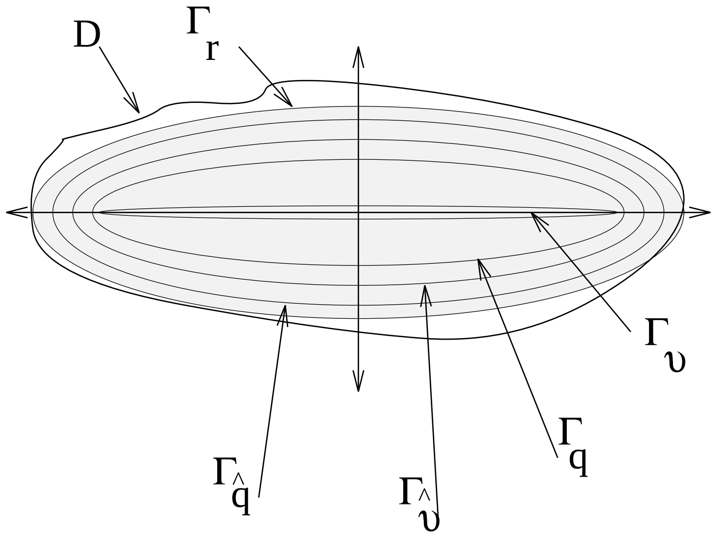

Figure 3.7: Illustration of condition **I** and **II** for any $g^t_\alpha(z)$. The outer curve represents the boundary of the domain of analyticity. The other closed curves represent a series of confocal ellipsi: : Γ_υ, an ellipse arbitrarily close to and enclosing the interval $[-1, 1]$; Γ_q another ellipse; $\Gamma_{\hat{\upsilon}}$, the smallest ellipse enclosing the image via $g^t_\alpha(z)$, of Γ_υ, $\Gamma_{\hat{q}}$, the smallest ellipse enclosing the image of Γ_q; and Γ_r the largest ellipse enclosing a domain where $g^t_\alpha(z)$ is analytic. The initial density must be analytic in a domain having in its interior $\Gamma_{\hat{q}}$ (condition **III**).

III the initial density is analytic in domain enclosed by an ellipse Γ_{r_0}, which contains the image of Ξ_q

A simple example of a system satisfying these conditions is illustrated in fig.3.5, where the system is extremely hyperbolic. In contrast, fig.3.7 demonstrates that the conditions above only require eventual hyperbolicity.

Proof:

The proof is identical to subsection 3.2.1 except that the discs C_r are substituted by the interior of ellipsi Ξ_r; the monomials z^n are substituted by Chebyshev polynomials $T_n(z)$, and $|W_{mn}|$ has its upper bound given by eq.(3.57) rather than eq.(3.13). Conditions **I** and **II** are satisfied by eqs. (3.2), (3.5) and the fact that we can choose ellipsi with arbitrarily small semi-axis minor (see eq.(3.56). This established the convergence of matrix multiplication in the infinite representation given that of $\rho_0(z)$ is analytic in Ξ_{r_0}, and $r_0 > q_{sup}$. That $r_0 > q_{sup}$ (so as condition **III** is satisfied) would seem at first sight to be a limitation, as it certainly is with the monomial representation. Fortunately, we may always choose any ellipse Γ_{q_s} with arbitrarily small semi-axis minor and as the interval $[-1, 1]$ is mapped into itself by each inverse branch, it follows $\hat{q}_s$ will have arbitrarily small semi-axis minor too.

$\square$

In fact we can relax the condition that the initial densities should be analytic. They need only be C_2 maps whose derivatives are functions of bounded variation.

3.3.3 A one parameter family of examples

In the last section we introduced two one parameter families of maps (see eqs.(3.19, (3.20)) and demonstrated in theory that for $0 < a < 1$ monomial representations of $\mathcal{U}$ are convergent. We will now explore numerically the spectral properties of the family that includes the tent map, using a Chebyshev representation. As said before, at $a = 1$, we get the cusp map, which displays type 3 intermittentcy (it possesses a marginally stable fixed point). The cusp map, therefore, does not satisfy our sufficient conditions to obtain a convergent matrix representation.

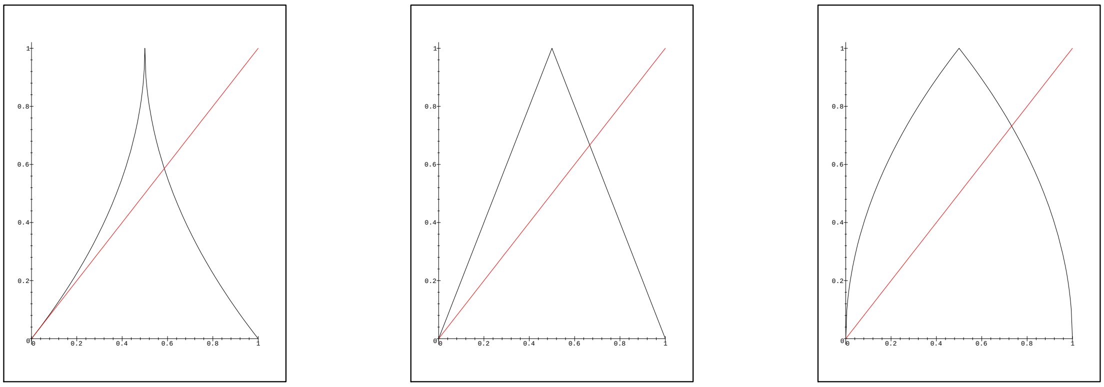

Figure 3.8: A one parameter family of maps eq.(3.20) where the parameter is the reciprocal of the expansion rate of the fixed point at zero: in the figures above above $f_1'(0) = 1$ (cusp map), $f_{1/2}'(0) = 2$ (tent map), and $f_0(0) = \infty$ (miter map).

In fig.(3.9) the spectra of $\mathcal{U}$ are displayed, determined with respect to a Chebyshev basis, where we have truncated the basis expansions at order 50, i.e $\mathcal{W}$ is a $50X50$ matrix. Extensive numerics indicate that for all parameter values but $a = 1/f'(0) = 1$, the dominant spectra have converged, and those neglected are close to zero in magnitude. The invariant densities have a surprisingly simple linear form due to certain symmetries,

$$\rho_{inv}(x) = \frac{d}{dx} L_a(x), \tag{3.64}$$

and all the systems are exact[2] and therefore mixing. The spectral properties of the cusp map are still not clear. Nevertheless, as the figure suggests, it appears that 1 as well as zero is an accumulation point of the spectra The dominant spectra exhibit two curious transitions as a functions of the parameter. Let us order the eigenvalues according to their magnitude, so that $\lambda_1 = 1$, corresponds to the invariant density, λ_2 corresponds to the slowest decay rate and so on. For $0 < a < (.389 \pm .001)$, λ_2 is negative (indicating that the asymptotic statistical behaviour is that of a exponentially decaying period 2 oscillation), and the third largest eigenvalue is positive. At $a \approx .389$ $\lambda_2 = -\lambda_3$. For

[2]Any arbitrarily small interval expands at an essentially exponential rate (λ_2^t) where λ_2 is the second largest eigenvalue of $\mathcal{U}$ acting on the space of analytic functions, and there exists no invariant set of subintervals having finite support

$(.389 \pm .001) < a < \frac{1}{2})$, λ_2 is positive (a decaying mode with no oscillation), and the third largest eigenvalue is negative. For $a > \frac{1}{2}$, all the spectra are real and positive, and $\lambda_2 \approx \frac{3x-1}{2}$.

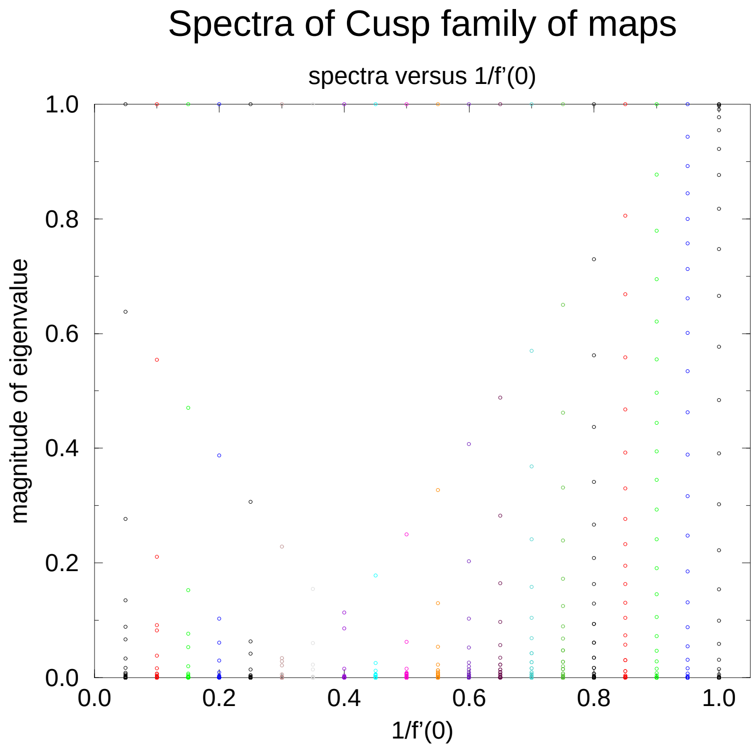

Figure 3.9: Spectra of the cusp family plotted against the reciprocal of the expansion rate of the fixed point 0.

3.4 Matrix representations of the Frobenius-Perron operator for any Markov map

In the last section, we considered hyperbolic and eventually hyperbolic maps whose corresponding Frobenius-Perron operator leave the space of analytic functions invariant. Markov analytic maps includes this class, and also those maps whose corresponding $\mathcal{U}$ leaves certain piecewise analytic function spaces invariant. We will see that the results of section 3.3 are applicable here too, after suitable changes of variable. Of course, in the previous chapter we considered piecewise linear Markov maps (and equivalent repellers), so the obvious generalization is to consider systems having curvature. First, a few definitions similar to those given in the previous chapter.

A piecewise analytic map $f : \mathbf{I} \to \mathbf{I}$, where $\mathbf{I} = [0, 1]$, is Markov if it has the following properties [70]:

(i) The number of non-analytic points $d_1, d_2, .., d_N$ is finite.

(ii) Their iterates form a finite set of points $\{a_0, a_1, .., a_{N_{min}}\}$, where $a_k < a_{k+1}, a_0 = 0$ and $a_{N_{min}} = 1$. Note that the points $\{a_i\}$ form a partition of the interval $[0,1]$ into cells $C_i = [a_i, a_{i+1}]$, which is known as the minimal Markov partition (P_M).

(iii) The inverse branches are of the form

$$f_\alpha{}^{-1}(x) = \sum_{i=1}^{N_{min}} g_{\alpha_i}(x)\chi_i(x), \tag{3.65}$$

where $g_{\alpha_i}(z)$ is analytic over a complex domain $D_i \supset C_i$, and $\chi_i(x)$ equals one if $Re(z) \in C_i$ and is zero otherwise.

(iv)

$$\exists\, \tau : \forall t \geq \tau,\ \forall z \in D_i, |\frac{d}{dz}g^t{}_{\alpha_i}(z)| \leq \Lambda < 1. \tag{3.66}$$

We remark that the cells of the partition $\mathcal{P_M}$ have the property

$$\forall i, j,\ f(Int(C_i)) \cap Int(C_j) \neq \emptyset \Rightarrow C_j \subset f(C_i). \tag{3.67}$$

Equivalently,

$$g_{\alpha_j}(Int(C_j)) \cap (Int(C_i)) \neq \emptyset \Rightarrow g_{\alpha_j}(C_j) \subset C_i \tag{3.68}$$

The Frobenius-Perron operator acting on a density can be written as

$$\mathcal{U}\rho(x) = \sum_\alpha \sum_i \sigma_\alpha g'_{\alpha_i}(x)\rho\left(g_{\alpha_i}(x)\right), \tag{3.69}$$

where

$$g'_{\alpha_i}(z_{\alpha_i}(z) = \frac{d}{dz}g_{\alpha_i}(z_{\alpha_i}(z), \tag{3.70}$$

and σ_α is defined as in the previous section.

We propose to use as a basis for eq.(3.69) the family of piecewise Chebyshev polynomials,

$$T_{ik}(x) = \begin{cases} T_k(h_i(x)) & \text{if } x \in C_i \\ 0 & \text{otherwise} \end{cases} \tag{3.71}$$

where

$$h_i(x) = \frac{x - .5(a_i + a_{i-1})}{.5(a_i - a_{i-1})} = \frac{x - e_i}{\Delta_i}. \tag{3.72}$$

The piecewise Chebyshev polynomials obey an orthogonality relation

$$\int_{c_j} T_{kj}(x)T_{mi}(x)w_j(x)dx = \delta_{j,i}\int_{-1}^{1} T_k(x)T_m(x)w(x)dx, \tag{3.73}$$

where,

$$w_j(x) = w(h_j(x))\frac{d}{dx}h_j(x) = w(h_j(x))\frac{1}{\Delta_j}, \tag{3.74}$$

and $w(x)$ is just the weighting factor of the standard Chebyshev polynomials (see eq. (3.45). The matrix representation $\mathcal{W}$ of $\mathcal{U}$ takes the form

$$\mathcal{U}T_{in}(x) = \sum_j \sum_{m=o}^{\infty} W_{jmin} T_{jm}(x). \tag{3.75}$$

To establish the convergence properties of $\mathcal{W}$ we will write

$$\mathcal{U} = \sum_\alpha \sum_i \mathcal{U}_{\alpha_i} \chi_i(x), \tag{3.76}$$

where

$$\mathcal{U}_{\alpha_i} T_{in}(x) = \sigma_\alpha g'_{\alpha_i}(x) T_{in}(g_{\alpha_i}(x). \tag{3.77}$$

Hence,

$$W_{jmin} = \sum_\alpha W_{\alpha jmin} \tag{3.78}$$

where

$$\mathcal{U}_{\alpha_i} T_{in}(x) = \sum_{m=0}^{\infty} W_{\alpha jmin} T_{jm}(x). \tag{3.79}$$

Thus, the problem of establishing the convergence properties of eq.(3.75) is transferred to eq.(3.79). This is advantageous because the right-hand side of eq.(3.77) is analytic if

$$\forall x \in C_j,\ g_{\alpha_i}(x) \in C_i, \tag{3.80}$$

as can be easily shown using property (iii) and eq.(3.68). Now from eqs.(3.73) and 3.79), for $m > 0$,

$$\begin{aligned} \pi W_{\alpha jmin} &= \sigma_\alpha \int_{C_j} g'_{\alpha_i}(x) T_{jm}(x) T_{in}(g_{\alpha_i}(x)) w_j(x) dx \\ &= \frac{\sigma_\alpha}{\delta_j} \int_{C_j} g'_{\alpha_i}(x) T_m(h_j(x)) T_n(h_i(g_{\alpha_i}(x))) w(h_j(x)) dx \\ &= \sigma_\alpha \int_{-1}^{1} {g'}_{\alpha_i}({h_j}^{-1}(x)) T_m(x) T_n(h_i(g_{\alpha_i}({h_j}^{-1}(x)))) w(x) dx \end{aligned} \tag{3.81}$$

Let

$$G(z) = h_i(g_{\alpha_i}({h_j}^{-1}(z))) \tag{3.82}$$

$G(z)$ is analytic in a domain $\mathcal{D}$ surrounding the interval $\mathcal{I}$. The convergence properties of eq.(3.79) are the same as that of the matrix representation of the Frobenius-Perron operator $\hat{\mathcal{U}}$ associated with $G(z)$ with respect to Chebyshev polynomials. Thus we can now exploit the results of section 3.3. We note first that, $G(z)$ has at least one fixed point $x^* \in \mathcal{I}$; and second, that through the chain rule and eq.(3.72)

$$\frac{d}{dz} G(z) = \frac{\Delta_i}{\Delta_j} g'({h_j}^{-1}(z)). \tag{3.83}$$

We see that $G'(z)$ can be greater than one even when $g'(z)$ is less than one, if the prefactor $\frac{\Delta_i}{\Delta_j}$ is large enough. However, as the original map is eventually expanding, there exists an $\hat{\tau} > \tau$ such that

$$\forall t \geq \hat{\tau},\ \forall z \in D,\ |\frac{d}{dz} G(z)| = \frac{\Delta_i}{\Delta_j} {g^t}'({h_j}^{-1}(z)) < 1. \tag{3.84}$$

Therefore the conditions for convergence of $\mathcal{W}$ (see subsection 3.3.2) are fulfilled.

3.5 Spectral Decompositions

For simplicity we shall first consider systems where the space of analytic functions F_r is invariant under $\mathcal{U}$. From this the generalization to systems possessing invariant piecewise analytic function spaces is automatic. F_r denotes the space of functions analytic in the domain Ξ_r enclosed by the ellipse Γ_r. Every such function has associated with it a number K which is the maximum value of the magnitude of the function in Ξ_r, which by the maximum modulus theorem[55] for analytic functions occurs on Γ_r[3]. Let us denote all functions with lowest upper bound K by $F_{r,K}$. We will establish the following spectral properties of $\mathcal{U}$:

1. Any eigenfunction $v(x) \in F_{r,K}$ can be expanded as

$$v(x) = \sum_{\ell=0}^{N} v_\ell T_\ell(x) + \sum_{\ell=N+1}^{\infty} v_\ell T_\ell(x), \tag{3.85}$$

   such that $\forall \epsilon > 0$, $\exists N$ where

$$\left| \sum_{\ell=N+1}^{\infty} v_\ell T_\ell(x) \right| < \epsilon. \tag{3.86}$$

   The truncation order N depends only on K, r and ϵ..

2. The vector representation of $v(x)$ and its corresponding eigenvalue λ satisfies the inequality

$$\left| \sum_{\ell=0}^{N} \mathcal{W}_{m\ell} v_\ell - \lambda v_m \right| < \frac{\epsilon}{r^m} \tag{3.87}$$

   Conversely, if $\mathcal{W}$ truncated at order N has an eigenvector $\vec{\hat{v}}$,

$$\sum_{\ell=0}^{N} \mathcal{W}_{m\ell} \hat{v}_\ell = \hat{\lambda} \hat{v}_m, \tag{3.88}$$

   such that

$$\hat{v}(x) = \sum_{\ell=0}^{N} v_\ell T_\ell(x) \in F_{r,K}, \tag{3.89}$$

   then

$$\left| \mathcal{U}\hat{v}(x) - \hat{\lambda}\hat{v}(x) \right| < \epsilon. \tag{3.90}$$

   Thus, $\vec{\hat{v}}$ and $\hat{\lambda}$ are practically indistinguishable from a true eigenfunction and eigenvalue of $\mathcal{U}$. Note that every eigenvector of the truncated matrix defines a function which is an element of $F_{r,K'}$ for some value of K'.

[3] For example, the bound of $|z^n|$ is the n^{th} power of the semi-axis major, while the bound of $|T^n(z)|$ equals the semi-axis major of the ellipse Γ_{r^n}.

3. There exists a $\hat{K}$ such that the magnitude of the eigenvalue corresponding to a $v(x) \in F_{r,K}$ decreases with increasing K if $K > \hat{K}$. This is also true for the eigenvalues of the truncated matrix where $\hat{v}(x) \in F_{r,K}$. The bound $\hat{K}$ can be determined from the the analytic properties of the map.

4. Any function $\rho(z) \in F_{r,\hat{K}}$ can be expanded in terms of a basis defined through the eigenvectors of the truncated representation of $\mathcal{W}$ (if it is diagonalizable), and in terms of its canonical basis more generally (where W is reduced to its Jordan form). The left and right canonical vectors of W form a bi-orthonormal set.

It is in the last sense that we can speak of spectral decompositions of $\mathcal{U}$. These results are also valid for more general transfer operators than just $\mathcal{U}$.

We assume that we have obtained a matrix representation $\mathcal{W}$ of $\mathcal{U}$ with respect to a basis of Chebyshev functions such that

$$W_{mn} \leq \frac{C}{2}\frac{\hat{r}^n + \hat{r}^{-n}}{r^m} < C\frac{\hat{r}^n}{r^m}, \tag{3.91}$$

where $1 \leq \hat{r} < r$, and C is a constant (see fig.(3.5) for a geometrical interpretation)). While this may not be possible for $\mathcal{U}$, it is always possible for $\mathcal{U}^\tau$, for some $\tau \geq 1$. In that case, we first consider the spectral properties of $\mathcal{U}^\tau$, which are then easily related to those of $\mathcal{U}$.

Let us first prove statement 1. Suppose that $v(x) \in F_{r,K}$ is an eigenfunction of $\mathcal{U}$,

$$\mathcal{U}v(x) = \lambda v(x),$$

then

$$v(x) = \sum_{n=0}^{\infty} v_n T_n(x), \tag{3.92}$$

where

$$v_n \leq \frac{K}{r^n}. \tag{3.93}$$

We choose the normalization of $v(x)$ so that its maximum magnitude in the interval $[-1,1]$ equals one. Thus,

$$\begin{aligned} \forall\epsilon > 0,\ \exists N_\epsilon : \forall N > N_\epsilon\ |v(x) - \sum_{n=0}^{N} v_n T_n(x)| &< \epsilon, & (3.94)\\ \sum_{n=N+1}^{\infty} |v_n| &< \epsilon, & (3.95)\end{aligned}$$

where

$$K\frac{r^{-N_\epsilon}}{r-1} \leq \epsilon. \tag{3.96}$$

□

We now turn to the proof of statement 2. By definition,

$$\mathcal{U}v(x) = \sum_{m=0}^{\infty}\sum_{n=0}^{\infty} W_{mn}v_nT_m(x) \;=\; \lambda\sum_{m=0}^{\infty} v_mT_m(x), \tag{3.97}$$

$$\sum_{n=0}^{\infty} W_{mn}v_n \;=\; \lambda v_m. \tag{3.98}$$

Suppose we truncate the expansion in eq.(3.98) at order N, we find

$$\left|\sum_{n=0}^{N} W_{mn}v_n - \lambda v_m\right| \;<\; \frac{cK}{r^m}\frac{(\frac{\hat{r}}{r})^{N+1}}{1-\frac{\hat{r}}{r}} \;=\; \epsilon_1. \tag{3.99}$$

We may choose the truncation order N so $\epsilon_1 \ll \epsilon$. Thus for all eigenfunctions $v(x) \in F_{r,K}$ we may obtain an approximate eigenvector equation, where the error is less than ϵ_1, and ϵ_1 decreases exponentially quickly with increasing truncation order. One can show in an almost identical way that if $\hat{v}(x) \in F_{r,K}$, and its vector represntation satisfies eq.(3.88) then

$$\left|\mathcal{U}\hat{v}(x) - \hat{\lambda}\hat{v}(x)\right| \;<\; \frac{KCr^{-N}}{(1-\frac{1}{r})(1-\frac{\hat{r}}{r})}. \tag{3.100}$$

$\square$

As the truncation order of the matrix is increased, we expect new eigenvalues to appear, but they maybe spurious unless they correspond to eigenfunctions which are elements of $F_{r,K}$. Two questions arise then, what is the nature of the new eigenvalues of $\mathcal{W}$ truncated at successively higher orders, and how are they related to the true spectrum of $\mathcal{U}$ acting on F_r ? We shall address these questions by proving statement 3 for the infinite dimensional eigenvalue problem, an identical argument holds for the truncated matrix representation. An immediate consequence of statement 3 is that if the expansion coefficients of $v(x)$ or $\hat{v}(x)$ for high order Chebyshev functions are non-negligible then the corresponding eigenvalue of $\mathcal{U}$ and the truncated matrix respectively is very small in magnitude. This implies that by choosing a sufficiently large truncation order we can guarantee that the only approximate eigenfunctions which do not satisfy eq.(3.100) have arbitrarily small eigenvalues (in magnitude) and can be neglected.

Let us now prove statement 3. We have already established that given a bound $\hat{K}$, all eigenfunctions $\{v(x)\} \in F_{r,\hat{K}}$, and approximate eigenfunctions $\{\hat{v}(x) \in F_{r,\hat{K}}$ satisfy eq.(3.99) or eq.(3.100) respectively. Let us consider then $v(x) \in F_{r,K}$, where $K > \hat{K}$.

$$v(x) = v_1(x) + v_2(x), \tag{3.101}$$

where

$$v_1(x) = \sum_{n=0}^{N_1} v_nT_n(x), \tag{3.102}$$

$$v_2(x) = \sum_{n=N_1+1}^{\infty} v_nT_n(x), \tag{3.103}$$

and $N_1 < N_\epsilon$. Let us denote the maximum value of $|v_1(z)|$ and $|v_2(z)|$ on Γ_r, by K_1 and K_2 respectively. If $K_2 < \hat{K}$ then we can already approximate the eigenvalue of $v(x)$ within an accuracy ϵ using a truncated basis of dimension N_ϵ. So we consider the case $K_2 > \hat{K}$. We may write eq.(3.98) as

$$\lambda v_m = \sum_{n=0}^{N_1} W_{mn} v_n + \sum_{n=N_1+1}^{\infty} W_{mn} v_n. \tag{3.104}$$

We will consider $m > N_1$, so that

$$v_m = \eta_m \frac{K_2}{r^m}, \tag{3.105}$$

where $0 \leq |\eta_m| \leq 1$. From Eq.(3.104) we obtain

$$\begin{aligned} |\lambda \eta_m| \frac{K_2}{r^m} &\leq \frac{C}{r^m} \left(K_1 \sum_{n=0}^{n=N_1} (\frac{\hat{r}}{r})^n + K_2 \sum_{n=N_1+1}^{\infty} (\frac{\hat{r}}{r})^n \right), \\ &= \frac{C_1}{r^m} \left(K_1 (1 - x_1) + K_2 x_1 \right), \end{aligned} \tag{3.106}$$

where

$$C_1 = \frac{C}{(1 - \frac{\hat{r}}{r})}, \ x_1 = (\frac{\hat{r}}{r})^{N_1+1}. \tag{3.107}$$

Thus,

$$|\lambda| \leq \frac{K_1}{\eta_m K_2} \left(C_1 (1 - x_1) \right) + C_1 x_1. \tag{3.108}$$

Now we are free to choose N_1 large enough that $C_1 x_1$ is very small. We then note that a basic property of Chebyshev function expansions for any smooth function having a bounded first derivative [18] implies

$$|v_k| \leq \frac{4}{\pi} max(|v(x)|)_{x \in [-1,1]}, \tag{3.109}$$

and as $max(|v(x)|)_{x \in [-1,1]} = 1$ we find that

$$K_1 \leq \frac{4}{\pi} \left(\frac{r^{N_1+1} - 1}{r - 1} + \frac{1 - r^{-(N_1+1)}}{1 - r^{-1}} \right). \tag{3.110}$$

Thus, for fixed N_1, K_1 is bounded. Now if

$$\forall m > N_1, \ K_2 \eta_m < \hat{K} \gg K_1$$

then the corresponding eigenfunction already satisfies eq.(3.87). Thus, any eigenfunction which does not satisfy eq.(3.87) must also not satisfy $\eta_m K_2 \geq \hat{K}$, for at least one value of η_m. We can now choose $\hat{K} \gg K_1$, so that λ is arbitrarily small, for example $\lambda \ll \epsilon$. An identical argument can be made for the functions $\hat{v}(x)$ associated with the eigenvectors of the truncated matrix representation, where ∞ is replaces by N, and in eq.(3.107)

$$x_1 = (\frac{\hat{r}}{r})^{N_1} - (\frac{\hat{r}}{r})^{N}.$$

□

As for statement 4, we may expand any initial density in terms of Chebyshev polynomials, and truncate the series so that the truncation error is arbitrarily small. The last three statements imply that all non-negligible approximate eigenfunctions satisfy eq.(3.100). Thus, we need only employ linear algebra for finite matrices to determine an approximate spectral decomposition of the initial density $\rho(x) \in F_{r\hat{K}}$, so the fourth statement is trivially true.

□

Our analysis so far has been restricted to matrix representations of $\mathcal{U}$ where $\hat{r} < r$, that is where every inverse branch map Ξ_r into $\Xi_{\hat{r}}$. In fact, we need only demand this property for $\mathcal{U}^t$, $t > \tau \geq 1$, to prove that the dominant eigenfunctions and spectra of $\mathcal{U}$ can be obtained through its truncated representation.
Proof :

We will denote the matrix representation of $\mathcal{U}^\tau$ by $W_{\tau\, mn}$. The eigenfunctions of $\mathcal{U}$ (with eigenvalues $\{\lambda\}$ are of coarse eigenfunctions of $\mathcal{U}^\tau$ with eigenvalues $\{\hat{\lambda}\} = \{\lambda^\tau\}$. By assumption we may determine a truncation order for $W_{\tau\, mn}$ such that the missing eigenvalues are of negligible magnitude, ϵ^τ. Thus, each analytic eigenfunction having a non-negligible eigenvalue has the property that

$$|v_n| \leq \frac{\hat{K}}{r_0}, \tag{3.111}$$

where $1 < r_0 < R$, and R is the largest ellipse within which this eigenfunction is analytic. The matrix representation is again of the form,

$$W_{mn} \leq \frac{C}{2}\frac{\hat{r}^n + \hat{r}^{-n}}{r^m}, \tag{3.112}$$

where $1 < r < R$, but unlike the hyperbolic case $\hat{r} > r$. The eigenfunction $v(x)$ and its eigenvalue λ satisfy the truncated eigenvector equation within an error ϵ_1. That is,

$$|\sum_{n=0}^{N_1} W_{mn} v_n - \lambda v_m| < \epsilon_1, \tag{3.113}$$

where

$$\epsilon_1 \leq KC\left(\frac{(\frac{\hat{r}}{r_0})^{N_1}}{(\frac{r_0}{\hat{r}}) - 1}\right). \tag{3.114}$$

Now, we may choose $\hat{r} = 1 + \hat{\delta}$ by setting $r = 1 + \delta$, where δ can be as small as desired. Hence, we can make ϵ_1 arbitrarily small by truncating the representation at a suitably high order. This means that the dominant eigenfunction and spectra of $\mathcal{U}$ satisfy eq.(3.99), but for a larger order of truncation than for $\mathcal{U}^\tau$. One can show similarly that the functions $\{\hat{v}(x)\}$ corresponding to the dominant eigenvectors of the truncated matrix satisfy eq.(3.100).

□

In light of the last result it is obvious that statements 1 to 4 are also valid for any Markov analytic map, where spaces of functions piecewise analytic over Markov partitions are invariant under $\mathcal{U}$. One just applies the same argument for each cell of the Markov partition, finding a suitable truncation order for each cell. Their supremum then defines the appropriate truncation order for the whole matrix.

3.6 Temporal behaviour of truncation error

The objective of this section is to determine useful upper bounds bounds on the temporal growth of the truncation error, so that it may be controlled, and in particular, rendered negligible. For simplicity we will assume that $\mathcal{U}$ leaves the space of analytic function invariant, but the more general case of invariant piecewise analytic function spaces is treated identically.

Let

$$E_n\rho(x) = \sum_{k=0}^{N} \rho_k T_k(x), \tag{3.115}$$

where ρ_k denotes the k^{th} order expansion coefficient of $\rho(x)$ with respect to a Chebyshev basis. Thus

$$\mathcal{U} \approx \sum_{m=0}^{N}\sum_{n=0}^{N} W_{mn}\rho_n T_m(x) = E_n\mathcal{U}E_n\rho(x). \tag{3.116}$$

Now,

$$\begin{aligned} &|\mathcal{U}^n\rho(x) - (E\mathcal{U}E)^n\rho(x)| = \\ &\left|\mathcal{U}^n\rho(x) - \mathcal{U}(E\mathcal{U}E)^{n-1}\rho(x) + \mathcal{U}(E\mathcal{U}E)^{n-1}\rho(x) - (E\mathcal{U}E)^n\rho(x)\right| \\ &\leq |\mathcal{U}(\mathcal{U}^{n-1}\rho(x) - (E\mathcal{U}E)^{n-1}\rho(x))| + |(\mathcal{U} - E\mathcal{U})(E\mathcal{U}E)^{n-1}\rho(x)| \end{aligned} \tag{3.117}$$

Thus,

$$\begin{aligned} &||\mathcal{U}^n\rho(x) - (E\mathcal{U}E)^n\rho(x)|| \leq \\ &||\mathcal{U}^{n-1}\rho(x) - (E\mathcal{U}E)^{n-1}\rho(x)|| + ||(\mathcal{U} - E\mathcal{U})(E\mathcal{U}E)^{n-1}\rho(x)|| \end{aligned} \tag{3.118}$$

Let

$$\hat{\epsilon}_k = ||\mathcal{U}^k\rho(x) - (E\mathcal{U}E)^k\rho(x)|| \tag{3.119}$$

and

$$\gamma_k = ||(\mathcal{U} - E\mathcal{U})(E\mathcal{U}E)^{n-1}\rho(x)||, \tag{3.120}$$

where $k = 1, 2, \cdots$. Then an upper bound on the measure error evolves according to

$$\hat{\epsilon}_n \leq \hat{\epsilon}_{n-1} + \gamma_{n-1}, \tag{3.121}$$

where $\gamma_0 = 0$. Now if

$$\forall t,\ (E\mathcal{U}E)^t\rho(x) \in F_{r,K}, \tag{3.122}$$

then we can use eq.(3.112) to show $\forall \epsilon > 0$ there exists a truncation order N such that

$$\begin{aligned} |\mathcal{U}\rho(x) - E\mathcal{U}E\rho(x)| &< \epsilon \\ |(\mathcal{U} - E\mathcal{U})(E\mathcal{U}E)^{n-1}| &< \epsilon. \end{aligned} \quad (3.123)$$

Integrating over the interval $[-1, 1]$ we find $\forall t > 1$, $\gamma_{t-1} < 2\epsilon$ and $\hat{\epsilon}_1 < 2\epsilon$, so that

$$\forall t > 1,\ \hat{\epsilon}_t \leq 2t\epsilon. \quad (3.124)$$

As ϵ decreases exponentially quickly as order of truncation is increased, we need at most increase the truncation order logarithmically in t, to have negligible measure error. If the magnitude of the leading eigenvalues of the truncated matrix are less than or equal to one, then eq.(3.124) will be valid. However, it is possible that the leading eigenvalues of the truncated matrix may be marginally greater than one. and then the bound K_t such that

$$(E\mathcal{U}E)^t \in F_{r,K_t} \quad (3.125)$$

may asymptotically diverge !

Nevertheless, we can still show that we need only increase the basis slightly faster than logarithmically in t, to ensure that the measure error remains vanishingly small. To see why, let us first note that the decomposition theorem for smoothing Markov operators[56, 67] (see eq.(2.9)) stated in section 2.1 implies that any eigenfunction having an eigenvalue of unit magnitude[4] is orthogonal to all other eigenfunctions, i.e if $\mathcal{U}v_\lambda(x) = \lambda v_\lambda(x)$ and $\mathcal{U}v'_\lambda(x) = \lambda v'_\lambda(x)$, where $|\lambda| = |\lambda'| = 1$, then

$$\int_\Omega v(x)v'(x)dx = 0. \quad (3.126)$$

This relation is also valid for the vector representations of $v_\lambda(x)$ and $v_{\lambda'}(x)$, i.e $\vec{v}_\lambda.\vec{v}_{\lambda'} = 0$, if $|\lambda| = 1$ or $|\lambda'| = 1$. From this fact, and eq.(3.99) it follows that for every eigenvalue λ of $\mathcal{U}$ of unit magnitude, there is a corresponding eigenvalue $\tilde{\lambda}$ of the truncated matrix such that $|\lambda - \tilde{\lambda}| < \epsilon_0$, and ϵ_0 decreases exponentially quickly with increasing truncation order. Let us also make the obvious remark that the asymptotic behaviour of $(E\mathcal{U}E)^t\rho(x)$ depends on the dominant eigenfunctions of $E\mathcal{U}E$ corresponding to these latter eigenvalue. One may readily show that there exists a constant κ such that

$$\gamma_t < \kappa|1 + \epsilon_0|^{t-1}\epsilon_1, \quad (3.127)$$

where the error ϵ_1 also decreases exponentially with the truncation order N. Finally, from our previous discussions, $|\mathcal{U}\rho(x) - E\mathcal{U}E\rho(x)| < \epsilon_2$, and again ϵ_2 decreases exponentially with the truncation order N. Now taking into account that the measure error is less than or equal to twice the absolute error, and plugging all the relations into eq.(3.121) we get,

$$\begin{aligned} \hat{\epsilon}_t &< \hat{\epsilon}_{t-1} + 2\kappa(1 + \epsilon_0)^{t-1}\epsilon_1 \\ \hat{\epsilon}_1 &< 2\epsilon_2. \end{aligned} \quad (3.128)$$

[4]If the system is mixing, then there will only be one such eigenfunction.

To simplify matters, let us redefine ϵ_1 and ϵ_2 to get rid of the constant factors of κ and 2,

$$\begin{aligned} \hat{\epsilon}_t &< \hat{\epsilon}_{t-1} + (1+\epsilon_0)^{t-1}\epsilon_1 \\ \hat{\epsilon}_1 &< \epsilon_2. \end{aligned} \tag{3.129}$$

If we iterate this equation, we get

$$\epsilon_t \leq \epsilon_2 + \epsilon_1 \left(\frac{(1+\epsilon_0)^t - 1 - \epsilon_0}{\epsilon_0} \right). \tag{3.130}$$

Now for small ϵ_0, we may expand the above relations up to second order in t,

$$\hat{\epsilon}_t \approx \epsilon_2 + \epsilon_1 \left(t - 1 + \frac{(t)(t-1)}{2}\epsilon_0, \right) \tag{3.131}$$

which shows that if we increase N logarithmically with the time T that we wish to make predictions, the measure error will be negligible. Let us stress that this is upper bound on the required increase of the basis with time is a worst case scenario. Moreover, once a system has settled into its asymptotic state, no new information is obtained by evolving distributions further in time.

3.7 Connection with the zeta function formalism

In section 2.3 of the last chapter on piecewise linear Markov maps we established a relation between the zeta function formalism and our matrix representations of $\mathcal{U}$ acting on the space of functions which are piecewise polynomial over the minimal Markov partition. It was shown that if $\mathcal{U}$ leaves the space of analytic functions invariant, then our method, and the dynamical zeta functions give the same decay rates of time correlation functions of analytic observables. This will be the case if the minimal Markov partition consists of one cell only, the unit interval, or equivalently, no fixed points or periodic orbits form the interface between cells of the minimal Markov partition. However, typical Markov analytic maps have multi-cell Markov partitions, and in this case, the dynamical zeta functions do not generally give the correct decay rates. For the linear case, we derived a general formula for the correction factor. In the present section, the latter results will be generalized to all Markov analytic maps (i.e also with curvature). The derivation is similar to the linear case, except that as piecewise polynomial function spaces are not invariant under $\mathcal{U}$, we are forced to exploit a lemma of D. Mayer[70] on generalized composition operators.

As stated previously, one of the purposes of the zeta function formalism is to relate the decay rates of time correlation functions of appropriate observables to the zeros of the function,

$$Z_s(z) = \det(1 - z\mathcal{U}), \tag{3.132}$$

through the zeros of the function

$$\tilde{Z}_s(z) = \prod_{k=1}^{\infty} \frac{1}{\zeta_k(z)}, \tag{3.133}$$

where

$$\zeta_k(z) = \prod_p \left(1 - \frac{z^{n_p}}{|\wedge_p| \wedge_p^{k-1}}\right)^{-1}, \tag{3.134}$$

$\prod_p$, n_p and $\wedge_p$ denote the product over all periodic orbits, the period of the p^{th} periodic orbit and its relative stability or instability factor $f'(x_1)f'(x_2)...f'(x_p)$ respectively. $\zeta_k(z)$ is an example of a dynamical zeta function. The zeros of $Z_s(z)$ equal the reciprocals of the eigenvalues of $\mathcal{U}$ if $\mathcal{U}$ is a nuclear operator[70] of order less than or equal to $\frac{2}{3}$[5]. In the zeta function formalism one seeks to relate the zeros of $Z_s(z)$ to the zeros of $\tilde{Z}_s(z)$. For all Markov analytic maps it was believed that

$$Z_s(z) = \tilde{Z}_s(z). \tag{3.135}$$

We will show that equality above generally holds only if the space of analytic functions is invariant under $\mathcal{U}$, and will derive a simple correction factor equal to

$$\frac{Z_s(z)}{\tilde{Z}_s(z)}$$

which is valid for all piecewise linear Markov maps. As before, we will use the trace formula

$$\begin{aligned} \det(1 - zT) &= \exp\left(\mathrm{Tr}\,(\ln(1 - zT)\right) \\ &= \exp(-\sum_{n=1}^{\infty} \frac{z^n}{n} \mathrm{Tr}\,(T^n)) \end{aligned} \tag{3.136}$$

to relate the eigenvalues of $\mathcal{W}$ to an expression involving $Z_s(s)$. Let us now apply formula (3.136) to $\det(1 - z\mathcal{W})$,

$$\begin{aligned} \det(1 - z\mathcal{W}) &= \exp[\mathrm{Tr}\,(\ln(1 - z\mathcal{W})] \\ &= \exp\left(-\sum_{n=1}^{\infty} \frac{z^n}{n} \mathrm{Tr}\,(\mathcal{W}^n)\right). \end{aligned} \tag{3.137}$$

We need now to determine $\mathrm{Tr}\,(\mathcal{W}^n)$. The trace of $\mathcal{W}^n$ is defined by,

$$\mathrm{Tr}\,(\mathcal{W}^n) = \sum_i \sum_{m=0}^{\infty} \mathcal{W}^n_{imim} \tag{3.138}$$

Now from eq.(3.78), we saw that

$$\mathcal{W}_{imin} = \sum_\alpha \mathcal{W}_{\alpha imin},$$

where the sum is over inverse branches. As in the last chapter, we note that the cell C_i can undergo a transition into itself via the inverse branch $g_\alpha(x)$ only if either $g_{\alpha x}$ has a fixed point in the interior of the cell C_i or has a fixed point on the boundary of the cell

[5]We do not know if $Z_s(z)$ equals $\tilde{Z}_s(z)$ under weaker conditions. Note also that the form of $\tilde{Z}_s(z)$ is slightly different in higher dimensions.

C_i and $g_{\alpha x}$ is monotonic increasing. Obviously, these are also necessary but not sufficient conditions for $\mathcal{W}_{\alpha imin}$ to be non-zero.

We observe from eqs.(3.81), (3.82) that

$$\begin{aligned}
\mathcal{W}_{\alpha imin} &= H_m \sigma_\alpha \int_{C_i} g'_{\alpha_i}(x) T_{im}(x) T_{in}(g_{\alpha_i}(x)) w_i(x) dx \\
&= H_m \frac{\sigma_\alpha}{\delta_i} \int_{C_i} g'_{\alpha_i}(x) T_m(h_i(x)) T_n(h_i(g_{\alpha_i}(x))) w(h_i(x)) dx \\
&= H_m \sigma_\alpha \int_{-1}^{1} g'{}_{\alpha_i}({h_i}^{-1}(x)) T_m(x) T_n(h_i(g_{\alpha_i}({h_i}^{-1}(x)))) w(x) dx \qquad (3.139)
\end{aligned}$$

If we let

$$G_{\alpha i}(z) = h_i(g_{\alpha_i}({h_i}^{-1}(z))) \qquad (3.140)$$

we see that $W_{\alpha imin}$ is the matrix representation of a Frobenius-Perron like operator,

$$\hat{U}_{\alpha i} \hat{\rho}(x) = \hat{\rho}(G_{\alpha i}(x)) |\frac{d}{dx} G_{\alpha i}(x)|, \qquad (3.141)$$

where $G_{\alpha i}(z)$ is an analytic map of the unit interval into itself. Moreover, if all the inverse branches of the Markov map are contractive, so will be $G_{\alpha i}$. In particular, every fixed point x_* of the the inverse branch $g_\alpha(x)$, where $x \in C_i$ defines an equivalent fixed point $\hat{x}_* = h_i^{-1}(x_*)$ of $G_{\alpha i}(x)$, having precisely the same contraction rate as x_*. We now use an elegant lemma presented by Mayer[70] which determines the spectra, and hence the trace of operators like $\hat{U}_{\alpha i}$ acting on the space of functions which are analytic in a complex domain containing the interval. *If ψ maps the domain $D \subset C$ strictly inside itself then the spectrum of the generalized composition operator $\mathcal{L}g = \varphi C_\phi g$ on the space $A_\infty(D)$ consists of the eigenvalues*

$$\lambda_n = \varphi(z*)(\psi'(z*))^n,\ n = 0, 1, 2,$$

converging to the point 0, where $z*$ is the unique fixed point of ψ in D. Every eigenvalue is simple. One can easily show that this lemma is also valid if $\psi(z)$ is only eventually contractive, i.e.

$$\exists \tau : \forall t > \tau, \forall z \in D,\ |\frac{d}{dz}\psi^t(z)| < 1, \qquad (3.142)$$

and there exists a real interval $I \subset D$ such that

$$\psi(I) \subset I. \qquad (3.143)$$

In our case,

$$\varphi \equiv \sigma \frac{d}{dx} G_{\alpha i}(x) = |\frac{d}{dx} G_{\alpha i}(x)|,$$

and

$$C_\psi g = g(\psi(z)) \equiv \hat{\rho}(G_{\alpha i}(z)).$$

Thus

$$\sum_{n=0}^{\infty} \mathcal{W}_{\alpha inin} = \sum_{k=0}^{\infty} (\frac{d}{dx} G_{\alpha i}(\hat{x}*))^k |\frac{d}{dx} G_{\alpha i}(\hat{x}*)|, \qquad (3.144)$$

Equivalently,

$$\sum_{n=0}^{\infty} \mathcal{W}_{inin} = \sum_{k=0}^{\infty} \left(\sum_{x_* \in Int(C_i)} \frac{1}{f^{n\prime k}(x_*)|f^{n\prime}(x_*)|} + \sum_{x_* \in B(C_i)} \frac{1}{f^{n\prime k}(x_*)|f^{n\prime}(x_*)|} \right) \tag{3.145}$$

where the first sum is over fixed points lying in the interior of the cell ($Int(C_i)$) and the second sum is over fixed points lying on the boundary of the cell ($B(C_i) = \{a_{i-1}, a_i\}$ associated with monotonic increasing branches. We may rearrange the right hand side of eq.(3.145),

$$\mathrm{Tr}\,(\mathcal{W}) = \sum_{k=0}^{\infty} \left(\sum_{x_*} \frac{1}{f'^k(x_*)|f'(x_*)|} + \sum_{y_{*1}} \frac{1}{f'^{k+1}(y_{*1})} - \sum_{y_{*2}} \frac{1}{f'^k(y_{*2})|f'(y_{*2})|} \right), \tag{3.146}$$

where the consecutive summations are over all fixed points, and fixed points having the following properties:

1. The inverse branch having y_{*1} as a fixed point is defined on either side of y_{*1}.
2. The inverse branch having y_{*2} as a fixed point is monotonic decreasing, but is defined only to one side of y_{*2}.

One may verify eq.(3.146) through the following observations. First, the fixed points $\{y_{*2}\}$ do not contribute to the trace. Second, consider two cells

$$C_i = [a_{i-1}, y_{*1}],\; C_{i+1} = [y_{*1}, a_i],$$

where y_{*1} forms the interface. If y_{*1} is a fixed point of a monotonic increasing branch, then

$$f_\alpha^{-1}(C_i) \subset C_i \text{ and } f_\alpha^{-1}(C_{i+1}) \subset C_{i+1}.$$

Thus the fixed point will give the same contribution twice. But, if $f_\alpha^{-1}(x)$ is monotonic decreasing, then the latter transitions do not occur, and the fixed point should not contribute to the trace[6]. One can show in a similar fashion that

$$\mathrm{Tr}\,(\mathcal{W}^n) = \sum_{k=0}^{\infty} \left(\sum_{x_*} \frac{1}{f^{n\prime k}(x_*)|f^{n\prime}(x_*)|} + \sum_{y_{*1}} \frac{1}{f^{n\prime k+1}(y_{*1})} - \sum_{y_{*2}} \frac{1}{f^{n\prime k}(y_{*2})|f^{n\prime}(y_{*2})|} \right). \tag{3.147}$$

where the sums are now over the fixed points of $f^n(x)$. In the sequel, any type of periodic orbit will be denoted by p. In addition, class 1 periodic orbits will also be denoted by p_1, and class 2 periodic orbits will be denoted by p_2

Let us now come back to eq.(3.137). Any periodic orbit p of period N_p will contributing to eq.(3.147) only if N_p is a divisor of n. We shall denote the set of all periodic orbits whose period N_p is a divisor of n by N_p/n. We shall adopt the argument and notation of Artuso et al[23, 7]. In general, the n^{th} order trace picks up contributions from N_p/n. Therefore

$$\mathrm{Tr}\,\mathcal{W}^n = \sum_{k=1}^{\infty} \left(\sum_{N_p/n} N_p t_p^{\frac{n}{N_p}} + \sum_{N_{p_1}/n} N_{p_1} \hat{t}_{p_1}^{\frac{n}{N_{p_1}}} - \sum_{N_{p_2}/n} N_{p_2} t_{p_2}^{\frac{n}{N_{p_2}}} \right), \tag{3.148}$$

[6] We note that due to the absolute convergence of the sums above, the summations can be reordered without changing their value.

where

$$t_p = \frac{1}{f^{N_p\prime}(x_*)^{k-1}|f^{N_p\prime}(x_*)|}, \text{ and } \hat{t}_{\hat{p}} = \frac{1}{f^{N_{\hat{p}}\prime}(x_*)^k} \tag{3.149}$$

and x_* is a fixed point of $f^{N_p}(x_*)$. Let $r = \frac{n}{N_p}$. We can express eq.(3.137) as

$$\begin{aligned}
det(1 - z\mathcal{W})) &= exp \sum_{k=1}^{\infty} \left(-\sum_p \sum_{r=1}^{\infty} \frac{(z^{N_p} t_p)^r}{r} - \sum_{p_1} \sum_{r=1}^{\infty} \frac{(z^{N_{p_1}} \hat{t}_{p_1})^r}{r} + \sum_{p_2} \sum_{r=1}^{\infty} \frac{(z^{N_{p_2}} t_{p_2})^r}{r} \right) \\
&= exp \sum_{k=1}^{\infty} \left(\sum_p \ln(1 - z^{N_p} t_p) + \sum_{p_1} \ln(1 - z^{N_{p_1}} \hat{t}_{p_1}) - \sum_{p_2} \ln(1 - z^{N_{p_2}} t_{p_2}) \right) \\
&= \prod_{k=1}^{\infty} \left(\prod_p (1 - z^{N_p} t_p) \prod_{p_1} (1 - z^{N_{p_1}} \hat{t}_{p_1}) \frac{1}{\prod_{p_2}(1 - z^{N_{p_2}} t_{p_2})} \right) \\
&= \prod_{k=1}^{\infty} \left(\frac{\eta_k(z) \xi_k(z)}{\zeta_k(z)} \right),
\end{aligned} \tag{3.150}$$

where

$$\eta_k(z) = \prod_{\hat{p}} (1 - z^{N_{\hat{p}}} \hat{t}_{\hat{p}}), \tag{3.151}$$

$$\xi_k(z) = \frac{1}{\prod_{p_2}(1 - z^{N_{p_2}} t_{p_2}).} \tag{3.152}$$

Thus,

$$det(1 - z\mathcal{U}) = \prod_{k=1}^{\infty} \frac{\eta_k(z)\xi_k(z)}{\zeta_k(z)} = \tilde{Z}_s(z) \prod_{k=1}^{\infty} \eta_k(z)\xi_k(z), \tag{3.153}$$

and

$$\frac{Z_s(z)}{\tilde{Z}_s(z)} = \prod_{k=1}^{\infty} \eta_k(z)\xi_k(z). \tag{3.154}$$

Let us repeat certain observations made for the piecewise linear case: (i) the number of periodic orbits producing in $\eta_k(z)$ $\xi(z)$ are finite; and (ii) the zeros of $\eta_k(z)$ describe a decaying oscillation with period $\hat{p}$ if $\hat{t}_{\hat{p}}$ is positive, and period $2\hat{p}$ is $\hat{t}_{\hat{p}}$ is negative. If more than one periodic orbit forms the interface between a periodic orbit (which can be the case if there is more than one critical point) then the above oscillations will occur for all such periodic orbits. Again, we stress that the functions $\eta_k(z)$ and $\xi_k(z)$ do not occur in eq.(3.153) if the space of analytic functions is invariant under $\mathcal{U}$. The nature of the link between our method and the zeta function formalism is thus clearly established.

3.8 Local statistical properties

Periodic orbits are believed to be densely distributed in the phase space for chaotic systems. The elements of orbits of low period tend to be well spaced, as the period increases, the distance between adjacent elements typically decreases. In this section we will show how this wealth of scales can be exploited to describe local statistical properties, such as the evolution of almost point like initial conditions, local fluctuations and patterns etc. We will also relate the correction factors appearing in eq.(3.153) to spectra associated with the periodic orbit(s) coinciding with elements of $\mathcal{P}_{min}$.

3.8.1 Partition self-refinement

In the last section we saw that given a Markov analytic map, the space F_{min} of functions piecewise analytic over $\mathcal{P}_{min}$ is invariant under $\mathcal{U}$. Invariance was a consequence of eqs. (3.65) - (3.68) being satisfied for $\mathcal{P}_{min}$. These equations are also satisfied for partitions $\mathcal{P}_M$ formed by the refinement of $\mathcal{P}_{min}$ through the addition of either (a) inverse images of some/all the points defining $\mathcal{P}_{min}$; or (b) all the elements of a finite number of periodic orbits. Thus, the results of the previous section are also valid for spaces of functions F_M piecewise analytic over any such $\mathcal{P}_M$. One may then ask does the spectra of $\mathcal{U}$ acting on such function spaces change for different choices of P_M ? Let's denote the spectra associated with $\mathcal{P}_{min}$ by sp_{min}, and the spectra associated with $\mathcal{P}_M$ by sp_M. As $F_{min} \subset F_M$ it follows that $sp_{min} \subset \mathcal{P}_M$. Let us first consider partitions formed by self-refinement (a). In this case any density which is initialy piecewise analytic over P_M will after a finite number of iterations (equal to the number of sucessive self refinements) be piecewise analytic over $\mathcal{P}_{min}$. It follows that $sp_M = sp_{min}$. The zero eigenvalue will become degenerate, with the trivial zero function as the only eigenfunction. Thus, associated with F_M is an infinite dimensional Jordan block, corresponding to an infinitely degenerate zero eigenvalue.

3.8.2 Partition refinement with periodic orbits

Suppose that $\mathcal{P}_M$ is constructed not through self-refinement of $\mathcal{P}_{min}$, but by adding all the elements of a periodic orbit of period p to $\mathcal{P}_{min}$. In this case (with the exception of accidental degeneracy) we get new additional spectra $sp_M \supset sp_{min}$. The eigenvalues are

$$\begin{aligned}\{\lambda\} &= \frac{1}{\sqrt[p]{(f^{p\prime}(x_l))^{k+1}}}, \\ &= \left|\frac{1}{\sqrt[p]{(f^{p\prime}(x_l))^{k+1}}}\right| \exp(i\gamma\pi j/p), \end{aligned} \tag{3.155}$$

where

$$\gamma = \begin{cases} 1, & \text{if } (f^{p\prime}(x_l))^{k+1} < 0; \\ 2, & \text{otherwise,} \end{cases}, \tag{3.156}$$
$$k = 0, 1, 2, 3..., \; and \; j = 1, 2, 3, ...p$$

and x_l belongs to a periodic orbit of period p. They describe a decaying oscillatory mode with period p if the argument of the p^{th} root is positive, and $2p$ if it is negative.
Proof:

Before deriving eqn.(3.155) we shall make a few observations. Let $\{X_1, X_2, ...X_p\}$ denote a periodic orbit of period p. Let

$$g(x) = \psi_{min}(x) + \phi(x)\chi_{[X_i,a_i]}(x), \tag{3.157}$$

where $X_i \in [a_{i-1}, a_i] = C_i$, and $\psi_{min}(x)$ is any function piecewise analytic over $\mathcal{P}_{min}$. If

$$\forall k \leq n, \; \frac{d^k}{dx^k}\phi(X_i) = 0, \tag{3.158}$$

then

$$\mathcal{U}g(x) = \hat{\psi}_{min} + \hat{\phi}(x)\chi_{[X_{i+1},a_j]}(x), \tag{3.159}$$

where $\phi(x)$ also satisfies eq.(3.158). Therefore we can construct nested extensions of the original function space F_{min}; $F_0 \supset F_1 \supset F_2 \supset F_3 \cdots \supset F_{min}$. The function spaces F_r are therefore invariant under $\mathcal{U}$.

For simplicity, lets first consider the case of the a periodic orbit being just a fixed point. Suppose there exists an eigenfunction $v(x) \in F_0$,

$$v(x) = v_{min}(x) + \hat{v}(x)\chi_{[X^*,a_j]}(x). \tag{3.160}$$

Then

$$\mathcal{U}v(x) = \lambda v(x) \tag{3.161}$$

and

$$\mathcal{U}v(x^* + \epsilon) - \mathcal{U}v(x^* - \epsilon) = \lambda(v(x^* + \epsilon) - v(x^* - \epsilon)), \tag{3.162}$$

where $0 < \epsilon \ll 1$. We note that only one inverse branch can have x^* as a fixed point, which we'll suppose is the α branch. Using eq.(3.157) and taking the limit of small ϵ we find

$$\sigma_\alpha \hat{v}(x^*)|\frac{d}{dx}f_\alpha^{-1}(x^*)| = \hat{v}(x^*)\frac{d}{dx}f_\alpha^{-1}(x^*) = \lambda\hat{v}(x^*). \tag{3.163}$$

Therefore $\lambda = \frac{d}{dx}f_\alpha^{-1}(x^*)$. Let's now note that

$$\frac{d^n}{dx^n}(\mathcal{U}v(x^* + \epsilon)) - \frac{d^n}{dx^n}(\mathcal{U}v(x^* - \epsilon)) = \lambda(\frac{d^n}{dx^n}(v(x^* + \epsilon)) - \frac{d^n}{dx^n}(v(x^* - \epsilon)), \tag{3.164}$$

which implies that

$$\frac{d^n}{dx^n}((\hat{v}(f_\alpha^{-1}(x)\frac{d}{dx}f_\alpha^{-1}(x)) = \lambda\frac{d^n}{dx^n}\hat{v}(x), \tag{3.165}$$

at $x = x^*$. In fact, we can completely determine $\hat{v}(x)$ by solving recursively the above equation, for which it is a unique solution up to a constant factor. Consider an eigenfunction $v(x) \in F_1$. By definition $\frac{d}{dx}\hat{v}(x^*) = 0$. Inserting this into eq.(3.165) for $n = 1$ we find $\lambda = \frac{d}{dx}f_\alpha^{-1}(x^*)^2$ and again $\hat{v}$ can be completely determined by solving recursively eq.(3.165) with this eigenvalue. In general if $v(x) \in F_k$ then $\mathcal{U}v(x) = \lambda_k v(x)$, where

$$\lambda_k = \frac{d}{dx}f_\alpha^{-1}(x^*)^k. \tag{3.166}$$

Let's now generalize the above construction to a periodic orbit of period p. We suppose that $\mathcal{U}v(x) = \lambda v(x)$

$$v(x) = v_{min}(x) + \hat{v}(x), \tag{3.167}$$

where

$$\hat{v}(x) = \sum_{\ell=1}^{p}\phi_\ell(x)\chi_{[X_\ell,a_{i*}]}(x). \tag{3.168}$$

If $v(x) \in F_r$ it is obvious that

$$\forall\ell,\ 1 \leq \ell \geq p,\ \frac{d^r}{dx^r}\phi_\ell(X_\ell) \neq 0). \tag{3.169}$$

Let's note that X_ℓ is mapped to $X_{\ell-1}$ by a unique inverse branch, which we'll refer to as $f^{-1}_{\ell\to\ell-1}(x)$, where we've adopted the convention that $X_{1-1} = X_p$. The generalization of eq.(3.164) is

$$\frac{d^n}{dx^n}(\mathcal{U}v(x_\ell+\epsilon)) - \frac{d^n}{dx^n}(\mathcal{U}v(x_\ell-\epsilon)) = \lambda(\frac{d^n}{dx^n}(v(x_\ell+\epsilon)) - \frac{d^n}{dx^n}(v(x_\ell-\epsilon)), \tag{3.170}$$

for all elements x_ℓ of the periodic orbit. This implies that

$$\frac{d^n}{dx^n}((\phi_{\ell-1}(f^{-1}_{\ell\to\ell-1}(x)\frac{d}{dx}f^{-1}_{\ell\to\ell-1}(x)) = \lambda\frac{d^n}{dx^n}\phi_\ell(x), \tag{3.171}$$

at $x = x_\ell$. Consider first the case that $v(x) \in F_0$. We get p coupled equations of the form

$$\phi_{\ell-1}(x_{\ell-1})\frac{d}{dx}f^{-1}_{\ell\to\ell-1}(x_\ell) = \lambda\phi_\ell(x_\ell). \tag{3.172}$$

Solving them for λ and using the chain rule we find

$$\begin{aligned}\lambda^p &= \frac{d}{dx}f^{-1}_{p\to p-1}(x_p)\frac{d}{dx}f^{-1}_{p-1\to p-2}(x_{p-1})\cdots\frac{d}{dx}f^{-1}_{2\to 1}(x_2)\\ &= \frac{d}{dx}f^p(x_l),\end{aligned} \tag{3.173}$$

where the roots are given by eq.(3.155) with $k = 0$. Now for any of these eigenvalues we can determine $\hat{v}(x)$ by solving recursively eq.(3.171) for $n = 1, 2, \cdots$. The general case of $v(x) \in F_r$ is treated in the same way, where we find the eigenvalues are given by eq.(3.155).

□

3.8.3 Example

To illustrate the results of subsection 3.8.2 let us return to the one parameter family of maps considered in subsection 3.3.3. This one parameter family of maps on the interval is defined as

$$f(x) = \begin{cases} f_L(x) = \frac{a-\sqrt{a^2-(4a-2)x}}{2a-1} & \text{if } 0 \le x < \frac{1}{2} \\ f_R(x) = f_L(1-x) & \text{otherwise} \end{cases}, \tag{3.174}$$

where $0 \le a \le 1$. We have already seen in fig. 3.9 the spectra (sp_{min}) of $\mathcal{U}$ acting on the space of analytic function for members of this family. Suppose for members of this family that we partition the interval two cells $[0, x^*]$ and $[x^*, 1]$ using the the fixed point x^* of the right branch of the map, and inquire about the nature of the spectra (sp_M) of $\mathcal{U}$ acting on corresponding space of piecewise analytic functions. The last subsection predicts that $sp_{min} \subset sp_M$, and eq.(3.155) states that $sp_M = sp_{min} \bigcup sp_*$ where

$$sp_* = \{f'(x^*)^{-k-1},\ k = 0, 1, \cdots\}, \tag{3.175}$$

and as $f'(x^*) < 0$, the eigenvalue $f'(x^*)^{-1}$ describes a period two exponentially decaying oscillatory mode. A plot of sp_{min} together with the new spectra (in magnitude) is given in fig. 3.10. This shows that there are parameters values (e.g. $a < 0.6$) where the asymptotic

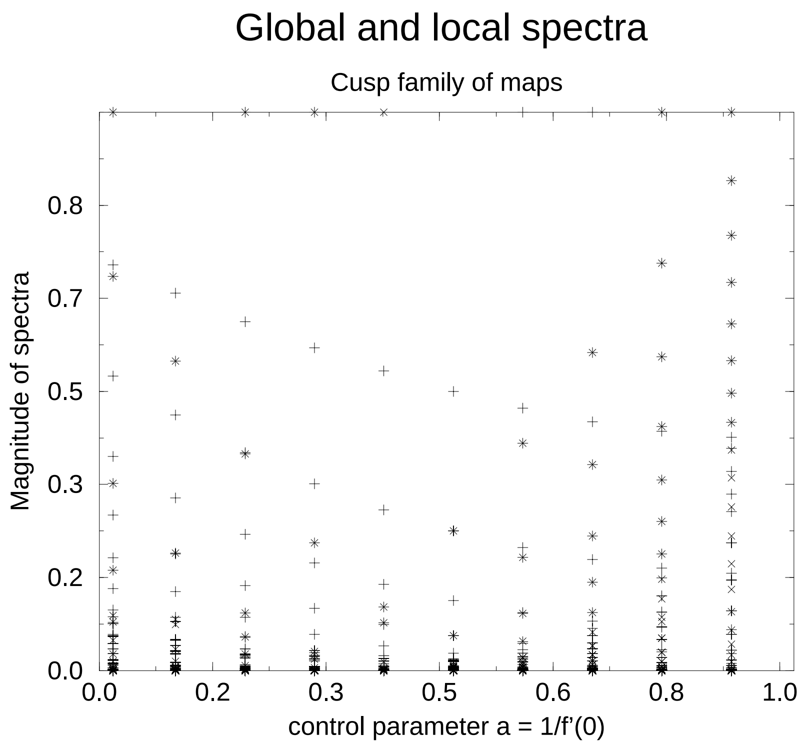

Figure 3.10: Global and local spectra versus the control parameter. The spectra of $\mathcal{U}$ acting on the space of analytic functions are denoted by $\times$'s (sp_{min}), and the spectra of $\mathcal{U}$ acting on the space of functions piecewise analytic over the partition $\{0, x^{*}, 1\}$ (sp_M) are denoted by $+$'s. Eigenvalues belonging to both sets are represented by $*$'s. Clearly, for $a < .6$, there exist eigenvalues of sp_{*} which are more dominant than those of sp_{min}.

decay rates of time correlation functions of observables with only local support are given by eq.(3.175), rather than sp_{min}. As a specific example, let us consider the map corresponding to $a = 0.01$. The dominant spectra of sp_{min} are:

$$1, -0.705776, 0.334810, -0.180066, \cdots,$$

and the dominant spectra of sp_M are

$$\begin{gathered} 1, -0.726296, \quad -0.705776 \quad, 0.5275, -0.383126, \\ 0.33481, 0.27826, \quad -0.20210 \quad, -0.18005, 0.146804, \cdots, \end{gathered}$$

respectively. Let us compare the new latter eigenvalues with the prediction of Eq.(3.175), which states that the new eigenvalues within the first 5 digits are

$$\begin{gathered} -0.726296, \quad 0.527506 \quad, -0.383126, \\ 0.278263, \quad -0.202101 \quad, 0.146785, \cdots. \end{gathered}$$

The accuracy within which the predicted values equal those obtained through the matrix representation is remarkable, given that the latter is obtained through numerical calculations. We also notice that the new spectra are comparatively large in magnitude with respect to sp_{min}, and so we may anticipate that time correlation functions of observables having support essentially over one or other cell may decay more slowly that observables having support over the entire interval. Accordingly, let us now compare the difference between local and global statistical properties from the perspective of the following time correlation functions:

$$C_{A,B}(\tau) = \int_0^1 A(x)\mathcal{U}^\tau[B(x)\rho_{inv}(x)]dx \tag{3.176}$$

$$A(x) = B(x) \quad \text{and} \quad B(x) = x \tag{3.177}$$

$$A(x) = B(x) \quad \text{and} \quad B(x) = \chi_{[x^*,1]}(x). \tag{3.178}$$

The results are displayed in fig. 3.11 (Left). Clearly, the local time correlation function[7]

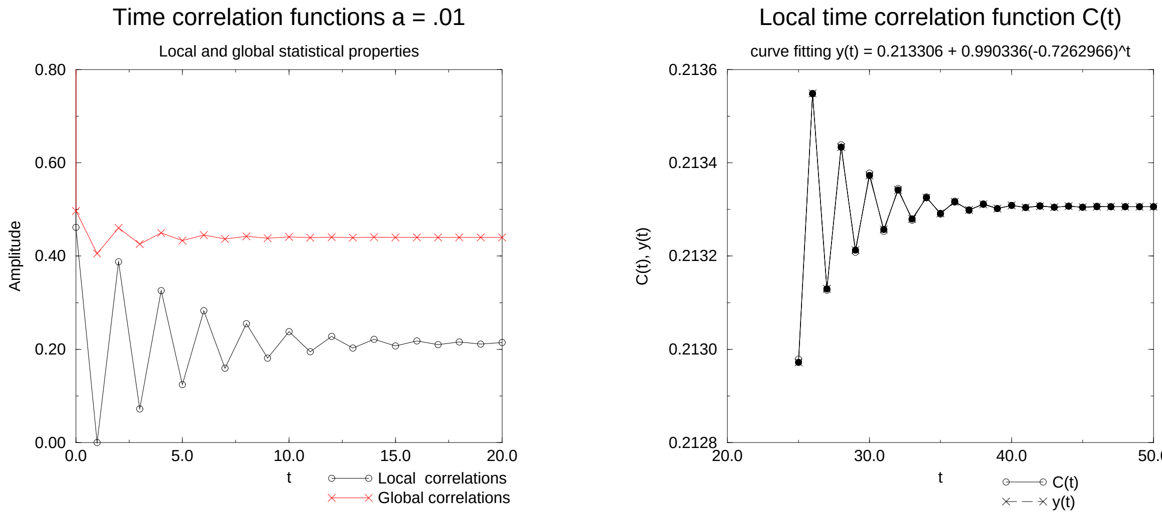

Figure 3.11: Left: Global and local time correlation correlation functions Right: The asymptotic decay rate of the time correlation function defined by eq.(3.178) is given by the largest (in magnitude) eigenvalue of sp_M, as expected.

corresponding to the observables eq.(3.178) decay more slowly than the autocorrelation function. Fig.3.11 (Right) shows that asymptotically it is characterised as a decaying period two oscillation, the exponent of which is equal to the second largest eigenvalue of sp_M.

3.9 Conclusion

We have demonstrated in this chapter that the choice of basis can be critical in obtaining convergent matrix representations of the Frobenius-Perron operator for arbitrary Markov analytic maps and equivalent repeller maps. But, by using piecewise Chebyshev basis convergence is guaranteed. Moreover, lower bounds on the convergence rate can be determined from the analytic properties of any map. We then proved that effective spectral

[7]We have also calculated these time correlation functions using a phase space trajectory one million iterations long. The results are within four digits of precision equal to those displayed here.

decompositions of $\mathcal{U}$ can be obtained using such a basis, and related the convergence of the representation as a function of the truncation order to the convergence of the spectral representation. One striking result for analytic (piecewise analytic) eigenfunctions concerns their expansions in terms of Chebyshev (piecewise Chebyshev) functions and the magnitude of their eigenvalues. It essentially states that the more irregular such an eigenfunction is (in the sense of the relative weighting of higher order expansion coefficients to lower order ones) the smaller the magnitude of the corresponding eigenvalue, and therefore, the faster the rate of decay. We then established the connection between our method, and the zeta function formalism, and pointed out that the dynamical zeta functions cannot be expected to give all the decay rates of analytical observables, if the minimal Markov partition consists of more than one cell. Fortunately, we were able to determine the correction factors, which it turns out, are related to the local statistical properties of the system. We derived a formula for the spectra associated with observables having support over local regions, and demonstrated its validity on concrete examples. In the following chapters, these results will be used, and generalized to non-hyperbolic chaotic maps, and two dimensional hyperbolic chaotic maps respectively.

Chapter 4

One dimensional non-hyperbolic chaos

4.1 Introduction

It is surprising that a simple looking map, $f_r(x) = rx(1-x)$, eq.(1.14), should serve as an paradigm of complexity for systems in fields as diverse as biology, chemistry, optics and hydrodynamics. The discovery, that the period doubling route to chaos is so common, and can be understood qualitatively and even quantitatively through the logistic map, is one of the greatest successes up to now, of non-linear science[22, 8, 69, 35]. Its origin lies in the fact that one-dimensional discrete time dynamics governed by a unimodal mapping are often observed when return maps are constructed from experimental time series pertaining to a single variable, or from mathematical models of multivariate continuous-time dynamical systems [20]. Indeed, many of the key properties of the logistic are shared by experimental systems where no unimodal first return map has been obtained[101].

Let us first outline some of general features of the logistic map. Later, we will come to the main subject of this chapter, a statistical description of non-hyperbolic chaos[3].

The dynamical complexity of the logistic map as the control parameter is varied is immediately apparent from the bifurcation diagram and corresponding Lyapunov exponent in figure 4.1. A sequence of bifurcations occurs for $1 < r < r_\infty = 3.5699456$, characterised by the existence of stable periodic orbits, except at the period doubling points r_n, which scale as

$$r_n = r_\infty - const\,\delta^{-n},$$

for $n \gg 1$. The number $\delta = 4.6692016091$ is one of the celebrated Feigenbaum constants. For $r > r_\infty$, chaos is possible, but the phase space is at first disjoint, which gives rise to periodic chaos. The disjoint intervals merge together by sucessive inverse bifurcations, the merging points being at

$$\tilde{r}_n = r_\infty + const\,\delta^{-n},$$

until the iterates fill the entire interval at $r = 4$. For $r > 4$ the map is a chaotic repeller. However, within the potentially chaotic regime, periodic windows occur, characterised by periodic p-cycles ($p = 3, 5, 6, ...$) with sucessive period doubling, described by other "universal" exponents. The periodic windows are densely distributed within $[r_\infty, 4]$. Nevertheless, chaotic parameter values occur in this interval with a probability[101, 19] of

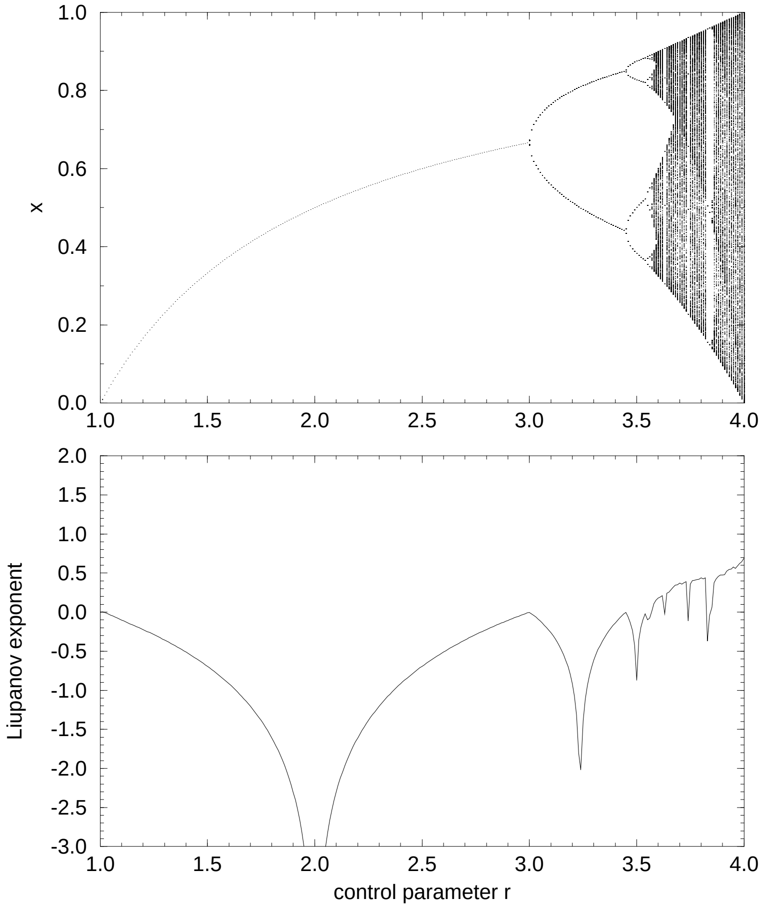

Figure 4.1: Bifurcation diagram and Lyapunov exponent for the logistic map

0.8979, and are distributed in the form a "fat" fractal[1]. Just before the period 3 window, at $r = 1 + \sqrt{8}$, type 1 intermittentcy[2] takes place, characterised by slowly evolving laminar behaviour, interspersed with chaotic bursts.

In addition to the principal features of unimodal maps in relation with the bifurcation of stable periodic orbits their ergodic properties have also been the subject of extensive studies. For example, proofs for the existence under certain conditions of an absolutely continuous invariant measure, and the exponential decay of time correlation functions are known, but are not very constructive. Our objective in the present chapter is to show that the statistical behaviour of such systems in the chaotic regime, including invariant densities, time-correlation functions and decay rates can be evaluated through an explicit matrix representation of the evolution operator $\mathcal{U}$.

The chief difficulty posed by the logistic map and several other experimentally obtained

[1] From a coarse grained perspective, the probability of finding a periodic window scales as $\mu(l) = \mu(0) + Al^{\beta}$, where $\mu(0) = 0.8979$ and $\beta = 0.45 \pm 0.005$. This has the result that given a chaotic parameter value, if one changes it by a small amount ϵ then the probability of it being in a periodic window is of the order ϵ^{β}

[2] Type 1 intermittentcy[101] is associated with tangent bifurcations, where a stable and unstable fixed point merge. To one side of (and close to) such critical parameter values the system is chaotic and intermittent, characterized by long laminar periods of evolution interspersed by explosive bursts

first-return maps, is due to existence of a quadratic extremum. The corresponding $\mathcal{U}$, when applied recursively on initialy analytic functions, produces singularities at all the iterates of the extremum. A method of treating these singularities is vital to any understanding of the statistical behavior of the system. Fortunately, these singularities are integrable if the Lyapunov exponent, when evaluated from the first iterate of the extremum, converges to a positive constant. The first goal of this chapter is the creation of basis sets of orthogonal functions capable of handling such singularities. This then permits one to obtain a matrix representation $\mathcal{W}$ of $\mathcal{U}$ which, typically, can be truncated when all periodic orbits are unstable. The eigenvectors and eigenvalues of $\mathcal{W}$ define, through the basis, a class of eigenfunctions and eigenvalues of $\mathcal{U}$. One can thus calculate time-correlation functions, spectra and invariant densities. The procedure will be illustrated on a few representative examples, especially to describe local statistical properties and to obtain a universal formula for the spectral gap as a function of the control parameter. This relation allows one to predict how quickly time correlation functions decay to their asymptotic values. Finally, we will prove from a statistical perspective, that all unimodal Markov maps with negative Schwarzian derivative, where the Lyapunov exponent calculated from the first iterate of the critical point is positive are equivalent to Markov analytic maps[70]. This result may be generalized to system with non-quadratic critical points if other assumptions are invoked. Henceforth, we shall refer to this class of maps as chaotic S-unimodal Markov maps.

The chapter is organized as follows.

- In section 4.2 we argue about the type of singularities generic to evolving probability densities, which give some insight on the nature of invariant function spaces $\{\mathcal{F}\}$ of $\mathcal{U}$. Following this ansatz, we construct an appropriate set of orthogonal functions and obtain matrix representations of $\mathcal{U}$ acting on each such $\mathcal{F}$.

- In section 4.3 we study some representative examples analytically and numerically, and show how non-Markov maps can be approximated by Markov ones. Next, for the logistic map (eq.(1.14)) we obtain a universal formula for the behaviour of the spectral gap as a function of the control parameter.

- In section 4.4 assuming the validity of the ansatz we investigate local statistical properties of, which provides one with a means to evolve almost point like probability distributions. We derive a formula for the spectra of $\mathcal{U}$ associated with local statistical properties, and related periodic orbits. We find complete agreement between the predictions of the formula and numerics.

- We prove the ansatz in section 4.5, which means that all the results of chapter three are also applicable here. Thus, matrix representations of $\mathcal{U}$ with respect to our basis sets converge exponentially quickly for any chaotic Markov S-unimodal maps. So, within any arbitrarily small error, the infinite matrix representations can be safely truncated to obtain spectral decompositions, evolve probability densities and calculate time correlation functions.

We conclude the chapter with a brief discussion.

4.2 Construction of a basis for singular densities

Let us consider a one-dimensional dynamical system on the unit interval, $x_{t+1} = f(x_t)$, an example of which is the logistic map. The corresponding Frobenius-Perron operator $\mathcal{U}$ is defined through the equation (cf (1.10)) [56]

$$\rho_{t+1}(x) = \mathcal{U}\rho_t(x) = \sum_\alpha \rho_t[f_\alpha^{-1}(x)]|f_\alpha^{-1'}(x)| \tag{4.1}$$

where $f_\alpha^{-1}(x)$ denote the local inverse branches of f.

Before proceeding to the study of the spectral properties of the Frobenius-Perron operator, we first discuss the formation of singularities when $\mathcal{U}$ is applied successively on a smooth initial probability density $\rho_0(x)$. Suppose first that the map $f(x)$ has a single quadratic critical point x_c, such that $f'(x_c) = 0$, $f"(x_c) \neq 0$ [with the notation $f'(x) = df/dx$]. For the logistic map (eq.(1.14)), the critical point is located at $x_c = 1/2$. The left and right local inverses, for $x \approx f(x_c)$, take the form,

$$f_\alpha^{-1}(x) \approx x_c \mp \sqrt{\frac{2}{f''(x_c)}(x - f(x_c))} \tag{4.2}$$

respectively. On inspecting $f_\alpha^{-1'}(x)$, it is clear that $\mathcal{U}\rho_0(x)$ will have a square root type singularity[3]. In the following, we will assume that each $f_\alpha^{-1'}(x)$ has a square root type singularity at $f(x_c)$, but is otherwise analytic in a narrow strip of the complex plain about the real interval wherein the dynamics is defined[4]. Let us denote the iterates of the critical point $f(x_c), f[f(x_c)], ..., f^{t+1}(x_c), ...$ by the set $\{x_{ct}\}$, with $t = 0, 1, 2, ...$, and consider first the case where they are finite in number $(N_c + 1)$. This happens when the critical point falls in a finite number of iterations onto a periodic orbit. We observe that the probability density $\mathcal{U}^t\rho_0$ develops an extra new singularity at each iteration until the last point of the periodic orbit is finally visited after N_c iterations. Because the critical point is quadratic and provided that the relative stability factor of the sequence, defined by

$$\Lambda = \prod_{t=1}^{N_c} |f'(x_{ct})| > 1, \tag{4.3}$$

is greater than one, we can conclude that all these singularities are of square root type. In subsection 4.3.2 we will consider the more general situation where the critical point never falls onto a periodic orbit, but

$$\lambda_c = \liminf_{N_c \to \infty} \prod_{t=0}^{N_c} \sqrt[N_c]{|f'(x_{ct})|} > 1. \tag{4.4}$$

The latter situation has been proven to occur for the logistic map for values of the control parameter which are of positive Lebesgue measure. In each of these situations, an invariant

[3]We will also consider the case where the singularities are of the type $(x - f(x_c))^{\beta - 1}$, where $\beta = \frac{1}{k}$ and k is an integer greater than two. They arise for instance[53], in polynomial maps of order k, where $\forall l < k$, $f^{[l]}(x_c) = \frac{d^l}{dx^l} f(x_c) = 0$ and $f^{[k]}(x_c) \neq 0$ at $f(x_c)$.

[4]These assumptions are probably too stringent, analyticity except at $f(x_c)$ can probably be relaxed to the condition that $f_\alpha^{-1'}(x)$ is smooth and bounded except at the singularity

density is known to exist. Indeed, it is known that if $f(x)$ has negative Schwarzian derivative and an invariant measure exists, then $f(x)$ is mixing up to a finite rotation. This means that there is a finite disjoint collection of p intervals, $I_0, I_1, ..., I_{p-1}$ which are cyclically permuted by f, and f^p, restricted to any of these intervals is unimodal and mixing. Moreover, Keller and Nowicki[53] have proven that time correlations for such systems decay exponentially.

Let us return to the case where N_c is finite. We shall make the hypothesis (to be proven later) that the evolved probability density behaves as

$$\mathcal{U}^t \rho_0 = \sum_{n=0}^{\infty} \alpha_n(t)|x - x_{ct}|^{(n-1)/2}, \tag{4.5}$$

on one side or the other of the points $\{x_{ct}\}$, and excluding these points is piecewise analytic over the appropriate Markov partitions (e.g. the minimal Markov one). For convenience, let us reorder the set $\{x_{ct}\}$ according to increasing values and denote the new set by $\{a_i\}_{i=0}^{N_c}$. The set can be used to partition the interval $[a_0, a_{N_c}]$ into N_c cells $C_i = [a_{i-1}, a_i]$ with $i = 1, 2, .., N_c$. In the literature, this partition is often referred to as the minimal Markov partition [70] and we will denote it by $\mathcal{P}_{min}$. To simplify the discussion without loss of generality, we shall only consider the non-transient dynamics which is restricted to the interval $[a_0, a_{N_c}]$.

We now observe that the square root-type singularities that occur in eq.(4.5) for $n = 0$ are accounted for naturally in the following singular function,

$$S(x) = \frac{1}{\pi} \sum_{i=1}^{N_c} \frac{(a_i - a_{i-1})\chi_i(x)}{\sqrt{((x - a_{i-1})(a_i - x)}} = \sum_{i=1}^{N_c} s_i(x)\chi_i(x), \tag{4.6}$$

where $\chi_i(x)$ equals one if $x \in C_i$ and is zero otherwise and the role of $\frac{1}{\pi}$ will be clear shortly. Consider the invertible transformation

$$\eta(x) = \int_{a_0}^{x} S(y)dy. \tag{4.7}$$

If $x \in C_i$, then it is clear that $\eta(x) - a_{i-1} \sim \sqrt{x - a_{i-1}}$ for $x \approx a_{i-1}$, and likewise $a_i - \eta(x) \sim \sqrt{(a_i - x)}$ for $x \approx a_i$, Thus, the expression $S(x)\eta(x)^m$ exhibits the same features as eq.(4.5) in the vicinity of any point of x_{ct}. Suppose now that we make the ansatz that

$$\rho_t = S(x)\hat{\rho}_t(\eta(x)), \tag{4.8}$$

where $\hat{\rho}(x)$ is piecewise analytic over $\mathcal{P}_{min}$. This is precisely the relation that pertains between the probability densities of two maps, $f(x)$, and $\hat{f}(x)$, which are conjugate (via a smooth invertible transformation) with respect to $\eta(x)$, i.e.

$$\hat{f}(x) = \eta^{-1} \circ f \circ \eta(x). \tag{4.9}$$

Hence, it would seem reasonable to propose that an appropriate basis should have the form,

$$\phi_{in}(x) = s_i(x)T_{in}(\eta(x))\chi_i(x), \tag{4.10}$$

where $\{T_{in}(x)\}, n = 0, 1, 2, ..., i = 1, 2, \cdots, N_c$ is any basis of orthogonal polynomials (Chebyshev functions[88, 25, 92] for example) with support on the cell C_i, and which are orthogonal with respect to a weighting function $w_i(x)$,

$$\int_0^1 T_{jm}(x)T_{in}(x)w_j(x)dx = \delta_{ji}\delta_{m,n}h(m). \tag{4.11}$$

Notice that, orthogonal functions and weighting factors with support on the cell C_i are related to those having support on the unit interval by the relations

$$\begin{aligned} T_{im}(x) &= T_m\left(\frac{x - a_{i-1}}{a_i - a_{i-1}}\right), \\ w_i(x) &= \frac{1}{a_i - a_{i-1}} w\left(\frac{x - a_{i-1}}{a_i - a_{i-1}}\right). \end{aligned} \tag{4.12}$$

An alternative way of deducing $\eta(x)$, is to first assume that $\{\phi_{in}(x)\}$ has the same form as eq.(4.10), except that $\eta(x)$ is an unknown function to be determined by demanding that the basis obey the same orthogonality relation as $\{T_n(x)\}$, but with a change in weighting factor $\hat{w}_i(x)$,

$$\int_{a_{i-1}}^{a_i} \phi_{jm}(x)\phi_{in}(x)\hat{w}_i(x)dx = \delta_{m,n}\delta(j,i)h(m). \tag{4.13}$$

We find the desired solution with

$$\hat{w}_i(x) = \frac{w_i(\eta(x))}{s_i(x)}\chi_i(x), \tag{4.14}$$

where $\eta(x)$ satisfies

$$s_i(x) = \frac{d\eta(x)}{dx}, x \in C_i, \tag{4.15}$$

$\eta(a_{i-1}) = a_{i-1}$ and $\eta(a_i) = a_i$. Hence, for $x \in C_i$,

$$\eta(x) = a_{i-1} + (a_i - a_{i-1})\frac{2}{\pi}\arcsin\left(\sqrt{\frac{x - a_{i-1}}{a_i - a_{i-1}}}\right). \tag{4.16}$$

Let us mention that another possible choice of singular function is the invariant density itself ($S(x) = \rho_{inv}(x)$), which is appealing. Unfortunately, one needs to first obtain $\rho_{inv}(x)$, which may be a non-trivial task itself. For now we shall make the following ansatz motivated by the above consideration, and explore its consequences with analytical and numerical examples.

I There exist invariant spaces of functions $\{\mathcal{F}\}$ which behave as

$$\mathcal{U}^t\rho_0 = \sum_{n=0}^{\infty} \alpha_n(t)|x - x_{ct}|^{(n-1)/2}, \tag{4.17}$$

for x in the vicinity of one side or the other of the points $\{x_{ct}\}$, and are otherwise analytic within each partition cell. $\mathcal{F}$ also includes all functions which are piecewise analytic over the partition, which is the form that we expect initial probability densities to have.

II Any function in such an $\mathcal{F}$ can be expanded in terms of the basis $\{\phi_{im}(x)\}$, in a rapidly convergent fashion.

III The corresponding matrix representation of $\mathcal{U}$ converges sufficiently quickly to be truncated.

IV To characterize local statistical properties, we will assume that the conjugate map $\hat{f}(x) = \eta \circ f \circ \eta^{-1}(x)$ is Markov analytic.

We may now obtain a matrix representation of $\mathcal{U}$,

$$(\mathcal{W})_{imjn} = \frac{1}{h_m} \int_0^1 dx \tilde{w}(x)\ \phi_{im}(x)\ (\mathcal{U}\phi_{jn})(x). \tag{4.18}$$

by simply regrouping the indices so that $(\mathcal{W})_{imjn} = M_{kl}$, where $k = mN_c + i$ and $l = nN_c + j$, for instance. Eigenvalues and eigenfunctions (such that $\mathcal{U}\psi_\nu = z_\nu \psi_\nu$) can then be found by truncating M_{kl} at a sufficiently high order, (corresponding to $m = n \leq N_p$, where typically $N_p \leq 10$) like for piecewise-linear maps [66]. In particular, the invariant density – when unique – corresponds to the eigenvector of $\mathcal{W}$ with unit eigenvalue.

Let $\rho_0(x)$ denote an initial density. The time-correlation function $C_{AB}(\tau)$ of two measurable functions $A(x)$ and $B(x)$,

$$C_{AB}(\tau) = \int_0^1 A(x)[\mathcal{U}^\tau(B\rho_{\text{eq}})](x)dx - \langle A\rangle_{\text{eq}}\langle B\rangle_{\text{eq}} \tag{4.19}$$

can also be easily calculated, where the role of such $\rho_0(x)$ is played by $B(x)\rho_{\text{eq}}(x)$. Then,

$$\rho_0(x) = \sum_{i=1}^{N_c} \sum_{m=0}^{N_p} c_{in}\ \phi_{im}(x)\ , \tag{4.20}$$

and

$$\mathcal{U}^t \rho_0(x) = \sum_{i,j=1}^{N_c} \sum_{m,n=0}^{N_p} \phi_{im}(x)\ (\mathcal{W}^t)_{imjn}\ c_{jn}\ , \tag{4.21}$$

so that correlation functions like (4.19) can be easily evaluated.

4.3 Examples

For some representative cases, we will now study the corresponding spectral properties and time correlation functions using matrix representations given by eq.(4.21). The examples belong to either of two classes: Markov maps, where the iterates of the critical point form a finite set, and non-Markov maps, where the number is countably infinite. We will show how **non-Markov maps can be approximated by Markov ones**, and then obtain a formula for the spectral gap for the logistic map, as a function of the control parameter r. Finally, we will outline some results from symbolic dynamics.

4.3.1 Markov maps

A particularly simple example is the logistic map at parameter 4. This map was first shown to be conjugate to the tent map at slope 2 by Ulam [105, 43]. In this case the singularities only occur at zero and one, so that $a_0 = 0$, $a_1 = 1$, and $N_c = 1$. The conjugacy to the tent map $g(y) = 1 - |2y - 1|$ is established by $g = \eta \circ f \circ \eta^{-1}$ with

$$\eta(x) = \frac{2}{\pi} \arcsin \sqrt{x} \quad \text{and} \quad s(x) \;=\; \eta'(x) = \frac{1}{\pi\sqrt{x(1-x)}}. \tag{4.22}$$

The Bernoulli polynomials $\{B_{2\nu}(y/2)\}$ [1] are eigenfunctions of the tent map with corresponding eigenvalues $z_\nu = 2^{-2\nu}$ for $\nu = 0, 1, 2, \ldots$ [27]. It is a simple matter to verify that the functions

$$\begin{aligned} \psi_\nu(x) &= \eta'(x)\; B_{2\nu}[\eta(x)/2] \\ &= \frac{1}{\pi\sqrt{x(1-x)}}\; B_{2\nu}\Big(\frac{1}{\pi}\arcsin\sqrt{x}\Big) \end{aligned} \tag{4.23}$$

are eigenfunctions of the logistic map with the same spectrum as the tent map. In fact, as $\eta'(x)$ is the invariant density of the logistic map for $r = 4$, our choice of basis is essentially equivalent to a local equilibrium hypothesis, where the densities are equal to continuous functions times the equilibrium density. A complete spectral decomposition can also be obtained.

More generally, one can find parameter values r where there exist finite minimal Markov partitions by demanding that the k^{th} iterate of the extremum falls onto a periodic orbit of period p, where $k = 2, 3, ...$ This reduces to solving for the roots of the fixed point equation,

$$f_m^{p+k}(\frac{1}{2}) = f_m^k(\frac{1}{2}), \tag{4.24}$$

and choosing those values of r which give rise to chaos. One representative example of eq.(4.24), $r = 3.6785735104283222651$, which exhibits a period 2 chaotic behaviour. Its dominant spectra are

$$1, -1, 0.595706, -0.595706, 0.457243, -0.457243, \ldots.$$

The fact that there is an eigenvalue equal to -1 is due to the existence of period 2 chaos, which is also manifested in the autocorrelation function of position (see Fig.4.2).

4.3.2 Non-Markov maps

We now come to the general case of parameter values of r below $r = 4$ where, typically no finite Markov partition exists[5]. In practice, the relative magnitude of the singularities at $f^k(x_c)$ decrease so rapidly with increasing k, that they quickly become negligible[64], suggesting that $\mathcal{U}$ can be well approximated through representations where only a finite

[5] Nevertheless we expect that the parameter values corresponding to Markov chaotic maps is dense in regions of parameter space where the corresponding systems are chaotic

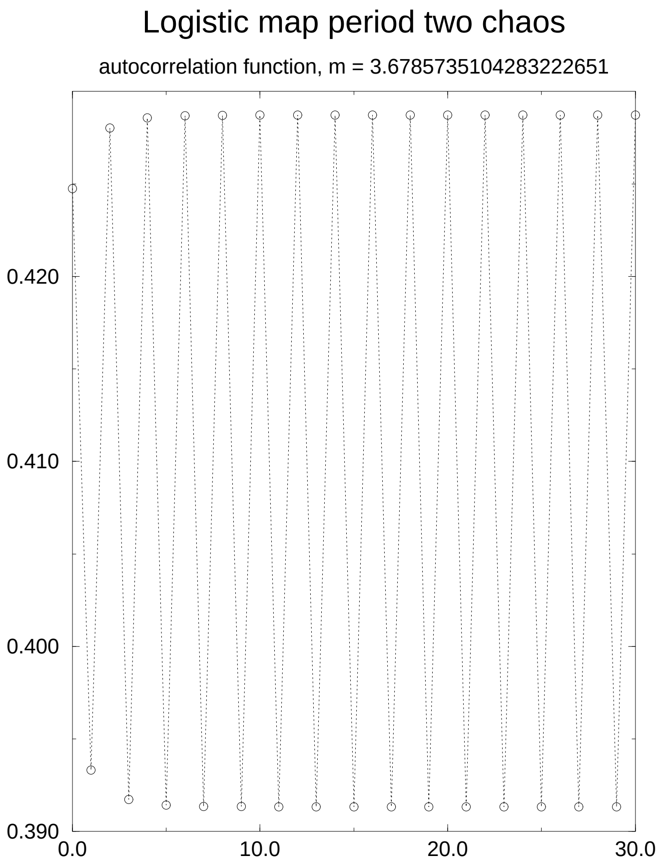

Figure 4.2: The autocorrelation function for the logistic map at the transition to period two chaos. Note that we have actually plotted $C_{x,x}(\tau) + < x >^2$.

number of singularities are considered[6]. The procedure is straightforward. One constructs a partition with the first $N_c + 1$ iterates of the critical point,

$$f(\frac{1}{2}), f^2(\frac{1}{2}), ..., f^{N_c+1}(\frac{1}{2}), \tag{4.25}$$

and a basis $\{\phi_{i,n}(x)\}$ using a convenient orthogonal set of polynomials (see eq.(4.10)). An approximation can then be made by simply treating the problem as if the number of iterates of the extremum was finite and one seeks a value of N_c and N_p such that one observes convergence in the quantities of interest as N_c and N_p are increased. Alternatively, exploiting eq.(4.24), one could try to approximate the the non-Markov system (having parameter r) by system $\hat{r}$, with

$$|r - \hat{r}| < \epsilon, \tag{4.26}$$

having a finite minimal Markov partition. The expectation is that if ϵ is small enough, the two systems should be virtually identical at least as far as statistical properties are

[6]A analogous situation occurs for hyperbolic analytic, but non-Markov maps, where the role of the singularities here is played by discontinuities.

concerned. A simple way of choosing $\hat{r}$ is to find the first time when the orbit of the extremum comes within $\hat{\epsilon} << 0$ of falling onto a periodic orbit. In other words we look for a value of p and k such that

$$|f^{p+k}(\frac{1}{2}) - f^{k}(\frac{1}{2})| < \hat{\epsilon}, \tag{4.27}$$

where $\hat{\epsilon} << 0$. One then chooses the solution of eq.(4.24) which also satisfies eq.(4.26). That values of $\hat{r}$ close to r exist satisfying eq.(4.27) follows from the work of Metropolis, Stein and Stein (see the appendix for a brief discussion). As a representative example, let us consider the case of $r = 3.95$. We followed the trajectory of the critical point for over 500 iterations by choosing the precision of the floating point calculations using Maple, so that all iterates were guaranteed to be accurate with 20 digits of precision (this entails doing intermediate calculations with 200 digit precision). All the numerics indicate that the 3.95 case is chaotic, but non-Markov. Now, if one examines the itinerary of $\frac{1}{2}$ one finds that it almost repeats itself after 22 and 46 iterations. The corresponding values of r which satisfy the above criteria are 3.9500001011218505454 and 3.9499999999999754036 respectively. We have calculated the time-correlation functions, invariant densities and spectra of the logistic map for the three mentioned values of r. As a check, we have also calculated the corresponding time-correlation functions through a long time series. Fig. (4.3) shows that the time-correlation functions of the three systems are virtually indistinguishable. The invariant density is given in Fig.(4.4).

In contrast, the spectra show a sensitivity to parametric perturbations although they have qualitatively the same structure (see Fig.(4.5).

4.3.3 Universal behaviour of the Spectral Gap

The method also allows one to study the spectral properties of the Frobenius-Perron operator in the inverse cascade of band-merging bifurcations $\{r_n\}$ accumulating from above at the onset of chaos like $(r_n - r_c) \sim \delta^{-n}$ where $\delta = 4.6692...$ is the Feigenbaum constant [35]. As a first result, the number of eigenvalues on the unit circle is equal to 2^n when 2^n bands merge leading to a period-2^n chaos, which is the spectral signature of an ergodic but non-mixing dynamics [62]. Moreover, the rest of the spectrum turns out to be separated from the unit circle by a gap which shrinks as the non-chaotic regime is approached as

$$\begin{aligned} \Delta_{\text{gap}} \quad &= \quad \text{Min}_{\nu=2^n+1,2^n+2,...}\{1 - |z_\nu|\} \ \sim \ (r_n - r_c)^\tau \\ \text{with} \quad & \tau = \frac{\ln 2}{\ln \delta} = 0.4498069... \end{aligned} \tag{4.28}$$

The universal exponent is determined by noting that the gap is of the order of the average Lyapunov exponent which is known to scale as $\bar{\lambda} \sim |r - r_c|^\tau$ [51]. We carried out a numerical verification of this prediction in the logistic map where the spectrum has been calculated down to the merging of 64 chaotic bands, giving an exponent $\tau_{\text{num}} \simeq 0.44$ in good agreement with eq. (4.28). This result shows that the spectrum of the Frobenius-Perron operator displays universal behaviors in the period-doubling cascade.

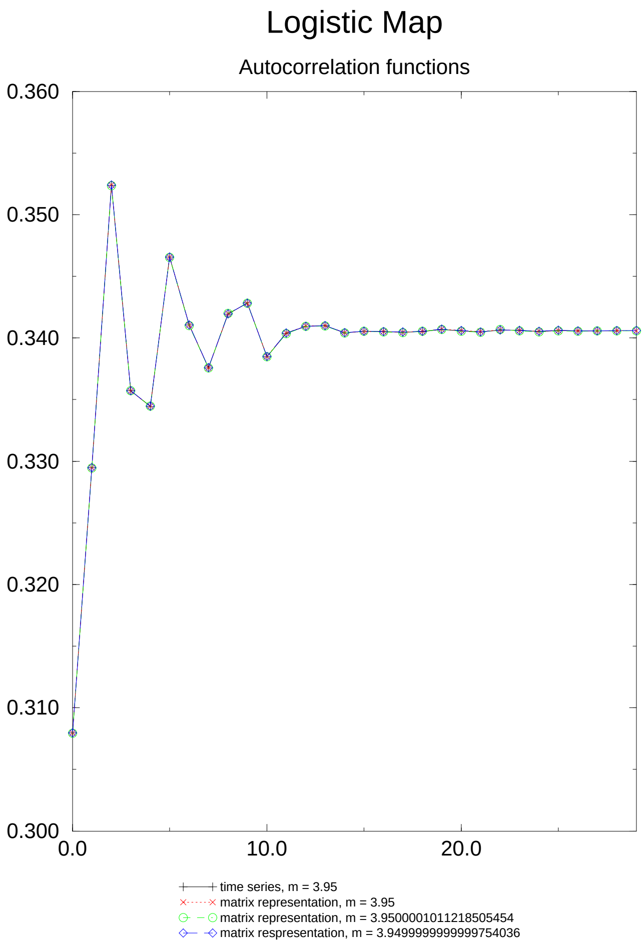

Figure 4.3: Plot of autocorrelation functions at $r = 3.95$ from a time series, through a truncated representation, and at nearby Markov parameter values. Note that we have actually plotted $C_{x,x}(\tau) + < x >^2$.

4.4 Local Statistical Properties

Up to now, the basis functions $\{\phi_{in}(x)\}$ have been defined so that each one has support over a given cell of the minimal Markov partition. One may ask whether the spectral properties of $\mathcal{U}$ change, if a different Markov partition (and corresponding function space) is used. Choosing a refined partition may be motivated by the desire to characterise local properties[66], occuring in small regions of the interval, much smaller, for example, than the typical size of the cells of the minimal Markov partition. We shall consider any Markov partition $\mathcal{P}_M$ formed by the refinement of $\mathcal{P}_{min}$ through the addition of either:

(a) inverse images of some/all the points defining $\mathcal{P}_{min}$; or

(b) all the elements of a finite number of periodic orbits.

Let us define to kinds of function space associated with any partition of type (a) or (b):

1. The space $\mathcal{F}_1$ of functions of the type

$$S_{min}(x)\psi(\eta_{min}(x)), \tag{4.29}$$

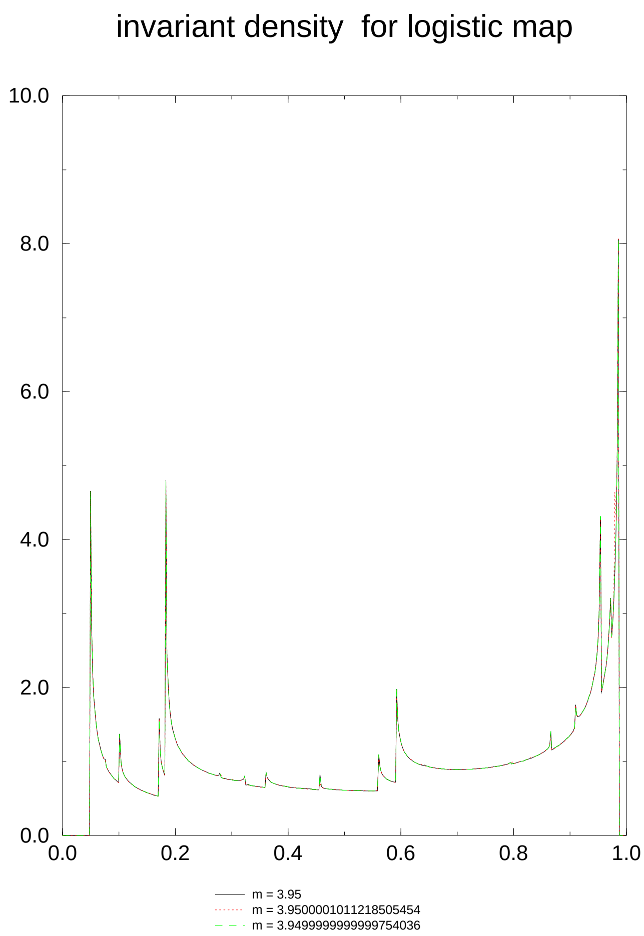

Figure 4.4: Plot of the invariant density for the logistic map at r = 3.95, and at nearby Markov parameter values

where $S_{min}(x)$ is the singular function associated with $\mathcal{P}_{min}$, $\eta_{min}(x)$ the corresponding conjugate transformation, and $\psi(x)$ is piecewise analytic over $\mathcal{P}_M$ (rather than just $\mathcal{P}_{min}$).

2. The space $\mathcal{F}_2$ of functions of the type

$$S_M(x)\psi(\eta_M(x)), \tag{4.30}$$

$\psi(x)$ is again piecewise analytic over $\mathcal{P}_M$,

$$S_M(x) = \frac{1}{\pi}\sum_{i=1}^{N_M} \frac{(a_i - a_{i-1})\chi_i(x)}{\sqrt{((x-a_{i-1})(a_i - x)}} = \sum_{i=1}^{N_c} s_i(x)\chi_i(x), \tag{4.31}$$

where N_M equals the number of cells of the $\mathcal{P}_M$, and

$$\eta_M(x) = \int_{a_0}^{x} S_M(y)dy. \tag{4.32}$$

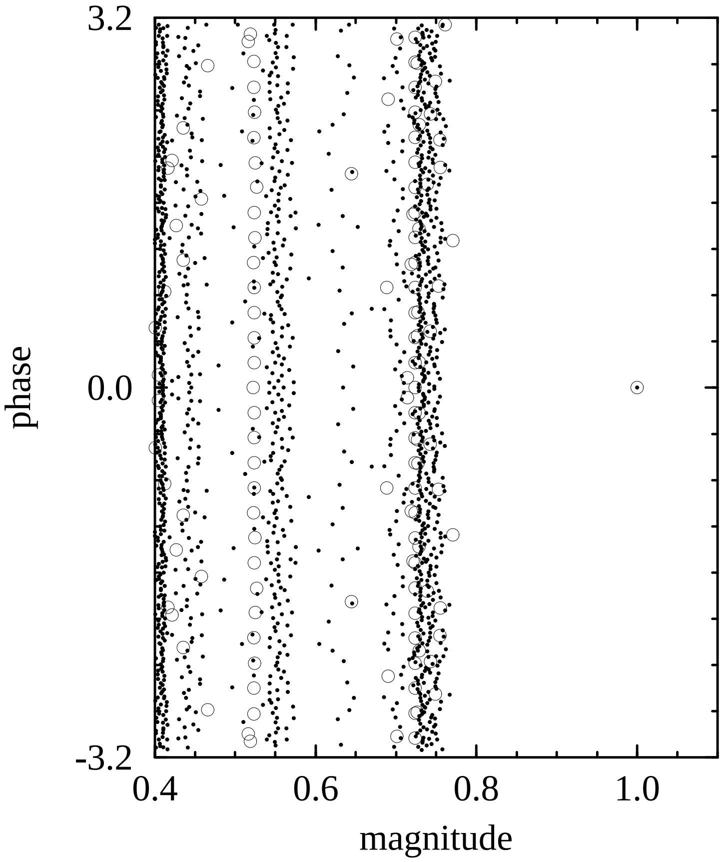

Figure 4.5: Plot of dominant spectra $|\lambda|e^{i\phi}$ in terms of magnitude $|\lambda|$ and phase ϕ for the logistic map at 3.95 (dots) and 3.9499999999999754036 (circles).

One may easily show that the ansatz is not valid for a type 2 function space if $\mathcal{P}_M$ is formed through self-refinement[7]. On the other hand, we will prove that the other combinations of partition and type of function space, as depicted in the following table do in fact satisfy the ansatz.

$\mathcal{P}_M$	**(a)**	**(b)**
$\mathcal{F}_1$	$\surd$	$\surd$
$\mathcal{F}_2$	X	$\surd$

Hence, the statistical properties of $f(x)$ can be determined through an analysis of a conjugate map $\hat{f}(x)$ which is Markov analytic[8] and therefore has its statistical properties detailed in chapter 3.

[7]This is evident if one considers eqs.(4.60,4.61), $\psi(x_{max}) = x_c$, but x_c is a point where $S_2(x)$ is singular, so the conjugate map cannot be piecewise analytic.

[8]Strictly speaking, these are not Markov analytic maps, as the derivative of $\hat{f}(x)$ can possess singularities. However, as we will see later, the inverse branches are C^3, piecewise analytic, and eventually contractive, so the methods of chapter 3 still apply.

The appropriate basis functions for $\mathcal{F}_1$ have the form

$$\phi_{ik}(x) = S_{min}(x)T_{ik}(\eta_{min}(x))$$

and for $\mathcal{F}_2$

$$\phi_{ik}(x) = S_M(x)T_{ik}(\eta_M(x)),$$

where $\{T_{ik}(x)\}, i = 1, 2, .., N_M;\ k = 0, 1, 2, ..$ are, for example, the Chebyshev polynomials with support on the cell C_i.

Let us denote the space of functions of the type given by eq.(4.8) by $\mathcal{F}_{min}$, and the spectra associated with $\mathcal{U}$ acting on F_{min} by sp_{min}, and the spectra of $\mathcal{U}$ acting on $\mathcal{F}_1$ or $\mathcal{F}_2$ by by sp_M. As $F_{min} \subset F_M$ it follows that $sp_{min} \subset \mathcal{P}_M$. Let us first consider partitions formed by self-refinement (a). In this case any density $\rho_0(x) \in \mathcal{F}_1$, will after a finite number of iterations (equal to the number of sucessive self refinements) be an element of $\mathcal{F}_{min}$. It follows that there is now a infinitely degenerate zero eigenvalue present in sp_M, which is otherwise identical to sp_{min}. Suppose on the other hand that $\mathcal{P}_M$ is a partition of type (b). Then, (with the exception of accidental degeneracy) we get new additional spectra $sp_M \supset sp_{min}$. The eigenvalues are

$$\begin{aligned} \{\lambda\} &= \frac{1}{\sqrt[p]{(\hat{f}^{p\prime}(x_l))^{k+1}}}, \\ &= \left|\frac{1}{\sqrt[p]{(\hat{f}^{p\prime}(x_l))^{k+1}}}\right| \exp(i\sigma\pi j/p), \end{aligned} \tag{4.33}$$

where

$$\sigma = \begin{cases} 1, & \text{if } (f^{p\prime}(x_l))^{k+1} < 0; \\ 2, & \text{otherwise,} \end{cases}, \tag{4.34}$$
$$k = 0, 1, 2, 3...,\ and\ j = 1, 2, 3, ...p$$

and x_l belongs to a periodic orbit of period p. They describe a decaying oscillatory mode with period p if the argument of the p^{th} root is positive, and $2p$ if it is negative. There is one subtlety, which will be explained in subsection 4.5.3, namely the relative stability factors of the conjugate map are related to those of the original map by,

$$\hat{f}^{p\prime}(y_l) = \begin{cases} f^{p\prime}(x_l) & \text{if } \mathcal{U} \text{ acts on } \mathcal{F}_1 \\ \frac{(|f^{p\prime}(x_l)|)^{\beta+1}}{f^{p\prime}(x_l)} & \text{if } \mathcal{U} \text{ acts on } \mathcal{F}_2 \end{cases}, \tag{4.35}$$

where $y_l = \eta_1(x_l)$ in the first case and $y_l = \eta_2(x_l) = x_l$ in the second respectively.

4.5 Validity of the Ansatz

We have seen analytic and numerical examples which support the ansatz of subsection 4.2

I There exist invariant spaces of functions $\{\mathcal{F}\}$ which behave as

$$\mathcal{U}^t\rho_0 = \sum_{n=0}^{\infty} \alpha_n(t)|x - x_{ct}|^{(n-1)/2}, \tag{4.36}$$

for x in the vicinity of one side or the other of the points $\{x_{ct}\}$, and are otherwise analytic within each partition cell. $\mathcal{F}$ also includes all functions which are piecewise analytic over the partition, which is the form that we expect initial probability densities to have.

II Any function in such an $\mathcal{F}$ can be expanded in terms of the basis $\{\phi_{im}(x)\}$, eq.(4.10) in a rapidly convergent fashion.

III The corresponding matrix representation of $\mathcal{U}$ converges sufficiently quickly to be truncated.

IV To characterize local statistical properties, we will assume that the conjugate map $\hat{f}(x) = \eta \circ f \circ \eta^{-1}(x)$ is Markov analytic.

We will establish the validity of the ansatz in four steps. In subsection 4.5 we prove part II of the ansatz. Then, in subsection 4.5.2 we show that the chaotic Markov S-unimodal maps are conjugate to Markov maps whose inverse branches are C^3 in the domain of definition, and also piecewise analytic over the associated Markov partition. The third step (subsection 4.5.3) consists of relating the relative stability/instability factors of periodic orbits of any chaotic Markov S-unimodal maps to its conjugate. In the final step, subsection 4.5.4, we show that the conjugate map is eventually hyperbolic, proving part IV of the ansatz which implies III and I.

4.5.1 Exponentially convergent basis expansions

Let us begin by considering the convergence of basis expansions of functions of the type

$$\hat{\psi}(x) = s(\beta, x)\psi(\eta(\beta, x)) \tag{4.37}$$

where

$$s(\beta, x) = \frac{c}{(x(1-x))^{(1-\beta)}}, \tag{4.38}$$

$\psi(x)$ is analytic in a complex domain containing the unit interval,

$$\eta(\beta, x) = \int_0^x s(\beta, y)dy, \tag{4.39}$$

$\beta = \frac{1}{N} \geq \frac{1}{2}$, and c is a normalization constant chosen so that $\eta(\beta, 1) = 1$. This allows us to consider systems where the extrema need not only correspond to quadratic critical points. We will focus attention on a one cell partition of the interval $[0, 1]$. The generalization to multi-cell partitions is automatic. In analogy with the case $\beta = \frac{1}{2}$, we propose that a suitable basis for such functions is

$$\phi_m(\beta, x) = s(\beta, x)T_m(\eta(\beta, x)), \tag{4.40}$$

where $T_m(x)$ is a any Jacobi polynomial having support on the unit interval, and $\eta(\beta, 1) = 1$. The weighting function is defined as

$$w(\beta, x) = \frac{w(\eta(\beta, x))}{s(\beta, x)}. \tag{4.41}$$

just as in eq.(4.14). If $\{T_n(x)\}$ are the Chebyshev polynomials, we can prove $\forall \epsilon > 0, \exists N$ such that $\forall n > N$,

$$\int_0^1 \left(\hat{\psi}(x) - \sum_{k=0}^{n} b_k \phi_k(\beta, x)\right) < \epsilon. \tag{4.42}$$

Moreover, the expansion coefficients C_n decrease exponentially quickly with increasing N. This is easy to see, as the expansion coefficient of $\hat{\psi}(x)$ are given by

$$\begin{aligned} & \frac{1}{h_m}\int_0^1 w(\beta, x)\hat{\psi}(x)\phi_m(\beta, x)dx \qquad (4.43)\\ = & \frac{1}{h_m}\int_0^1 w(\eta(\beta, x))\psi(\eta(\beta, x))s(\beta, x)T_m(\eta(\beta, x))dx \\ = & \frac{1}{h_m}\int_0^1 w(x)\psi(x)T_m(x)dx. \end{aligned}$$

Exponentially decreasing expansion coefficients follows from the properties of Chebyshev expansions of analytic functions.

We now want to show that any analytic function $\Upsilon(x)$ can be expressed as eq.(4.37),

$$\Upsilon(x) = s(\beta, x)u(\eta(\beta, x)) \tag{4.44}$$

where $u(x)$ is another analytic function. Clearly,

$$\psi(x) = \frac{\Upsilon(\eta^{-1}(\beta, x))}{s(\beta, \eta^{-1}(\beta, x))} = \Upsilon(\eta^{-1}(\beta, x))\frac{d}{dx}\eta^{-1}(\beta, x) \tag{4.45}$$

So we require that $\eta^{-1}(\beta, x)$ has an analytic complex extension in a region enclosing the unit circle and its first derivative is bounded away from zero. Now $\eta(\beta, x) : [0, 1] \to [0, 1]$ is a continuous function, so that

$$\frac{d}{dx}\eta^{-1}(\beta, x) > \frac{2^{\beta-1}}{c} \tag{4.46}$$

Now, $s(\beta, x)$ is analytic and non-zero in a small complex domain D_ϵ including $[\epsilon, 1-\epsilon]$, i.e. in this domain, $\eta(\beta, z)$ is a conformal map. Therefore, $\eta^{-1}(\beta, x)$ is analytic at least in a complex domain including $[\eta(\epsilon), \eta(1-\epsilon)] = [\epsilon', 1-\epsilon'']$, where $\epsilon, \epsilon', \epsilon''$ are arbitrarily small and positive. We only have left to show that $\eta^{-1}(\beta, x)$ is analytic in a small complex domain about 0, and 1 respectively. Using the Taylor expansion for for $x < 1$,

$$s(\beta, x) = cx^{\beta-1}(1 - (1-\beta)x + \cdots). \tag{4.47}$$

Thus

$$\eta(\beta, x) = x^\beta(c_0 + c_1 x + \cdots), \tag{4.48}$$

where all the expansion coefficients above are greater than zero. We now notice that $\eta(\beta, z)^{\frac{1}{\beta}}$ is analytic, and it also is a conformal map as its first derivative is non-zero for all z in a small complex domain containing $[0, 1-\epsilon]$ (but excluding the possibly non-analytic point at 1. Therefore, there exists a conformal map $\vartheta(z)$, at least in a domain about $[0, 1-\epsilon']$ such that

$$\eta^{-1}(\beta, x) = \vartheta(x^{\frac{1}{\beta}}) = d_0 + d_1 x^{\frac{1}{\beta}} + d_2 x^{\frac{2}{\beta}} + \cdots \tag{4.49}$$

So $\eta^{-1}(\beta, x)$ is analytic in a complex extension about $[0, 1-\epsilon]$, for some small ϵ. It is clear that $d_0 = 0$, and $d_1 c_0^{\frac{1}{\beta}} = 1$. Using the symmetry of $s(\beta, x)$, it is easy to show that $\eta^{-1}(\beta, 1-x) = 1 - \eta^{-1}(\beta, x)$.

Finally, suppose a function or one of its derivatives has a root β type singularity at 0, i.e.

$$\hat{\varsigma}(x) = x^{\beta-1}\varsigma(x^{\beta}), \tag{4.50}$$

where $\varsigma(x)$ is analytic. It is obvious that we can also express $\hat{\varsigma}(x)$ as $s(\beta, x)\psi(\beta, \eta(\beta, x))$ where $\psi(x)$ is another analytic function.

The generalization to a multi-cell partition is straight forward. We simply define

$$\varpi_i(x) = \frac{x - a_{i-1}}{a_i - a_{i-1}}, \tag{4.51}$$

for every cell C_i of the partition. For $x \in C_i$ the corresponding conjugate transformation and its inverse have the form

$$\begin{aligned} \hat{\eta}(x) &= \varpi_i^{-1} \circ \eta(\beta, \varpi_i(x)) \\ &= a_{i-1} + (a_i - a_{i-1})\eta(\beta, \frac{x - a_{i-1}}{a_i - a_{i-1}}), \end{aligned} \tag{4.52}$$

$$\begin{aligned} \hat{\eta}^{-1}(x) &= \varpi_i^{-1} \circ \eta^{-1}(\beta, \varpi_i(x)) \\ &= a_{i-1} + (a_i - a_{i-1})\eta^{-1}(\beta, \frac{x - a_{i-1}}{a_i - a_{i-1}}), \end{aligned} \tag{4.53}$$

where the singular function becomes

$$\hat{S}(x) = s(\beta, \varpi_i(x)) = s(\beta, \frac{x - a_{i-1}}{a_i - a_{i-1}}), \tag{4.54}$$

for $x \in C_i$. The new basis is defined like eq.(4.10),

$$\hat{\phi}_{in}(x) = \hat{S}(x) T_{in}(\hat{\eta}(x))\chi_i(x), \tag{4.55}$$

where the β dependence in $\hat{\eta}(x), \hat{S}(x), \{\hat{\phi}_{in}(x)\}$ is implicitly understood. Thus, it is clear that assumption II of the ansatz is valid.

$\square$

4.5.2 Conjugacy to piecewise analytic maps

We will now show that the inverse branches of the conjugate map $\hat{f}(x)$ are C^3 over their domains of definition, and are also piecewise analytic over $\mathcal{P}_{min}$ and appropriate refinements.

Consider the cell to cell transition represented by $f_{\alpha}^{-1}(x) \in C_j$, where $x \in C_i$, and assume that $f_{\alpha}^{-1}(x)$ is monotonic increasing (the argument is identical if it is monotonic decreasing). Let

$$g_{\alpha}(x) = \hat{\eta} \circ f_{\alpha}^{-1} \circ \hat{\eta}^{-1}(x). \tag{4.56}$$

We will demonstrate that $g_\alpha(x)$ has an analytic extension about each $[a_{i-1}, a_i]$, that is

$$g_\alpha(x) = \sum_{i=1}^{N_c} \tilde{g}_i(x)\chi_i(x), \tag{4.57}$$

where $\tilde{g}_i(z)$ is analytic in a complex domain D_i containing the cell C_i. Let us first list the key properties necessary for our proof.

1. $f_\alpha^{-1}(x)$ is defined in the domain $[x_{min}, x_{max}]$, where $x_{max} = f(x_c)$ and $x_{min} = f(x_{max})$.
2. $f_\alpha^{-1}(x)$ can be analytically continued into a complex domain including the interval $[x_{min}, x_{max} - \epsilon]$
3. $f'_\alpha(x)$ has an integrable singularity of the type $(x_{max} - x)^{\beta-1}$ at $x = x_{max}$.
4. The Markov property of the partition implies

$$f_\alpha^{-1}(C_j) \bigcap C_i \neq \emptyset \Rightarrow f_\alpha^{-1}(C_j) \subset C_i. \tag{4.58}$$

5. Thus, if $f^{-1}(a_{j-1}) = a_{i-1}$ then for $a_{j-1} \leq x \ll a_j$

$$f_\alpha^{-1}(x) = a_{i-1} + \hat{c}_1(x - a_{j-1}) + \hat{c}_2(x - a_{j-1})^2 + \cdots, \tag{4.59}$$

where the first expansion coefficient $\hat{c}_1$ is non-zero, similarly for for $a_{j-1} \ll x \leq a_j$.

Proof :

Due to eqs.(4.48,4.49,4.52,4.53, 4.58, 4.59) the only points about which $g_\alpha(x)$ may possibly be non-analytic are $x = a_{i-1}$, or $x = a_i$. First, consider x in the vicinity of x_{max}. From eq.(4.50) we may write

$$f_\alpha^{-1}(x) = \psi(\hat{\eta}(x)). \tag{4.60}$$

Thus,

$$f^{-1}(\hat{\eta}^{-1}(x) = \psi(x) \tag{4.61}$$

and is analytic at least for x in the right most cell. Now $f_\alpha^{-1}(x_{max}) = x_c$, and x_c does not coincide with points where $\hat{\eta}(x)$ is non-analytic, so $g_\alpha(x) = \hat{\eta}(\psi(x))$ has an analytic extension in a domain containing x_{max}.

Second, suppose $f_\alpha^{-1}(a_j)$ lies within a cell C_i, i.e. $a_{i-1} < f_\alpha^{-1}(a_j) < a_i$, but $a_j \neq x_{max}$. Then it is easy to show that $g'_\alpha(a_j) = 0$, and that $g''_\alpha(x)$ has a discontinuity at a_j. Nevertheless, $g_\alpha(x)$ is piecewise analytic at this point.

Third, suppose $f_\alpha^{-1}(a_{j-1}) = a_{i-1}$, and $a_{j-1} \leq x \ll a_j$ (the case of $f_\alpha^{-1}(a_{j-1}) = a_{i-1}$ is treated identically). Eqs.(4.49,4.53,4.59) imply that

$$f_\alpha^{-1} \circ \hat{\eta}^{-1}(x) = a_{i-1} + b'_1(x - a_{j-1})^{\frac{1}{\beta}} \left(1 + b'_2(x - a_{j-1})^{\frac{1}{\beta}} + b'_3(x - a_{j-1})^{\frac{2}{\beta}} + \cdots\right) \tag{4.62}$$

where the $b'_1, b'_2, \cdots$ are expansion coefficients, and $b'_1 \neq 0$. Therefore,

$$\hat{\eta}(f_\alpha^{-1} \circ \hat{\eta}^{-1}(x) = a_{j-1} + c_0 {b'_1}^{\beta}(x - a_{i-1}) + O^2, \tag{4.63}$$

where O^2 denotes terms of order 2 and higher in $(x - a_{j-1})$. The cases of $a_{j-1} \ll x \leq a_j$, and $f_\alpha^{-1}(x)$ being monotonic decreasing are treated in the same way. Therefore g_α can be analytically continued into a complex domain enclosing the cell C_j, and $g_\alpha(x)$ is piecewise analytic over the partition. Let us remark again that at points $a_j \neq x_{max}$, where $g_\alpha(a_j) \neq a_i$, we find $|{g_\alpha}'(a_j)| = 0$, which so that $g_\alpha(x)$ is C^3 across such points.

$\square$

We notice that $|\hat{f}'(a_i)| = \infty$ at the points $a_j \neq x_{max}$, where $g_\alpha(a_j) \neq a_i$, which is quite a surprise. These observations are illustrated in Fig. 4.6, which corresponds to the conjugate map of the logistic map, $m = 3.9500001011218505454$, where the conjugate transformation is defined by eq.(4.16), and the minimal Markov partition consists of 21 cells.

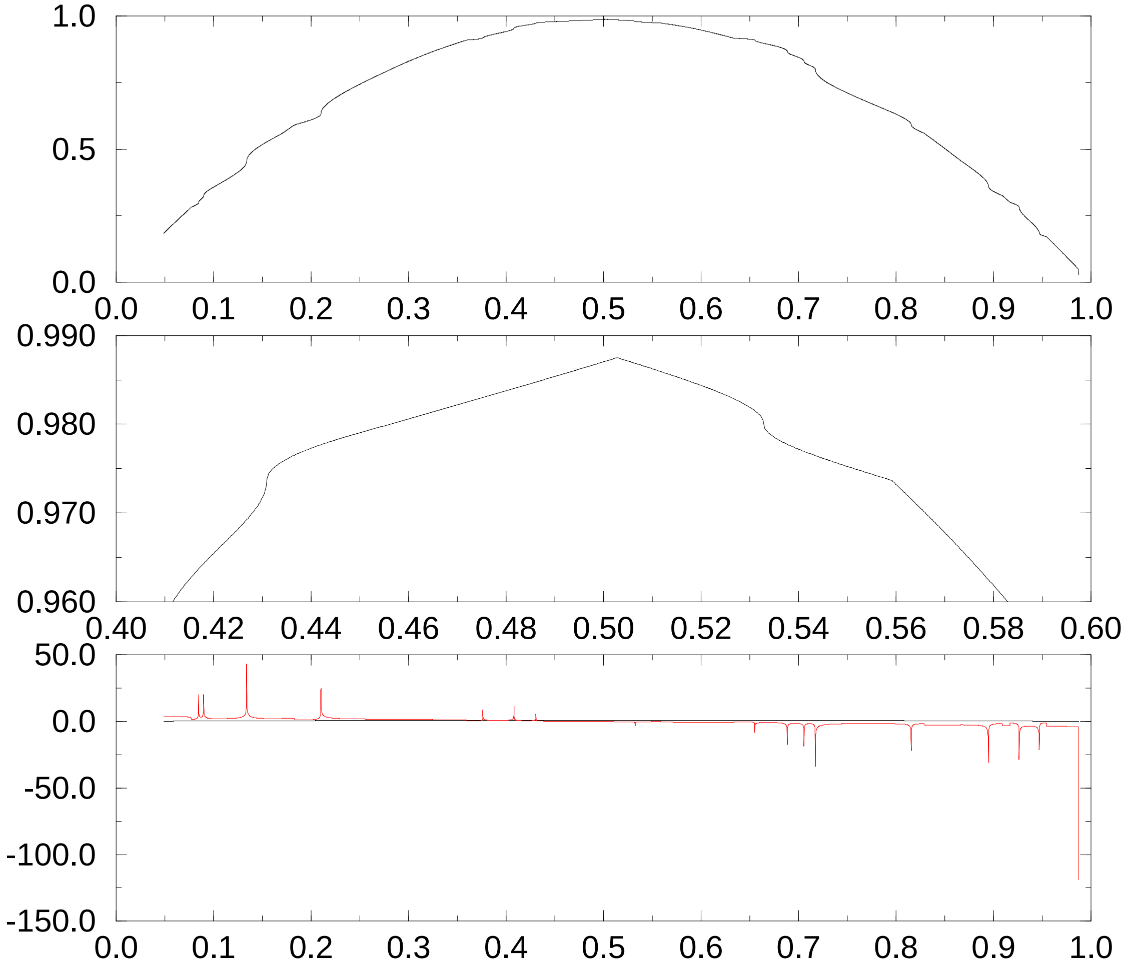

Figure 4.6: The conjugate map to the logistic map, $m = 3.9500001011218505454$ defined with respect to the 21 cell minimal Markov partition. The upper figure is the conjugate map, the middle one is a blow-up of the region around $(0.5, 1)$ illustrating the removal of the extremum, and the lower figure is the derivative of the conjugate map demonstrating that there are several points where its derivative is infinite as predicted.

Thus, the conjugate map, unlike its local inverses, is generally not piecewise analytic over $\mathcal{P}_{min}$. We observe that the latter condition is not satisfied for the logistic map at parameter 4 (when the singular function $S(x) = S_{min}(x)$), which is expected given its conjugacy to the tent map.

4.5.3 Conjugacy and periodic orbits

It is obvious that there is a one to one correspondence between the periodic orbits of the non-hyperbolic map, and its conjugate, for suppose $x*$ is a element of a periodic orbit of period p, and that $x \in C_j$. Then there exists an inverse branch f_α^{-p} such that $f_\alpha^{-p}(x*) = x*$. Moreover,

$$\hat{\eta} \circ f_\alpha^{-p} \circ \hat{\eta}^{-1}(y*) = y*, \tag{4.64}$$

where $x* = \hat{\eta}^{-1}(y*)$. The equivalence also extends to the relative instability factors of the periodic orbits, provided that the elements of the periodic orbit does not coincide with the points where the local conjugate transformations ($\{\hat{\eta}(x)\}$) are non-analytic. To see this, recall that

$$\frac{d}{dx} g_\alpha^p(y) = s_j(f_\alpha^{-p} \circ \hat{\eta}^{-1}(y)) f^{-p\prime}(\hat{\eta}^{-1}(x))\hat{\eta}^{-1\prime}(y), \tag{4.65}$$

and as each factor on the right hand-side is analytic at and in the vicinity of $y = y*$,

$$\frac{d}{dx} g_\alpha^p(y*) = f^{-p\prime}(x*). \tag{4.66}$$

A simple example is given by the fixed point in $[\frac{1}{2}, 1]$ of the logistic map ($f(x)$) at parameter 4, and the tent map ($\hat{f}(x)$) at slope 2, where

$$\hat{f}'(\frac{2}{3}) = f'(\frac{3}{4}) = -2$$

On the other hand, if all the elements of a periodic orbit coincide with points where local conjugate transformations (of type β) are non-analytic, then

$$\frac{d}{dx} g_\alpha^p(y*) = \sigma(|f_\alpha^{-p\prime}(x*)|)^\beta, \tag{4.67}$$

where $\sigma = 1$ if $f_\alpha^{-p}(x)$ is monotonic increasing, and equals $\sigma = -1$ otherwise. Before demonstrating this, lets again use the logistic and tent maps as an illustration where $\beta = \frac{1}{2}$,

$$\hat{f}'(0) = f'(0)^\beta = 2,$$

which obviously satisfies the eq.(4.67). A general proof is as follows.

From eqs. (4.48, 4.49, 4.52, 4.53), the local conjugate functions for the j^{th} cell may be written as

$$\hat{\eta} = a_{j-1} + c_0(x - a_{j-1})^\beta + r_1 \tag{4.68}$$

$$\hat{\eta}^{-1} = a_{j-1} + d_0(x - a_{j-1})^{\frac{1}{\beta}} + r_2, \tag{4.69}$$

where the remainder terms r_1, r_2 are analytic are analytic at $x = a_{j-1}$, and $r_1(a_{j-1}) = r_2(a_{j-1}) = 0$. It is easy to show that $d_0 = c_0^{\frac{-1}{\beta}}$. Next, one writes

$$f_\alpha^{-p}(x*) = x * + f_\alpha^{-p\prime}(x*)(x - x*) + O^2, \tag{4.70}$$

where $x* = a_{j-1}$ or $x* = a_j$, and O^2 denotes terms of order 2 and higher in $(x - x*)$. Consider the case where $x* = a_{j-1}$ and $f_\alpha^{-p}(x)$ is monotonic increasing. Then,

$$\hat{\eta} \circ f_\alpha^{-p} \circ \hat{\eta}^{-1}(x) = x * + f_\alpha^{-p\prime}(x*)^\beta (x - x*) + O^2, \tag{4.71}$$

and the result is immediate. The cases of $x = a_j$ or $f_\alpha^{-p}(x)$ being monotonic decreasing are treated in the same way.

□

In light of these results we should make a few comments

1. Clearly, if all the periodic orbits of $f(x)$ are hyperbolic, then this must also be true for the conjugate map $\hat{f}(x)$.
2. If $\hat{f}(x)$ is eventually expanding, then the formula for the spectra of local statistical properties is certainly valid

4.5.4 Equivalence to eventually hyperbolic maps

To prove eventual hyperbolicity we need only two more properties.

1. There exists a $\Lambda < 1$ and a constant K such that

$$\forall \alpha, \forall t, |\frac{d}{dx} f_\alpha^{-t}(x*)| < K\Lambda^{-t} < 1, \tag{4.72}$$

   where $x*$ is the fixed point of $f_\alpha^{-t}(x)$.

2. There exists an $\epsilon > 0$ such that

$$\forall \alpha, \forall t, |\frac{d}{dx} f_\alpha^{-t}(x)| < 1, \tag{4.73}$$

   for all $x \in [x * -\epsilon, x * +\epsilon]$.

Nowicki and Van Strien[83] have proven that the first condition is satisfied for any unimodal map with negative Schwarzian derivative. The second condition is also satisfied for this class of maps, and follows from the fact that if a map $f(x)$ has negative Schwarzian derivative, then $\left|\frac{d}{dx} f_\alpha^{-t}(x)\right|$ is a convex function[72]. To see why, simply assume that the second condition is not satisfied. For an arbitrarily small ϵ, one can then choose an inverse branch such that

$$\forall \alpha, \forall t, |\frac{d}{dx} f_\alpha^{-t}(x * \pm \epsilon)| \geq 1, \tag{4.74}$$

where one is free to choose the appropriate sign (in $\pm\epsilon$). Now as $\left|\frac{d}{dx}f_\alpha^{-t}(x)\right|$ is a convex function, and its domain is finite, its value must increase to the right or left of $x * \pm\epsilon$ so $f_\alpha^{-t}(x)$ has another fixed point y where

$$\forall\alpha,\, \forall t,\, |\frac{d}{dx}f_\alpha^{-t}(y))| > 1. \tag{4.75}$$

But this implies that $f^t(x)$ has a stable fixed point which contradicts the fact that all periodic orbits are unstable, and the demonstration is complete.

Now in eqs.(4.72-4.73) we may replace $f_\alpha^{-t}(x)$ by the conjugate inverse branches $g_\alpha^t(x)$ due to the results of subsection 4.5.4, and the fact that the conjugate transformations are bounded monotonic C_2 functions.

To prove eventual hyperbolicity, we note that we may write any sequence of inverse branches as

$$g_\alpha^{t+s}(x) = g_{\alpha_s} \circ g_{\alpha_{s-1}} \cdots \circ g_{\alpha_r} \circ \cdots \circ g_{\alpha_1} \circ g_{\alpha'}^t(x), \tag{4.76}$$

where $0 \leq r \leq s < t$. As all $\frac{d}{dx}g_\alpha(x)$ are bounded, we can choose t sufficiently large that $g_\alpha^{t+s}(x)$ is contractive in finite regions $\{\epsilon_{r+t}\}$ about each fixed point x_{r+t} of the subsequences

$$g_{\alpha_r} \circ \cdots \circ g_{\alpha_1}. \circ g_{\alpha'}^t(x),$$

In particular, we can choose t sufficiently large, that $\epsilon_{r+t} > \epsilon$, $\forall r \leq s$. Moreover, as the domain of $g_\alpha^{t+s}(x)$ is bounded, we can increase t and s further until all the regions $\{\epsilon_{r+t}\}$ overlap, so that $g_\alpha^{t+s}(x)$ is contractive in its entire domain. Thus, the proof is complete, and the ansatz is verified.

$\square$

Chapter 5

Two Dimensional Chaos

5.1 Introduction

Periodically forced nonlinear oscillators produce flows which through Poincaré sections sometimes reduce to a two dimensional first return map. Two well known examples are the Van der Pols and Duffing oscillators, which for certain values of their control parameters behave chaotically. In particular, the action of map on a region of the two dimensional surface of section can be likened to the making of a horseshoe: the region is first stretched in one direction, (the unstable direction) and contracted in a transverse one (the stable direction), and then the elongated form is folded (see figure 5.1). "Indeed, the presence of

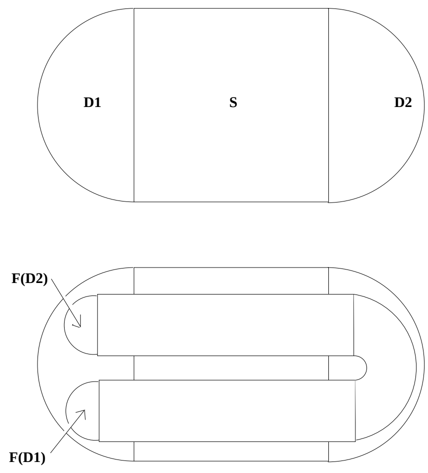

Figure 5.1: The Smale horseshoe map

horseshoes is essentially synonymous with what most authors mean by the term chaos"[44]. Shil'nikov discovered sufficient conditions for the return maps obtained from the Poincare section of three dimensional flows be of the horseshoe type. One requires **1** the existence of a particular type of fixed point known as a saddle focus, **2** a homoclinic orbit and **3** that a specific inequality[44, 103] to be satisfied which will be stated shortly. A flow

$$\frac{d\vec{x}}{dt} = \vec{f}(\vec{x}) \tag{5.1}$$

when linearized about the saddle-focus $\vec{x_*}$, has two complex conjugate eigenvalues ω_1, ω_2 and one real one ω_3, where either $Re(\omega_1) < 0 < \omega_3$ or $\omega_3 < 0 < Re(\omega_3)$. In the former case, the conjugate pair, and the corresponding set of eigenvectors define the local stable manifold of $\vec{x_*}$, whereas the eigenvector of ω_3 defines the local unstable manifold of $\vec{x_*}$, and in the vicinity of $\vec{x_*}$ trajectories appear to spiral up the surface of an inverted funnel[77, 41, 24]. In the latter case, the situation is reversed: the conjugate pair and their eigenvectors defines the local unstable manifold of $\vec{x_*}$, and the eigenvector of ω_3 define locally the stable manifold of $\vec{x_*}$, and the trajectories appear to spiral up the surface of the a non-inverted funnel. The non-linearities present in system can cause these trajectories, which otherwise would escape to infinity, to be re-injected close to the saddle-focus, permitting the possibility of chaos. The occurrence of chaos[1] is guaranteed if homoclinic orbit exists, which is a closed loop, emanating from $\vec{x_*}$ along the unstable manifold, and returning along the stable manifold, and $|\omega_3| > Re(\omega_1)$. A simple example of such a flow is the Rössler model

$$\begin{aligned} \frac{dx}{dt} &= -y - z \\ \frac{dy}{dt} &= x + ay \\ \frac{dz}{dt} &= bx - cz + xz, \end{aligned} \tag{5.2}$$

with $a = 0.38$, $b = 0.30$.

Two dimensional maps can also arise from flows without performing a Poincaré section, if the coefficients of the dynamical equations are periodic. A simple example is a bouncing ball on a massive oscillating table. If the coefficient of restitution equals one, the map is area preserving, while if is less than one, the map contacts areas uniformly. This example when conservative, has been widely studied, on account of its relevance to certain problems in particle and plasma physics, and most recently in quantum chaos. In a slightly different coordinate system, it is known as the standard map. In fact, any diffeomorphism with a homoclinic point p[2] will resemble a horseshoe at least in the vicinity of that point.

A glance at the horseshoe depicted in fig.5.1 reveals a local decoupling of the dynamics along the horizontal (expanding) direction, and the vertical (contracting) direction. If the map is applied repeatedly on $S \bigcup D_1 \bigcup D_2$, it is clear that most points will escape from S into D_1, and that the set of points that remain should be so fractured in the contracting direction that it becomes a Cantor set in the limit of an infinite number of iterations. This set, Λ is invariant, and the map is clearly hyperbolic on all points in Λ. The map is an example of a Axiom A diffeomorphism. Now one can imagine maps defined on a phase space Ω, where there is essentially no gap between either side of the horseshoe, so that Λ is not fractal but rather $\Lambda = \Omega$, but in all other respects it is like the horseshoe map. The map then is still axiom A, but is also a Anosov diffeomorphism. The local decoupling between the contracting and expanding directions follows from the stable (and unstable) manifold theorem, and the fact that all points of Ω are hyperbolic. The

[1] All periodic orbits are unstable and dense.

[2] A point of transversal intersection of the stable and unstable manifolds of a hyperbolic fixed or periodic point.

horseshoe map and any Anosov diffeomorphism where Ω is the 2-torus are also examples of K systems[6]. A K-system has the property that the corresponding Perron Frobenius operator acting on L^2 has denumerable Lebesgue spectrum (loosely speaking the spectra is continuous on the unit circle), and is consequently mixing. Other examples of K systems include Bernoulli schemes, the Baker map[75], geodesic flows on compact Riemannian manifolds with negative curvature and the Bolzmann-Gibbs model of a gas consisting of hard spheres in a box undergoing elastic collisions. The situation is more delicate for general axiom A systems. The main results are concerned with the ergodic properties of axiom A attractors[32, 14], with respect to the SRB measures. These are invariant ergodic measures which are smooth along the unstable foliations of the system. Their importance lies in the fact that the long time average properties of almost any point trajectory in an axiom A attractor are the same as those of the SRB measure.

We are interested primarily in the statistical properties of these systems. Despite the vast literature available, it appears, that the only concrete cases where, for example, time correlation functions have been explicitly calculated (excluding a numerical determination through a long time series) are restricted to systems where the one dimensional maps associated with the unstable direction leave the space of analytic functions invariant. Ruelle[95, 96], for example, essentially projects the dynamics of the system onto the unstable foliations, and under exceptional conditions, the resulting one dimensional map has an associated Frobenius-Perron operator which leaves the space of analytic functions invariant. Unlike Ruelle, Rugh[98, 97] does not perform such a projection, however concrete results (i.e. actual numbers) are again limited to essentially the same classes of systems and corresponding observables.

Another approach to this problem has been to seek representations of the Frobenius-Perron operator with respect to a basis consisting of tensor products of Schwarz distributions (e.g. derivatives of Dirac delta distributions) times polynomials[65], which for certain choices of basis amounts to a spectral decomposition[5, 38, 39, 49] of the operator, where basis elements are generalized eigenvectors of $\mathcal{U}$. The representation acquires meaning in suitable test spaces of observables, within the context of correlation function like integrals. While this method has proved fruitful in the examination of diffusion-like phenomena, it has only been applied to linear maps, and its extension for more general systems is not obvious.

In this chapter we consider the statistical properties of two dimensional chaotic maps defined either on the unit rectangle or the unit torus. The maps fall into two classes: conservative, and non-conservative but reversible. We suppose that the dynamics is described by the iterative equation,

$$\vec{x_{n+1}} = \vec{f}(\vec{x_n}), \tag{5.3}$$

where

$$\vec{x} = \begin{pmatrix} x \\ y \end{pmatrix}. \tag{5.4}$$

The associated probability density $\rho(\vec{x})$ evolves with the Frobenius-Perron operator,

$$\rho_{n+1}(\vec{x}) = \mathcal{U}\rho_n(\vec{x}) = \rho_n(\vec{f}^{-1}(\vec{x}))J(\vec{f}^{-1}(x)), \tag{5.5}$$

where the jacobian $J(\vec{x})$ equals one if the map is conservative.

The probability of finding the system in a region of phase space at a time t, given some initial preparation, or the calculation of a time correlation function, entails the evaluation of expressions such as

$$C_{ab}(t) = \int_I \int_I dxdy a(x,y)\mathcal{U}^t b(x,y), \tag{5.6}$$

where I denotes the unit interval, and $a(x,y)$ and $b(x,y)$ are observables. Therefore, the "physical" quantity is the value of the integral, not $\mathcal{U}^t a(x,y)$ (which can be interpreted as a probability density), or the integrand.

The method we will advocate in this chapter exploits the local decoupling of the dynamics into two one dimensional maps, and the fact that we can manipulate the integrand of eq.(5.6) through changes of variable without changing the value of the integral. Using local coordinates or canonical coordinates aligned with the stable and unstable directions, we construct a linear operator Θ consisting locally of a product of two Frobenius-Perron-like operators associated with the stable, and unstable directions respectively. By virtue of our manipulations of the fore-mentioned integrand, each of these individual operators is associated with a one dimensional expanding map, and leaves the corresponding space of piecewise analytic functions invariant. Thus we can use our results for one dimensional Markov analytic maps, to obtain matrix representations of Θ, and the representations converge extremely rapidly as in the one dimensional case. The great advantage of this method is that it can be applied to classes of nonlinear two dimensional maps, and is easily implemented numerically as the representations are obtained with respect to non-esoteric basis functions such as Chebyshev polynomials. It also explains why a generalized Markov coarse graining is not only possible for these systems, but is natural, which is not totally unexpected given earlier results on "traditional" Markov coarse graining[33, 21, 78].

One may still ask why not just obtain a representation of $\mathcal{U}$ acting on L^2, with respect to, for example Fourier functions or some other complete basis. Indeed, it is a simple matter for a number of conservative hyperbolic maps to obtain such a representation. There is, unfortunately a snag: as we already alluded to for K systems, the spectrum of $\mathcal{U}$ is continuous on the unit circle. Indeed it must be so for the system to be ergodic[46], let alone mixing. Thus, while time correlation functions must decay, and may decay even at an exponential rate, there is no eigenvalue of $\mathcal{U}$ corresponding to this decay. We will show that the exponential decay of time correlation functions for a large class of reversible chaotic systems is due to the fact that one needs only partial information about an evolving probability density to determine exactly the value of a time correlation function, which one might characterise as a statistical measurement. This is provided that the corresponding observables are not any possible measurable functions, but belong to a restricted set, for example analytic functions, piecewise analytic functions and so on. Of course, these are precisely the kind of observables that are typically used in statistical measurement. The surprise is that such calculations can be performed exactly, through matrix representations of a linear operator such as Θ, where the signature of exponential decay is contained in the fact that the eigenvalues lie within the unit disc. It is the hyperbolic nature of these systems, together with local decoupling of the dynamics along the stable and unstable manifolds which enables such representations to be obtained.

- In section 5.2 we consider a class of 2-d reversible maps which are constructed for any 1-d Markov analytic maps whose corresponding Frobenius-Perron operator leaves the space of analytic functions invariant. We show how time correlation function can be evaluated through matrix representations of a new linear operator Θ, which leaves tensor products of analytic functions in x and y invariant. In this setting, we explain why a generalized Markov coarse graining is both possible, and natural. We establish the relationship between our method, and representations of $\mathcal{U}$ with respect to generalized basis functions/ generalized eigenvectors.

- In section 5.3 we generalize or results to any 1-d Markov analytic map whose corresponding $\mathcal{U}$ leaves spaces of piecewise analytic functions invariant, with the condition that range of each monotonic branch include the unit interval.
- In section 5.4 we consider Anosov automorphisms of the torus.
- In section 5.5 we relate the spectra of our matrix representations to the zeta function formalism, and point out how subtle the counting problem can be.
- In section 5.6 we obtain the spectra associated with local statistical properties.
- We outline how our results are applicable to general 2-d hyperbolic systems on the torus in section 5.7.
- In section 5.8 we conclude the chapter with an assessment of its relevance to more general problems both from a practical perspective, and as a possible dynamical explanation of macroscopic irreversability.

5.2 Simple 2-d reversible chaotic maps

5.2.1 The basic idea

One of the simplest two dimensional chaotic maps is the baker, which is constructed from the Bernouili shift in the following way. The Bernouli shift maps the interval onto itself,

$$f(x) = \begin{cases} f_L(x) = 2x & \text{if } x < \frac{1}{2} \\ f_R(x) = 2x - 1 & \text{otherwise.} \end{cases} \tag{5.7}$$

The baker map is defined as

$$\vec{f}(\vec{x}) = \begin{cases} f_\alpha(x) & \text{if } x \in I_\alpha \\ f_\alpha^{-1}(y) & \end{cases} \tag{5.8}$$

where I_α is the domain of the α branch, ($I_l = [0, \frac{1}{2}]$, $I_r = (\frac{1}{2}, 1]$ and f_α^{-1} is the corresponding local inverse. It's inverse has the form,

$$\vec{f}^{-1}(\vec{x}) = \begin{cases} f_\alpha^{-1}(x) & \\ f_\alpha(y) & \text{if } y \in I_\alpha \end{cases} \tag{5.9}$$

Clearly the map is one to one, and conservative as the the expansion by a factor of two along g the x-axis is compensated by a contraction of $\frac{1}{2}$ along the y-axis. Moreover, there is a decoupling in $\vec{f}(\vec{x})$ between x and y for $x \in I_\alpha$, so that locally we may consider Baker as two independent one dimensional maps, one contractive, the other expansive. While this remark is trivial for the Baker, we may exploit this observation to consider much more complicated two dimensional maps, where either by design, or by a judicious choice of local coordinates, a similar decoupling takes place. In particular, we may generalize the latter construction to define reversible two dimensional maps from two one dimensional chaotic maps $f_x(x)$ and $f_y(y)$ as,

$$\vec{f}(\vec{x}) = \begin{cases} f_{x\alpha}(x) & \text{if } x \in I_\alpha \\ f_{y\alpha}^{-1}(y) & . \end{cases} \tag{5.10}$$

where each $f_{x\alpha}(x)$ is monotonic and analytic in the domain $I_{x\alpha}$, $f_{x\alpha}(I_{x\alpha}) = J_{x\alpha} \supset I$, and domains $I_{x\alpha}$ which are mutually disjoint cover the unit interval. Similarly, $f_{y\alpha}(y)$ is monotonic and analytic in the domain $I_{y\alpha}$, $f_{y\alpha}(I_{y\alpha}) = J_{y\alpha} \supset I$, and domains $I_{y\alpha} \subset I$ which are mutually disjoint cover the unit interval.

$$\vec{f}^{-1}(\vec{x}) = \begin{cases} f_{x\alpha}^{-1}(x) & \\ f_{y\alpha}(y) & \text{if } y \in I_{y\alpha} \end{cases} \tag{5.11}$$

A simple example of such a two dimensional map, is where $f_x(x)$ is the Bernoulli shift, and $f_y(y)$ is the tent map with slope two. Now the two dimensional map will be conservative if $f_x(x)$ and $f_y(y)$ are piecewise linear, and $|f_x'(x)| = |f_y'(y)| =$ constant. Otherwise, the new map will be reversible, but not conservative. If $J_{x\alpha}$ or $J_{y\alpha}$ is greater than the unit interval, then the system is a repeller. That is there are points which escape the unit rectangle, and never come back. This is the case where $f_x(x)$ is the tent map with slope greater than two. Another example is the Smale horseshoe map. For these maps, the Frobenius-Perron operator takes the form

$$\mathcal{U}\rho(x,y) = \sum_\alpha \rho(f_{x\alpha}^{-1}(x), f_{y\alpha}(y))|\frac{d}{dx}f_{x\alpha}^{-1}(x)\frac{d}{dy}f_{y\alpha}(y)|\chi_{I_{y\alpha}}(y) \tag{5.12}$$

Our goal is to calculate $C_{ab}(t)$ for representative classes of observables. Let's assume that each observable can be written as a product of two terms, of which one depends on x, and the other depends only on y,

$$a(x,y) = a_x(x)a_y(y);\; b(x,y) = b_x(x)b_y(y). \tag{5.13}$$

Using eq.(5.9) one can easily show that right hand side of eq.(5.6) takes the form

$$\begin{aligned} C_{ab}(t) &= \sum_{\alpha_t,\alpha_{t-1},\cdots,\alpha_1} \{[\int_I a_x(x)U_{x\alpha_t}U_{x\alpha_{t-1}}\cdots U_{x\alpha_1}b_x(x)] \\ &\times [\int_I a_y(y)U^\dagger{}_{y\alpha_t}U^\dagger{}_{y\alpha_{t-1}}\cdots U^\dagger{}_{y\alpha_1}b_y(y)dy]\} \end{aligned} \tag{5.14}$$

where

$$U_{x\alpha}b_x(x) = b_x(f_{x\alpha}^{-1}(x))\left|\frac{d}{dx}f_{x\alpha}^{-1}(x)\right|, \tag{5.15}$$

and

$$U^{\dagger}_{y\alpha}b_y(y) = b_y(f_{y\alpha}(y))|\frac{d}{dy}f_{y\alpha}(y)|\chi_{I_{y\alpha}}(y). \tag{5.16}$$

Now, we can make a change in variable so that

$$\int_I a_y(y){U^{\dagger}}_{y\alpha_t}{U^{\dagger}}_{y\alpha_{t-1}}\cdots {U^{\dagger}}_{y\alpha_1}b_y(y)dy \;=\; \int_I b_y(y)U_{y\alpha_1}U_{y\alpha_2}\cdots U_{y\alpha_t}a_y(y)dy, \tag{5.17}$$

where

$$U_{y\alpha}a_y(y) = a_y(f^{-1}_{y\alpha}(y)). \tag{5.18}$$

Thus, the properties of $C_{ab}(t)$ can be deduced by through the properties of a new linear operator Θ_t acting on the function $b_x(x)a_y(y)$,

$$\begin{gathered}\Theta_t b_x(x)a_y(y) \;= \\ \textstyle\sum_{\alpha_t,\alpha_{t-1},\cdots,\alpha_2,\alpha_1}\{\,U_{x\alpha_t}U_{y\alpha_1}U_{x\alpha_{t-1}}U_{y\alpha_2}\cdots U_{x\alpha_2}U_{y\alpha_{t-1}}U_{x\alpha_1}U_{y\alpha_t}\,\}b_x(x)a_y(y)\end{gathered} \tag{5.19}$$

and

$$\Theta_1 b_x(x)a_y(y) = \sum_{\alpha} U_{x\alpha}U_{y\alpha}b_x(x)a_y(y). \tag{5.20}$$

Thus,

$$C_{ab}(t) = \int_I\int_I dxdya_x(x)b_y(y)\Theta_t b_x(x)a_y(y). \tag{5.21}$$

Let us now mention a remarkable difference between $\mathcal{U}^t$ and Θ_t, using the baker map as an example. Suppose $b_y(y) \neq 1$, and $b_x(x)$ and $b_y(y)$ are polynomials or order N, in x and y respectively. Observe that $\mathcal{U}b_x(x)b_y(y)$ will have a discontinuity at $y = \frac{1}{2}$. Similarly, $\mathcal{U}^t b_x(x)a_y(y)$ will have discontinuities at

$$y = \frac{j}{2^t},\; j = 1, 2, ..., 2^t - 1.$$

Thus, as the density evolves it becomes progressively more fractured in y, while its x dependence remains that of a polynomial of order no greater than N. Yet if $b_x(x)$ and $a_y(y)$ are each polynomials of order N in x and y respectively, then the x and y dependence of $\Theta_t b_x(x)a_y(y)$ will not be fractured, but rather will be that polynomial type, no higher that N in each of its variables. Thus, Θ_t leaves the space of polynomial functions in x and y of finite order invariant, and can be represented easily as a matrix using a polynomial basis. For a general expanding map, where each $f^{-1}_{\alpha}(x)$ is analytic, the space of analytic functions in x and y respectively is invariant under Θ_t, but becomes progressively more fractured under $\mathcal{U}^t$ (unless $b_y(y) = 1$. Therefore, Θ_t would seem to be an easier operator to study, except for the awkward ordering in

$$U_{x\alpha_t}U_{y\alpha_1}U_{x\alpha_{t-1}}U_{y\alpha_2}\cdots U_{x\alpha_2}U_{y\alpha_{t-1}}U_{x\alpha_1}U_{y\alpha_t}b_x(x)a_y(y).$$

We now will show that this ordering is not in fact a problem.

We may exploit our results for one dimensional Markov analytic maps as $f^{-1}_{x\alpha}(x)$ and $f^{-1}_{y\alpha}(y)$ are contractive analytic function of their arguments. If $b_x(x)$ and $a_y(y)$ are analytic, we may use Chebyshev polynomials in x and in y to obtain a matrix representation of $U_{x\alpha}$ and $U_{y\alpha}$ respectively. The Chebyshev polynomials obey an orthogonality relation

$$\int_I T_n(x)T_m(x)w(x)dx = h_n\delta_{n,m}, \tag{5.22}$$

with respect to the weighting factor $w(x)$. The matrix representation of eq.(5.15) and eq.(5.18) are

$$W_{x\alpha n_k n_{k-1}} = \frac{1}{h_{n_k}}\int_I T_{n_k}(x)[U_{x\alpha}T_{n_{k-1}}(x)]w(x)dx, \tag{5.23}$$

and

$$W_{y\alpha m_k m_{k-1}} = \frac{1}{h_{m_{k-1}}}\int_I T_{m_{k-1}}(y)[U_{y\alpha}T_{m_k}(y)]w(y)dy, \tag{5.24}$$

Hence,

$$\begin{aligned}[\textstyle\int_I a_x(x)U_{x\alpha_t}U_{x\alpha_{t-1}}\cdots U_{x\alpha_1}b_x(x)] &= \textstyle\sum_{n_t=0}^{\infty}\sum_{n_{t-1}=0}^{\infty}\cdots\sum_{n_0=0}^{\infty} \\ \{[\textstyle\int_I a_x(x)T_{n_t}(x)dx]W_{x\alpha_t n_t n_{t-1}}W_{x\alpha_{t-1}n_{t-1}n_{t-2}}&\cdots W_{x\alpha_1 n_1 n_0}b_{xn_0}\},\end{aligned} \tag{5.25}$$

and

$$\begin{aligned}[\textstyle\int_I b_y(y)U_{y\alpha_1}U_{y\alpha_2}\cdots U_{y\alpha_1}a_y(y)] &= \textstyle\sum_{m_t=0}^{\infty}\sum_{m_{t-1}=0}^{\infty}\cdots\sum_{m_1=0}^{\infty} \\ \{a_{ym_t}W_{y\alpha_t m_t m_{t-1}}W_{y\alpha_{t-1}m_{t-1}m_{t-2}}&\cdots W_{y\alpha_1 m_1 m_0}[\textstyle\int_I b_y(y)T_{m_0}(y)dy]\},\end{aligned} \tag{5.26}$$

where

$$b_{xn_0} = \frac{1}{h_{n_0}}\int_I T_{n_0}(x)b_x(x)w(x)dx \tag{5.27}$$

and

$$a_{ym_t} = \frac{1}{h_{m_t}}\int_I T_{m_t}(y)a_y(y)w(y)dy. \tag{5.28}$$

From chapter 3 we know that these representations converge extremely rapidly. Indeed, if $f(x)$ is piecewise linear, any polynomial function space of finite order remains invariant under each of these operators. In this case, if $a_y(y)$ and $b_x(x)$ are polynomials of order N in y, and x respectively, then the summations in eq.(5.25) and eq.(5.26) are bounded by N rather than ∞. On the other hand, if $f(x)$ is not piecewise linear, or $a_y(y)$ and $b_x(x)$ are not polynomials, we may still truncate the expansions at a finite order with negligible error. Therefore,

$$\begin{aligned}C_{ab}(t) = \textstyle\sum_{n_t=0}^{\infty}\sum_{n_{t-1}=0}^{\infty}\cdots\sum_{n_0=0}^{\infty}\sum_{m_t=0}^{\infty}\sum_{m_{t-1}=0}^{\infty}\cdots\sum_{m_0=0}^{\infty}\sum_{\alpha_t,\alpha_{t-1},\cdots,\alpha_1}\{ \\ a_{ym_t}\hat{a}_{xn_t}W_{x\alpha_t n_t n_{t-1}}W_{y\alpha_t m_t m_{t-1}}W_{x\alpha_{t-1}n_{t-1}n_{t-2}}W_{y\alpha_{t-1}m_{t-1}m_{t-2}}\cdots W_{x\alpha_1 n_1 n_0}W_{y\alpha_1 m_1 m_0}b_{xn_0}\hat{b}_{ym_0}\} \\ \simeq \textstyle\sum_{m_t=0}^{N}\sum_{n_t=0}^{N}\sum_{m_1=0}^{N}\sum_{n_1=0}^{N} a_{ym_t}\hat{a}_{xn_t}W^t_{m_t n_t m_0 n_0}b_{xn_0}\hat{b}_{ym_0},\end{aligned} \tag{5.29}$$

where

$$\hat{a}_{xn_t} = \int_I a_x(x)T_{n_t}(x)dx,$$

$$\hat{b}_{ym_0} = \int_I b_y(y)T_{m_0}(y)dy,$$

$$W_{m_k n_k m_{k-1} n_{k-1}} = \sum_{\alpha} W_{y\alpha m_k m_{k-1}} W_{x\alpha n_k n_{k-1}}, \tag{5.30}$$

and N is an appropriate truncation order. Thus, the awkwardness of the ordering in eq.(5.19) is no longer a problem. Let us stress that if $f(x)$ is piecewise linear and $a_y(y)$ and $b_x(x)$ are polynomials in x and y of order N, then no error is produced by truncation, so that the corresponding time correlation functions may be determined exactly with a N^2XN^2 dimensional matrix. More generally, from section 2 we know that that there exists a τ such that

$$\forall t > \tau,\ |W^t_{n_1 m_1 n_0 m_0}| < C\frac{\hat{r}^{n_0+m_1}}{r^{n_1+m_0}}, \tag{5.31}$$

where C is a constant and $\hat{r} < r > 1$.

5.2.2 Spectral properties of Θ_t and W

One may wonder how the spectral properties of Θ_t acting on functions $a_y(y)b_x(x)$ which are analytic in x and y are related to the spectral properties of W^t ? Their eigenvalues are identical, as we will now show. Let

$$\hat{W}_{tm_0n_tm_tn_0} = \frac{1}{h_{m_0}h_{n_t}}\int_I\int_I dydxw(y)w(x)T_{m_0}(y)T_{n_t}(x)\Theta_t T_{m_t}(y)T_{n_0}(x) \tag{5.32}$$

so that

$$\begin{aligned} C_{ab}(t) &= \textstyle\sum_{m_t=0}^{\infty}\sum_{n_t=0}^{\infty}\sum_{m_0=0}^{\infty}\sum_{n_0=0}^{\infty} \hat{b}_{ym_0}\hat{a}_{xn_t}\hat{W}_{tm_0n_tm_tn_0}a_{ym_t}b_{xn_0} \\ &= \textstyle\sum_{m_t=0}^{\infty}\sum_{n_t=0}^{\infty}\sum_{m_0=0}^{\infty}\sum_{n_0=0}^{\infty} a_{ym_t}\hat{a}_{xn_t}\hat{W}^{\ddagger}_{tm_tn_tm_0n_0}\hat{b}_{ym_0}b_{xn_0} \\ &= \textstyle\sum_{m_t=0}^{\infty}\sum_{n_t=0}^{\infty}\sum_{m_0=0}^{\infty}\sum_{n_0=0}^{\infty} a_{ym_t}\hat{a}_{xn_t}W^{t}_{m_tn_tm_0n_0}\hat{b}_{ym_0}b_{xn_0}, \end{aligned} \tag{5.33}$$

$\ddagger$ is a partial transpose operation on $\hat{W}_t$ which leaves its determinant invariant. The following diagram illustrates the operation on a matrix where each of the indices m_t, n_t, m_0, n_0 can only take on two values, 0 or 1.

$$\hat{W}_{tm_0n_tm_tn_0} = \begin{pmatrix} \hat{W}_{t0000} & \hat{W}_{t0001} & \hat{W}_{t0010} & \hat{W}_{t0011} \\ \hat{W}_{t0100} & \hat{W}_{t0101} & \hat{W}_{t0110} & \hat{W}_{t0111} \\ \hat{W}_{t1000} & \hat{W}_{t1001} & \hat{W}_{t1010} & \hat{W}_{t1011} \\ \hat{W}_{t1100} & \hat{W}_{t1101} & \hat{W}_{t1110} & \hat{W}_{t1111} \end{pmatrix}. \tag{5.34}$$

Then,

$$\hat{W}^{\ddagger}_{tm_0n_tm_tn_0} = \begin{pmatrix} \hat{W}_{t0000} & \hat{W}_{t0001} & \hat{W}_{t1000} & \hat{W}_{t1001} \\ \hat{W}_{t0100} & \hat{W}_{t0101} & \hat{W}_{t1100} & \hat{W}_{t1101} \\ \hat{W}_{t0010} & \hat{W}_{t0011} & \hat{W}_{t1010} & \hat{W}_{t1011} \\ \hat{W}_{t1110} & \hat{W}_{t0111} & \hat{W}_{t1110} & \hat{W}_{t1111} \end{pmatrix}. \tag{5.35}$$

Eq.(5.33) implies that $\hat{W}_t^{\ddagger} = W^t$. Equivalently $\hat{W}_t = W^{t\ddagger}$, which means that Θ_t can be generated by simple matrix multiplication, when acting on functions which are analytic in x and y. The partial transpose operation is well defined here because of the rapid convergence of the representation. Let us be more formal and define a product space

$\mathcal{F}_x X \mathcal{F}_y$, and consider the case where $\mathcal{F}_x$ and $\mathcal{F}_y$ are the space of functions analytic in x and y respectively. As remarked before, this space is invariant under Θ_t In particular, $\hat{W}_1 = W^{\ddagger}$, so that the spectral properties of Θ_1 acting on $\mathcal{F}_x X \mathcal{F}_y$ is the same as W. Thus as regards the evaluation of $C_{ab}(t)$, where $a_y(y)$ and $b_x(x)$ are analytic in y and x, we need only study the properties of Θ_t. Let $\mathcal{F}$ denote the function space consisting of $\{a_y(y)b_x(x)\}$, where each of these functions is an analytic functions of its argument. This function space is invariant. Thus we have the extraordinary result the statistical properties of $C_{ab}(t)$ determined through $\mathcal{U}$ which not not leave $\mathcal{F}$ invariant is entirely equivalent to Θ_t. Moreover, while the spectra of $\mathcal{U}$ must lie on the unit circle, and are continuous the spectra of Θ_1 are discrete, lie within the unit circle[3] (except for the eigenvalue 1), and equal the decay rates of $C_{ab}(t)$.

5.2.3 Two simple examples

Let us now illustrate these results with two simple examples, the baker map, and Smale's horseshoe map, which is a repeller. First let us consider the baker. From eqs.(5.7),(5.8) we observe that

$$\begin{aligned} U_{xl} b_x(x) &= \frac{1}{2} b_x(\frac{x}{2}), \qquad & U_{yl} a_y(y) a_y(\frac{y}{2}) \\ U_{xr} b_x(x) \frac{1}{2} b_x(\frac{1+x}{2}), \qquad & & U_{yr} a_y(y) = a_y(\frac{1+y}{2}). \end{aligned} \tag{5.36}$$

Now

$$W_{x\alpha n_k n_{k-1}} = \begin{cases} \frac{1}{2}^{n_k+1} & \text{if } n_k = n_{k-1} \\ 0 & \text{if } n_k > n_{k-1} \end{cases}, \tag{5.37}$$

and

$$W_{y\alpha m_k m_{k-1}} = \begin{cases} \frac{1}{2}^{m_k} & \text{if } m_k = m_{k-1} \\ 0 & \text{if } m_{k-1} > m_k \end{cases}. \tag{5.38}$$

Hence,

$$W_{m_k n_k m_{k-1} n_{k-1}} = \begin{cases} \frac{1}{2}^{m_k+n_k} & \text{if } m_k = m_{k-1} \text{ and } n_k = n_{k-1} \\ 0 & \text{if } m_{k-1} > m_k \text{ or } n_k > n_{k-1} \end{cases}. \tag{5.39}$$

Now, as mentioned before, may make a partial transpose of this matrix without changing its spectra,

$$W_{m_k n_k m_{k-1} n_{k-1}} \to W_{m_{k-1} n_k m_k n_{k-1}} \equiv W^{\ddagger},$$

and $W^{\ddagger}$ is upper triangular, so we may simply read the eigenvalues from its diagonal elements,

$$\lambda_{nm} = \frac{1}{2}^{n+m}, \tag{5.40}$$

and observe that each eigenvalue $\frac{1}{2}^N$, for $N > 1$ is $2N+1$ fold degenerate. It is easy to show that each $\lambda = exp(-z)$, where z is the corresponding Zeta Ruelle resonance.

[3]this is because the one dimensional maps $f_x(x)$ are exact and therefore U_x has only one eigenvalue of unit magnitude. More generally, the number of eigenvalues of unit magnitude of Θ_1 acting on the fore-mentioned function spaces is the same as the associated U_x.

Let us now consider the Smale horseshoe map[26][44]

$$\vec{x}_{n+1} = F(\vec{x}_n), \tag{5.41}$$

which arises whenever one has transverse homoclinic orbits. A simple, "linear" one is displayed in Fig.(5.1).

A great deal is known about this map. For example, for forward time evolution, there is an invariant set which is the form of a cantor set along the expanding direction, and a similar invariant set along the contracting direction for backward time evolution. There is also a complete symbolic dynamics. We will not go into these details, but rather focus on the statistical properties of the system, within the rectangle **S** . We can characterise the action of the map as an expansion by a constant factor $\delta > 2$ along the horizontal direction, and a contraction, by a factor $\frac{1}{\delta}$ along the vertical direction, followed by a folding. Consider the set of points,

$$\Xi = \{\vec{x} : \vec{x} \in S \text{ and } F(\vec{x}) \in S\}, \tag{5.42}$$

and let S be the unit square $[0,1]X[0,1]$. For these points, the map $F(\vec{x})$ is piecewise linear, and resembles the baker map in that we can describe its action just as eq.(5.8). Thus, there exists a one dimensional map

$$f(x) = \begin{cases} f_l(x) = \delta x + b & \text{if } 0 \geq x < \frac{1}{2} \\ f_r(x) = -\delta(x-1) + b & \text{if } \frac{1}{2} \leq x \leq 1 \end{cases}, \tag{5.43}$$

where $\frac{1}{2}(\delta - 2) < b < 0$. The linear two dimensional map is then defined as,

$$\vec{f}(\vec{x}) = \begin{cases} f_\alpha(x) & \text{if } x \in I_\alpha \\ f_\alpha^{-1}(y) & , \end{cases} \tag{5.44}$$

where I_α is the domain of the α branch, and f_α^{-1} is the corresponding local inverse. It's inverse has the form,

$$\vec{f}^{-1}(\vec{x}) = \begin{cases} f_\alpha^{-1}(x) & \\ f_\alpha(y) & \text{if } y \in I_\alpha \end{cases}. \tag{5.45}$$

The statistical properties of time correlation functions of observables that have support S can be obtained in the same way as was done for the baker. Hence,

$$W_{xln_kn_{k-1}} = \begin{cases} \frac{1}{\delta}^{n_k+1} & \text{if } n_k = n_{k-1} \\ 0 & \text{if } n_k > n_{k-1} \end{cases}, \quad W_{xrn_kn_{k-1}} = \begin{cases} -(\frac{-1}{\delta})^{n_k+1} & \text{if } n_k = n_{k-1} \\ 0 & \text{if } n_k > n_{k-1} \end{cases}, \tag{5.46}$$

$$W_{ylm_km_{k-1}} = \begin{cases} \frac{1}{\delta}^{m_k} & \text{if } m_k = m_{k-1} \\ 0 & \text{if } m_{k-1} > m_k \end{cases}, \quad W_{yrm_km_{k-1}} = \begin{cases} (\frac{-1}{\delta})^{m_k} & \text{if } m_k = m_{k-1} \\ 0 & \text{if } m_{k-1} > m_k \end{cases}. \tag{5.47}$$

Therefore,

$$W_{m_kn_km_{k-1}n_{k-1}} = \begin{cases} 2\frac{1}{\delta}^{m_k+n_k+1} & \text{if } m_k = m_{k-1} \text{ and } n_k = n_{k-1} \text{ and } n_km_k \text{ is even} \\ 0 & \text{if } n_k = n_{k-1} \text{ and } n_km_k \text{ is odd} \\ 0 & \text{if } m_{k-1} > m_k \text{ or } n_k > n_{k-1} \end{cases}. \tag{5.48}$$

Again, we may perform a partial transpose on W to reveal that $W^{\ddagger}$ is upper triangular so that its eigenvalues are given by the elements of W_{mnmn} of eq.(5.48). The leading eigenvalue $\frac{2}{\delta}$ is less than one, which is expected as S is a repeller, and so the probability of being in S asymptotically must vanish. We could in a similar way consider a dissipative horseshoe map with an expansion rate $\delta > 2$ along the horizontal direction and a contraction rate $\mu < \frac{1}{\delta}$ along the vertical direction, as described by Guckenheimer and Holmes. In that case the spectra have the form

$$\lambda_{nm} = \begin{cases} 2\frac{1}{\delta}^{n+1}\mu^m & \text{if } nm \text{ is even} \\ 0 & \text{otherwise} \end{cases} . \tag{5.49}$$

5.2.4 Generalized Markov Coarse Graining

Let us briefly mention why only partial information about an evolving probability density is necessary to determine the values of time correlation functions. As we have seen, time correlation functions may be exactly determined through the matrix representation

$$W_{m_k n_k m_{k-1} n_{k-1}} = \sum_\alpha W_{y\alpha m_k m_{k-1}} W_{x\alpha n_k n_{k-1}},$$

where

$$W_{x\alpha n_k n_{k-1}} = \frac{1}{h_{n_k}} \int_I T_{n_k}(x)[U_{x\alpha} T_{n_{k-1}}(x)]dx,$$

and

$$\begin{aligned} W_{y\alpha m_k m_{k-1}} &= \tfrac{1}{h_{m_{k-1}}} \textstyle\int_I T_{m_{k-1}}(y)[U_{y\alpha} T_{m_k}(y)]w(y)dy \\ &= \tfrac{1}{h_{m_{k-1}}} \textstyle\int_I U^{\dagger}_{y\alpha} \left[[T_{m_{k-1}}(y) w(y)\right] T_{m_k}(y)dy \\ &= \tfrac{1}{h_{m_{k-1}}} \textstyle\int_I w(f_{y\alpha}(y)) U^{\dagger}_{y\alpha} \left[[T_{m_{k-1}}(y))\right] T_{m_k}(y)dy \end{aligned}$$

$$= \tfrac{1}{h_{m_k}} \tfrac{h_{m_k}}{h_{m_{k-1}}} \textstyle\int_I w(y) \tfrac{w(f_{y\alpha}(y))}{w(y)} T_{m_k}(y) U^{\dagger}_{y\alpha} \left[[T_{m_{k-1}}(y))\right] dy. \tag{5.50}$$

To make our point as transparent as possible, instead of Chebyshev polynomials lets use Legendre polynomials, as the weighting function $w(x)$ is a constant. Hence, we may write

$$W^t_{m_t n_t m_0 n_0} = \frac{1}{h_{m_t}} \frac{h_{m_t}}{h_{m_0}} \frac{1}{h_{n_t}} \int_I \int_I w(y)w(x) T_{m_t}(y) T_{n_t}(x) U^t T_{m_0}(y) T_{n_0}(x) dy dx \tag{5.51}$$

Now, as we have already observed, if $m_0 > 0$, $U^t T_{m_0}(y) T_{n_0}(x)$ will be highly fractured along the y axis, in fact it will have generally have $r^t - 1$ discontinuities, where $f_x(x)$ and $f_y(y)$ each have r branches. It is obvious that if we wish to approximate such a fractured functions with Legendre polynomials, i.e through the representation, then we will need m_1 to be very large. In fact we can expect that order M of the polynomials should be such that the number of zeros is at least equal to the number of discontinuities. But if the order necessary to evaluate eq.(5.29) exactly or with high accuracy is N, then the only relevant details of the fractured form of $Ub(x, y)$ along the y axis, is that which can be picked up by polynomials in y of order no higher than N. Indeed, if the dynamical systems is piecewise linear, and the observable $a(x, y)$ is polynomial in y and of order 1 say, that the time correlation function may be evaluated exactly, using polynomials in y or order no greater than 1. Thus, most of the complicated features present in evolving densities along the contracting directions is redundant. We have then a simple physical explanation of why time correlation functions decay, independently of any error in their computation, at least for the dynamical systems being considered in this chapter. More importantly, we see why this a priori infinite dimensional problem naturally reduces to a finite one.

5.2.5 Generalized basis and eigenvectors

Another method used to study the statistical properties of two dimensional linear conservative hyperbolic maps seeks a representation of $\mathcal{U}$ using a bi-orthonormal set of generalized basis functions

$$\begin{aligned} \phi_{n,m}(x,y) &= \tilde{\phi_m}(y)\phi_n(x), \\ \tilde{\phi_{n,m}}(x,y) &= \phi_m(y)\tilde{\phi_n}(x), \\ \int_0^1\int_0^1 dxdy\tilde{\phi}_{n_1,m_1}(x,y)\phi_{n_0,m_0}(x,y) &= \delta_{n_1,n_0}\delta_{m_1,m_0}, \\ \int_0^1 \tilde{\phi}_{n_1}(x)\phi_{n_0}(x)dx &= \delta_{n_1,n_0}. \end{aligned} \tag{5.52}$$

The $\phi_n(x)$'s are polynomials in x, and are used to expand functions lying in some space of analytic functions. For example, if $\phi_n(x) = x^n$, then we are simply making a Taylor series expansion, and for uniform convergence, the space consists of functions which are analytic in a disc of radius r, where r of coarse depends on the interval where the dynamics are defined, and the choices of zero for the monomials. The $\tilde{\phi}_n(x)$'s simply determine the expansion coefficients, and are Schwarz distributions (consisting of Dirac delta distributions and their derivatives). So, in the case of monomials, the expansion coefficients of an analytic functions $g(x)$ are given by,

$$\tilde{\phi}_n(x) = \frac{(-1)^n\delta^{(n)}(x)}{n!}, \ \int_0^1 \tilde{\phi}_n(x)g(x)dx = \frac{g^{(n)}(0)}{n!}. \tag{5.53}$$

We want to relate matrix representation of $\mathcal{U}$,

$$\hat{W}_{m_1n_1m_0n_0} = \int_0^1\int_0^1 \tilde{\phi}_{n,m}(x,y)\mathcal{U}\phi_{n,m}(x,y)dxdy. \tag{5.54}$$

Let us first recall that

$$\mathcal{U}\tilde{\phi_m}(y)\phi_n(x) = \sum_\alpha U_{x\alpha}\phi_n(x)U^\dagger_{y\alpha}\tilde{\phi_m}(y). \tag{5.55}$$

Thus,

$$\begin{aligned} \hat{W}_{m_1n_1m_0n_0} &= \sum_\alpha \int_0^1 \phi_{m_1}(y)U^\dagger_{y\alpha}\hat{\phi}_{m_0}(y)dy\int_0^1 \hat{\phi}_{n_1}(x)U_{x\alpha}\phi_{n_0}(x)dx \\ &= \sum_\alpha \int_0^1 \hat{\phi}_{m_0}(y)U_{y\alpha}\phi_{m_1}(y)dy\int_0^1 \hat{\phi}_{n_1}(x)U_{x\alpha}\phi_{n_0}(x)dx \\ &= \int_0^1\int_0^1 \hat{\phi}_{m_0}(y)\hat{\phi}_{n_1}(x)\Theta_1\phi_{m_1}(y)\phi_{n_0}(x)dydx. \end{aligned} \tag{5.56}$$

Hence, the matrix representation of Θ_1 with respect to the basis

$$\phi_{m_1}(y)\phi_{n_0}(x), \tag{5.57}$$

is the same as the partial transpose of eq.(5.54), where the indices m_0 and m_1 are interchanged. Therefore, the spectra of the two representations are identical. We conclude then that from the perspective of time correlation functions the two formulations are equivalent to generalized coarse graining. Let us add that we could have used other bi-orthonormal sets, formed, for example, from Bernouli polynomials and their corresponding duals. The advantage of working with Θ is that we can see which sort of basis should be chosen so that the corresponding matrix representation will converge (in advance of any calculation), and the reason for such convergence is clear. This is not true of representations of $\mathcal{U}$ with respect to a generalized basis, where the choice of basis is generally justified post facto, once it is known to work for a given system. While this distinction is not very important for linear systems, it is very relevant for more complex and general systems, where one is forced to employ numerical methods.

5.3 Multi-cell minimal Markov partitions

Up to now, we have constructed two dimensional reversible maps from one dimensional Markov analytic maps, where the minimal Markov partition consisted of one cell only, the unit interval itself. We shall now generalize the construction (see eq.(5.8)) to the case of multi-cell Markov partitions and piecewise analytic observables. Two simple maps and Markov partitions displayed in fig.(5.2) illustrate what we have in mind. The 2-d map is

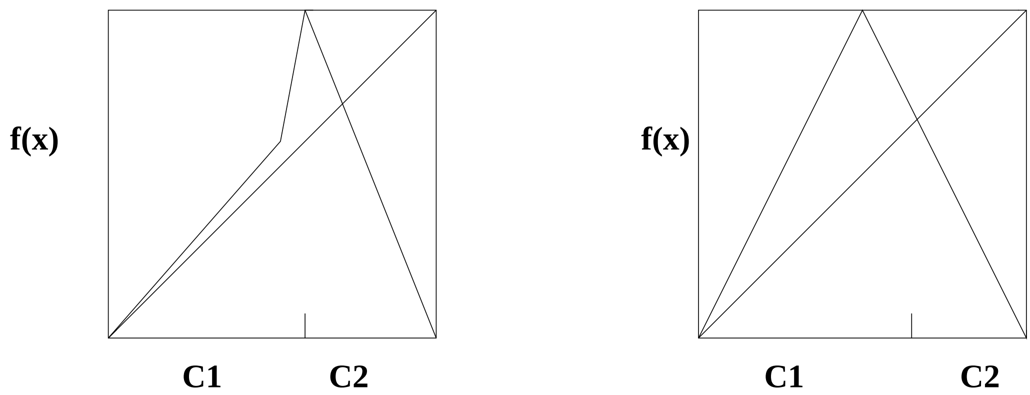

Figure 5.2: A simple Markov map where the minimal Markov partition consists of two cells, and the tent map with a two cell Markov partition

constructed again using eq.(5.10), so

$$\vec{f}(\vec{x}) = \begin{cases} f_{x\alpha}(x) & \text{if } x \in I_\alpha \\ f_{y\alpha}^{-1}(y) & . \end{cases} \tag{5.58}$$

The analysis is identical with the last section up to eq.(5.21). From hereon the treatment must be adapted to include a cellular perspective of the initial and final observables.

Let $\mathcal{F}_x$ denote the space of functions piecewise analytic over a Markov partition $\mathcal{P}_M$ of the unit interval for $f_x(x)$. Similarly, $\mathcal{F}_y$ denote the space of functions piecewise analytic over a partition $\mathcal{P}_{M'}$ of unit interval for $f_y(y)$. Obviously, we may use $\mathcal{P}_M$ and $\mathcal{P}_{M'}$ to define a two dimensional partition of the rectangle. Now, from the one dimensional Markov analytic case studied in chapter 2 we know that $\mathcal{F}_x$, $\mathcal{F}_y$ are invariant under $U_{x\alpha}$ and $U_{y\alpha}$ respectively if $\mathcal{P}_M$ and $\mathcal{P}_{M'}$ are each either the minimal Markov partition of $f_x(x)$, or a refinement thereof. Thus, the product space, $F_x X F_y$ is invariant under Θ_t. We then proceed as in the one dimensional case by introducing piecewise Chebyshev polynomials $\{T_{in}(x)\}$ and $\{Tjn(y)\}$ corresponding to the partitions P_M and $P_{M'}$ respectively. For a complete derivation of the following see appendix B.1. The matrix representations of $U_{x\alpha}$ and $U_{y\alpha}$ are

$$W_{x\alpha_k i_k n_k i_{k-1} n_{k-1}} = \frac{1}{h_{n_k}} \int_I T_{i_k n_k}(x)[U_{x\alpha_k} T_{i_{k-1} n_{k-1}}(x)] w_{i_k}(x) dx, \tag{5.59}$$

and

$$W_{y\alpha_k j_k m_k j_{k-1} m_{k-1}} = \frac{1}{h_{m_{k-1}}} \int_I T_{j_{k-1} m_{k-1}}(y)[U_{y\alpha_k} T_{j_k m_k}(y)] w_{j_{k-1}}(y) dy, \tag{5.60}$$

We said that the partitions $\mathcal{P}_M$ and $\mathcal{P}_{M'}$ define two dimensional cells of the rectangle. Conversely, the two dimensional cells $\hat{i}_t$ and $\hat{i}_0$ uniquely determine the one dimensional cells j_t, i_t, j_0, i_0. Hence,

$$C_{ab}(t) = \sum_{\hat{i}_t} \sum_{m_t=0}^{\infty} \sum_{n_t=0}^{\infty} \sum_{\hat{i}_0} \sum_{m_0=0}^{\infty} \sum_{n_0=0}^{\infty} a_{y\hat{i}_t m_t} \hat{a}_{x\hat{i}_t n_t} W^t_{\hat{i}_t m_t n_t \hat{i}_0 m_0 n_0} b_{x\hat{i}_0 n_0} \hat{b}_{y\hat{j}_0 m_0}, \tag{5.61}$$

where

$$\begin{aligned} b_{x\hat{i}_0 n_0} = b_{x\hat{i}_0 n_0} &= \frac{1}{h_{n_0}} \int_I T_{i_0 n_0} b_x(x) w_{i_0}(x) dx, \\ a_{y\hat{i}_t m_t} = a_{y j_t m_t} &= \frac{1}{h_{m_t}} \int_I T_{j_t m_t} a_y(y) w_{j_t}(y) dy, \qquad (5.62) \\ \hat{b}_{y\hat{i}_0 m_0} = \hat{b}_{y j_0 m_0} &= \int_I b_y(y) T_{j_0 m_0}(y) dy, \\ \hat{a}_{x\hat{i}_t n_t} = \hat{a}_{x i_t n_t} &= \int_I a_x(x) T_{i_t n_t}(x) dx, \qquad (5.63) \end{aligned}$$

and

$$W_{\hat{i}_k m_k n_k \hat{i}_{k-1} m_{k-1} n_{k-1}} = \sum_{\alpha} W_{y\alpha j_k m_k j_{k-1} m_{k-1}} W_{x\alpha i_k n_k i_{k-1} n_{k-1}}. \tag{5.64}$$

The spectral properties of W are the same as those of Θ_1 acting on $F_x X F_y$. We shall exploit this fact in section 5.6 by studying directly the action of Θ_1 on various invariant function spaces, rather than through a numerically determined W. But first, let us consider another class of maps closely related to those which we have already scrutinized.

5.4 Anosov automorphisms

We shall consider here simple linear Anosov automorphisms of the torus. The generic form of the map is

$$\vec{x}_{n+1} = \vec{f}(\vec{x}_n) = A \begin{pmatrix} x_n \\ y_n \end{pmatrix} mod(1), \tag{5.65}$$

where $\det(A) = 1$, and the eigenvalues of A do not equal one in magnitude. The coefficients of A are integers, which implies that the x and y coordinates of any periodic point, $\vec{f}^p(\vec{x}_p) = \vec{x}_p$ must be rational numbers between zero and one [26]. Through each point there exists one stable eigendirection ($\vec{e_s}$) and and unstable eigendirection ($\vec{e_u}$), with corresponding eigenvalues $\frac{1}{\Lambda}$ and Λ respectively. A rectangle partition $\mathcal{P}_M = (C_1, C_2, \cdots, C_{N_c})$ is a Markov partition [36] if

$$\begin{aligned} \vec{f}(\bigcup_{i=1}^{N_c} \delta^s C_i) &\subset \bigcup_{i=1}^{N_c} \delta^s C_i \\ \vec{f}^{-1}(\bigcup_{i=1}^{N_c} \delta^u C_i) &\subset \bigcup_{i=1}^{N_c} \delta^u C_j, \end{aligned} \tag{5.66}$$

where $\delta^u C_j$ and $\delta^s C_j$ correspond to the sides of the cell C_j parallel to the unstable and stable directions respectively, and

$$\forall i, j = 1, \cdots, N_c,\ \vec{f}(C_i) \bigcap C_j \text{ is connected.} \tag{5.67}$$

Markov partitions of the 2−torus can be constructed, for example, by tracing out the stable and unstable manifolds through the hyperbolic fixed point following the method of Adler and Weiss [6], until the entire torus is partitioned into rectangles/parallelograms satisfying eqs. (5.66) and (5.67). Such a Markov partition P_0 can be refined to produce a new partition P_1 by:

(1) self-refinement, namely using either the forward images of cells ($\vec{f}(C_i) \bigcap C_j$), the inverse images of cells ($\vec{f}^{-1}(C_i) \bigcap C_i$)), or

(2) In the Adler-Weiss partition construction, continuing the stable (unstable) manifold direction for further intersections,

(3) finding a periodic orbit(s), and tracing out the stable and unstable manifolds through each point of the orbit(s), until, for example, the first intersection with the boundary of the cell containing the point.

In this context, methods (1) and (2) are equivalent. One could alternatively construct P_0 by choosing all the elements of a periodic orbit, and trace out each of their stable and unstable manifolds until a Markov partition is obtained. An example of a toral automorphism is the map,

$$\vec{x}_{n+1} = \vec{f}(\vec{x}_n) = \begin{pmatrix} 1 & 1 \\ 1 & 0 \end{pmatrix} \begin{pmatrix} x_n \\ y_n \end{pmatrix} mod(1). \tag{5.68}$$

The map is clearly area preserving, has eigenvalues $\Lambda_u = \frac{1+\sqrt{5}}{2}$, and $\Lambda_s = \frac{1}{\Lambda_u}$, and eigenvectors

$$\vec{e}_u = \sqrt{\frac{\sqrt{5}-1}{2\sqrt{5}}}\left(\vec{e}_x\frac{2}{\sqrt{5}-1} + \vec{e}_y\right),\ \vec{e}_s = \sqrt{\frac{\sqrt{5}+1}{2\sqrt{5}}}\left(\vec{e}_x\frac{2}{\sqrt{5}+1} - \vec{e}_y\right) \tag{5.69}$$

We may trace the unstable and stable directions through the fixed point at the origin to construct a Markov partition, as is illustrated in fig.(5.3).

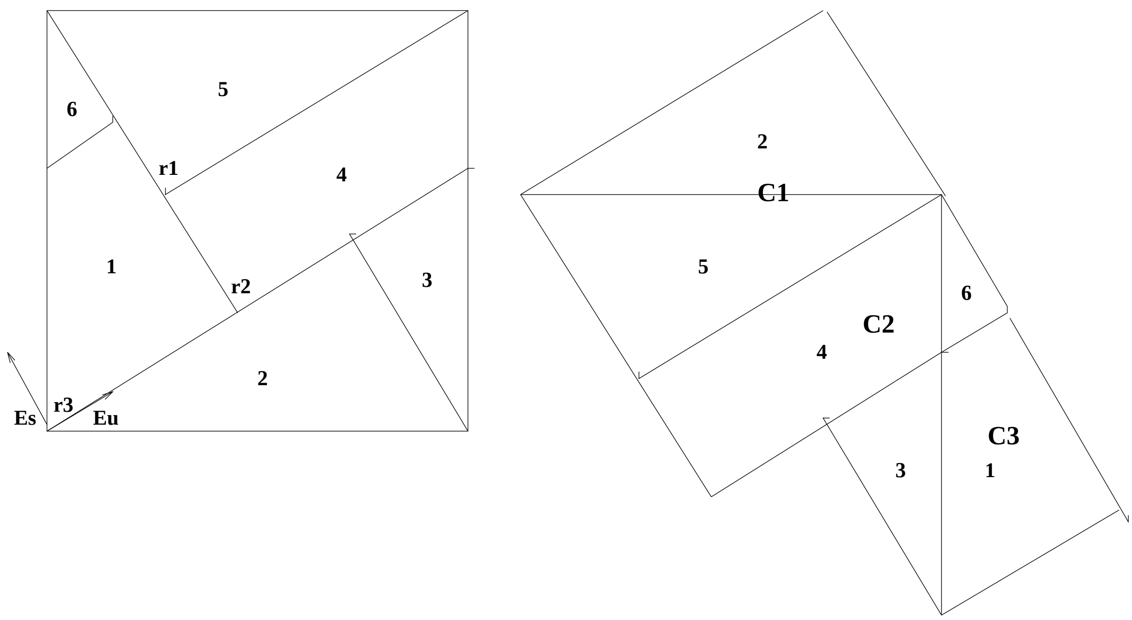

Figure 5.3: Left, A Markov partition for a toral automorphism obtained by tracing out the stable and unstable manifolds emanating from the hyperbolic fixed point at the origin. Due to the toroid geometry its not always obvious that the partition has generated a set of rectangles. Right, Demonstration that partition has indeed generated a set of rectangles. The local coordinates associated with each cell are simply the distance along its sides, where the (local) origin is defined as the left bottom vertex.

Clearly, there is always a coupling in $\vec{f}(x)$ between the x and y coordinates, but we may suspect that if we use a local coordinate system, aligned along the unstable, and stable directions, that a decoupling within each cell is possible. This is indeed the case, as we shall now see. The local coordinates (u, s) are defined via

$$\text{if } \vec{x} \in C_j,\ \vec{x} - \vec{r}_j = u\vec{e}_u + s\vec{e}_s, \tag{5.70}$$

where $\vec{r}_j$ denotes the bottom corner of each rectangle if neither the stable nor unstable directions are parallel to the x-axis, otherwise it denotes the bottom left corner. Thus, $0 < u < L_{uj}$ and $0 < s < L_{sj}$, where L_{uj} and L_{sj} denote the length of the sides of j^{th} cell parallel to the unstable and stable directions respectively. So, we may represent any point $\vec{x}$

$$\vec{x} \equiv (j, u, s), \tag{5.71}$$

where j corresponds to the cell C_j containing $\vec{x}$. Lets now consider the form of the map in local coordinates when describing a transition from cell C_i to cell C_j.

$$\vec{x} \in C_i \rightarrow \vec{x} = \vec{r}_i + u\vec{e}_u + s\vec{e}_s, \tag{5.72}$$

Due to the Markov property and the stable and unstable manifold theorem if $\vec{x} \in C_i \bigcap \vec{f}^{-1}(C_j)$ we may write

$$\vec{f}(\vec{x}) = \vec{r}_j + f_{uij}(u)\vec{e}_u + f_{sji}^{-1}(s)\vec{e}_s. \tag{5.73}$$

Equivalently,

$$\vec{f}(i,u,s) = \left(j, f_{uij}(u), f_{sji}^{-1}(s)\right) \quad \text{if } u \in I_{uij}, \tag{5.74}$$

where $I_{uij} = \delta^u \left(C_i \bigcap \vec{f}^{-1}(C_j)\right) \subset [0, L_{ui}]$, which is simply the domain of $f_{uij}(u)$. Thus, it is clear that a local decoupling of $\vec{f}(\vec{x})$ occurs. Indeed, eq.(5.73) resembles eq.(5.10), where the local coordinates u, s here play the role of x, y, Moreover, as

$$\begin{aligned} \frac{d}{du} f_{uij}(u) &= \Lambda_u \\ \frac{d}{ds} f_{sji}^{-1}(s) &= \Lambda_s, \end{aligned} \tag{5.75}$$

the local one dimensional maps $f_{uij}(u)$ and $f_{sji}^{-1}(s)$ are piecewise linear. Accordingly, we may anticipate that an analysis of the statistical properties of this type of map should be similar to the last two sections. Let us denote the range of $f_{sji}^{-1}(s)$ by $I_{sji} = \delta^s \left(C_j \bigcap \vec{f}(C_i)\right)$. We find if $x \in C_j$ and $s \in I_{sji}$ that

$$\vec{f}^{-1}(\vec{x}) = \vec{r}_i + f_{uij}^{-1}(u)\vec{e}_u + f_{sji}(s)\vec{e}_s, \tag{5.76}$$

or in local coordinates

$$\vec{f}(j,u,s) = \left(i, f_{uij}^{-1}(u), f_{sji}(s)\right) \quad \text{if } s \in I_{sji}. \tag{5.77}$$

Thus, for $x \in C_j$,

$$\begin{aligned} U\rho(\vec{x}) &= \rho(\vec{f}^{-1}(\vec{x})) \\ &= \sum_{C_i} M_{ji}\rho(\vec{r}_i + f_{uij}^{-1}(u)\vec{e}_u + f_{sji}(s)\vec{e}_s)\chi_{I_{sji}}(s), \end{aligned} \tag{5.78}$$

where M_{ji} is a topological transition matrix, its entries equal one if a given cell to cell transition occurs and is zero otherwise. Equivalently,

$$U\rho(j,u,s) = \sum_{C_i} M_{ji}\rho\left(i, f_{uij}^{-1}(u), f_{sji}(s)\right)\chi_{I_{sji}}(s). \tag{5.79}$$

Let us now turn to the calculation of

$$C_{ab}(t) = \int_I \int_I dxdya(x,y)\mathcal{U}^t b(x,y) = \sum_j \int_{C_j} dxdya(x,y)\mathcal{U}^t b(x,y). \tag{5.80}$$

The observables may be written in the equivalent form,

$$
\begin{aligned}
b(\vec{x}) &\equiv \sum_i b_i(\vec{x})\chi_i(\vec{x}) && (5.81)\\
a(\vec{x}) &\equiv \sum_j a_j(\vec{x})\chi_j(\vec{x}), && (5.82)
\end{aligned}
$$

where $\chi_i(\vec{x}) = 1$, if $\vec{x} \in C_i$ and is zero otherwise. We will assume that the observables are locally separable in the sense that,

$$
\begin{aligned}
b_i(r_i + u\vec{e}_u + s\vec{e}_s) = b_{ui}(u)b_{si}(s)\\
a_j(r_j + u\vec{e}_u + s\vec{e}_s) = a_{ju}(u)a_{sj}(s).
\end{aligned} \tag{5.83}
$$

We will also write

$$
\begin{aligned}
b_u(i,u) = b_{ui}(u), \qquad b_s(i,s) = b_{si}(s);\\
a_u(i,u) = a_{ui}(u), \qquad a_s(i,s) = a_{si}(s);
\end{aligned} \tag{5.84}
$$

and denote by b_u the set of functions $\{b_{ui}(u)\}$, and by b_s the set of functions $\{b_{si}(s)\}$, where the index i runs over all the cells of the partition. a_u and a_s are similarly defined. Now, suppose $b(\vec{x})$ is locally separable, then for $\vec{x} \in C_j$,

$$
\begin{aligned}
Ub(\vec{x}) &\equiv Ub(j,u,s)\\
&= \sum_i M_{ji} b_{ui}(f_{uij}^{-1}(u)) b_{si}(f_{sji}(s))\chi_{I_{sji}}(s)\\
&= \sum_i U_{uji}U_{sji}^{\dagger} b_{ui}(u)b_{si}(s),
\end{aligned} \tag{5.85}
$$

where

$$
\begin{aligned}
U_{uji}b_{ui}(u) &= \frac{1}{|\Lambda_u|} M_{ji} b_{ui}(f_{uij}^{-1}(u)), && (5.86)\\
U_{sji}^{\dagger} b_{si}(s) &= \frac{1}{|\Lambda_s|} M_{ji} b_{si}(f_{sji}(s))\chi_{I_{sji}}(s). && (5.87)
\end{aligned}
$$

Hence, $C_{ab}(1)$ may be rewritten as,

$$
\begin{aligned}
C_{ab}(1) &= \sum_{i_1,i_0} \int_{C_{i_1}} dxdy\, a_{i_1}(\vec{x}) U^1 b_{i_0}(\vec{x})\chi_{i_0}(\vec{x})\\
&= sin(\theta) \sum_{i_1,i_0} \int_0^{L_{ui_1}} a_{ui_1}(u) U_{ui_1i_0} b_{ui_0}(u) du \int_0^{L_{si_1}} a_{si_1}(s) U_{si_1i_0}^{\dagger} b_{si_0}(s) ds,
\end{aligned} \tag{5.88}
$$

where $sin(\theta) = |\vec{e}_u \wedge \vec{e}_s|$. Making a change in variable, we obtain,

$$
\begin{aligned}
&\textstyle\int_0^{L_{si_1}} a_{si_1}(s) U_{si_1i_0}^{\dagger} b_{si_0}(s) ds\\
&= \textstyle\int_0^{L_{si_0}} b_{si_0}(s) U_{si_0i_1} a_{si_1}(s) ds,
\end{aligned} \tag{5.89}
$$

where

$$U_{si_0i_1}a_{si_1}(s) = M_{i_1i_0}a_{si_1}(f^{-1}_{si_1i_0}(s)). \tag{5.90}$$

Therefore,

$$C_{ab}(1) = sin(\theta)\sum_{i_1,i_0}\int_0^{L_{ui_1}}\int_0^{L_{si_0}} b_{si_0}(s)a_{ui_1}(u)U_{ui_1i_0}U_{si_0i_1}\left[b_{ui_0}(u)a_{si_1}(s)\right]duds. \tag{5.91}$$

While $U_{ui_1i_0}$ is a linear operator associated with a transition from the cell C_{i_0} to the cell C_{i_1}, $U_{si_0i_1}$ is associated with the same cellular transition but in reverse/backward in time, i.e. from C_{i_1} to C_{i_0}. More generally,

$$\begin{aligned} C_{ab}(t) = \textstyle\sum_j\sum_i\int_{C_j} dxdya_j(\vec{x})U^tb_i(\vec{x})\chi_i(\vec{x}) \\ = sin(\theta)\textstyle\sum_{i_t,i_{t-1},\cdots,i_0} \\ \textstyle\int_0^{L_{ui_t}} a_{ui_t}(u)U_{ui_ti_{t-1}}U_{ui_{t-1}i_{t-2}}\cdots U_{ui_1i_0}b_{ui_0}(u)du \quad (5.92) \\ X\ \textstyle\int_0^{L_{si_t}} a_{si_t}(s)U^{\dagger}_{si_ti_{t-1}}U^{\dagger}_{si_{t-1}i_{t-2}}\cdots U^{\dagger}_{si_1i_0}b_{si_0}(s)ds. \quad (5.93) \end{aligned}$$

Again, making a change in variable, we obtain,

$$\begin{aligned} \textstyle\int_0^{L_{si_t}} a_{si_t}(s)U^{\dagger}_{si_ti_{t-1}}U^{\dagger}_{si_{t-1}i_{t-2}}\cdots U^{\dagger}_{si_1i_0}b_{si_0}(s)ds \\ = \textstyle\int_0^{L_{si_0}} b_{si_0}(s)U_{si_0i_1}U_{si_1i_2}\cdots U_{si_{t-1}i_t}a_{si_t}(s)ds, \end{aligned} \tag{5.94}$$

Thus

$$\begin{gathered} C_{ab}(t) = \\ sin(\theta)\textstyle\sum_{i_t,i_{t-1},\cdots,i_0}\int_0^{L_{ui_t}}\int_0^{L_{si_0}} dudsa_{ui_t}(u)b_{si_0} \\ U_{ui_ti_{t-1}}U_{ui_{t-1}i_{t-2}}\cdots U_{ui_1i_0}U_{si_0i_1}U_{si_1i_2}\cdots U_{si_{t-1}i_t}a_{si_t}(s)b_{ui_0}(u) \end{gathered} \tag{5.95}$$

Imitating the earlier sections, we define

$$\begin{gathered} \left[\Theta_tb_ua_s\right](i_t,u)(i_0,s) = \textstyle\sum_{i_{t-1},i_{t-2},\cdots,i_2,i_1} \\ \chi_{I_{si_t}}(s)\chi_{I_{ui_0}}(u)U_{ui_ti_{t-1}}U_{ui_{t-1}i_{t-2}}\cdots U_{ui_1i_0}U_{si_0i_1}U_{si_1i_2}\cdots U_{si_{t-1}i_t}b_{ui_0}(u)a_{si_t}(s), \end{gathered} \tag{5.96}$$

and

$$\left[\Theta_1b_ua_s\right](i_1,u)(i_0,s) = U_{ui_1i_0}U_{si_0i_1}b_{ui_0}(u)a_{si_1}(s). \tag{5.97}$$

Thus,

$$C_{ab}(t) = sin(\theta)\sum_{i_t,i_0}\int_0^{L_{ui_t}}\int_0^{L_{si_0}} duds\left[a_u(i_t,u)b_s(i_0s)\,\Theta_ta_sb_u(i_t,u)(i_0,s)\right] \tag{5.98}$$

Now $U_{ui_1i_0}$ and $U_{si_0i_1}$ are Frobenius-Perron like operators, associated with one dimensional expanding analytic maps (in fact just linear ones). Thus, if $b_{ui_0}(u)$ and $a_{si_1}(s)$ are polynomial functions of order N in u over $[0, L_{ui_0}]$ and s over $[0, L_{si_1}]$ respectively, then

$$U_{ui_1i_0}b_{ui_0}(u),\ \text{and}\ U_{si_0i_1}a_{si_1}(s),$$

will be polynomial functions of order no higher than N in u over $[0, L_{ui_1}]$ and s over $[0, L_{si_0}]$ respectively. This leads us to define invariant piecewise analytic function spaces $\mathcal{F}_u$ and $\mathcal{F}_s$ respectively, where

$$\mathcal{F}_u = \{b_{ui_0}(u)\} \text{ and } \mathcal{F}_s = \{a_{si_1}(s)\}, \tag{5.99}$$

each $b_{ui_0}(u)$ and $a_{si_1}(s)$ being analytic functions (we could be more restrictive and define them to be polynomial functions of order N) of their arguments, and the indices i_0 and i_1 run over all the cells of the partition. Therefore, the product space $\mathcal{F}_s X \mathcal{F}_u$ is invariant under Θ_t. Just as in the earlier sections, there exist other function spaces which are invariant under Θ_t, where the observables are separable with respect to $\mathcal{P}_0$, and b_u, a_s are piecewise analytic over a Markov partition $\mathcal{P}_1$, which is a refinement of $\mathcal{P}_0$. For now, however, let us focus on obtaining a matrix representation for Θ_t acting on $\mathcal{F}_s X \mathcal{F}_u$.

Copying section 5.3 we introduce piecewise Chebyshev functions, where each family has domain $[0, L_{ui}]$, $[0, L_{si}]$, where i denotes any Markov cell. Thus, the matrix representations of $U_{ui_k i_{k-1}}$ and $U_{si_{k-1} i_k}$ are

$$W_{ui_k n_k i_{k-1} n_{k-1}} = \frac{1}{h_{n_k}} \int_0^{L_{ui_k}} T_{ui_k n_k}(u)[U_{ui_k i_{k-1}} T_{ui_{k-1} n_{k-1}}(u)] w_{ui_k}(u) du, \tag{5.100}$$

and

$$W_{si_k m_k i_{k-1} m_{k-1}} = \frac{1}{h_{m_{k-1}}} \int_0^{L_{si_k}} T_{si_{k-1} m_{k-1}}(s)[U_{si_{k-1} i_k} T_{si_k m_k}(s)] w_{si_{k-1}}(s) ds, \tag{5.101}$$

Dissecting eq.(5.95) and using the representations above we find,

$$\begin{gathered}\textstyle\int_0^{L_{ui_t}} a_{ui_t}(u) U_{ui_t i_{t-1}} U_{ui_{t-1} i_{t-2}} \cdots U_{ui_1 i_0} b_{ui_0}(u) du \; = \\ \textstyle\sum_{n_t=0}^{\infty} \sum_{n_{t-1}=0}^{\infty} \cdots \sum_{n_0=0}^{\infty} \\ \{[\textstyle\int_{I_{ui_t}} a_{ui_t}(u) T_{un_t i_t}(u) du] W_{ui_t n_t i_{t-1} n_{t-1}} W_{ui_{t-1} n_{t-1} i_{n-2} n_{t-2}} \cdots W_{ui_1 n_1 i_0 n_0} b_{ui_0 n_0}\},\end{gathered} \tag{5.102}$$

and

$$\begin{gathered}= \textstyle\int_0^{L_{si_0}} b_{si_0}(s) U_{si_0 i_1} U_{si_1 i_2} \cdots U_{si_{t-1} i_t} a_{si_t}(s) ds, \\ \textstyle\sum_{m_t=0}^{\infty} \sum_{m_{t-1}=0}^{\infty} \cdots \sum_{m_0=0}^{\infty} \sum_{i_t} \sum_{i_0} \\ \{a_{si_t m_t} W_{si_t m_t i_{t-1} m_{t-1}} W_{si_{t-1} m_{t-1} i_{t-2} m_{t-2}} \cdots W_{si_1 m_1 i_0 m_0} [\textstyle\int_{I_{si_0}} b_{si_0}(s) T_{si_0 m_0}(s) ds]\},\end{gathered} \tag{5.103}$$

where

$$b_{ui_0 n_0} = \frac{1}{h_{n_0}} \int_{I_{ui_0}} T_{ui_0 n_0}(u) b_{ii_0}(u) w_{ui_0}(u) du \tag{5.104}$$

and

$$a_{ui_t m_t} = \frac{1}{h_{m_t}} \int_{I_{si_t}} T_{i_t m_t}(s) a_{si_t}(y) w_{ui_t}(s) ds. \tag{5.105}$$

We may now reassemble the patient, by inserting eqs.(5.102) and (5.103) into eq.(5.95),

$$
\begin{aligned}
C_{ab}(t) = sin(\theta) \textstyle\sum_{n_t=0}^{\infty} \sum_{n_{t-1}=0}^{\infty} \cdots \sum_{n_0=0}^{\infty} \sum_{m_t=0}^{\infty} \sum_{m_{t-1}=0}^{\infty} \cdots \sum_{m_0=0}^{\infty} \sum_{i_t, i_{t-1}, \cdots i_0} \\
\{ a_{s i_t m_t} \hat{a}_{u i_t n_t} W_{u i_t n_t i_{t-1} n_{t-1}} W_{s i_t m_t i_{t-1} m_{t-1}} W_{u i_{t-1} n_{t-1} i_{t-2} n_{t-2}} W_{s i_{t-1} m_{t-1} i_{t-2} m_{t-2}} \cdots \\
\cdots W_{u i_1 n_1 i_0 n_0} W_{s i_1 m_1 i_0 m_0} b_{u i_0 n_0} \hat{b}_{s i_0 m_0} \} \\
= sin(\theta) \textstyle\sum_{i_t} \sum_{m_t=0}^{\infty} \sum_{n_t=0}^{\infty} \sum_{i_0} \sum_{m_0=0}^{\infty} \sum_{n_0=0}^{\infty} a_{s i_t m_t} \hat{a}_{u i_t n_t} W^{t}_{i_t m_t n_t i_0 m_0 n_0} b_{u i_0 n_0} \hat{b}_{s i_0 m_0}
\end{aligned}
\tag{5.106}
$$

where

$$
\hat{b}_{s i_0 m_0} = \int_{I_{s i_0}} b_s(s) T_{s i_0 m_0}(s) ds,
$$

$$
\hat{a}_{u i_t n_t} = \int_{I_{u i_t}} a_u(u) T_{u i_t n_t}(u) du,
$$

and

$$
W_{i_k m_k n_k i_{k-1} m_{k-1} n_{k-1}} = W_{s i_k m_k i_{k-1} m_{k-1}} W_{u i_k n_k i_{k-1} n_{k-1}}. \tag{5.107}
$$

As in the previous sections, the spectral properties of W are the same as Θ_1 acting on $\mathcal{F}_u X \mathcal{F}_s$. On the other hand, suppose we define another product space $\mathcal{F}_u' X \mathcal{F}_s'$ with respect to a Markov partition $\mathcal{P}_1$ which is a refinement of the original partition $\mathcal{P}_0$. We may still use Θ_t to calculate $C_{ab}(t)$, where the observables are associated with $\mathcal{F}'_u X \mathcal{F}'_s$. In particular, the spectral properties of Θ_1 acting on this new space will correctly describe the characteristic times/ decay rates of $C_{ab}(t)$. This observation will be very useful in the next section, where we characterise the properties of $C_{ab}(t)$ for different types of observables, associated with, for example, local statistical properties. Let us complete this section by determining some of the statistical properties of the automorphism described by eq.('5.68),

5.4.1 A Model Example

As we saw already, the map in question is,

$$
\vec{x}_{n+1} = \vec{f}(\vec{x}_n) = \begin{pmatrix} 1 & 1 \\ 1 & 0 \end{pmatrix} \begin{pmatrix} x_n \\ y_n \end{pmatrix} mod(1), \tag{5.108}
$$

and the Markov partition is given in fig.(5.3). In local coordinates, $\vec{x} \in C_i \bigcap \vec{f}^{-1}(C_j)$, the map has the form,

$$
\vec{f}(\vec{x}) = \vec{r}_j + f_{uij}(u)\vec{e}_u + f_{sji}^{-1}(s)\vec{e}_s. \tag{5.109}
$$

It is quite easy to show that $\{f_{uij}(u)\}$ have the form

$$
\begin{aligned}
f_{u13}(u) = \Lambda_u u, \text{ if } u \in [0, \frac{L_{u3}}{\Lambda_u}], \qquad & f_{u12}(u) = \Lambda_u u - L_{u3} \text{ if } u \in [\frac{L_{u3}}{\Lambda_u}, L_{u1}] \\
f_{u21}(u) = \Lambda_u u - L_{u3} \text{ if } u \in [\frac{L_{u3}}{\Lambda_u}, L_{u2}], \qquad & f_{u23}(u) = \Lambda_u u \text{ if } u \in [0, \frac{L_{u3}}{\Lambda_u}],, \\
f_{u31}(u) = \Lambda_u u \text{ if } u \in [0, \frac{L_{u3}}{\Lambda_u}]. &
\end{aligned}
\tag{5.110}
$$

The topological transition matrix M_{ji} describing the possible transitions from cell C_i to C_j is given by

$$M = \begin{pmatrix} 0 & 1 & 1 \\ 1 & 0 & 0 \\ 1 & 1 & 0 \end{pmatrix}. \tag{5.111}$$

Similarly, its inverse, for $\vec{x} \in C_j \bigcap \vec{f}(C_i)$,

$$\vec{f}^{-1}(\vec{x}) = \vec{r}_i + f_{uij}^{-1}(u)\vec{e}_u + f_{sji}(s)\vec{e}_s. \tag{5.112}$$

The $\{f_{sji}(s)\}$ take the form,

$$\begin{gathered} f_{s12}(s) = L_{s2} + \frac{s}{\Lambda_s} \text{ if } s \in [0, |\Lambda_s|L_{s2}], \qquad f_{s13}(s) = \frac{1}{\Lambda_s}(s - L_{s1}) \text{ if } s \in [|\Lambda_s|L_{s2}, L_{s1}], \\ f_{s21}(s) = L_{s1} + \frac{s}{\Lambda_s} \text{ if } s \in [0, L_{s2}], \\ f_{s31}(s) = L_{s1} + \frac{s}{\Lambda_s} \text{ if } s \in [0, |\Lambda_s|L_{s1}, \qquad f_{s32}(s) = L_{s2} + \frac{1}{\Lambda_s}(s - |\Lambda_s|L_{s1}) \text{ if } s \in [|\Lambda_s|L_{s1}. \end{gathered} \tag{5.113}$$

Now, as the local maps are linear maps, we know immediately that Θ_1 leaves $\mathcal{F}_s X \mathcal{F}_u$ invariant, where

$$\mathcal{F}_u = \{b_{ui_0}(u)\} \text{ and } \mathcal{F}_s = \{a_{si_1}(s)\}, \tag{5.114}$$

each $b_{ui_0}(u)$ and $a_{si_1}(s)$ polynomial functions of order $N, N = 0, 1, 2, \cdots$, and $M, M = 0, 1, 2, \cdots$. of their arguments, and the indices i_0 and i_1 run over all the cells of the partition. This means that the transition matrix $W_{i_k m_k n_k i_{k-1} m_{k-1} n_{k-}}$ has a block form

$$W = \begin{pmatrix} \star & \bullet & \bullet & \bullet \cdots \\ 0 & \star & \bullet & \bullet \cdots \\ 0 & 0 & \star & \bullet \cdots \\ \vdots & \vdots & \vdots & \ddots \end{pmatrix}, \tag{5.115}$$

where the $\bullet$'s and $\star$'s represent $3X3$ matrices, and $\star \equiv W_{i_1 m_1 n_1 i_0 m_1 n_1}$. Thus the eigenvalues of W equal the eigenvalues of the $\star$'s. Now, as the local maps are piecewise linear, it is easier to calculate W with respect to a piecewise monomial basis, rather than with a piecewise Chebyshev basis. The eigenvalues in either representation will be the same. Indeed, the $\star$ parts of the two representations are related by the similarity transformation

$$D_{ji} = L_{uj}^{-n} L_{sj}^{m} \delta_{j,i}. \tag{5.116}$$

The $\star$ parts of the matrix in the piecewise monomial representation have the simple form,

$$\star \equiv W_{i_1 mn i_0 mn} = M_{i_1 i_0} \Lambda_s^m \Lambda_u^{-n-1}. \tag{5.117}$$

It turns out that the eigenvalues of M are $-1, \Lambda_u, \Lambda_s$. Thus the eigenvalues of W are the numbers above multiplied by $\Lambda_s^m \Lambda_u^{-n-1}$, i.e.

$$\{\lambda\} = \Lambda_s^m \Lambda_u^{-n}, \; -\Lambda_s^m \Lambda_u^{-n-1}, \; \Lambda_s^{m+1} \Lambda_u^{-n-1}, \; m, n = 0, 1, 2, \cdots. \tag{5.118}$$

In fact the spectra of W for any linear toral automorphism will be the eigenvalues of the corresponding topological transition matrix times $\Lambda_s^m \Lambda_u^{-n-1}$.

Finally, it is straight forward to generalize these results to the piecewise linear automorphisms of the torus considered by Chernov[16].

5.5 Connection with the zeta function formalism

In chapter 3 we established the connection between our matrix representations of $\mathcal{U}$ acting on the space of analytic functions piecewise analytic over the minimal Markov partition and the dynamical zeta function. We now will generalize those results to all the classes of two dimensional maps considered so far in the present chapter.

As stated previously, one of the purposes of the zeta function formalism is to relate the decay rates of time correlation functions of appropriate observables to the zeros of the function,

$$Z_s(z) = \det(1 - z\mathcal{U}), \tag{5.119}$$

through the zeros of the function

$$\tilde{Z}_s(z) = \prod_{k=1}^{\infty}\prod_{\ell=1}^{\infty}\frac{1}{\zeta_{k,\ell}(z)}. \tag{5.120}$$

The dynamical zeta function in two dimensions has the form

$$\zeta_{k,\ell}(z) = \prod_p \left(1 - \frac{z^{n_p}\wedge_{sp}^{\ell-1}}{\mid \wedge_{up}\mid \wedge_{up}^{k-1}}\right)^{-1}, \tag{5.121}$$

and $\prod_p$ denotes the product over all periodic orbits, N_p, the period of the p^{th} periodic orbit, and $\wedge_{up}$, $\wedge_{sp}$ denote the expansion and contraction rates of the periodic orbit along the expanding and contracting directions,i.e.

$$\wedge_{up} = \frac{d}{du}\vec{f}^p(x_p) \text{ and } \wedge_{sp} = \frac{d}{ds}\vec{f}^p(x_p). \tag{5.122}$$

For one dimensional Markov analytic maps, we have seen that if the space of analytic functions is not invariant under $\mathcal{U}$, then the poles of the dynamical zeta functions do not generally give the correct decay rates of time correlation functions of analytic observables. This fact was apparently first noticed by Manning, although no general correction formula was derived, as we have done[4]. Deriving a general correction formula in two dimensions is more difficult, because fixed points or an element of a periodic orbit can lie in the interface not just between two cells, but also between three or even four. We will show how the correction formula,

$$\Gamma(z) = \frac{Z_s(z)}{\tilde{Z}_s(z)},$$

can be derived, but the precise form of the correction should be determined for each particular system.

Let us first consider the case where no correction is required. We will use again the trace formula,

$$\begin{aligned}\det(1 - z\mathcal{W}) &= \exp[\mathrm{Tr}\,(\ln(1 - z\mathcal{W})]\\ &= \exp\left(-\sum_{n=1}^{\infty}\frac{z^n}{n}\mathrm{Tr}\,(\mathcal{W}^n)\right).\end{aligned} \tag{5.123}$$

[4]Related work has been reported by H.H. Rugh[99] (P. Cvitanovic', private communication)

We need now to determine $\mathrm{Tr}\,(\mathcal{W}^n)$. For the systems considered in section 5.2

$$\mathcal{W}_{m_k n_k m_{k-1} n_{k-1}} = \sum_{\alpha} \mathcal{W}_{y\alpha m_k m_{k-1}} \mathcal{W}_{xan_{k-1}}, \tag{5.124}$$

so

$$\mathrm{Tr}\,\mathcal{W} = \sum_{\alpha} \left(\sum_{m=0}^{\infty} \mathcal{W}_{y\alpha m_k m_{k-1}} \right) \left(\sum_{n=0}^{\infty} \mathcal{W}_{x\alpha n_k n_{k-1}} \right). \tag{5.125}$$

Now, recall that

$$\begin{aligned} \mathcal{W}_{x\alpha n_k n_{k-1}} &= \frac{1}{h_{n_k}} \int_I T_{n_k}(x)[U_{x\alpha} T_{n_{k-1}}(x)] w(x) dx, \\ \mathcal{W}_{y\alpha m_k m_{k-1}} &= \frac{1}{h_{m_{k-1}}} \int_I T_{m_{k-1}}(y)[U_{y\alpha} T_{m_k}(y)] w(y) dy, \end{aligned} \tag{5.126}$$

where

$$\begin{aligned} U_{x\alpha} b_x(x) &= b_x(f_{x\alpha}^{-1}(x)) |\frac{d}{dx} f_{x\alpha}^{-1}(x), \\ U_{y\alpha} a_y(y) &= a_y(f_{y\alpha}^{-1}(y)), \end{aligned} \tag{5.127}$$

and each of these operators leaves the space of analytic functions invariant. Thus,

$$\mathrm{Tr}\,\mathcal{W} = \sum_{\alpha} ((\mathrm{Tr} U_{y\alpha})(\mathrm{Tr} U_{x\alpha})) \tag{5.128}$$

We a note that each $f_{x\alpha}^{-1}(x)$ and $f_{y\alpha}^{-1}(y)$ has a fixed point either in the unit interval or at zero or one, in which case the branches are monotonic increasing, and maps the unit interval into itself (in x and y respectively). We may now take advantage of the lemma used for one dimensional Markov maps which determines the spectra, and hence the trace of operators like $U_{\alpha x}$ and $U_{\alpha y}$, acting on the space of functions which are analytic in a complex domain containing the interval. For clarity, lets repeat the lemma. *If ψ maps the domain $D \subset C$ strictly inside itself then the spectrum of the generalized composition operator $\mathcal{L}g = \varphi C_{\phi} g$ on the space $A_{\infty}(D)$ consists of the eigenvalues*

$$\lambda_n = \varphi(z*)(\psi'(z*))^n, \; n = 0, 1, 2,$$

converging to the point 0, where $z*$ is the unique fixed point of ψ in D. Every eigenvalue is simple. As we mentioned before, this lemma is also valid if $\psi(z)$ is only eventually contractive, i.e.

$$\exists \tau : \forall t > \tau, \forall z \in D, \; |\frac{d}{dz} \psi^t(z)| < 1, \tag{5.129}$$

and there exists a real interval $I \subset D$ such that

$$\psi(I) \subset I. \tag{5.130}$$

Relating the generalized composition operator to $U_{x\alpha}$, and $U_{\alpha y}$ respectively, we see,

$$\varphi \equiv |\frac{d}{dx} f_{\alpha x}^{-1}(x)| \text{ and } C_{\psi} g = g(\psi(z)) \equiv b_x(f_{\alpha x}^{-1}(x)), \tag{5.131}$$

or

$$\varphi \equiv 1 \text{ and } C_\psi g = g(\psi(z)) \equiv a_y(f_{\alpha y}^{-1}(y)). \tag{5.132}$$

Using eq.(5.122) for the fixed points of $f_{x\alpha}$ and $f_{y\alpha}$ (which are just the x and y components of the fixed points of $\vec{f}(\vec{x})$ we find

$$\mathrm{Tr}\,\mathcal{W} = \sum_{\vec{f}(\vec{x}_*)=x_*} \left(\sum_{\ell=0}^{\infty} \sum_{k=0}^{\infty} \frac{\wedge_{s1}(\vec{x}_*)^{\ell}}{\wedge_{u1}(\vec{x}_*)^{k} | \wedge_{u1}\,(\vec{x}_*)|} \right), \tag{5.133}$$

where we have explicitly written the $\vec{x}_*$ dependence of the contraction and expansion rates for each fixed point to avoid confusion. In the following, the dependence will be implicit. Similarly,

$$\mathrm{Tr}\,\mathcal{W}^p = \sum_{\vec{f}^p(\vec{x}_*)=x_*} \left(\sum_{\ell=0}^{\infty} \sum_{k=0}^{\infty} \frac{{\wedge_{sp}}^{\ell}}{{\wedge_{up}}^{k} | \wedge_{up}\,|} \right), \tag{5.134}$$

As in previous chapters, we follow the argument and notation of Artuso et al[23, 7]. Any periodic orbit p of period N_p will contribute to eq.(5.133) only if N_p is a divisor of n. We shall denote the set of all periodic orbits whose period N_p is a divisor of n by N_p/n. In general, the n^{th} order trace picks up contributions from N_p/n. Therefore

$$\mathrm{Tr}\,\mathcal{W}^n = \sum_{\ell=1}^{\infty} \sum_{k=1}^{\infty} \left(\sum_{N_p/n} N_p t_p^{\frac{n}{N_p}} \right), \tag{5.135}$$

where

$$t_p = \frac{\wedge_{sp}^{l-1}}{\wedge_{up}^{k-1} | \wedge_{up}\,|}. \tag{5.136}$$

Let $r = \frac{n}{N_p}$. We can express eq.(5.123) as

$$\begin{aligned} det(1 - z\mathcal{W})) &= exp \sum_{\ell=1}^{\infty} \sum_{k=1}^{\infty} \left(- \sum_{p} \sum_{r=1}^{\infty} \frac{(z^{N_p} t_p)^r}{r} \right) \\ = exp \sum_{\ell=1}^{\infty} \sum_{k=1}^{\infty} \left(\sum_{p} ln(1 - z^{N_p} t_p) \right) &= \prod_{\ell=1}^{\infty} \prod_{k=1}^{\infty} \left(\prod_{p} (1 - z^{N_p} t_p) \right) \\ = \prod_{k=1}^{\infty} \prod_{\ell=1}^{\infty} \frac{1}{\zeta_{k,\ell}(z)} &= Z_s(z). \end{aligned} \tag{5.137}$$

We now turn to the more general case for the systems where the simplest invariant function space under Θ_t consists of a product space of piecewise analytic functions. As in the one dimensional case, care must be taken when relating the trace of $\mathcal{W}$ to the periodic orbits of the system. In the case of the systems studied in section 5.3 the matrix representation has the form

$$\mathcal{W}_{\hat{i}_k m_k n_k \hat{i}_{k-1} m_{k-1} n_{k-1}} = \sum_{\alpha} \mathcal{W}_{y\alpha j_k m_k j_{k-1} m_{k-1}} \mathcal{W}_{x\alpha i_k n_k i_{k-1} n_{k-1}}, \tag{5.138}$$

whereas for linear Anosov automorphisms,

$$\mathcal{W}_{i_k m_k n_k i_{k-1} m_{k-1} n_{k-1}} = \mathcal{W}_{s i_k m_k i_{k-1} m_{k-1}} \mathcal{W}_{u i_k n_k i_{k-1} n_{k-1}}. \tag{5.139}$$

In each case, the transition from a two dimensional cell into itself can take place only $\vec{f}(\vec{x})$ has at least one fixed point $\vec{x}_*$ either in the cell interior, or a fixed point at the boundary and such that both $\wedge_{u1}(\vec{x}_*) > 0$ and $\wedge_{s1}(\vec{x}_*) > 0$. This is also true for $\vec{f}^p(\vec{x})$, where the role of fixed points is played by periodic orbits of period p (or divisors of p, i.e in this sense a fixed point is also a periodic orbit of period p), and $\wedge_{up}(\vec{x}_p) > 0$ and $\wedge_{sp}(\vec{x}_p) > 0$. Employing the same arguments as before we find,

$$\sum_{\ell=0}^{\infty}\sum_{k=0}^{\infty}\mathcal{W}_{i\ell ki\ell k} = \sum_{\ell=0}^{\infty}\sum_{k=0}^{\infty}\left(\sum_{\vec{x}_*\in Int(C_i)}\frac{\wedge_{s1}(\vec{x}_*)^{\ell}}{\wedge_{u1}(\vec{x}_*)^{k}|\wedge_{u1}(\vec{x}_*)|} + \sum_{\vec{x}_*\in B(C_i)}\frac{\wedge_{s1}(\vec{x}_*)^{\ell}}{\wedge_{u1}(\vec{x}_*)^{k}|\wedge_{u1}(\vec{x}_*)|}\right), \tag{5.140}$$

where the sum $\sum_{x_*\in B(C_i)}$ is over fixed points on the cell boundary provided that both $\wedge_{u1}(\vec{x}_*) > 0$ and $\wedge_{s1}(\vec{x}_*) > 0$. Similarly,

$$\sum_{\ell=0}^{\infty}\sum_{k=0}^{\infty}\mathcal{W}^p_{i\ell ki\ell k} = \sum_{\ell=0}^{\infty}\sum_{k=0}^{\infty}\left(\sum_{\vec{x}_p\in Int(C_i)}\frac{\wedge_{sp}(\vec{x}_p)^{\ell}}{\wedge_{up}(\vec{x}_p)^{k}|\wedge_{up}(\vec{x}_p)|} + \sum_{\vec{x}_p\in B(C_i)}\frac{\wedge_{sp}(\vec{x}_p)^{\ell}}{\wedge_{up}(\vec{x}_p)^{k}|\wedge_{up}(\vec{x}_p)|}\right). \tag{5.141}$$

The trace of $\mathcal{W}^p$ is just the sum over all the cells of eq.(5.141). Unfortunately, unlike the one dimensional case, a fixed point or an element of a periodic orbit can form the interface between two, three or even four cells, depending on the system, and in the case of linear automorphisms, on the construction of the partition, which is somewhat arbitrary. For example, one could construct the partition from all the elements of another periodic orbit, rather than the hyperbolic fixed point. The sum over the boundary periodic orbits will induce a correction to eq.(5.137), so that

$$det(1 - z\mathcal{W}) = \tilde{Z}_s(z)\Gamma(z), \tag{5.142}$$

where $\Gamma(z)$ is generally a rational function determined from a finite number of periodic orbits, which can be obtained for each system case by case. The need for such corrections has already been noted in the literature[13], as well as in the earlier chapters of this thesis. In particular, Manning[68] has shown that Axiom A diffeomorphisms have rational zeta functions. For the systems that we are studying, it seems easier, and is certainly more informative to just use matrix representations, and avoid the zeta function formalism. We shall now see that the periodic orbits that form interfaces between cells give rise to spectra which can be easily characterized. Indeed, they can be used to explore the local statistical properties of a given system.

5.6 Local statistical properties

Markov partitions played a crucial role in the last two sections. There existence enabled us to obtain matrix representations of Θ_t, through which we are able to calculate $C_{ab}(t)$. There are however, an infinite number of Markov partitions for the system we have studied, so which should one choose? Two other issues are how can local statistical properties be described - and to what extent does the choice of observable(s) give rise to different characteristic times of the system ? From the previous chapters on one dimensional Markov maps we know that these questions are related. Indeed the one dimensional results extend, with little change, to two dimensions, as we will now show.

First, let us recapitulate the relevant findings of chapter 2. For any one dimensional Markov analytic map, the space of functions $\mathcal{F}_{min}$ piecewise analytic over the minimal Markov partition is invariant under $\mathcal{U}$, and we denote the corresponding spectra by SP_{min}. Any space $\mathcal{F}_M$ of functions which are piecewise analytic over a Markov partition $\mathcal{P}_M$ constructed by refining $\mathcal{P}_{min}$ with either: (a) the inverse images of the cell boundaries of $\mathcal{P}_{min}$ (self-refinement) or (b) all the elements of a periodic orbit, is also invariant. The spectra of $\mathcal{U}$ acting on F_M, SP_M, include SP_{min} and possibly additional spectra. The additional spectra are in case (a) just degenerate zero eigenvalues, while in case (b) are given by a simple formula, and describe decaying periodic oscillations.

Turning now to two dimensional maps, we need first to introduce a single notation for coordinates to describe all the systems so far considered (so as not to be repetitive). Let us assume that we know a two dimensional Markov partition $\mathcal{P}_0$. We will denote the coordinates by $(i,u),(j,s)$, which were used for toral automorphisms. For the maps studied in the first two sections, $i=j=1$ (i.e. these indices only have one value) and $u=x, s=y$, and

$$\begin{aligned}
[\Theta_1 b_u a_s](1,u)(1,s) &= \sum_\alpha U_{u\alpha}U_{s\alpha}b_u(u)a_s(s) \\
&= \sum_\alpha b_u(f_{u\alpha}^{-1}(u))a_s(f_{s\alpha}^{-1}(s))|\frac{d}{du}f_{u\alpha}^{-1}(u)|. \qquad (5.143)
\end{aligned}$$

For linear toral automorphisms,

$$\begin{aligned}
[\Theta_1 b_u a_s](i_1,u)(i_0,s) &= U_{ui_1i_0}U_{si_0i_1}b_{ui_0}(u)a_{si_1}(s) \\
&= b_{ui_0}(f_{ui_0i_1}^{-1}(u))a_{si_1}(f_{si_1i_0}^{-1}(s))|\frac{d}{du}f_{ui_0i_1}^{-1}(u)|. \qquad (5.144)
\end{aligned}$$

Let

$$\mathcal{F}_0 = F_u X F_s$$

be the invariant product spaces associated with the $\mathcal{P}_0$, as defied in the last two sections. Thus for the systems of section 5.3,

$$\mathcal{P}_0 = \mathcal{P}_M X \mathcal{P}_{M'} \text{ and } F_u X F_s \equiv F_x X F_y,$$

where F_u consists of functions which are piecewise analytic over $\mathcal{P}_M$ and F_s consists of functions which are piecewise analytic over $\mathcal{P}_{M'}$. For Anosov automorphisms, if

$$b_u a_s \in F_u X F_s,$$

then $b_u(i,u)$ and $a_s(j,s)$ are analytic functions for $u \in [0, L_{u_i}]$ and for $s \in [0, L_{s_j}]$ respectively. For each Markov partition $\mathcal{P}_1$ obtained through refinement of $\mathcal{P}_0$, we may define a product space $\mathcal{F}_1$ invariant under Θ_1, as was done in the last two sections. We wish to characterise the spectra sp_1 of Θ_1 acting on $\mathcal{F}_1$. Now,

$$\mathcal{F}_1 \supset \mathcal{F}_0 \Rightarrow sp_1 \supset sp_0.$$

What then, is the nature of the additional spectra sp_1/sp_0 ? Let us first consider the case where $\mathcal{P}_1$ is obtained through self-refinement of $\mathcal{P}_0$.

This case can be understood by simply partitioning any cell C_i of $\mathcal{P}_0$ into two cells using a line ℓ parallel with the stable (unstable) direction, and such that $\vec{f}(\ell)$ $(\vec{f}^{-1}(\ell)$ falls onto the stable (unstable) side of the cells of $\mathcal{P}_0$. This is precisely what happens through self-refinement, and defines $\mathcal{P}_1$. We first remark that $\mathcal{F}_1$ is invariant under Θ_1. It is easy to show $\forall b_u a_s \in \mathcal{F}_1$ that $\Theta_1 b_u a_s \in \mathcal{F}_0$. Therefore the only additional spectra, sp_1/sp_0 are zero, and infinitely degenerate. Thus, we obtain the same result as for one-dimensional maps. We now turn to refinement with periodic orbits.

5.6.1 Refinement with periodic orbits

Lets now consider the effect of refining P_0 with elements of periodic orbits (drawing their stable or/and unstable manifolds until the first intersection with a cell wall. The spectra of Θ_1 obey virtually the same formula as in the 1-d case. The derivations are also similar.

Before deriving formulae for the spectra we shall make a few observations. Let

$$\{\vec{X}_1, \vec{X}_2, ...\vec{X}_p\}$$

denote a periodic orbit of period p. For the system of section 5.3, $\vec{X}_k \equiv (u_k, s_k)$, and the cell C_i has coordinates,$[L_{ui-1}, L_{ui}]X[L_{si-1}, L_{si}]$. For toral automorphisms, $\vec{X}_k \equiv (i, u_k, s_k)$, where $\vec{X}_k \in C_i$. and L_{ui}, L_{si} have already been defined. We may identify three subspaces of $\mathcal{F}_1$ which are invariant under Θ_t:

1. the space of functions having discontinuities along the stable manifold passing through elements of the periodic orbit,

$$\vartheta = \psi_0 + \phi_u \phi_s \sum_{\ell=1}^{p} \chi_{[u_\ell, L_{ui}]}(u); \tag{5.145}$$

2. the space of functions having discontinuities along the unstable manifold passing through elements of the periodic orbit,

$$\vartheta = \psi_0 + \phi_u \phi_s \sum_{\ell=1}^{p} \chi_{[s_\ell, L_{si}]}(s); \tag{5.146}$$

3. the space of functions having discontinuities along both the stable and unstable manifolds passing through elements of the periodic orbit,

$$\vartheta = \psi_0 + \phi_u \phi_s \sum_{\ell=1}^{p} \sum_{\ell'=1}^{p} \chi_{[u_\ell, L_{ui}]}(u) \chi_{[s_{\ell'}, L_{sj}]}(s). \tag{5.147}$$

In the equations above, ψ_0 and $\phi_u \phi_s$ are elements of $\mathcal{F}_0$, and L_{ui}, L_{si}, L_{sj} correspond to the cells containing the points $\vec{X}_l$ and $\vec{X}_{l'}$ respectively. Each of these function spaces may in turn be separated into sets of nested invariant function spaces, by noting that if ϑ has the properties

$$\forall \ell,\ \forall k < n_u \frac{d^k}{du^k}\phi_{u1}(u_\ell) = 0 \text{ and } \frac{d^{n_u}}{du^{n_u}}\phi_{u1}(u_\ell) \neq 0 \tag{5.148}$$

or

$$\forall \ell',\ \forall k < n_s,\ \frac{d^k}{ds^k}\phi_{s1}(s_{\ell'}) = 0 \text{ and } \frac{d^{n_s}}{ds^{n_s}}\phi_{s1}(s_{\ell'}) \neq 0, \tag{5.149}$$

for the systems of section 5.3, and

$$\forall \ell,\ \forall k < n_u \frac{d^k}{du^k}\phi_{ui}(u_\ell) = 0 \text{ and } \frac{d^{n_u}}{du^{n_u}}\phi_{ui}(u_\ell) \neq 0 \tag{5.150}$$

or

$$\forall \ell',\ \forall k < n_s,\ \frac{d^k}{ds^k}\phi_{sj}(s_{\ell'}) = 0 \text{ and } \frac{d^{n_s}}{ds^{n_s}}\phi_{sj}(s_{\ell'}) \neq 0, \tag{5.151}$$

for linear Anosov automorphisms, then so must $\Theta_1\vartheta$. In the following, each of these invariant spaces will be denoted by $\mathcal{F}_{n_u,u}, \mathcal{F}_{s,n_s}$ and $\mathcal{F}_{n_u,n_s}$.

Let us now derive formulae for the spectra of Θ_1 when acting on the above spaces for the systems described by section 5.3. The derivation for linear toral automorphisms is identical, except for a plethora of indices. For simplicity, we first consider the case of the a periodic orbit being just a fixed point $\vec{X}^* = (u^*, s^*)$. Suppose there exists an eigenfunction $v(u, s)) \in F_{0,u}$,

$$\Theta_1 v(u, s) = \lambda v(u, s). \tag{5.152}$$

Now

$$\Theta_1 v(u^* + \epsilon, s^*) - \Theta_1 v(u^* - \epsilon, s^*) = \lambda(v(u^* + \epsilon, s^*) - v(u^* - \epsilon, s^*)), \tag{5.153}$$

where $0 < \epsilon \ll 1$. We note only one “branch” in eq.(5.8) can have $\vec{X}^*$ as a fixed point, which we'll denote as the α branch. Thus, only one term in the sum of eq.(5.143),

$$U_{u\alpha} U_{s\alpha} v(u, s)$$

can have a discontinuity passing through the fixed point. Using eq.(5.145)) we may write

$$v(u, s) = \psi_0(u, s) + \phi_s(s)\phi_u(u)\chi_{[u^*, L_{ui}]}(u). \tag{5.154}$$

We find in taking the limit of small ϵ that,

$$\sigma_{u\alpha}\phi_u(u^*)\phi_s(s^*)|\frac{d}{du}f_{u\alpha}^{-1}(u^*)| = \lambda\phi_u(u^*)\phi_s, s^*), \tag{5.155}$$

where $\sigma_{u\alpha}$ equals one if $f_{u\alpha}^{-1}(u)$ is monotonic increasing and minus one otherwise. Therefore

$$\lambda = \frac{d}{du}f_{u\alpha}^{-1}(u^*).$$

Let's now note that

$$\frac{d^n}{du^n}(\Theta_1 v(u^*+\epsilon, s^*) - \frac{d^n}{du^n}(\Theta_1 v(x^*-\epsilon, s^*) = \lambda(\frac{d^n}{du^n}(v(u^*+\epsilon, s^*) - \frac{d^n}{du^n}v(u^*-\epsilon, s^*), \tag{5.156}$$

which implies that

$$\frac{d^n}{du^n}((\phi_u(f_{u\alpha}^{-1}(u)\frac{d}{du}f_{u\alpha}^{-1}(u)) = \lambda\frac{d^n}{du^n}\phi_u(u), \tag{5.157}$$

at $u = u^*$.

Now consider an eigenfunction

$$v(u,s) \in \mathcal{F}_{1u}.$$

By definition $\phi_u(u^*) = 0$ but $\frac{d}{du}\phi_u(u^*) \neq 0$. Inserting this into eq.(5.157) for $n = 1$ we find $\lambda = \frac{d}{du}f_{u\alpha}^{-1}(u^*)^2$.

In general if $v(u,s)) \in \mathcal{F}_{ku}$ then $\Theta_1 v(u,s) = \lambda_k v(u,s)$, where

$$\lambda_{ku} = \frac{d}{du}f_{u\alpha}^{-1}(u^*)^{k+1}. \tag{5.158}$$

The case of $v(x,y) \in \mathcal{F}_{sk}$ is treated analogously, where we find the formula for the spectra associated with $\mathcal{F}_{sn_s}$ is

$$\lambda_{sk} = \sigma_{s\alpha}|\frac{d}{du}f_{u\alpha}^{-1}(u^*)|\frac{d}{ds}f_{s\alpha}^{-1}(s^*)^k \tag{5.159}$$

where $\sigma_{s\alpha}$ equals one if $f_{s\alpha}^{-1}(u)$ is monotonic increasing and minus one otherwise. The case of $v(x,y) \in \mathcal{F}_{0,0}$ is only slightly more complicated. Eq.(5.153) is now replaced by

$$\Theta_1 v(u^*+\epsilon, s^*+\epsilon) - \Theta_1 v(u^*-\epsilon, s^*-\epsilon) = \lambda\left(v(u^*+\epsilon, s^*+\epsilon) - v(u^*-\epsilon, s^*-\epsilon)\right). \tag{5.160}$$

We find in taking the limit of small ϵ that

$$\begin{aligned} \sigma_{u\alpha}\sigma_{s\alpha}\phi_u(u^*)\phi_s(s^*)|\frac{d}{du}f_{u\alpha}^{-1}(u^*)| &= \lambda_{00}\phi_u(u^*)\phi_s(s^*) \\ &\Rightarrow \lambda_{00} = \sigma_{s\alpha}\frac{d}{du}f_{u\alpha}^{-1}(u^*). \end{aligned} \tag{5.161}$$

To treat the general case, we first replace Eq.(5.156) by

$$\begin{aligned} \frac{d^n}{du^n}\frac{d^m}{ds^m}\Theta_1 v(u^*+\epsilon, s^*+\epsilon) &- \frac{d^n}{du^n}\frac{d^m}{ds^m}\Theta_1 v(u^*-\epsilon, s^*-\epsilon) \\ = \lambda(\frac{d^n}{du^n}\frac{d^m}{ds^m}v(u^*+\epsilon, s^*+\epsilon) &- \frac{d^n}{du^n}\frac{d^m}{ds^m}v(u^*-\epsilon, s^*-\epsilon)), \end{aligned} \tag{5.162}$$

from which it follows

$$\begin{aligned} &\sigma_{u\alpha}\sigma_{s\alpha}\tfrac{d^n}{du^n}\tfrac{d^m}{ds^m}\left(\phi_u(f_{u\alpha}^{-1}(u^*))\phi_s(f_{s\alpha}^{-1}(s^*))|\tfrac{d}{du}f_{u\alpha}^{-1}(u^*)|\right) \\ &= \lambda\left(\tfrac{d^n}{du^n}\tfrac{d^m}{ds^m}\phi_u(f_{u\alpha}^{-1}(u^*))\phi_s(f_{s\alpha}^{-1}(s^*))\right). \end{aligned} \tag{5.163}$$

Suppose now that $v(u,s) \in \mathcal{F}_{nm}$. Solving eq.(5.163) and using eqs.(5.158), (5.159) we find that

$$\lambda_{nm} = \left(\frac{d}{du}f_{u\alpha}^{-1}(u*)\right)^{n+1}\sigma_{s\alpha}\left(\frac{d}{ds}f_{s\alpha}^{-1}(s*)\right)^m = \sigma_{u\alpha}\lambda_{n-1u}\lambda_{sm}, \tag{5.164}$$

where for the last equality we assume $n > 0$.

Let's now generalize the above construction to a periodic orbit of period p. In the following we'll adopt the convention that $(u_{p+1}, s_{p+1}) = (u_1, s_1)$ and $(u_{1-1}, s_{1-1}) = (u_p, s_p)$. First, suppose that $v(u,s) \in \mathcal{F}_{n*}$. Eq.(5.156) is valid here too, except that (u^*, s^*) now is an element of the periodic orbit, say (u_k, s_k). We then note that only one "inverse branch' is associated with the discontinuity through (u_k, s_k), namely that inverse branch which maps u_k to u_{k-1}, which we denote by $f^{-1}_{u\,k\to k-1}$. Hence

$$\frac{d^r}{du^r}\left((\phi_u(f^{-1}_{u\,k\to k-1}(u)\frac{d}{du}f^{-1}_{u\,k\to k-1}(u)\right) = \lambda\frac{d^r}{du^r}\phi_u(u), \tag{5.165}$$

at $u = u_k$. In particular we find for each element of the periodic orbit,

$$\frac{d^n}{du^n}(\phi_u(u_{k-1})(\frac{d}{du}f^{-1}_{u\,k\to k-1}(u_k)^{n+1} = \lambda\frac{d^n}{du^n}\phi_u(u_k). \tag{5.166}$$

Solving these p coupled equation we find

$$\{\lambda_{n\infty}\} = ((\frac{d}{du}f^{-p}_{u\,k\to k}(u_k)^{n+1}))^{\frac{1}{p}}. \tag{5.167}$$

Suppose now that $v(u,s) \in \mathcal{F}_{sm}$. We perform the analogous derivations, by first noting that only one "inverse branch' is associated with the discontinuity through (u_k, s_k), namely that inverse branch which maps s_k to s_{k+1}, which we denote by $f^{-1}_{s\,k\to k+1}$.

$$\{\lambda_{sm}\} = \left(\sigma_s|\frac{d}{du}f^{-p}_{u\,k\to k}(u_k)|(\frac{d}{ds}f^{-p}_{s\,k\to k}(s_k))^m\right)^{\frac{1}{p}}, \tag{5.168}$$

where σ_s equals one if $f^{-p}_{s\,k\to k}(s_k)$ is monotonic increasing, and minus one otherwise. Now if $v(u,s) \in \mathcal{F}_{nm}$ we can use eq.(5.162) to obtain

$$\begin{aligned} &\sigma_s\sigma_u\tfrac{d^n}{du^n}\tfrac{d^m}{ds^m}\left(\phi_u(f^{-1}_{u\,k\to k-1}(u_k))\phi_s(f^{-1}_{s\,k\to k+1}(s_k))|\tfrac{d}{du}f^{-1}_{u\,k\to k-1}(u_k)|\right) \\ &= \lambda\left(\tfrac{d^n}{du^n}\tfrac{d^m}{ds^m}\phi_u(f^{-1}_{uk\to k-1}(u_k))\phi_s(f^{-1}_{sk\to k+1}(s_k))\right), \end{aligned} \tag{5.169}$$

where σ_u equals one if $f^{-p}_{u\,k\to k}(u_k)$ is monotonic increasing, and minus one otherwise. We find that the eigenvalues are given by

$$\{\lambda_{nm}\} = \left(\sigma_s\sigma_u|\frac{d}{du}f^{-p}_{u\,k\to k}(u_k)|(\frac{d}{du}f^{-p}_{u\,k\to k}(u_k))^n(\frac{d}{ds}f^{-p}_{s\,k\to k}(s_k))^m\right)^{\frac{1}{p}} \tag{5.170}$$

For a simple example of such spectra, we need only look at our example of a linear automorphism on the torus, and the spectra given by eq.(5.118), that is the eigenvalues given by $-\Lambda_s^m\Lambda_u^{-n-1}$.

5.7 General 2-d conservative hyperbolic maps

All our analysis has assumed the existence of finite Markov partitions, where the cell walls were straight lines parallel to the stable/unstable directions of the map. Each of these assumptions may not be true more generally. We can argue heuristically, and provide numerical evidence that the first assumption is not crucial, as we can construct quasi-Markov partitions. The second assumption is more drastic, so let us suggest how this problem may be solved where the cell walls have curvature, and the map is defined on the torus.

Let us assume that there exists a finite Markov partition. A local coordinate system can be constructed as follows. Let $\vec{e}_j$ denote the origin of the cell ,which we define as the bottom left corner. Each point $\vec{x}$ in the C_j lies on a stable manifold $\omega_s(\vec{x})$ and an unstable manifold $\omega_u(\vec{x})$. $\omega_s(\vec{x})$ and $\omega_u(\vec{x})$ each intersect with the unstable and stable sides of C_j containing $\vec{e}_j$ (see figure). The points of intersection $\vec{x}_u$, $\vec{x}_s$ can be parameterized as the distance of $\vec{x}_u$ and $\vec{x}_s$ from $\vec{e}_j$ along the unstable and stable sides of C_j respectively (u, s). The stable and unstable manifold theorem together with the Markov property imply that the map described in our coordinate system u, s decouples locally so that if

$$\vec{x} \in C_i \bigcap \vec{f}^{-1}(C_j) \equiv (u, s)$$

then

$$\vec{f}(\vec{x}) \equiv (f_{uij}(u), f_{sji}^{-1}(s) \text{ if } u \in I_{uij}. \tag{5.171}$$

Similarly, if

$$\vec{x} \in C_j \bigcap \vec{f}(C_i) \equiv (u, s)$$

then

$$\vec{f}^{-1}(\vec{x}) \equiv (f_{uij}^{-1}(u), f_{sji}(s) \text{ if } s \in I_{sji}. \tag{5.172}$$

Thus, in local coordinates the map decouples in the same way as Anosov automorphisms, except that $f_{uij}^{-1}(u)$ and $f_{sji}(s)$ are nonlinear functions in u and s respectively. If these are analytic functions of their argument, then the analysis of the systems statistical properties proceeds as in the earlier sections[5]. In this case, we use orthogonal polynomials with argument u and s respectively. There are however at least two sources of difficulty. First, we need our observables to be separable $a(u, s) = a_u(u)a_s(s)$, which may not always be possible given the curvature in the system. Second, we have to construct the Markov partition, which even numerically can be problematic.

5.8 Conclusion

In this chapter we have focused on the measurable statistical properties of a large class of two dimensional hyperbolic dynamical systems including systems that are reversible and conservative. By measurable statistical properties, we mean statements such as the probability of the system to be found in a a specified region of phase given some initial preparation, or the value of a statistical moment of the system with respect to an observable. These statements entail the evaluation of correlation function type integrals, which

[5]In fact if the map is C^r, then the stable and unstable manifolds of a point will also be C^r[26].

we have shown can be performed through finite matrix representations of a linear operator Θ closely related to the Frobenius-Perron operator. The representations are valid only in the context of such integrals, and cannot generally be used to evolve probability densities. No assumptions are made about the system being close to or far from equilibrium, but rather that observables/measurable functions and initial probability densities are reasonably regular functions, for example piecewise analytic along the canonical co-ordinates. The spectra of the representations lie in the unit circle, implying directly the exponential decay of time correlation functions, and for simple systems and observables, correspond to the zeros of the dynamical zeta functions. We have also shown how local statistical properties can be described using a finite number of periodic orbits, and that the the associated spectral properties are given by a simple formula. This local perspective is suitable for describing the evolution of highly localised initial densities, which may model, for instance, almost point-like initial conditions. Finally we have outlined how these techniques may be applied to more general axiom A dynamical systems.

One may ask if these results shed any light on the long-standing issue of the origins of macroscopic irreversability[58, 59] That is, suppose that a system consisting of a large number of particles, can is some sense be approximated as an Anosov dynamical system, as proposed by Gallavotti and Cohen[37], and that our results can be extended to such a model. We observed for our systems that the probability to be in a region of phase space at some time, given an initial preparation of the system, and time correlation functions, can be evaluated error free with only partial information about the evolving probability density, provided that our observables belong to restricted classes of functions, such as analytic functions, or piecewise analytic functions, etc. Through judicious changes of variable taking into account the hyperbolic nature of the system we were able to define a new operator whose spectra lie within the unit disc, and are the signatures of exponential decay of time correlation functions, and irreversability. We established the relation between these spectra and the zeta function formalism. What is intriguing, for these simple models at least, is not just irreversability, but the microscopic mechanisms that permit time correlation functions (and statements of probability) to be evaluated exactly through finite matrix representations.

From this pragmatic view, we may inquire about how these results may be extended to more complex and concrete systems. The last section sketched how the results may apply to general axiom A systems. We may be able to relax the condition of hyperbolicity. For instance, we could couple two logistic maps, or cusp maps, in the manner of the Baker map. One could also consider the statistical properties of multi-Baker like maps [38, 39] which exhibit diffusion like phenomena. The novelty here would be to replace the Baker map, with a reversible non-linear map. Finally, let us remark that one of virtues of the techniques presented here, is that numerical investigations should be more easily implemented, which is necessary if one wishes to study more general, and complex systems.

Chapter 6

Epilogue

Almost all the maps considered in this dissertation share two key features. First, all periodic orbits are unstable, and second the existence of a Markov partition, which in the case of one dimensional maps is the minimal Markov partition [1]. We shall briefly discuss how these restrictions can be relaxed, for one-dimensional non-Markov maps, and certain type three intermittent maps respectively. We will then mention an application to stochastic resonance-like phenomena. Finally, we will give an outlook for future work.

6.1 Non-Markov chaotic maps

Let us consider a piecewise analytic expanding map on or in the interval, with the property that the iterates of at least one of the non-analytic points[2] (henceforth called critical points) does not fall onto a periodic orbit[3]. To simplify the discussion, we will suppose that the system has only one critical point (x_c) whose iterates never fall onto a periodic orbit. The idea underlying our analysis is that a density evolved for t iterations can be expressed as a sum over an exponentially increasing number (γ^t, $\gamma > 1$) of inverse trajectories, and groups of trajectories can be identified with specific non-analyticities which are ordered. The summations over inverse trajectories can be rearranged taking this into account to prove that the relative amplitude of higher-order non-analyticities decreases exponentially with increasing order.

Let us restrict our attention to that region of the interval where at least one inverse branch is defined, and call this region $\mathcal{I}$. Any probability density $\rho_0(x)$ which is analytic over $\mathcal{I}$, will if it is evolved for t iterations generally have non-analytic points at all the iterates of the critical points. Let us define the order of the non-analytic points to be the iterate at which they first appear. We will demonstrate that amplitude of the density associated with non-analytic points decreases exponentially quickly with the order of the point. This will allow us to neglect higher order discontinuities, and within any stipulated accuracy, determine the statistical properties of the system through a finite matrix representation of $\mathcal{U}$.

[1] the exception is the logistic map with $r = 3.95$ considered in 4.3.2

[2] There are either discontinuities in the map, or its first derivative

[3] The map has therefore a countably infinite minimal Markov partition. See Baladi and Keller[11] for another approach to this problem.

Proof:

We first note that

$$\rho_t = \mathcal{U}^t \rho_0(x) = \sum_{\{q_t\}} \rho_0(q_t(x))|\frac{dq_t(x)}{dx}|, \tag{6.1}$$

where the sum is over all sequences $q_t(x)$,

$$q_t(x) = f_{\alpha_t}^{-1} \circ f_{\alpha_{t-1}}^{-1} \circ \cdots \circ f_{\alpha_1}^{-1}(x), \tag{6.2}$$

and as usual, if $q_t(x)$ is not defined at a point x then the corresponding contribution to 6.1 is set to zero at x. Each sequence can be written in terms of two subsequences,

$$q_t(x) = r_{t-\ell} \circ p_\ell(x), \tag{6.3}$$

where the principal subsequence $p_\ell(x)$ has the property that x_c is contained in its range ($p_\ell(\mathcal{I})$) and the remainder subsequence $r_{t-\ell}(y)$ is an analytic function of $y \in p_\ell(\mathcal{I})$. The sequences $\{r_{t-\ell} \circ p_\ell(x)\}$ give rise to non-analytic points in eq.(6.1) of order no higher than ℓ. Thus, we can reorder the sum in eq.(6.1),

$$\begin{aligned}
\rho_t(x) &= \sum_{\ell=1}^{t} \sum_{\{r_{t-\ell}\}} \rho_0(r_{t-\ell} \circ p_\ell(x))|r'_{t-\ell}(p_\ell(x))p'_\ell(x)| && (6.4)\\
&= \sum_{\ell=1}^{t} [\mathcal{U}^{t-\ell}\rho_0](p_\ell(x))|p'_\ell(x)| && (6.5)\\
&= \sum_{\ell=1}^{t} \rho_{t-\ell}(p_\ell(x))|p'_\ell(x)|, && (6.6)
\end{aligned}$$

where the last two equations are valid if the critical point is not an element of a periodic orbit, which is precisely the case here. Now, $|p'_\ell(x)|$ is decreasing exponentially quickly with increasing ℓ, so provided $[\mathcal{U}^{t-\ell}\rho_0](p_\ell(x))$ is a bounded function $\forall(t-\ell)$, we can truncate the sum in eq.(6.6) at an appropriate value of ℓ with negligible error. To show that $[\mathcal{U}^{t-\ell}\rho_0](p_\ell(x))$ is indeed a bounded function we can either use the result of Lasota and Yorke[57] establishing the fact that for C_2 piecewise expanding maps, the space of functions of bounded variation is invariant under $\mathcal{U}$, or we can use the fact that for $y \in p_\ell(\mathcal{I})$, $\mathcal{U}^{t-\ell}\rho_0(x)$ is analytic, and exploit the results of chapter 2. Thus, we can state that $\forall\epsilon > 0$, $\exists N$ such that $\forall x, \forall t$,

$$\sum_{\ell=N+1}^{t} \rho_{t-\ell}(p_\ell(x))|p'_\ell(x)| < \epsilon. \tag{6.7}$$

It is even easier to establish similar statement in a measure sense, for

$$\sum_{\ell=N+1}^{t} \int_{\mathcal{I}} \rho_{t-\ell}(p_\ell(x))|p'_\ell(x)|dx \leq \sum_{\ell=N+1}^{t} \int_{\mathcal{I}} |p'_\ell(x)|dx < \epsilon. \tag{6.8}$$

$\square$

It follows straight forwardly that we need only take account of a finite (and small) number of non-analytic points to evolve the probability density with very high accuracy. We use these points to form a quasi minimal Markov partition, and then apply the methods explored in chapter 2, but with the restriction that the initial probability density can have non-analytic points at only the first few iterates of the critical point. It follows trivially from the above analysis that the magnitude of discontinuities in corresponding invariant densities also decreases exponentially quickly with increasing order. The case of there being more than one critical point that does not fall into a periodic orbit in a finite number of iterations is treated in the same way.

6.2 Intermittent Chaos

We will now consider one of the prototypes of type 3 intermittentcy, namely the cusp map (see fig. 6.1). The cusp map was first obtained as the first return map from a Poincare section of the Lorenz set of ordinary differential equations. The map is clearly expansive

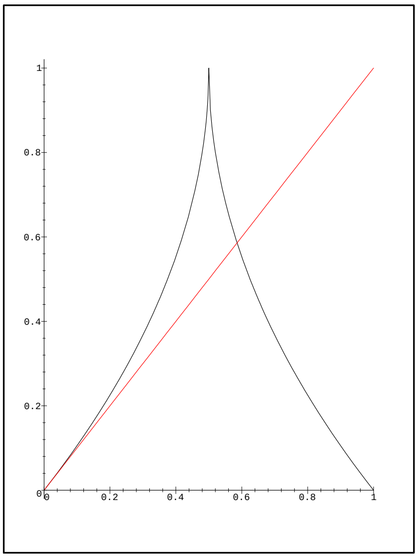

Figure 6.1: The cusp map defined on the unit interval. The marginally stable fixed point at 0 gives rise to laminar behaviour, which is interrupted by bursts of explosive change when a trajectory enters the central region which is highly expansive.

everywhere in the interval except at 0 which is a fixed point which is marginally stable. A trajectory which passes close to 0 will evolve very slowly, but if after some time it enters the central region, it will evolve extremely quickly. As these two types of evolution are coupled in a typical trajectory, it is not evident which time scales will play the dominant role in the systems dynamics. In fact type 3 intermittentcy is poorly understood. We will outline how the methods developed in chapter 3 can be used to investigate both the spectral properties of these systems, and to calculate time-correlation functions where the matrix representation based technique is of the order of 10^4 times faster than methods based on times series analysis.

The inverse branches of the cusp map on the unit interval are given by

$$f_L^{-1}(x) = x - \frac{x^2}{2},\ f_R^{-1}(x) = 1 - f_L^{-1}(x). \tag{6.9}$$

This system has a very simple invariant density $\rho_{inv}(x) = 2 * (1 - x)$, and a positive Lyapunov exponent. Let us now investigate its statistical properties using the results of chapter 2. We seek matrix representations $\mathcal{W}$ of $\mathcal{U}$ acting on, for example, the space of analytic functions. We observe that the inverse branches are analytic functions for any bounded region of the complex plane. Thus, conditions **I, II, III** of subsection 3.2.2 and 3.3.2 are satisfied. However, owing to the marginally stable fixed point at 0 the cusp is not eventually expansive, so we cannot guarantee that that there exists a τ such that $\forall t \geq \tau$, $|\mathcal{W}^t_{mn}| < C\frac{\hat{r}^n}{r^m}$. Therefore, we cannot be sure that our method of obtaining spectral decompositions of $\mathcal{U}$ through $\mathcal{W}$ will work[4]. With this caveat, we may still calculate the spectra of the truncated representations, and investigate their convergence (if any) as a function of the truncation order. The results of this numerical investigation are displayed in Fig.6.2. No clear convergence of the spectra is evident, in contrast with maps which

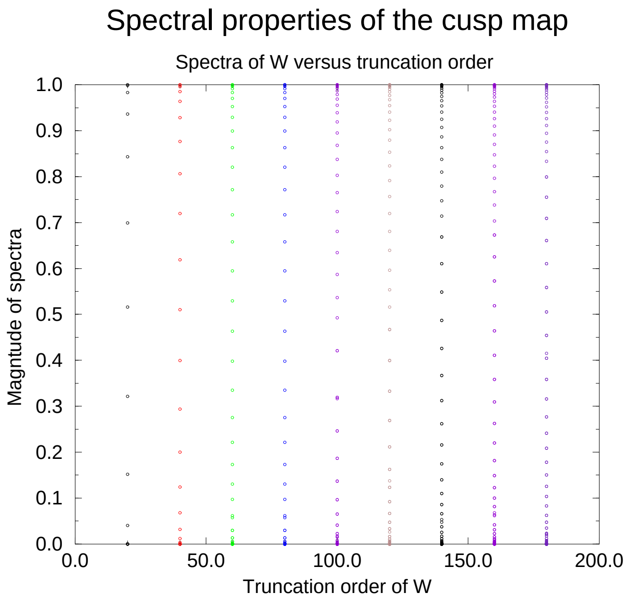

Figure 6.2: Spectra of the $\mathcal{W}$ truncated at successively higher orders. While no clear convergence is evident, it still appears that 1 as well as 0 may be an accumulation point.

are eventually expanding. Nevertheless, it appears that 1 as well as 0 is an accumulation point for the spectra[5]. Now, we made the same observation in sub-section 3.3.3 where we considered the dependence of the spectra of the cusp family of maps as a function of

[4] Indeed, eventual hyperbolicity also plays a key role in the theorem of Lasota and Yorke proving that spaces of functions of bounded variation is invariant.

[5] See also a recent work of H.H. Rugh[100] which we became aware of after submission of this thesis.

the control parameter $\frac{1}{f'(0)}$. In that case, provided $f'(0) > 1$, we are guaranteed that the spectral calculations are reliable (as the map is hyperbolic). The spectral properties of cusp map were then investigated by extrapolating to $(f'(0) = 1)$, where strictly speaking, we cannot be sure that our results are reliable. Never-the-less, as these are two completely independent mathematical approaches (extrapolate by increasing the truncation order, or by varying the control parameter) to the same question, yielding the same result, we can have some confidence that the spectral result is not merely a numerical artifact. This result would suggest that time correlation functions should decay very slowly, perhaps at a non-exponential rate. Now, for $f'(0) = 1$, in contrast with the spectra, time correlation functions of the type,

$$C_{A,B}(\tau) = \int_0^1 A(x)\left[\mathcal{U}^\tau B(x)\rho_{inv}(x)\right]dx = \sum_{j=0}^{N}\sum_{j=0}^{N} a_j \mathcal{W}^\tau b_i + \psi(\tau), \tag{6.10}$$

can be reliably calculated through truncated matrix representations of $\mathcal{U}$, although a priori, we may have to increase the order of truncation rapidly with increasing τ. In the equation above, a_j, b_i are time independent expansion coefficients, and ψ_τ is the error. Therefore, it comes as a very pleasant surprise to see that typically, time correlation function can be calculated reliably for values of τ as long as 300 iterations or more with matrix representations truncated at only order 20. The numerical results are displayed in Fig.6.3. We have also calculated $C_{A,A}(\tau)$ for $A = x^2, x^3, x^4$ for $0 < \tau \leq 300$ with high precision

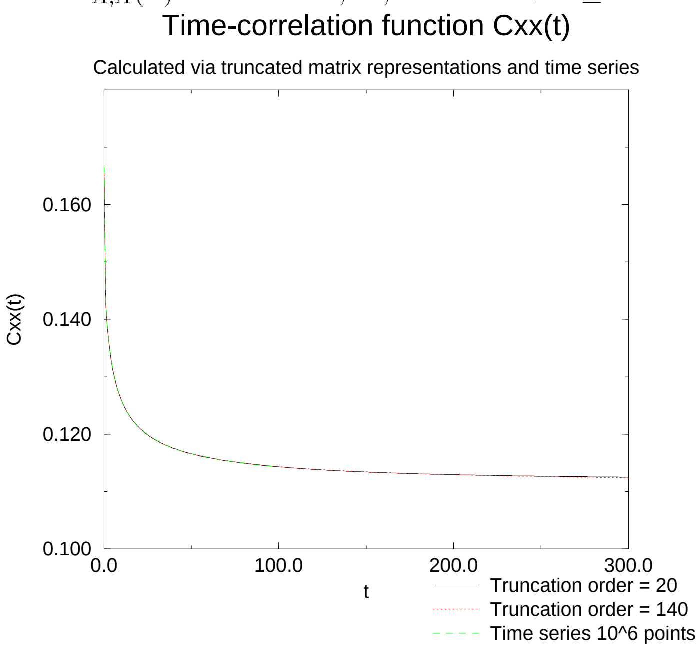

Figure 6.3: The correlation function $C_{x,x}(\tau)$ can be calculated with high precision for values of τ as long as 300 or more, with a matrix representation truncated at surprisingly low orders. Here, the truncation order is 20 and 140. For comparison, we have also calculated $C_{x,x}(\tau)$ from a time series of 10^6 points for $0 < \tau < 100$.

using a matrix representation truncated at order 20. The time taken to perform these calculations through a matrix representation is of the order of 10^{-4} of the time to make the equivalent traditional calculations through a time series,

$$C_{x,x}(\tau) = 10^{-6} \sum_{n=0}^{10^6-1} f^{n+\tau}(x_0) f^n(x_0), \tag{6.11}$$

with the same accuracy. Moreover for large τ the computation time is so long with traditional methods that it becomes prohibitive. It is believed that type three intermittent

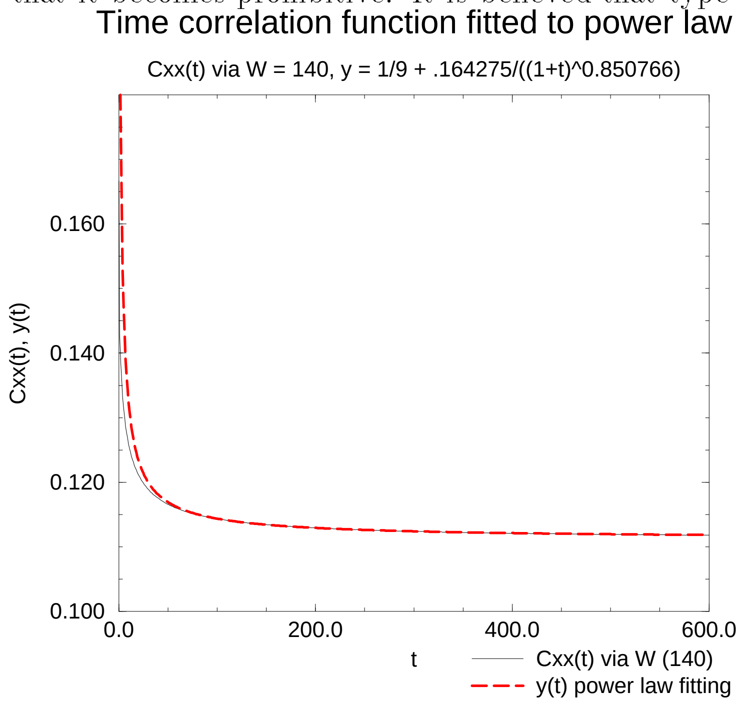

Figure 6.4: The time correlation function $C_{x,x}(\tau)$ appears to decay asymptotically as a power law. If the system is mixing, then the asymptotic value of $C_{x,x}(\tau)$ equals $\frac{1}{9}$, which is also what we observe numerically.

systems decay according to a power law. Fig.6.4 supports this assertion, where we have fitted $C_{x,x}(\tau)$ for $100 \leq \tau \leq 300$ to the curve

$$y = \bar{x}^2 + \frac{0.164275}{(1+\tau)^{0.850766}}, \tag{6.12}$$

where $\bar{x} = \frac{1}{3}$ is the mean value of x with respect to the invariant density, $\rho_{inv}(x)$. Note, that if the system is mixing, then

$$\lim_{\tau \to \infty} C_{x,x}(\tau) = \frac{1}{9},$$

which is, as we see, also expected from the numerics. We note that the exponent is $0.850766\cdots$ rather than 1, which would be the case for a continuous spectral density $(\rho(\lambda))$ were we to make the hypothesis

$$C_{x,x}(\tau) \approx \int_{1-\gamma}^{1} \rho(\lambda) \lambda^\tau d\lambda, \tag{6.13}$$

where $\gamma \ll 1$. Thus, the asymptotic behaviour of $C_{x,x}(\tau)$ may be consistent with our observation that in Fig.6.2 1 appears be an accumulation point for the eigenvalues of $\mathcal{U}$ acting on the space of analytic functions as well as 0.

6.3 Stochastic resonance-like phenomena in chaos

Some time ago we devised a class of chaotic dynamical systems to exhibit, when perturbed with weak periodic perturbations, stochastic resonance like behaviour[80, 64]. In its classical setting, stochastic resonance[76, 12, 71, 87, 74] deals with one-variable bistable systems subjected simultaneously to a stochastic forcing and to a weak periodic forcing. Such systems respond very sensitively[6] when the period of the forcing is of the order of the Kramers time τ_k, which is the average time jumping time from well to well in the presence of noise with no periodic forcing. They have the interesting property that the sensitivity of the system to the periodic perturbations can be enhanced by increasing the noise strength. The origin of this sensitivity can be understood through a perturbative solution of the associated Fokker-Planc equation, which reveals that a bistable weakly noisy system is in an almost critical state due to the existence of an eigenvalue μ_1 close to zero, and having the property $\mu_1 \approx \frac{1}{\tau_k}$. Note that the corresponding form of these eigenvalues for discrete time mappings is $\lambda_1 = \exp(\mu_1)$.

The class of chaotic systems were designed to have the following the properties.

1. The system should have two regions in phase space such that if a trajectory enters a region, it remains there for a long time before jumping to the other one and vice-versa.

2. The invariant density should be symmetric with respect to a point lying equidistant between the two regions.

3. There exists a control parameter which increases the rate of transition from region to region (in analogy for the stochastic system to the effect of increases in the noise intensity or decreases of the depth of the potential wells).

Two examples of such a map are given in fig. 6.5 Property (2) is achieved by demanding

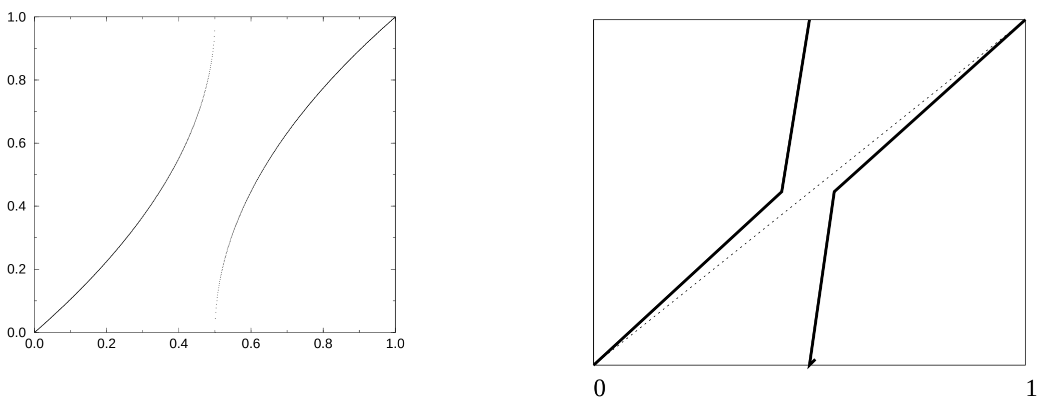

Figure 6.5: A symmetric type 3 intermittent map, and a piecewise linear map which has intermittent-like behaviour. The maps are symmetric about the point $(\frac{1}{2}, \frac{1}{2})$, which implies that any density which is initialy symmetric about $\frac{1}{2}$ will remain if is evolved by $\mathcal{U}$.

[6]The strength of response can be measured for instance, in terms of the signal to noise ratio, or changes in the residence times in the potential wells.

that the maps by symmetric about reflection through the point $(\frac{1}{2}, \frac{1}{2})$. This in turn implies that each map obeys the relation,

$$f(x) = \begin{cases} f_L(x) & \text{if } 0 \leq x < \frac{1}{2} \\ 1 - f_L(1-x) & \text{if } \frac{1}{2} < x \leq 1 \end{cases}, \qquad (6.14)$$

where

$$f_L(0) = 0,\ f_L(\frac{1}{2}) = 1,\ \text{and } f_L'(x) \geq 1 \text{ for } 0 < x \leq \frac{1}{2}.$$

The fixed point 0 is either unstable or marginally stable. Now, we may choose $f_L'(x) \approx 1$ for $x \ll 1$, which will trap trajectories in the laminar regions for suitably long times, thus satisfying property (1). The role of the control parameter (3) can be played by $f_L^{-1\prime}(0)$ for a suitably defined one parameter family of maps. The first map in Fig.6.5 is intimately related to the cusp family of subsection 3.3.3. That is, it is a member of the one parameter family defined by

$$\begin{aligned} f_L^{-1}(x) &= f_L^{-1\prime}(0)x - (\frac{1}{2} - f_L^{-1\prime}(0)x^2 \qquad (6.15) \\ f_L^{-1\prime}(0) &\geq 1, \end{aligned}$$

where $f_L^{-1\prime}(0) \geq 1$. This family has the surprising property that for every member, the invariant density is uniform. When $f_L^{-1}(0) = 1$, the corresponding system exhibits type three intermittentcy, whereas if $f_L^{-1}(0) = \frac{1}{2}$ the system is simply the Bernouli shift map. These maps are Markov analytic provided the fixed point at 0 is unstable, so the corresponding spectral properties can be easily obtained. The second map is a member of the following two parameter family of piecewise linear maps, defined from

$$\begin{aligned} f_L(x) = (1+\delta)x &= f_L^{-1\prime}(0)x,\ 0 \leq x < a < \frac{1}{2} \\ \delta \ll 1,\ f_L(0) &= 0,\ f_L(\frac{1}{2}) = 1. \qquad (6.16) \end{aligned}$$

We can choose Markov members of this family demanding that a falls onto a periodic orbit in a finite number of iterations. A particularly simple case is to demand that $f_L^N(a) = \frac{1}{2}$, e.g. $N = 2$, so the minimal Markov partition consists of the elements

$$0, f(a), \frac{1}{2}, f(1-a), 1.$$

From chapter 2 is is clear that the space of functions piecewise constant over this partition is invariant under $\mathcal{U}$. If we choose $\delta = 0.01$ we find the eigenvalues of $\mathcal{U}$ corresponding to this space are

$$\lambda_1 = -0.0848,\ \lambda_2 = -0.0863,\ \lambda_3 = 0.9818 \text{ and } \lambda_4 = 1.$$

Much as in the case of stochastic resonance, the relevant time scale governing the residence time in the laminar region is given by $\frac{1}{|\ln \lambda_3|} \approx 54.4$.

Let us now turn to the effect of weak periodic perturbations on the chaotic system. We considered three types of perturbation:

(a) weak multiplicative forcing in the form of a periodic square wave[7], to the control parameter

$$f'(0)(t) = 1 + \delta + \epsilon(-1)^{div(t,\frac{p}{2})}; \tag{6.17}$$

(b) weak additive forcing in the form kicks of a periodic square wave to the trajectory with periodic boundary conditions imposed to ensure that the system remain in the unit interval

$$x_{t+1} = F(x_t) = f(x_t) + \epsilon(-1)^{div(t,\frac{p}{2})}; \tag{6.18}$$

(c) weak multiplicative forcing in the form kicks of a periodic square wave to the trajectory except when it is within ϵ of the boundary

$$x_{t+1} = F(x_t) = f(x_t) + \epsilon(-1)^{div(t,\frac{p}{2})}(1 - \chi_{[0,\epsilon]}(x_t) - \chi_{[1-\epsilon,1]}(x_t)); \tag{6.19}$$

For each of the above types of perturbation the system exhibits enhanced sensitivity for long periodic perturbations. In the cases of (a) and (b) this first occurs at $p \approx \frac{1}{|log(\lambda_2)|}$, and is manifest in significant changes in the residence times. For perturbation of type (c), the strength of the response is far greater, but at forcing periods much longer than $\frac{1}{|log(\lambda_2)|}$. The strength of this response can be understood by investigating the properties of the system during long half periods, when it is kicked in only one direction, e.g. the right. If only right multiplicative kicks were to be applied a small attractor close to 1 would form, and all trajectories would ultimately fall into this region. Using the approximate methods of section 6.1 the dominant spectra of the evolution operator (if the system was only to receive kicks from one direction) can be calculated. It turns out that the second largest eigenvalue, which describes accurately the decay rate from the large region into the small attractor, is much closer to unity than is the second largest eigenvalue of the unperturbed system. Of course, after a half period the kick reverses and a "temporary" small attractor on the left is formed. The strong response of the system to long forcing periods is manifested in changes in the residence times, and the power spectrum about the forcing frequency (e.g. increases of the order of 100).

6.4 Outlook

Let us enumerate some of the obvious open questions/problems suggested by the results of this thesis.

1. Many theories require the existence of finite Markov partitions, which is problematic, as such partitions are atypical for most systems. In section 6.1 we have demonstrated for one-dimensional piecewise analytic non-Markov maps that a quasi-Markov partition can be defined, where the effect of the non-Markov property of the partition is of negligible. It is natural therefore, to inquire about the implications of this result for higher dimensional systems.

2. Intermittentcy[101] has attracted much attention for a variety of reasons. It has been observed experimentally in, for example, Bénard experiments, where the velocity of

[7] Note that by $div(a, b)$, we mean the integer part of the quotient of a and b.

the fluid is monitored (types one and three for different Rayleigh numbers), and in simple nonlinear RCL circuits (type three). It has also been suggested as a possible mechanism for the generation of "$\frac{1}{f}$ noise", which is observed in phenomena as diverse as carbon films, super-conductors, and nerve membranes. Experimentally, the power spectrum of these systems diverges with a power law $f^{-\delta}$, $0.8 < \delta < 1$. Type three intermittent maps also exhibit (numerically) such divergences in the power spectrum of autocorrelation functions. Nevertheless, type three intermittentcy is still poorly understood, which increases the interest of the preliminary results stated in section 6.2. The techniques described in chapter 4 are, in principle, applicable for the logistic map at parameter values where type one intermittentcy occurs, for example, chaotic regimes close to period three windows.

3. Stochastic resonance is expected to be present in a wide variety of nonlinear noisy systems. It is also believed that it may be important in applied science, particularly for low frequency detection and processing, where the frequency of the signal is of prime importance. We have outlined in section 6.3 how stochastic resonance-like phenomena are also observable in chaotic systems, where the role of noise is played by the chaotic nature of the system. The phenomena are not yet completely understood, especially for the most spectacular case of a weak multiplicative periodic forcing which is almost additive (see eq.(6.19)), nevertheless, we believe that the principle results of this thesis should lead to a better understanding of them.

4. All the examples we have discussed have been for idealized maps, yet the results of this thesis should be applicable to the first return maps obtained in many experiments. To our knowledge, there has been very little work done on the statistical properties of experimental chaotic systems. One obvious difficulty not present when systems are not chaotic is the relation between the statistical properties of a flow, and its first return map. One may also ask if some of the techniques developed here can be generalized to flows independently of a knowledge of the first return map.

5. Our results for the statistical properties of two dimensional conservative chaotic maps showed how the critical role of the choice of observable is in reducing an a priori infinite dimensional problem to a finite one. Might this shed any light on our understanding of macroscopic phenomena of systems which microscopically are reversible ?

6. Finally, we have shown constructively how to obtain rapidly converging matrix representations of the Frobenius-Perron operator, and that such representations can also be used to obtain spectral decompositions, if desired. There are other operators which we could have analysed, for example, the generalized Frobenius-Perron operators which appear in the thermodynamic formalism. We may then naturally ask are other interesting linear operators operator to which we can apply our techniques?

Appendix A

Non-hyperbolic chaos

In chapter 1 we mentioned the relation between symbolic dynamics and Markov coarse graining, and the ability of the former to unravel complexities of system. A particularily good example is provided by one parameter families of unimodal maps of the interval. Briefly, the itinerary of the critical point determines the topology of the system, which can be represented symbolically in terms of a sequence of L's, R's and C (corresponding to whether an iterate is to the left or to the right of the critical point or coincides with the critical point), and is known as the kneading sequence. The symbolic sequences are ordered, in the sense that one can say that one sequence is greater or less than another. An enormous number of results have been obtained using symbolic dynamics. The importance of these results is evident from the fact that the period doubling route to chaos is generic to (a) any unimodal[19] map with negative Schwartzian derivative and a quadratic critical point. Morover, many of the results extend to large classes (b) of one-parameter families of unimodal maps. Let us list a few of them.

1. One example valid for class (b) is the Sarkovskii theorem which gives simple criteria to determine which periodic orbits exist for a given system (however, it does not distinguish between stable and unstable orbits).

2. Another example, is the work of Metropolis, Stein and Stein, who have discovered and systematically exploited certain combinatorial regularities of one parameter families of maps. In particular, suppose that one knows that at the parameter value $\mu = \mu_0$ the kneading sequence is ω_0, and at parameter value μ_1 the kneading sequence is ω_1, and $\omega_0 < \omega_1$. Then corresponding to any $\omega : \omega_0 < \omega < \omega_1$, there exists a parameter value μ lying between μ_0 and μ_1.

3. Indeed for systems of type (a) one can determine from the nature of a kneading sequence, whether the corresponding system has a stable periodic orbit (periodic or finite number of L's and R's followed by C), is sensitive to initial conditions and even if it definitely has has an absolutely continuous invariant ergodic measure (the kneading sequence is eventually periodic).

The work of Metropolis and Stein explains why given a non-Markov map, we were able to find Markov ones close by in parameter space, having identical kneeding sequences for the first 22 and 44 iterates respectively. The kneeding sequence of a Markov map is eventually periodic, so the corresponding system must have an absolutely continuous invariant ergodic measure. Let us recall that spectral formula given by eq.(4.33) tells us that if a phase space partition is formed in part by the elements of a periodic orbit of period p, then there will exist decaying oscillations of period p or $2p$. From the Sarkovskii theorem, we clearly know which periodic decaying oscillations can occur.

Appendix B

Two dimensional hyperbolic chaos

B.1 Two dimensional invertible maps

The piecewise Chebyshev polynomials are defined as,

$$T_{ik}(x) = \begin{cases} T_k(h_i(x)) & \text{if } x \in C_i \\ 0 & \text{otherwise} \end{cases} \tag{B.1}$$

where

$$h_i(x) = \frac{x - .5(a_i + a_{i-1})}{.5(a_i - a_{i-1})} = \frac{x - e_i}{\Delta_i}. \tag{B.2}$$

They obey the orthogonality relation

$$\int_{c_j} T_{kj}(x) T_{mi}(x) w_j(x) dx = \delta_{j,i} \int_{-1}^{1} T_k(x) T_m(x) w(x) dx, \tag{B.3}$$

where,

$$w_j(x) = w(h_j(x)) \frac{d}{dx} h_j(x), \tag{B.4}$$

and $w(x)$ is just the weighting factor of the standard Chebyshev polynomials. The matrix representations of $U_{x\alpha}$ and $U_{y\alpha}$ are

$$W_{x\alpha_k i_k n_k i_{k-1} n_{k-1}} = \frac{1}{h_{n_k}} \int_I T_{i_k n_k}(x) [U_{x\alpha_k} T_{i_{k-1} n_{k-1}}(x)] w_{i_k}(x) dx, \tag{B.5}$$

and

$$W_{y\alpha_k j_k m_k k_{k-1} m_{k-1}} = \frac{1}{h_{m_{k-1}}} \int_I T_{j_{k-1} m_{k-1}}(y) [U_{y\alpha_k} T_{j_k m_k}(y)] w_{j_{k-1}}(y) dy, \tag{B.6}$$

Eqs.(5.25) and (5.26) are now replaced by

$$\begin{aligned} [\textstyle\int_I a_x(x) U_{x\alpha_t} U_{x\alpha_{t-1}} \cdots U_{x\alpha_1} b_x(x)] \;=\; & \textstyle\sum_{n_t=0}^{\infty} \sum_{n_{t-1}=0}^{\infty} \cdots \sum_{n_0=0}^{\infty} \sum_{i_t} \sum_{i_0} \\ \{[\textstyle\int_I a_x(x) T_{n_t i_t}(x) dx] & W_{x\alpha_t i_t n_t i_{t-1} n_{t-1}} W_{x\alpha_{t-1} i_{t-1} n_{t-1} i_{n-2} n_{t-2}} \cdots W_{x\alpha_1 i_1 n_1 i_0 n_0} b_{x i_0 n_0}\}, \end{aligned} \tag{B.7}$$

and

$$[\int_I b_y(y) U_{y\alpha_1} \cdots U_{y\alpha_{t-1}} U_{y\alpha_t} a_y(y)] \; = \; \sum_{m_t=0}^{\infty} \sum_{m_{t-1}=0}^{\infty} \cdots \sum_{m_0=0}^{\infty} \sum_{j_t} \sum_{j_0}$$
$$\{a_{yj_tm_t} W_{y\alpha_t j_t m_t j_{t-1} m_{t-1}} W_{y\alpha_{t-1} j_{t-1} m_{t-1} j_{t-2} m_{t-2}} \cdots W_{y\alpha_1 j_1 m_1 j_0 m_0} [\int_I b_y(y) T_{j_0 m_0}(y) dy]\}, \tag{B.8}$$

where

$$b_{xi_0n_0} = \frac{1}{h_{n_0}} \int_I T_{i_0 n_0} b_x(x) w_{i_0}(x) dx \tag{B.9}$$

and

$$a_{yj_tm_t} = \frac{1}{h_{m_t}} \int_I T_{j_t m_t} a_y(y) w_{j_t}(y) dy. \tag{B.10}$$

We know that eqs. (B.7) and (B.8) converge from our analysis of the corresponding one dimensional case in subsection 3.4. Indeed the results of that section also imply that our representation of Θ converges uniformly and absolutely. We may now use eqs.(B.7) and (B.8) to calculate $C_{ab}(t)$. The only change from eq.(5.29) are additional summations over the initial and final cells.

$$C_{ab}(t) = \sum_{n_t=0}^{\infty} \sum_{n_{t-1}=0}^{\infty} \cdots \sum_{n_0=0}^{\infty} \sum_{m_t=0}^{\infty} \sum_{m_{t-1}=0}^{\infty} \cdots \sum_{m_0=0}^{\infty} \sum_{i_t} \sum_{j_t} \sum_{i_0} \sum_{j_0}$$
$$\sum_{\alpha_t, \alpha_{t-1}, \cdots, \alpha_1}$$
$$\{ a_{yj_tm_t} \hat{a}_{xi_tn_t} W_{x\alpha_t i_t n_t i_{t-1} n_{t-1}} W_{y\alpha_t j_t m_t j_{t-1} m_{t-1}} W_{x\alpha_{t-1} i_{t-1} n_{t-1} i_{t-2} n_{t-2}} W_{y\alpha_{t-1} j_{t-1} m_{t-1} j_{t-2} m_{t-2}} \cdots$$
$$\cdots W_{x\alpha_1 i_1 n_1 i_0 n_0} W_{y\alpha_1 j_1 m_1 j_0 m_0} b_{xi_0n_0} \hat{b}_{xi_0n_0} \}$$
$$= \sum_{\hat{i}_t} \sum_{m_t=0}^{\infty} \sum_{n_t=0}^{\infty} \sum_{\hat{i}_0} \sum_{m_0=0}^{\infty} \sum_{n_0=0}^{\infty} a_{y\hat{i}_tm_t} \hat{a}_{x\hat{i}_tn_t} W^t_{\hat{i}_t m_t n_t \hat{i}_0 m_0 n_0} b_{x\hat{i}_0n_0} \hat{b}_{y\hat{j}_0m_0}, \tag{B.11}$$

where the two dimensional cells $\hat{i}_t$ and $\hat{i}_0$ uniquely determine the one dimensional cells j_t, i_t, j_0, i_0,

$$\hat{b}_{y\hat{j}_0m_0} = \hat{b}_{yj_0m_0} = \int_I b_y(y) T_{j_0m_0}(y) dy,$$

$$\hat{a}_{x\hat{i}_tn_t} = \hat{a}_{xi_tn_t} = \int_I a_x(x) T_{i_tn_t}(x) dx,$$

and

$$W_{\hat{i}_k m_k n_k \hat{i}_{k-1} m_{k-1} n_{k-1}} = \sum_\alpha W_{y\alpha j_k m_k j_{k-1} m_{k-1}} W_{x\alpha i_k n_k i_{k-1} n_{k-1}}. \tag{B.12}$$

B.2 Two dimensional non-invertible maps

We may define families of two dimensional maps

$$\vec{f}(\vec{x}) = \left\{ \begin{array}{ll} f_\alpha(x) & \text{if } x \in I_\alpha \\ g_\alpha(y) & , \end{array} \right. \tag{B.13}$$

where

$$f_\alpha(x) = f_\alpha(x) \text{ if } x \in I_\alpha, \tag{B.14}$$

$$g_\alpha(y) = g_{\alpha\beta}(y) \text{ if } y \in I_\beta, \tag{B.15}$$

$f(x)$ is a one dimensional Markov analytic map and $g_\alpha(y)$ is a family of one dimensional Markov analytic maps each of which leaves the space of analytic functions invariant under their respective Frobenius-Perron operators. By construction their is a coupling between the x and y directions. Thus we may divide the unit square into rectangles where $f(x)$ and $g(y)$ are each monotonic. Hence the Frobenius-Perron operator takes the form

$$\mathcal{U}\rho(x,y) = \sum_\alpha \sum_\beta \rho(f_\alpha^{-1}(x), g_{\alpha\beta}^{-1}(y))|\frac{d}{dx}f_\alpha^{-1}(x)\frac{d}{dy}g_{\alpha\beta}^{-1}(y)|. \tag{B.16}$$

The space $\mathcal{F}$ of functions $\{\rho(x,y)\}$ where $\rho(x,y) = \rho_x(x)\rho_y(y)$, and $\rho_x(x)$ is piecewise analytic over the minimal Markov partition of $f(x)$ (or refinements thereof), and $\rho_y(y)$ is an analytic function $\forall y \in \mathcal{I}$ is invariant under $\mathcal{U}$. We may immediately apply our results from one dimensional Markov maps to obtain convergent matrix representations of $\mathcal{U}$ acting on $\mathcal{F}$. Moreover, all our results regarding local statistical properties are valid here too.

Bibliography

[1] M. Abramowitz and A. Stegun. *Handbook of Mathematical Function.* Dover, New York, 1972.

[2] R.L. Adler and T.J. Rivlin. *Proceedings of the Americal mathematical society*, 15:794, 1992.

[3] D. Alonso, D. MacKernan, P. Gaspard, and G. Nicolis. *Physical review E*, 54:2474, 1996.

[4] I. Antoniou and S. Tasaki. *Journal of physica A*, 26:73, 1992.

[5] I. Antoniou and S. Tasaki. *Physica A*, 190:303, 1992.

[6] V.I. Arnold and A. Avez. *Ergodic Problems of Classical Mechanics.* W.A. Benjamin, New York, 1968.

[7] R. Artuso, E. Aurell, and P. Cvitanović. *Nonlinearity*, 3:325, 1990.

[8] Hao Bai-Lin, editor. *Chaos II: a reprint selection*, Singapore, 1990. World scientific.

[9] V. Baladi. *Periodic orbits and dynamical spectra*, To appear in Ergodic theory dynamical systems:preprint, 1997.

[10] V. Baladi, J. P. Eckmann, and D. Ruelle. *Nonlinearity*, 2:119, 1989.

[11] V. Baladi and G. Keller. *Communications in mathematical physics*, 127:459, 1990.

[12] R. Benzi, G. Parisi, A. Sutera, and A. Vulpiani. *Tellus*, 34:10, 1982.

[13] R. Bowen. *American journal of mathematics*, XCV:429, 1973.

[14] R. Bowen. On axiom a diffeomorphisms. *Regional conference series in mathematics, American mathematical society*, 35, 1978.

[15] B. Branner and P. Hjorth, editors. *Dynamical zeta functions*, volume Real and complex dynamical systems. Kluwer academic publishers, 1995.

[16] N.I. Chernov. *Journal of statistical physics*, 69:111, 1992.

[17] B. Chirikov. *Physics Reports*, 52:263, 1979.

[18] C.W. Clenshaw. Chebytshev series for mathematical functions. Technical report, Her majesty's stationary office, London, 1962.

[19] P. Collet and J.P. Eckmann. *Iterated Maps on the interval as dynamical systen.* Progress in Physics, Birhauser, Boston, 1980.

[20] P. Collet, J.P. Eckmann, and H. Koch. *Journal of statistical physics*, 25:1, 1981.

[21] M. Courbage and G. Nicolis. *Europhysics letters*, 11:1, 1990.

[22] P. Cvitanović, editor. *Universality in Chaos: a reprint selection*, Bristol and New York, 1989. Adam Hilger.

[23] P. Cvitanović. *Physical Review Letters*, 61:2729, 1992.

[24] D. Daems and G. Nicolis. *Journal of statistical physics*, 76:1287, 1994.

[25] P.J. Davis. *Interpolation and Approximation.* Dover, 1975.

[26] R.L. Devaney. *An introduction to chaotic dynamical systems.* Addison-Wesley, 1987.

[27] M. Dörfle. *Journal of statistical physics*, 40:93, 1985.

[28] W. Ebeling, J. Freund, and K. Rateitschak. *Internalional journal of bifurcations and chaos*, 6:611–625, 1996.

[29] W. Ebeling and G. Nicolis. *Chaos, Solitons and fractals*, 2:635–650, 1992.

[30] W. Ebeling, T. Pp̈schel, and K.F. Albrecht. *Internalional journal of bifurcations and chaos*, 5:51–61, 1995.

[31] J.P. Eckmann. Resonances in dynamical systems. In B. Simon, editor, *Proceedings of the IX International Congress on Mathematical Physics*, London, 1989. IOP Publishing company.

[32] J.P. Eckmann and D. Ruelle. *Reviews of modern physics*, 57:617, 1985.

[33] Y. Elskins and R. Kapral. *Journal of statistical physics*, 38:1027–1049, 1985.

[34] M. Feigenbaum, I. Procaccia, and T. Tel. *Physical Review A*, 39:5359, 1989.

[35] M.J. Feigenbaum. *Communications in mathematical physics*, 77:65, 1980.

[36] V. Franceschini and F. Zironi. *Journal of statistical physics*, 40:69, 1985.

[37] G. Gallavotti and E.G. Cohen. Dynamical ensembles in stationary states. preprint, Fisica, Universita di Roma La Sapienz, 1995.

[38] P. Gaspard. *Physics Letters A*, 168:13, 1992.

[39] P. Gaspard. *Journal of statistical physics*, 68:673, 1992.

[40] P. Gaspard and D. Alonso. *Physical Review A*, 45:8283, 1992.

[41] P. Gaspard and G. Nicolis. *Journal of statistical physics*, 32:499, 1983.

[42] A. Goldbeter. *Biochemical oscillations and cellular rhythms: the molecular bases of periodic and chaotic behaviour.* Cambridge university press, 1996.

[43] S. Grossman and S. Thomae. *Zeitung für naturforschung*, 32:1353, 1977.

[44] J. Guckenheimer and P. Holmes. *Nonlinear oscillations, Dynamical systems, and Bifurcations of Vector Fields.* Springer, New York, 1983.

[45] G. Györgi and P. Szepfalusy. *acta physica Hungarica*, 64, 1988.

[46] P. Halmos. *Lectures on ergodic theory.* Chelsea publishing company, New York, 1955.

[47] P. Hanks, editor. *Collins Pocket Reference Thesaurus.* HarperCollins, 1988.

[48] H. Hasegawa and W. Saphir. *Physical review A*, 46:7201, 1992.

[49] H.H. Hasegawa and D. Driebe. *Physical review E*, 50:1, 1995.

[50] F. Hofbauer and G. Keller. *Journal für mathematik*, 352:100, 1983.

[51] B. A. Huberman and J. Rudnick. *Physical review letters*, 45:154, 1980.

[52] C. Jung, T. Tél, and E.M. Ziamniak. *Chaos*, 3(4):555, 1993.

[53] G. Keller and T. Nowicki. *Communications in mathematical physics*, 149:31–69, 1992.

[54] R. Kluiving. *Fully developed chaos and phase transitions in one dimensional iterated maps.* PhD thesis, Department of physics and astronomy, University of Amsterdam, Amsterdam, 1992.

[55] E. Kreyszig. *Advanced engineering mathematics.* John Wiley and sons, New York, 1983.

[56] A. Lasota and M. Mackey. *Probabilitic description of Deterministic systems.* Cambridge university press, 1985.

[57] A. Lasota and J. A. Yorke. *Transactions of the Americam mathematical society*, 186:481, 1976.

[58] J.L. Lebowitz. *Physica A*, 194:1, 1993.

[59] J.L. Lebowitz. *Physics today*, September:32, 1993.

[60] T. Li. *Journal of Approximation theory*, 17:177, 1976.

[61] E.N. Lorenz. *Predictability: Does the flap of a butterfly's wing in Brazil set of a tornado in Texas ?* Lecture held at annual meeting of thee American association for the advancement of science, Washinton D.C., December 29, 1979.

[62] J. Losson and M.C. Mackey. *Physica D*, 72:324, 1994.

[63] D. MacKernan. Dissipative deterministic chaotic dynamics between the lyapunov time and the long time limit: A probabilistic description. In T. Bountis, editor, *Chaos: Theory and Practice*. Plenum Press, 1992.

[64] D. MacKernan. *Chaos, solitons and fractals*, 4:59, 1994.

[65] D. MacKernan. *Nuovo Cimento D*, 17:863, 1995.

[66] D. MacKernan and G. Nicolis. *Physical Review E*, 50:25, 1994.

[67] M. Mackey. *Reviews of Modern Physics*, 61(4):981–1015, 1989.

[68] A. Manning. *Bulletin of the London mathematical society*, 3:215, 1971.

[69] R. May. *Nature*, 261:459, 1976.

[70] D. H. Mayer. Continued fractions and related transformations. In T. Bedford, M. Keane, and C. Series, editors, *Ergodic theory, symbolic dynamics and hyperbolic spaces*, pages 175–222. Oxford University Press, Oxford, 1991.

[71] B. McNamera and K. Weisenfeld. *Physical review A*, 39:4854, 1989.

[72] M. Misiurewic. *Institut des Hautes Etudes Scientifiques, publications mathematiques*, 53:17, 1981.

[73] H. Mori, B. So, and T. Ose. *Progress in theoretical physics*, 66:4, 1981.

[74] F. Moss. *Stoscastic resonance; from the ice ages to the monkeys ear.* Preprint, Department of physics, university of Missouri at Saint Louis, St. Louis, MO 63121, U.S.A., 1992.

[75] M.Reed and B. Simon. *Methods of Modern Mathematical Physics*, volume 1: Funtional Analysis. Academic Press, New York, 1972.

[76] C. Nicolis. *Tellus*, 34:1, 1982.

[77] G. Nicolis. *Introduction to Nonlinear Science.* Cambridge University Press, 1995.

[78] G. Nicolis, S. Martinez, and E. Tirepegui. *Chaos, solitons and fractals*, 1(2):25, 1991.

[79] G. Nicolis and C. Nicolis. *Physical review A*, 38:1, 1988.

[80] G. Nicolis, C. Nicolis, and D. MacKernan. *Journal of statistical physics*, 70:125, 1993.

[81] G. Nicolis, J. Piasecki, and D. MacKernan. Toward a probabilitis description of deterministic chaos. In L. Savari G. Györgi, I Kondor and T. Tel, editors, *From phase transitions to chaos*, Singapore, 1992. World scientific.

[82] G. Nicolis and I. Prigogine. *Exploring Complexity.* W.H. Freeman and Company, New York, 1989.

[83] T. Nowicki and S. Van Strien. *Transactions of the American mathematical society*, 321:793, 1990.

[84] A. Péntek, T. Tél, and Z. Toroczkai. *J. Phys. A: Math. Gen.*, 28:2191, 1995.

[85] A. Péntek, T. Tél, and Z. Toroczkai. *Fractals*, 3(1):331, 1995.

[86] A. Péntek, Z. Torockzai, T. Tél, C. Grebogi, and J.A. Yorke. *Physical Review E*, 51(2):4076, 1995.

[87] I. Peterson. *Science*, February 23:127, 1991.

[88] W.H. Press, S.A. Teukolsky, and V.T. Vetterling. *Nunerical Recipes.* Cambridge university press, Cambridge, 1992.

[89] S. N. Rasband. *Chaotic Dynamics of Nonlinear Systems.* Wiley-Interscience, 1989.

[90] K. Rateitschak, W. Ebeling, and J. Freund. *Europhysics letters*, 35:401–406, 1996.

[91] L.E. Reichl. *The Transition to chaos in coservative classical systems: quantum manifestations.* Springer, New York, 1992.

[92] T. Rivlin. *Chebyshev polynomials.* Wiley-Interscience, New York, 1990.

[93] G. Roeperstorff. On the exponential decay of correlations for exact dynamical systems. Unpublished, Institüt für Theoretische Physik, RWTH D-51 Aachen, Germany, 1987.

[94] Rokhlin. *American mathematical society translations*, 39:1, 1964.

[95] D. Ruelle. *Physical review letters*, 56:405, 1986.

[96] D. Ruelle. *Journal of statistical physics*, 44:281, 1986.

[97] H.H. Rugh. *Nonlinearity*, 5:1239, 1992.

[98] H.H. Rugh. *Time evolution and correlations in chaotic dynamical systems.* PhD thesis, Niels Bohr Institute, University of Copenhagen, September 1992.

[99] H.H. Rugh. *Ergodic theory dynamical systems*, 16:805, 1996.

[100] H.H. Rugh. *Intermittency and regularized Fredholm determinants*, Preprint, University of Warwick, 1996.

[101] H. G. Schuster. *Deterministic Chaos.* VCH. Weinheim (Germany), 1988.

[102] H. Shigematsu, H. Mori, T. Yoshida, and H. Okamoto. *Journal of statistical physics*, 30:649, 1983.

[103] L.P. Shil'nikov. *International journal of bifurcation and chaos*, 4:489, 1994.

[104] P. Szepfalusy and T. Tel. *Physical Review A*, 34:2520, 1986.

[105] S. Ulam. *A collection of mathematical problems*, volume 8 of *Interscience tracts in pure and applied mathematics*. Interscience, New York, 1960.

[106] T. Yoshida, H. Mori, and H. Shigematsu. *Journal of statistical physics*, 31:279, 1983.

[107] E.M. Ziamniak, C. Jung, and T. Tél. *Physica D*, 76:123, 1994.